

HEAT AND MATTER TRANSFER IN BODY ORGANS
WITH SPECIAL REFERENCE TO
SKIN BLOOD FLOW AND LOCALISED HYPERTHERMIA

Thesis presented for the Degree of Doctor of Philosophy

by

James Patterson B.Sc.

Bioengineering Unit
University of Strathclyde
Glasgow.

May 1982

ABSTRACT

Analytical and numerical models are developed to describe the transport and re-distribution of a highly diffusible substance in the tissues of the body, by the processes of blood flow and diffusion. The models are applied to analagous problems involving, in one case, transfer of matter, specifically an inert gas, and in the other, heat. The specific clinical problems investigated are the measurement of skin blood flow by the clearance of a radioactive inert gas, ^{133}Xe , and the temperature distributions produced in tissue during localised hyperthermia in cancer therapy.

The models show that significant exchange of both an inert gas and heat can occur, between the blood and tissue, in blood vessels larger than capillaries. Traditional models based on capillary exchange are therefore limited in small regions of tissue and the implications of this are discussed for both problems.

The clearance of ^{133}Xe from the skin, after epicutaneous application, is shown to be dependent on the diffusion properties of the epidermal barrier as well as the blood flow. The technique is therefore considered unsuitable as a method of measuring skin blood flow.

The temperature distributions produced during localised hyperthermia are shown to be greatly influenced by blood flow and thermal conduction. In

practical situations the interaction between these two processes can produce complex effects. The possible biological effects of the resulting temperature non-uniformities are outlined and the implications for cancer therapy discussed.

ACKNOWLEDGEMENTS

The author would like to express his thanks to the following people:

The late Dr. F. C. Gillespie of the Department of Clinical Physics and Bioengineering, Glasgow, for his constant advice, guidance and encouragement. To him I owe an immeasurable debt.

Dr. R. Strang of the Department of Clinical Physics and Bioengineering, Glasgow, with whom much of the work on hyperthermia was carried out, and who provided many valuable discussions.

Dr. J. C. Barbenel and Professor J. P. Paul of the Bioengineering Unit, for their critical eye and immense patience.

Mr. M. H. C. Webster, Consultant Plastic Surgeon at Canniesburn Hospital, for help in many aspects of the work on skin blood flow.

Mrs. June Henderson who has both typed this thesis and been of considerable help in its preparation.

My wife, Sandra, for her support and understanding during the writing of the thesis.

Part of this work was carried out under a grant from the Scottish Home and Health Department.

UNITS

Many of the terms used in this thesis, for example diffusion coefficient, blood flow and density, are still widely quoted, particularly in clinical usage, in units which do not adhere strictly to the SI system. For this reason they are used in their common form here and, to provide consistency, other terms are converted to the same units, based mainly on g, cm and ml. Conversion factors to proper SI units are given in Appendix E.

CONTENTS

	Page
Title Page	i
Abstract	ii
Acknowledgements	iv
Units	v
Contents	vi
Chapter 1 Introduction	1
Chapter 2 Review of Previous Literature	23
Chapter 3 Mathematical Models of Heat and Matter Transfer	43
Chapter 4 Skin Blood Flow - Techniques and Radiation Dose	73
Chapter 5 Skin Blood Flow - Model of Xenon-133 Clearance	109
Chapter 6 Skin Blood Flow - Results and Discussion	134
Chapter 7 Localised Hyperthermia - Techniques and Tissue Characteristics	191
Chapter 8 Localised Hyperthermia - Results and Discussion	207
Chapter 9 Heat and Matter Transfer - Conclusions	272
References	278
Appendix A Calculation of the radiation dose in the use of ^{133}Xe	308
Appendix B Program to fit clearance curve with double exponential function	315
Appendix C Program to calculate the partial pressure of ^{133}Xe throughout the skin	318
Appendix D Program to calculate the temperature distribution in tissue during localised hyperthermia	321
Appendix E Conversion factors to SI units	325

CHAPTER 1

INTRODUCTION

1.1 INTRODUCTION

1.2 THERMAL CONDUCTION AND DIFFUSION OF MATTER

1.2.1 Fourier's law of heat conduction

1.2.2 Fick's law of diffusion

1.3 SKIN BLOOD FLOW IN PLASTIC SURGERY

1.3.1 The aim of the present study

1.4 ANATOMY OF SKIN AND ITS BLOOD SUPPLY

1.4.1 The epidermis

1.4.2 The dermis

1.4.3 Subcutaneous tissue

1.4.4 Blood supply of the skin and subcutaneous
tissue

1.5 HYPERTHERMIA IN THE TREATMENT OF CANCER

1.5.1 The effect of heat on body cells and tissues

1.5.2 Variation of hyperthermic effect with
temperature

1.5.3 The aim of localised hyperthermia

1.5.4 The aim of the present study

1.1 INTRODUCTION

If heat is produced locally within a tissue of the body it will, over a period of time, be redistributed both locally to adjacent parts of the tissue and remotely to other tissues of the body. Likewise, if an amount of an inert, diffusible material is deposited in a tissue it, too, will undergo redistribution both within and away from the tissue. The processes responsible for this transport of heat and matter are essential to metabolism in tissue. Exchange of heat between the cells of the tissue and the blood contained within the blood vessels occurs by way of thermal conduction; exchange of matter occurs principally by diffusion. Within the blood vessels bulk transport by the blood flow becomes the dominant process and accounts for the transfer of heat and of matter over longer distances. A description of heat transfer within a tissue will therefore incorporate both thermal conduction and blood flow; a description of matter transfer will incorporate diffusion and blood flow.

Thermal conduction and diffusion are, however, fundamentally similar processes and as such can be described by analagous mathematical equations. Consequently if a mathematical model is constructed to describe the transfer of heat within a tissue then the same model can be adopted to describe matter transfer in that tissue provided, of course, that appropriate substitutions are made for the particular constants of conduction and diffusion.

The aim of this study, then, is to develop such analagous mathematical models and to use the resulting models to investigate two clinical problems, one involving matter transfer and the other heat transfer. The three objectives are summarised here.

Objective A - To develop analytical and numerical models of the transport and distribution of a highly diffusible substance in tissues of the body.

Objective B - To use the models to investigate the roles played by blood flow and diffusion in the clearance of a radioactive gas, Xenon-133, from the skin; and subsequently to assess the use of the clearance rate as an index of skin blood flow in plastic surgery.

Objective C - To use the models to investigate the roles played by blood flow and thermal conduction in modifying temperature distributions produced in localised hyperthermia; and on the basis of the findings to examine the use of localised hyperthermia in cancer therapy.

This chapter first of all examines the analogy between thermal conduction and diffusion (section 1.2) and then introduces the two clinical problems to be investigated by the mathematical models. Section 1.3 describes the importance of the measurement of skin blood flow in plastic surgery and the method recently proposed to do this. A brief description of the anatomy of skin and its blood supply follows in section 1.4. The use of increased tissue temperatures in cancer therapy is illustrated in section 1.5 and the importance of the uniformity of such

temperature distributions is described.

1.2 THERMAL CONDUCTION AND THE DIFFUSION OF MATTER

Classically the conduction of heat is explained on the basis of a simple molecular exchange of kinetic energy. The thermal energy of a solid, for example, consists mainly of the vibrational energy of the molecules about their equilibrium positions. In the course of these oscillations each molecule interacts or "collides" with each of its neighbours and in so doing exchanges kinetic energy with them. In a medium with a uniform temperature no net exchange of energy occurs over a period of time. However if one region of a solid is at a higher temperature than another the kinetic energy of these molecules will be greater. During the molecular interactions, then, more energy will be transferred from the hot area to the cold than in the opposite direction. This is termed thermal conduction.

Similarly if molecules of type A within a uniform temperature medium, B, are free to move (rather than just vibrate) the continual interactions and collisions result in each particular molecule following a rather erratic or random pathway. If the concentration of these molecules within the medium is uniform there will be no net movement, each molecule which leaves a part of the medium being just as likely to be replaced by one from another part. However if there is a larger concentration of molecules within one region then more molecules are likely to leave that region at any specific time than

will enter. There will thus be a net flow away from the region of high concentration. This is termed diffusion. The above are certainly oversimplifications of both processes. No single physical mechanism has been shown to be responsible for either process and in fact there are radical differences between the mechanisms involved in gases, liquids and solids. Despite this each process has been shown to be described by a rather simple, and largely empirical, equation.

1.2.1 Fourier's law of heat conduction

This law, which was described by Fourier in 1822, states that the rate of heat transfer over a unit surface area, due to a temperature gradient within an isotropic medium, is directly proportional to the size of that gradient

$$\dot{Q} = -k \frac{\partial T}{\partial x} \quad 1.1$$

where \dot{Q} is the heat flux, T the temperature and x the direction of the gradient.

The constant of proportionality k is the thermal conductivity.

1.2.2 Fick's law of diffusion

Similarly, Fick's law (1855) states that the rate of transfer of matter is proportional to the concentration gradient of the particular species within a medium

$$J = -D \frac{\partial C}{\partial x} \quad 1.2$$

where J is the mass flux, C the mass concentration.

In this case the constant of proportionality is known as the diffusion coefficient of the substance in the medium.

In both cases, then, the equations state that the flux is proportional to the gradient of the driving force which in one case is temperature and the other concentration. By appropriate substitutions of k and D these equations then become analogous.

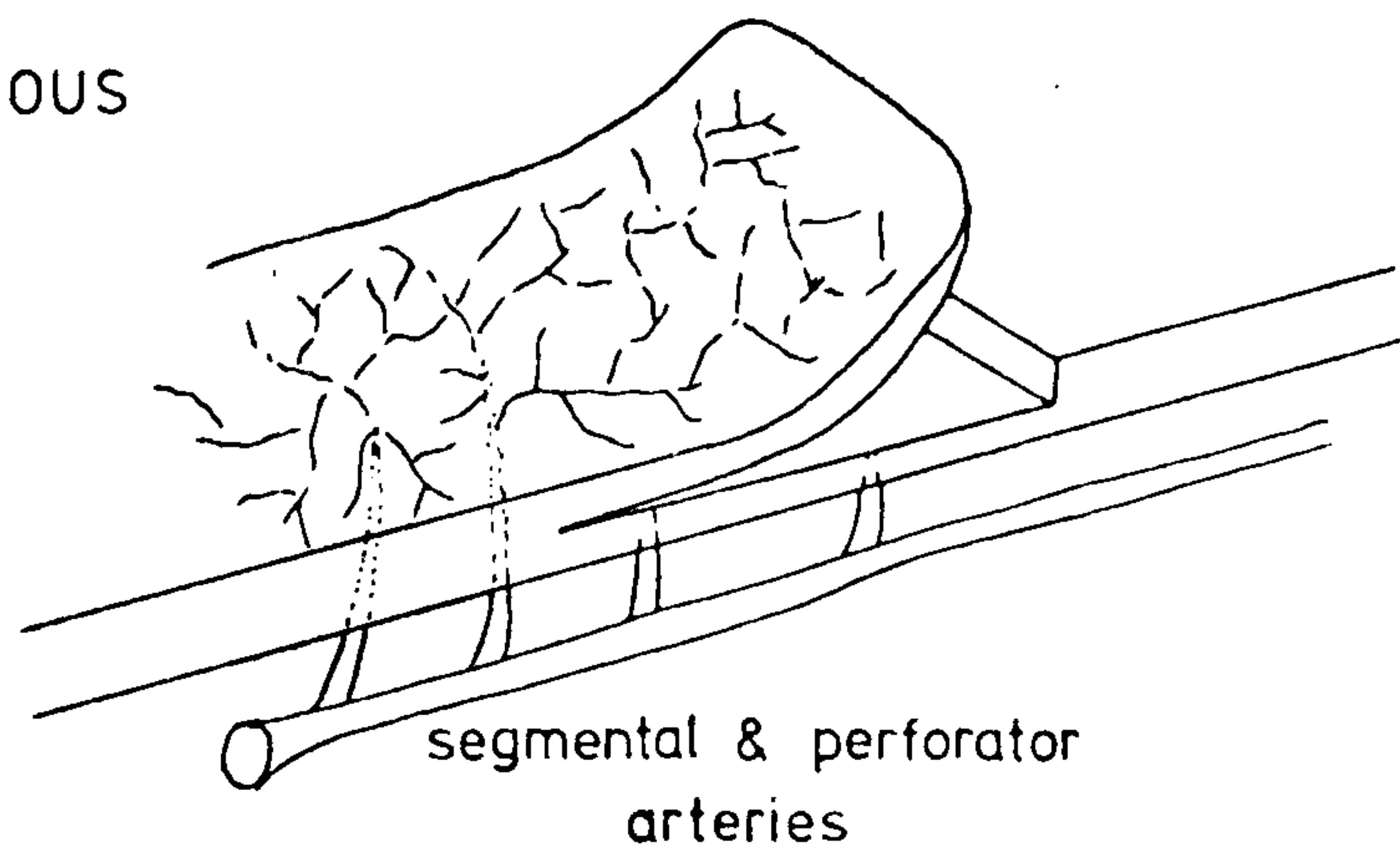
1.3 SKIN BLOOD FLOW IN PLASTIC SURGERY

The raising and transfer of flaps of skin form an important part of the practice of plastic surgery (Fig. 1.1). Such procedures are employed to restore the protective layer of skin to a damaged area or to provide an improved cosmetic appearance. Failure of these operations results in necrosis of all or part of the flap which is subsequently detrimental to the patient's health, comfort and expectations. In almost all cases this failure has its roots in an inadequate blood supply.

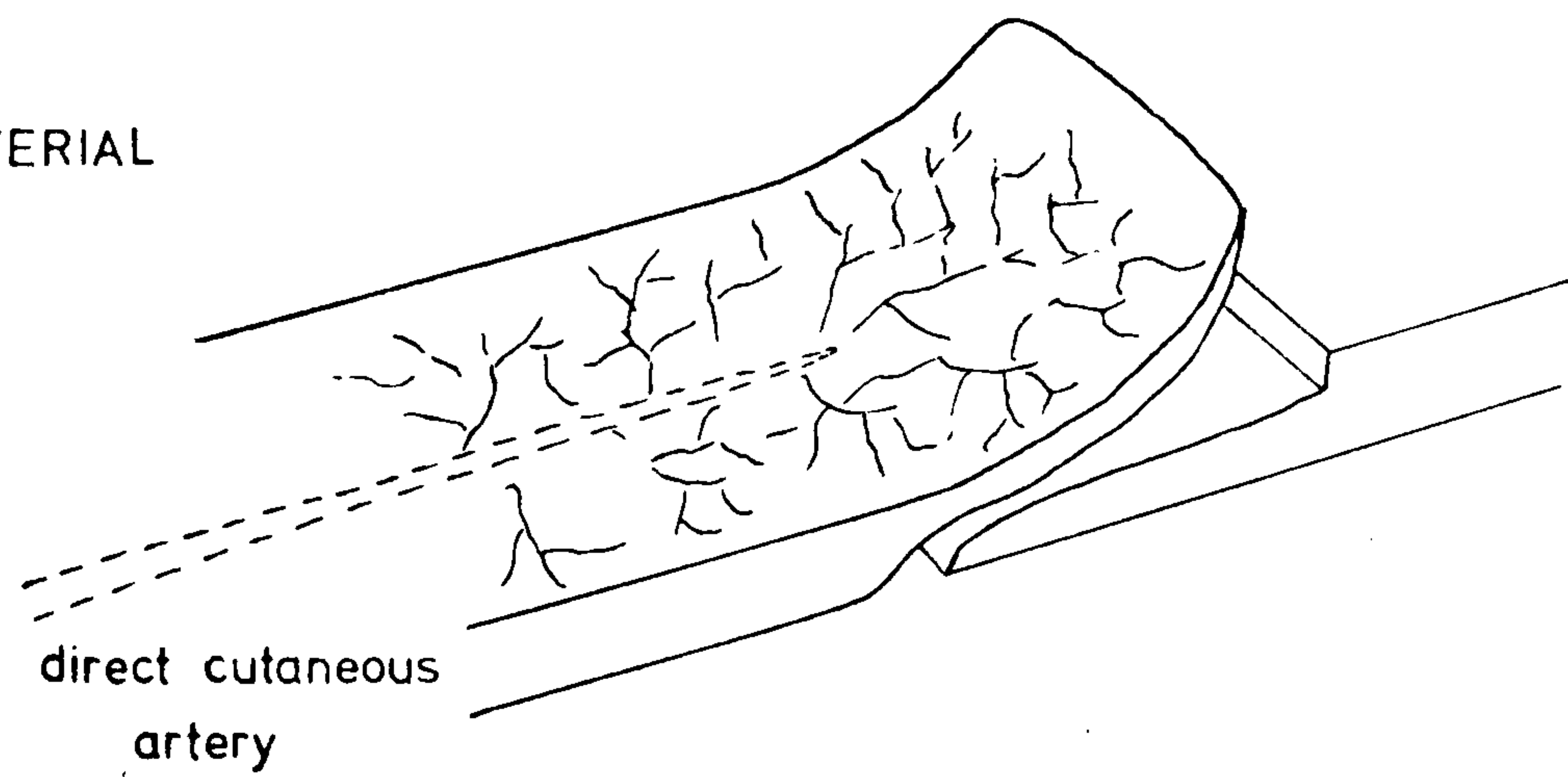
Transplantation of skin from one part of the body to another is required when a wound is too extensive to close by simple suturing. In most cases a skin graft is sufficient to cover the area but in many instances, especially when the recipient bed is poorly vascularised or when padding bony surfaces, a skin flap is required. A skin flap is a piece of skin and subcutaneous tissue which has a vascular attachment to the body maintained at all times for nourishment.

Generally flaps are designed, raised, transferred and divided (Grabb and Smith, 1973) according to rules which result from the accumulated experience of the surgeons. What is known of the circulation of the flap at any stage

1. CUTANEOUS



2. ARTERIAL



3. FREE

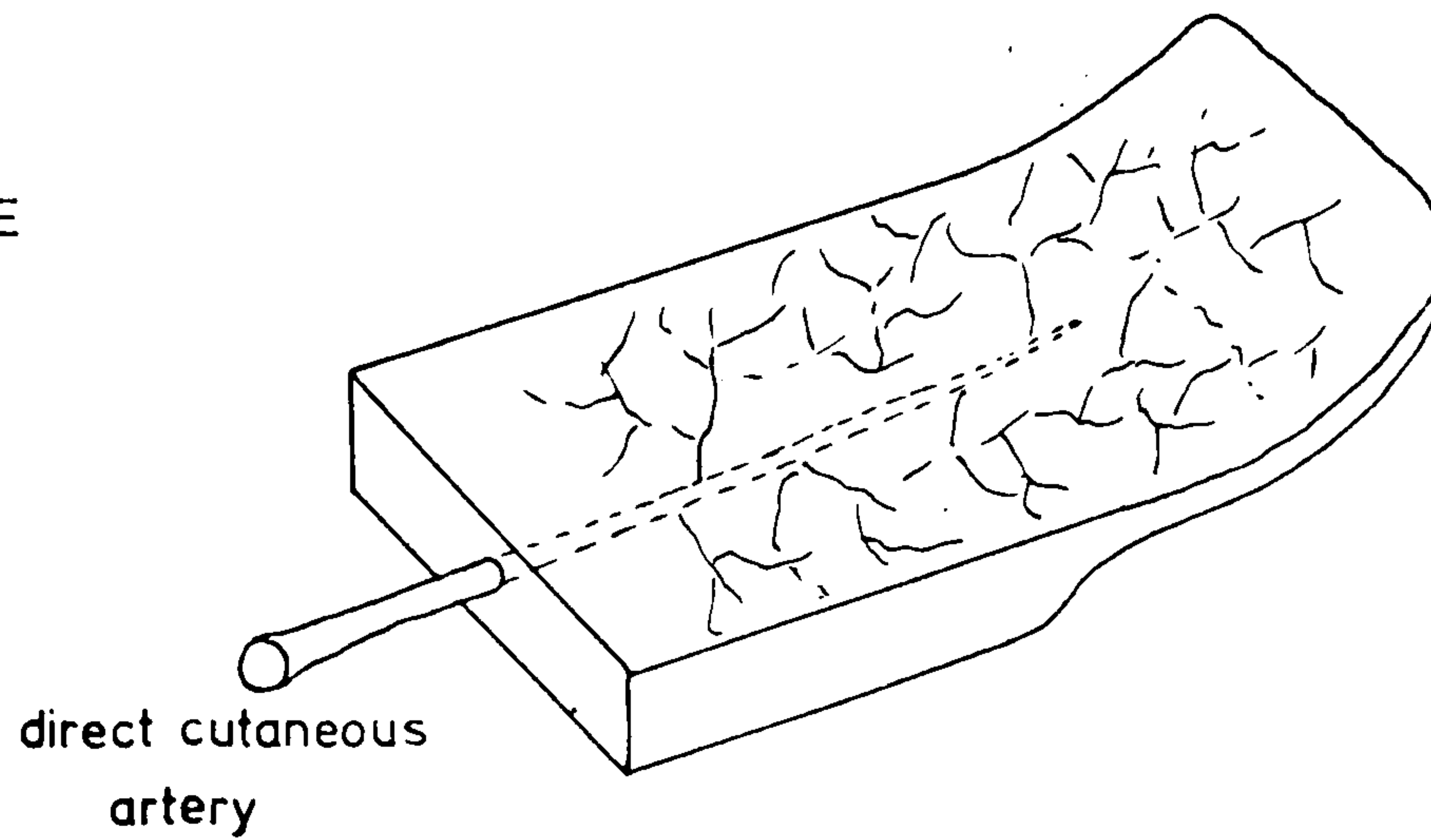


Figure 1.1 Types of skin flaps.

is similarly dependent on the surgeon's expertise and clinical intuition; his subjective assessment is based mainly on skin colour and temperature. Since McLure and Aldrich (1923) introduced the first test based on a physical measurement a very large number of methods have been suggested for assessing the circulation of a flap. These have included physical measurements such as rate of hair growth (Douglas and Buchholz, 1943), skin temperature (Hackett, 1974; Taubenfligel et al, 1965), light transmission (Hertzman et al, 1946; Stranc et al, 1971) and oxygen tension (Guthrie et al, 1972); inflow methods using fluorescein (McGregor and Morgan, 1973), vital dyes (Teich-Alasia, 1971) or microspheres (Reinisch, 1974); and clearance methods using saline (McLure and Aldrich, 1923), atropine (Hynes, 1948) or radioactive isotopes (Tauxe et al, 1970; Tsuchida and Tsuya, 1978). Each of these methods has added to the knowledge of the general behaviour of flap circulation but none has provided the combination of simplicity and accuracy to enable it to be adopted for routine clinical use. This means that skin flaps may be unnecessarily limited or they may be too ambitious; they may be left attached to the donor site for longer than is necessary or they may be divided too early; or they may be subject to a reversible but undetected insult to their blood supply. What is required then is a simple but accurate method of measuring skin blood flow which can be used in the clinical setting of plastic surgery.

1.3.1 The aim of the present study

In 1966 Sejrsen reported on the use of a radioactive inert gas, Xenon-133, in the measurement of skin blood flow and claimed that his technique was both simple and quantitative. This technique involved the introduction of ^{133}Xe into the skin and subsequent monitoring of its rate of clearance from the site. Although other radioactive materials have also been used in this way, even as early as 1948 (Kety), the exact relationship between the rate of clearance of the isotope and the skin blood flow has always been subject to some considerable doubt (Tauxe et al, 1970; Challoner, 1972). Prompted by Sejrsen's claims that his technique overcame the previous objections, this study set out to re-examine the clearance of ^{133}Xe from the skin and in particular to use mathematical models to assess the relationship between the clearance rate and skin blood flow.

1.4 ANATOMY OF SKIN AND ITS BLOOD SUPPLY

The skin is a complex, glandular organ which, because of its intimate contact with the environment, primarily serves to protect the body from external insults and conditions. In this respect it mediates sensation, provides thermoregulation, resists bacterial and chemical penetration by producing a horny covering, affords some protection from light and radiation and lends mechanical support to the body structures. One of its most striking features is its variability, varying not only between races and individuals but showing considerable differences between one part of the body and another. This is most

clearly described by Kligman (1965) who contrasts "the tropical rain forests of the axillae with the oily tundras of the face and the comparative deserts of the trunk". Consequently any investigation of the properties of skin requires that the particular area of the body be recorded; applying the results obtained in one area to the situation in another will surely result in serious error.

The human skin consists of two distinct layers (Fig. 1.2), of different biological origin: these are a) an avascular surface layer, the epidermis and b) an underlying vascular layer, the dermis or true skin. A third layer, sometimes considered separately but more often as part of the "whole skin", is the subcutaneous fatty tissue lying beneath the dermis.

1.4.1 The epidermis

The epidermis (Fig. 1.2a) consists of corrugated layers of cells which are penetrated in places by hair follicles and sweat glands, both of which extend deeper down into the dermis. It varies in thickness from 40 μm or less on parts of the face and body to 1 mm or more on the palms of the hands and soles of the feet (Southwood, 1955). It has no blood supply but the lower layers derive nutrition, by diffusion, from the blood vessels contained within the ridges of the dermal-epidermal junction.

The cells of the epidermis arise from the reproductive basal cell layer adjacent to the dermis. In this layer a

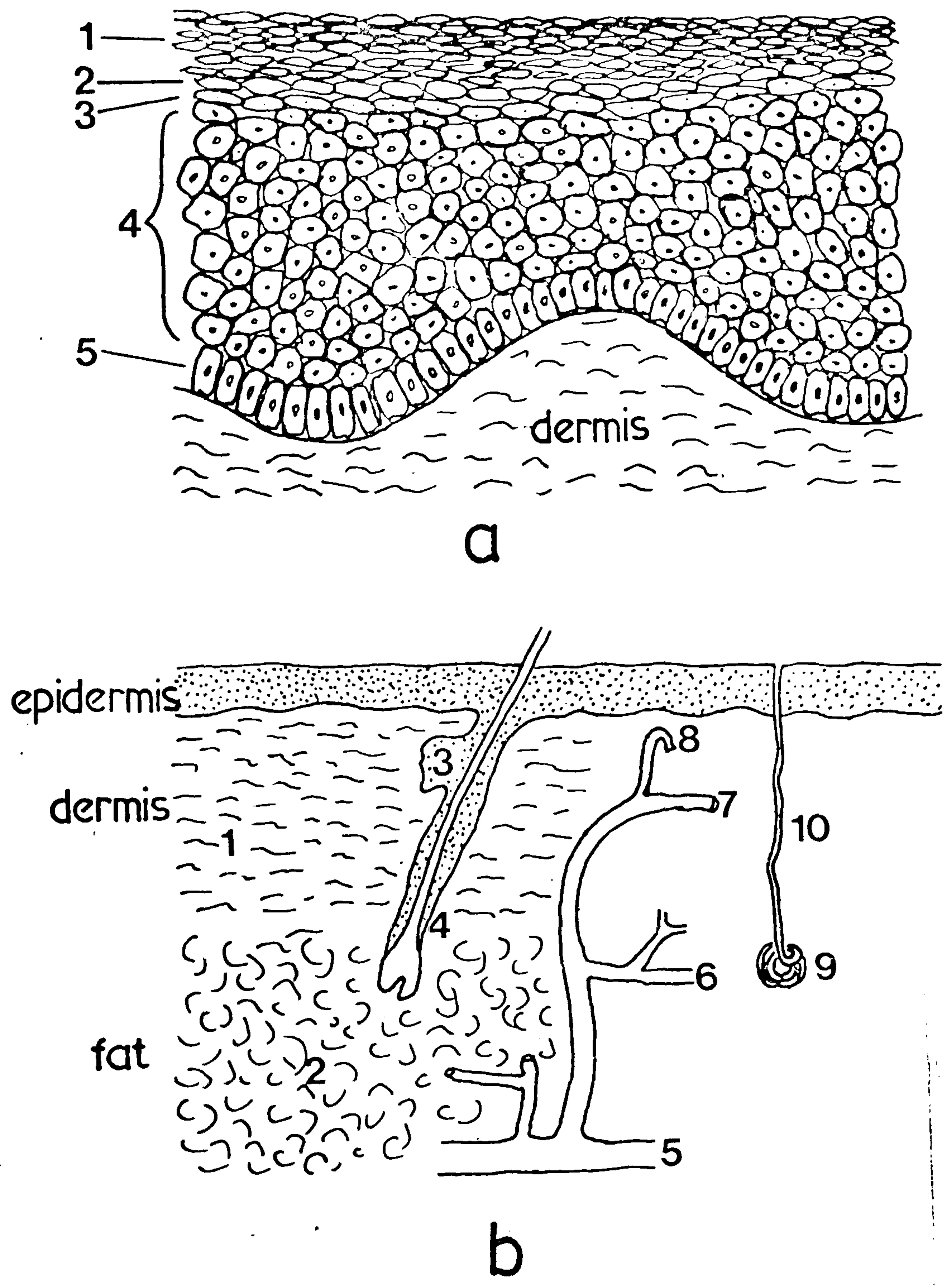


Figure 1.2 a) The epidermis: 1 - stratum corneum 2 - stratum lucidum 3 - granular layer 4 - prickle cell layer 5 - basal cell layer.

b) The whole skin: 1 - collagen and elastin 2 - fat globules 3 - sebaceous gland 4 - hair follicle and hair 5 - deep arterial plexus 6 - middle arterial plexus 7 - superficial arterial plexus 8 - capillary 9 - sweat gland 10 - sweat duct.

continual process of division forms new cells which push against those above them, resulting in a steady upward migration. As the cells approach the surface a complex process of dehydration, polymerisation and compaction of the intracellular material occurs and finally keratin filled, metabolically inactive cells are produced, which are then imperceptibly shed.

Histologists have classified the epidermis into five layers although in some cases these are ill-defined and even indistinguishable. These are a) the stratum germinativum or basal cell layer, where regeneration takes place, b) the stratum Malpighi or prickle cell layer, c) the stratum granulosum, the final living layer, d) the stratum lucidum, which is often indistinct, and finally at the surface e) the stratum corneum.

The horny cell layers of the stratum corneum undoubtedly provide the barrier function of the epidermis (Scheuplein, 1978) rather than any of the viable layers as was originally postulated. This is a passive barrier dependent simply on the dense structure within the stratum corneum and, while almost impermeable to large molecules, allows all small molecules to pass through to some extent.

1.4.2 The dermis

Although the epidermis and dermis are well bound together to form a single unit they are strikingly different. In contrast to the cellular structure of the epidermis the dermis (Fig.1.2b) is mainly a network of collagen and elastin fibres, packed densely and with relatively few

cells, in a colloidal ground substance. The bulk of the fibrous material is collagen which makes up about 70% of the weight of the skin. In addition this tissue contains numerous appendages

- a) blood vessels, to be described in section 1.4.4
- b) lymph vessels - which in general parallel the course of the blood vessels but whose flow is considerably less (Mayerson, 1963)
- c) hair follicles and sebaceous glands which form a single unit and whose root lies in the dermis but penetrates upwards through the epidermis. The sebaceous gland secretes sebum which forms a very thin layer on the surface of the skin (Tregear, 1966). The distribution of hair follicles varies considerably with site
- d) sweat glands - these consist of a coil situated in the dermis and a long winding duct which again penetrates the epidermis and opens out onto the surface. The rate of secretion of the sweat glands increases considerably at ambient temperatures higher than 30°C
- e) muscle fibres
- f) nerve fibres

Also sparsely distributed in the dermis are several types of cells which have important functions in the processes of repair.

1.4.3 Subcutaneous tissue

Lying beneath the dermis and merging almost

imperceptibly with it is the subcutaneous tissue which consists mainly of fat cells. The thickness of this layer varies considerably according to anatomical site and the individual.

1.4.4 Blood supply of the skin and subcutaneous tissue

The blood supply of the skin performs the dual tasks of fulfilling the nutritional requirements of the tissue and controlling body temperature. This double function is reflected by the remarkably wide range of blood flow which can be achieved. In addition because of its high proportion of supporting rather than metabolic tissue the minimum blood flow which is necessary for its survival is extremely small.

As with the structure of the skin, there is a general pattern of the blood vessels which applies to most skin for most of the time, but again considerable variation from this pattern has been observed. In particular this applies to the changes which are apparent in pathological states (Ryan, 1976).

A flat network or plexus of small arteries lies just below the lower surface of the dermis in the subcutaneous tissue. This network sends branches throughout the subcutaneous tissue and also up into the dermis. These branches run vertically or obliquely through the dermis dividing and subdividing many times, producing the characteristic candelabra pattern (Fig. 1.3). As the arteries enter the dermis they are about 100 μ in diameter but this falls to 50 μ in the middle of the tissue

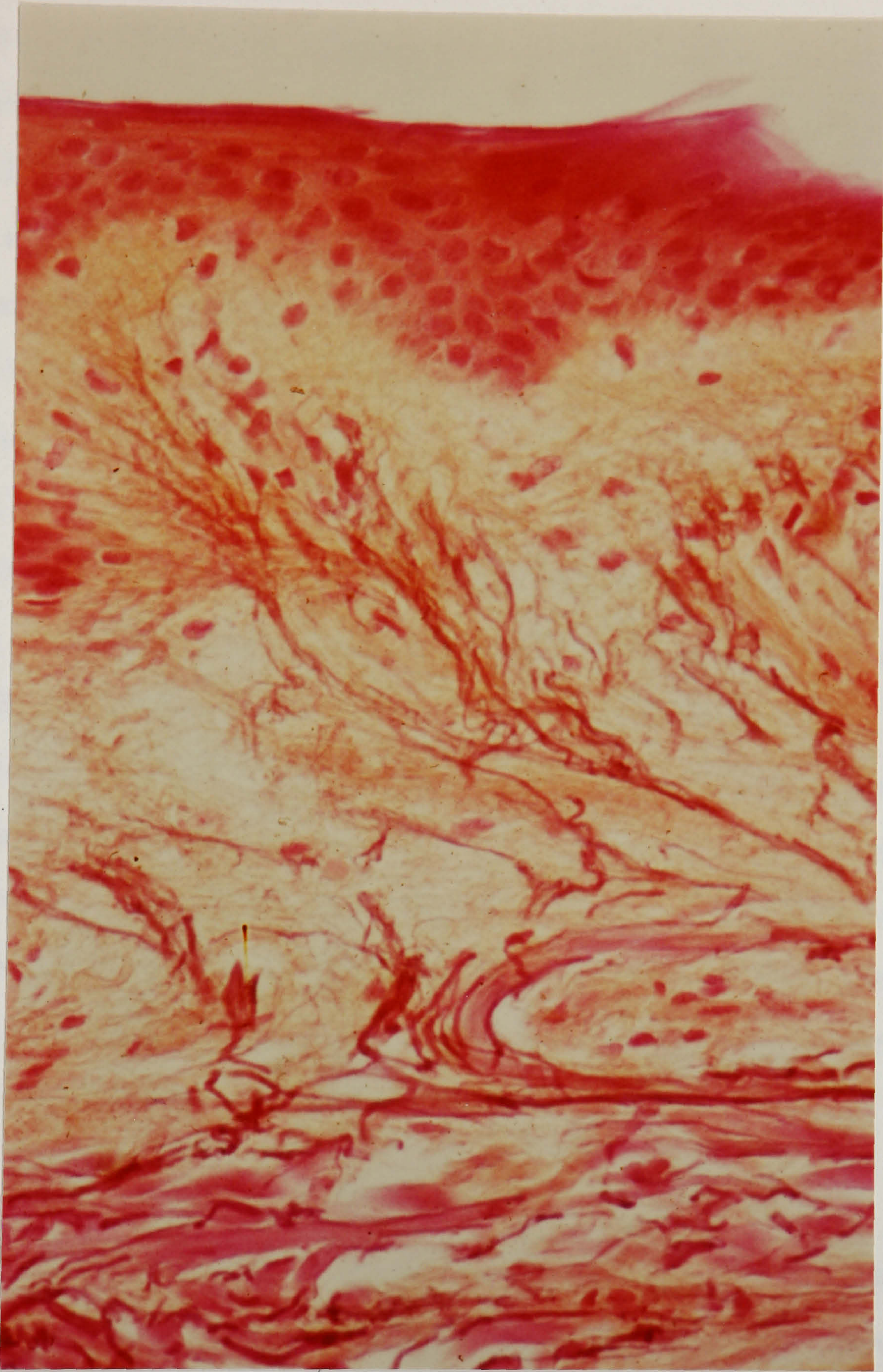


Figure 1.3 The blood supply of the skin.

(Ryan, 1973). The dermis receives a rather poor capillary blood supply, as noted above, although a large number of capillaries are found around the sweat glands and hair follicles. In contrast a much richer capillary supply is found close to the epidermis in the papillary ridges (Fig. 1.2b). This arises from a sub-papillary arterial plexus and each capillary is made up of a vertical loop, rather like a hair pin. In most cases only one capillary, about 10-15 μ in diameter and 0.2-0.4 mm in length, is found in each papilla. Venous plexuses are found in the sub-papillary layer - it is this plexus which governs the colour of the skin - in the middle of the dermis and in the area just below the dermis. Drainage from the sub-cutaneous tissue occurs into this subdermal plexus. The veins of the skin, which are more numerous than the arteries, are 40-60 μ in diameter in the middle of the skin rising to 100-400 μ in the subdermal region.

1.5 HYPERTHERMIA IN THE TREATMENT OF CANCER

The ability of heat to alter the course of tumour progression was first recognised more than 100 years ago by Busch (1866) who noted spontaneous tumour regression in patients who had a severe fever caused by bacterial infection. This finding was adopted by Coley (1893) who then deliberately induced fever in his patients by injecting them with various bacterial toxins and obtained some cases of remarkable and sustained regression in patients with advanced and inoperable malignant disease. The most successful results were apparently in the patients

who developed high and sustained fever. Therefore, despite the fact that the effects of this treatment were undoubtedly due to the combination of the bacterial actions and the role of the body's immune system as well as the increased temperatures, Westermarck in 1927 carried out investigations into the treatment of cancer using localised hyperthermia. These studies supported the previous observations and suggested a differential effect of heat on tumour and normal tissue. However, as the effects were rather inconsistent and since other new and exciting forms of cancer treatment were being developed at that point in time (viz., radiotherapy, chemotherapy and surgical techniques), the use of hyperthermia was temporarily pushed into the background. More recently new technical advances in heating techniques and the failings of conventional treatments to provide a universal cure for malignant disease have resulted in a revival of interest in hyperthermia. This stems in particular from the work of Crile in 1963 and Cavaliere et al in 1967. Dickson (1979), Field^{& Bleehen} (1979), Stehlin (1977) and many others (Streffer et al, 1977) have since advanced the studies through scientific research to limited examples of clinical practice, utilising hyperthermia on its own and in combination with drugs or radiotherapy.

1.5.1 The effect of heat on body cells and tissues

Increasing the temperature of body cells and tissues only a few degrees above their normal temperature results in considerable changes within the cells and eventually cell death. Although much is known of the effects of

hyperthermia the critical target for thermal damage has not so far been identified (Connor et al, 1977; Dickson and Calderwood, 1980). It appears that the thermal energy required for cell killing corresponds to protein denaturation (Westra and Dewey, 1971) and this could inhibit replication of DNA and synthesis of protein (Mondovi et al, 1969b). Inhibition of cellular respiration (Mondovi et al, 1969a) and disruption of cell membranes (Dickson, 1975; Janiak and Szmigielski, 1978) have also been suggested as important targets. In addition there are other physical and physiological factors which must be considered when evaluating the effect of hyperthermia in vivo. These include the blood flow, tissue pH, metabolic rate, differential thermal sensitivity and immune response (Dickson and Calderwood, 1980).

The effectiveness of hyperthermia in cancer therapy depends on a differential effect on tumour tissue compared to normal tissue. Despite the fact that there is a lack of convincing evidence that tumour cells are more sensitive to heat than normal cells in vitro (Song et al, 1980) it is clear that most tumours are more heat sensitive in vivo (Kim and Hahn, 1979; Le Veen et al, 1976). Field and Bleehen (1979) have summarised the possible factors responsible for this, and these include reduced blood flow in the tumour, low pH and lack of nutrition.

1.5.2 Variation of hyperthermic effect with temperature

The thermal damage produced in a tissue will depend on the temperature obtained within the tissue and the

time of application of the heat. The higher the temperature the less time is required to produce the same biological effect (Overgaard and Overgaard, 1977). Figure 1.4 shows a typical thermal response curve of the heating time required to produce a given biological effect at various temperatures (from Dickson and Calderwood, 1980, and Field and Bleehen, 1979). It is seen that a change of 1°C in tissue temperature is equivalent to altering the heating time by a factor of more than two (Dickson, 1977). Similarly, Field and Bleehen (1979) show that an increase in heating time of only 20% or a change in temperature of 0.5°C is sufficient to increase the probability of necrosis in a tissue from 0 to 100%, at the critical point.

These results have several important implications in the clinical practice of hyperthermia.

- a) First of all, and of vital importance, accurate monitoring of the temperature within the heated region will be required.
- b) Since both normal and tumour tissue may be contained within the heated region then, to avoid appreciable normal tissue change, a high degree of uniformity of heating will be required.
- c) Only small differences in heat sensitivity or small differences in temperature within a tumour, caused for example by poor heat dissipation, will produce a decided therapeutic advantage.

In order to maximise the differences between normal

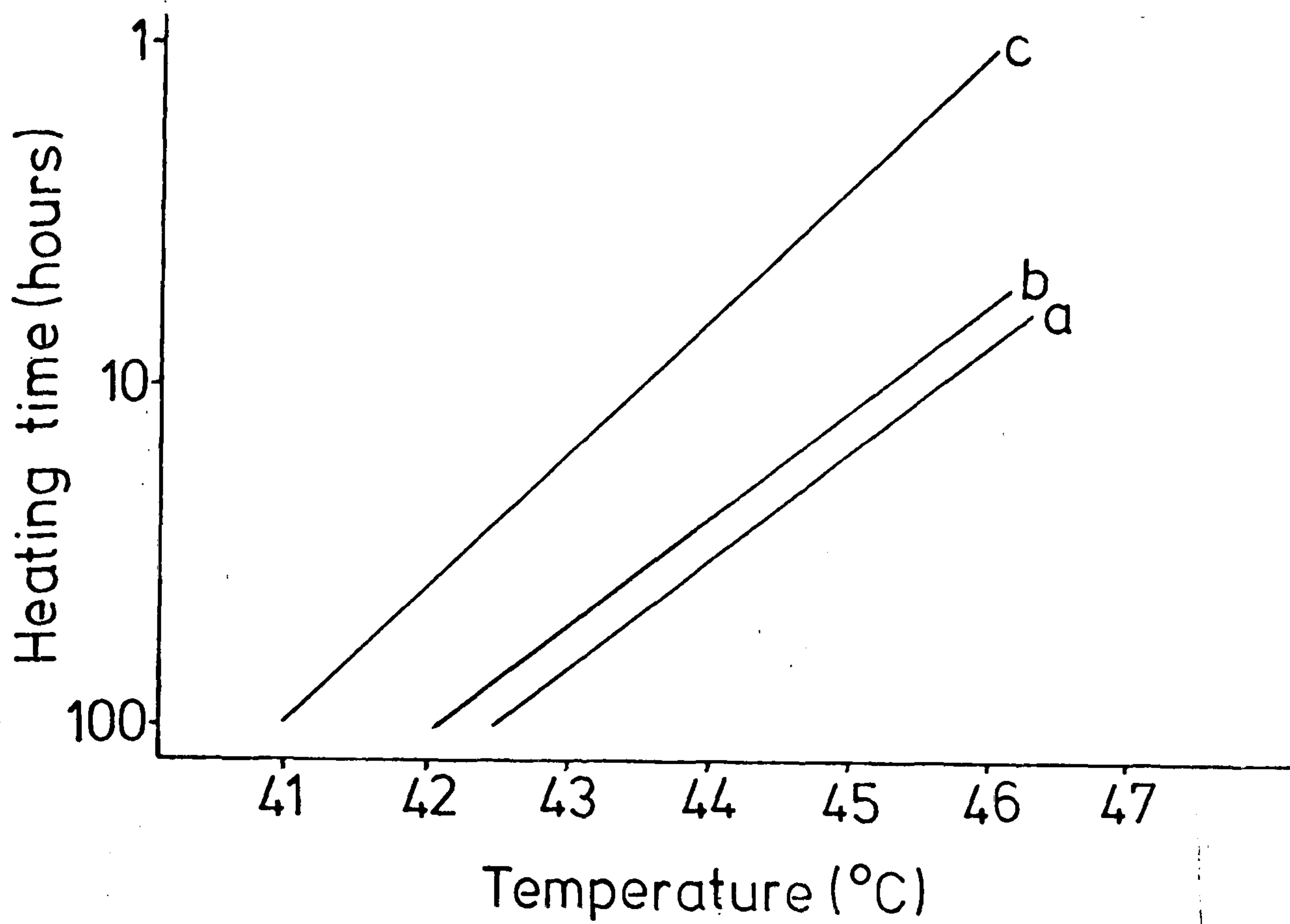


Figure 1.4 Thermal response curves - the relationship between heating time and temperature for the following effects (a) the probability of producing necrosis in rat tails is 100% (b) the probability of producing necrosis in rat tails is zero (c) the thermal death times for human skin.

and tumour tissue a temperature of 42°C has been suggested for clinical hyperthermia (Dickson and Calderwood, 1980) although specific tumours may require higher temperatures than this. Such a temperature would require a heating time of 20 hours (Dickson and Calderwood, 1980), which, for practical reasons, would be given in separate treatments of about one hour each.

1.5.3 The aim of localised hyperthermia

The temperature of tissues of the body can be increased either as a whole body effect, by use of hot air, wax or space suit technology (Pettigrew, 1975), a regional effect by perfusion with heated fluid (Cavaliere et al, 1967) or as a local effect using various physical techniques such as ultrasound (Ter Haar, 1979), high frequency electromagnetic waves (Guy et al, 1974; Mendecki et al, 1978), low frequency electric currents (Doss and McCabe, 1976) or by simple conduction of heat (Robinson et al, 1974).

Localised hyperthermia has considerable practical advantages and with it temperature differentials between tumour and normal tissues may be produced, unlike whole body or regional heating by perfusion. Its application depends on the ability to direct heat to a particular volume of tissue while at the same time producing little or no heat in the surrounding tissues. Ideally the heating pattern should be uniform within the region of interest. However, even with this heating pattern, the temperature distribution produced will depend on the

physical properties of heat dissipation (conduction) and also on biological properties such as blood flow. The biological effect produced by this temperature distribution will, as previously discussed, depend on many other factors.

1.5.4 Aim of the present study

Although a large amount of research has been carried out on the effects of increased temperatures on the cells and tissues of the body and on the theoretical heating patterns delivered by different physical techniques very little has been undertaken on the true temperature distributions achieved in vivo and in particular on the factors affecting these. In most studies the temperature at only one point within the heated region is monitored and the biological effects are related to this one temperature. Hume et al (1979) have recently illustrated the existence of non-uniform temperatures within the treatment volumes and have discussed the significance of this with regard to the interpretation of the biological effects.

The aim of the present study is to investigate, with the aid of mathematical models, the effect of heat transfer processes, viz. thermal conduction and blood flow, in modifying the temperature distributions produced in vivo during localised hyperthermia. The roles of these processes in producing both beneficial and detrimental effects will be discussed and the significance of these effects in relation to cancer therapy examined.

CHAPTER 2REVIEW OF PREVIOUS LITERATURE

- 2.1 INTRODUCTION
- 2.2 PHYSICAL PROCESSES INVOLVED IN THE TISSUE CLEARANCE
OF A LOCALLY DEPOSITED MATERIAL
- 2.3 MEASUREMENT OF SKIN BLOOD FLOW USING XENON-133
- 2.4 GENERAL MODELS OF HEAT TRANSFER IN BIOLOGICAL TISSUES
- 2.5 HEAT TRANSFER MODELS IN HYPERTHERMIA

2.1 INTRODUCTION

Clearly there is an extensive amount of literature on the ways in which materials and heat are transported and distributed in the human body. In line with the aims of the present study this review concentrates primarily on models of local clearance of a material, as applied to tissue blood flow measurement, and on models of localised, as opposed to whole body, heat transfer.

2.2 PHYSICAL PROCESSES INVOLVED IN THE TISSUE CLEARANCE OF A LOCALLY DEPOSITED MATERIAL

Interest in the mathematical description and modelling of the transport of diffusible substances in the body has developed mainly from three areas of investigation, viz.,

- a) the analysis of the uptake of anaesthetic gases (Morales and Smith, 1948),
- b) the analysis of the supply of oxygen to the tissues (Krogh, 1919), and
- c) the measurement of tissue blood flow (Kety, 1951).

It is with this third area of investigation that the present review concentrates.

In 1923 McLure and Aldrich injected saline into the skin, producing a small bleb, and used the subjective assessment of the rate of disappearance of this bleb as a measure of skin blood flow. This was probably the first attempt to relate the rate of clearance of a locally deposited substance to the rate of blood flow. Further development of this technique was slow, however, since the only tissue open to this visual assessment was, of course,

the skin. Hynes (1948) reported a modification of this technique whereby atropine was injected into a tissue. Since atropine produces blurring of the vision when it reaches the eyes the time taken for this to occur was adopted as a measure of its clearance time from the injected area and subsequently of the blood flow. The time taken to travel from the local injection site to the eyes was assumed to be relatively small.

In both of the above cases a proper objective measurement of the rate of clearance was not possible. This awaited the development of tracer substances which could be quantitatively monitored from outside the body - artificially produced radioactive isotopes.

In 1951 Kety, prompted by the emergence of these radioisotopes, gave a comprehensive review of the exchange of inert gases at the lungs and tissues. He defined an inert gas as a substance which dissolves in the blood and tissues of the body according to Henry's Law and undergoes no chemical change within it. Inherent in his assumptions was also the fact that exchange between blood and tissue occurs only by a passive diffusion process with no active transport mechanism involved. All of these characteristics relate directly to the present study.

Kety (1951) proposed that, in a homogeneous tissue, in order for a substance to be cleared from it two distinct steps are involved

- a) the material has to pass from the intracellular and extracellular spaces of the tissue through the

capillary walls to the blood, and this occurs by diffusion

b) the material is then transported away from the tissue by the blood flow.

He then showed that, for capillaries, the time taken to achieve complete diffusion equilibrium, between the blood and the cylinder of tissue served by each capillary, is much less than one second. In these calculations the value of the diffusion coefficient of oxygen was used, and this is similar to most other gases. Since this diffusion time is less than the time taken for blood to pass through a typical capillary he suggested that the clearance rate from tissue is therefore dominated by the rate of blood flow and not by the time taken to diffuse to the capillaries. Furthermore, he demonstrated that in such a homogeneous tissue, the blood flow would remove a constant fraction of the deposited material in each time interval. Mathematically the rate of clearance is then represented by a single exponential function whose rate constant is proportional to the blood flow.

This analysis was in direct contrast to that of Teorell (1937) who considered the clearance rate to be diffusion limited, although he gave no justification for this. More recently Hills (1967) has expressed support for this "diffusion limited" approach. He investigated the diffusion of inert gases ⁸⁵Krypton and acetylene in muscle tissue and reported intracellular diffusion coefficients which were several orders of magnitude less

than previously accepted values for the bulk diffusion coefficients. Using a detailed mathematical model he then deduced that diffusion to the capillaries played a much more significant role than previously imagined and that much of the experimental data could be equally well explained by a diffusion or perfusion limited theory. Subsequently Hennessy (1971, 1974) produced even more elaborate models based on this approach.

Hills' theory, however, is inconsistent with a large amount of the experimental findings. Jones (1950), for example, showed that the rate of clearance of two gases of widely different diffusion coefficients was identical. Betz et al (1966) have shown similar results when comparing the clearance of an inert gas and heat, whose diffusion coefficients are two orders of magnitude different. Larsen and Lassen (1967), in subcutaneous tissue and Haggendal et al (1965), in white matter of the brain, have shown that the clearance rate in these tissues follows a single exponential course for a considerable time contrary to what would be expected if a diffusion limitation was present. Above all, however, Unsworth and Gillespie (1971) and Evans et al (1974) have also measured diffusion coefficients in tissue and have not been able to demonstrate the very low values reported by Hills for intracellular diffusion coefficients. Accordingly they have pointed out several potential sources of uncertainty in Hills' experimental methods.

In the present study Kety's original assumption has

therefore been adopted, i.e. that the diffusion coefficient of an inert gas is high enough to ensure that a complete diffusion equilibrium is achieved between the tissue and the blood in the capillaries. In addition it has been assumed that each tissue is represented by a single, bulk diffusion coefficient. Paradoxically this relatively high diffusion coefficient of an inert gas introduces two further important factors in the modelling of tissue clearance which Kety neglected. Indeed, although these factors have since received limited investigations they are, with few exceptions, ignored in practical applications of the clearance techniques.

Firstly the size, total surface area, linear velocity of blood flow, etc., of capillaries combine to maximise the exchange of nutrients within these vessels (Folkow and Neil, 1971). For this reason they are often known as the exchange vessels. However several studies have indicated that exchange of highly diffusible substances such as heat (Bazett et al, 1948) and inert gases (Stosseck, 1970; Broderson et al, 1973; Sejrsen and Tonnessen, 1972; Sejrsen, 1970) occurs through the walls of blood vessels larger than capillaries. In essence this simply indicates that there is not a step change in the properties of the blood vessels going from capillaries to larger vessels. Complete diffusion equilibrium occurs in the capillaries themselves while small arteries and veins presumably allow limited diffusion and large arteries and veins virtually no diffusion. The exchange properties, in relation to

inert gases, of the various branches of the circulatory network have never been properly defined. There are several consequences of this limited exchange. Sejrsen (1967) has shown that, with an intra-arterial bolus input of inert gas to a tissue some of the gas is lost from the arterial vessels and then picked up again as the arterial bolus passes. This produces an extension of the bolus. Similarly with this technique, the often close proximity of arteries and veins allows the gas to diffuse from one vessel to the other producing a diffusion shunt and allowing gas to bypass the capillary bed of the tissue (Gillespie, 1967; Broderson et al, 1973). This led Broderson et al to claim that "at low blood flow the ^{133}Xe clearance method becomes ambiguous as an indicator of brain blood flow". No account of this is taken, however, in present day use of the technique. More important for a local clearance technique Sejrsen (1971) and Challoner (1973) have demonstrated, in skin, that inert gas may be lost from venous vessels as they pass through other tissues which have a lower partial pressure of the gas. In this way a considerable amount of ^{133}Xe is deposited in the fatty tissue below the skin, leading Challoner (1973) to claim that this method is therefore unsuitable for skin blood flow measurements.

The second factor of importance, because of the high diffusion coefficient of the inert gases, is that they will not only be able to diffuse rapidly from tissue to the capillary blood but will also be able to diffuse

from one tissue to another (Gillespie, 1967). This, of course, will occur where two tissues have different partial pressures of the gas and this may be due to the initial labelling of the tissue, different solubilities of the tissues or to different blood flows in them causing one tissue to clear more rapidly than another. Despite the fact that Gillespie (1967) illustrated the importance of this problem in the brain, again no account of it is taken in present day use of the technique, even though it was experimentally verified by Espagno and Lazorthes (1965) and Nilsson (1965). This effect will be greatest in thin tissues and this has been ably demonstrated by Strang^{et al} (1979) who found intertissue diffusion to be a major factor in measuring blood flow in the eye. Sejrsen (1967, 1971) likewise notes that intertissue diffusion takes place in the skin but does not include it in his final model, even though its relative importance increases considerably at low blood flows.

2.3 MEASUREMENT OF SKIN BLOOD FLOW USING XENON-133

In a series of papers from 1966 Sejrsen (1966, 1968, 1969, 1971) described the processes involved in the clearance of a local deposit of the radioactive inert gas, Xenon-133, from the skin. By then neglecting what he considered to be the least important processes he produced a mathematical function describing the clearance curve and using this he showed how a value for the dermal blood flow could be obtained. Later Challoner (1973) repeated some of the basic investigations and, in a much

less detailed fashion, produced support for Sejrsen's model. The accuracy of this technique, in measuring skin blood flow, has never been determined due solely to the lack of a direct method with which to compare it. Despite this it has subsequently been adopted in a large number of clinical and research investigations (Nyfors and Rothenborg, 1970; LeRoy et al, 1971; Fox et al, 1972; Greeson et al, 1973; Moore, 1973; Kostuick et al, 1976; Handel et al, 1976; Kristensen and Wadskov, 1977; Tsuchida and Tsuya, 1978; Prather et al, 1979; Daly and Henry, 1980). Doubts about the validity of Sejrsen's model have been raised only once before (Chimoskey, 1972) and therefore because of this almost complete acceptance of his model a detailed description is left to chapter 4 and only a brief summary given here.

Two ways of introducing the ^{133}Xe into the skin were presented (Sejrsen, 1971), one by a direct dermal injection and the other by diffusing it through the epidermis (known as the epicutaneous diffusion method). Clearance from the dermis was then said to occur almost entirely by the dermal blood flow. A proportion of the ^{133}Xe removed from the dermis then travelled to the lungs where it was lost to the air while the rest of it was transferred from the dermal venous blood to the subcutaneous fatty tissue. This was then removed in a similar way by the subcutaneous blood flow. Sejrsen presented evidence to show that both the dermis and subcutaneous tissue act like Kety's simple homogeneous tissue, as described in the previous section,

each of them producing a single exponential clearance rate. Because of the high solubility of ^{133}Xe in fatty tissue the rate of clearance from the subcutaneous tissue was considerably slower than from the dermis. The composite clearance curve, obtained by radiation detectors positioned over the skin, was therefore made up of two different exponentials, a fast one representing the ^{133}Xe removed by the dermal blood flow and a slow one due to the ^{133}Xe transferred to the fatty tissue and removed by the subcutaneous blood flow. Challoner (1973), using only the injection technique, suggested that the fatty tissue accumulation was considerable and that this reduced the sensitivity of the technique for measuring dermal blood flow. Sejrsen, however, felt that this was only true at very low values of blood flow.

Both Sejrsen and Challoner claimed that the process of injecting the skin increased the skin blood flow in a variable way. Therefore, although the injection technique was theoretically capable of measuring the dermal flow it was in fact reflecting a disturbed situation and not the resting blood flow. Sejrsen concluded that in order to obtain a true measure of the resting skin blood flow the epicutaneous diffusion technique must be used.

Chimoskey (1972) attempted to validate the technique by comparing it with venous-occlusion plethysmography (VOP), a procedure which can be used only on the limbs and which reflects skin blood flow only when used on the fingers. Unfortunately he chose to assess only the direct injection of ^{133}Xe and to ignore the epicutaneous diffusion

method. Since he obtained a direct relationship between the flow values measured by ^{133}Xe clearance and by VOP he concluded a) that the direct injection method is an accurate measure of skin blood flow b) that there was therefore no evidence for injection trauma and c) that since, according to Sejrsen, the epicutaneous method gave lower values of flow than the injection method then the former must label structures other than dermis to produce this low clearance rate. In his study, however, Chimoskey used the initial slope of the clearance curve to determine skin blood flow but failed to acknowledge that this would underestimate the fast exponential component representing the dermis (Kristensen and Wadskov, 1977). This would therefore tend to cancel out any overestimation of flow caused by injection trauma. He may, of course, have considered (although he did not mention it) that since the VOP essentially measured a mean value of the flow between dermis and subcutaneous tissue then the use of the initial slope of the clearance curve was therefore more appropriate. However, in an in-series system such as this the initial slope will be as greatly affected by the relative amplitude of the two components as by their clearance rates. As already indicated by Sejrsen (1971) the relative amplitude depends on the amount of ^{133}Xe transferred from the dermal venous blood to the subcutaneous tissue and so the initial slope is not necessarily well correlated with a mean blood flow.

Without exception the papers which have appeared

using Xenon-133 in skin blood flow measurements have referred to Sejrsen's original work. It is surprising, however, that very few of them have accepted his advice concerning the method of introduction of ^{133}Xe and the analysis of the clearance curve. Most have preferred to use the injection technique, calculating the blood flow from the initial slope of the curve, although they do not justify these modifications to Sejrsen's technique. Kristensen and Wadskov (1977) showed that the use of the initial slope failed to demonstrate the reduction in skin blood flow caused by application of corticosteroids and clearly evident from a more complete analysis of the clearance curve. By using the initial slope after injection, Greeson et al (1973) in a drug study, Nyfors and Rothenborg (1970) in psoriasis, and LeRoy et al (1971) in scleroderma leave doubts as to whether the changes in flow they reported were true changes or whether they were due to a difference in reactivity of the vessels or to a difference in the transfer processes occurring between the blood and subcutaneous tissue.

In some papers the technique has been accorded quite unrealistic capabilities. For example, Moore (1973), in assessing the level at which a leg may be amputated, presented a value, 0.60 ml/100g/min, for the skin blood flow below which the skin would not survive. In his study the three patients who had flows lower than this level all developed necrotic wounds, while all others, with higher flows, healed well. Since he used only the

initial 10 minutes of the clearance curve it can be calculated from his results that, in order to differentiate between the two groups of patients, an accuracy of better than 0.5% would have to be attributed to the technique. Clearly this is an impossible level to achieve in measurements of this kind and a more realistic assessment of the reproducibility, of 20%, was given by Challoner (1972). Kostuik et al (1976) assumed similar levels of accuracy to that of Moore but their clinical results reflected the inability to achieve this.

The most thorough use of Sejr'sen's technique has been made by Handel et al (1976), appropriately, for the present study, using the epicutaneous technique on skin flaps. They not only split the clearance curve into its component parts, but also used a computerised method of assessing the goodness of fit to the experimental curve. In this way they attempted to show in each situation that only two exponential components were present and where this was not true the data was rejected. However, as has been emphasised before (Riggs, 1963) the ability to provide a good fit to a clearance curve by using a number of components does not prove that these components exist. Handel et al did not investigate the effect of further components on the adequacy of fit of the curves. The importance of this will be discussed in chapter 6.

2.4 GENERAL MODELS OF HEAT TRANSFER IN BIOLOGICAL TISSUES

The many studies devoted to the modelling of heat

transfer in tissues of the human body can be classified into three categories.

(a) those dealing with the thermal behaviour of the body as a whole and concerned in particular with thermal regulation and comfort (Hardy et al, 1970).

(b) those dealing with the temperature profiles produced over relatively long distances and related mainly to studies of the limbs (Pennes, 1948; Mitchell et al, 1970).

(c) those dealing with heat transfer and temperature distributions in a localised region of the body, over distances of a few centimetres or even millimetres, and concerned primarily with the therapeutic aspects of heat and the use of heat in tissue blood flow studies (Perl, 1962; Klinger, 1974).

It is on this third category that the present review concentrates.

Any model of a physical or biological system must, of necessity, simplify it. The large number of models developed to describe heat transfer in a biological tissue differ mainly in the extent to which each of them introduce simplifying assumptions, in the complexity of the geometrical arrangement of tissues and in the boundary conditions which are required in each particular investigation. Most of the fundamentals of the physical processes are understood; the problem is often one of applying the knowledge to a particular practical situation.

The most basic model of heat transfer in a tissue is to assume that the tissue is homogeneous and isotropic and that heat is transferred within the tissue solely by the process of conduction. Fourier's equations can then be used to determine the temperature distribution at any time and solutions for almost every conceivable physical situation of this kind have been reported (Crank, 1975). Although this simple description forms the basis of all heat transfer models and is sometimes even the only process taken into account (Lin, 1972; Draper and Boag, 1971), it neglects one very important parameter. Pennes, in 1948, recognised the significant role played by the circulation in transporting heat within the body. In developing what has come to be known as the "bio-heat transfer equation" (Cravalho^{et al,} 1980) Pennes, and later Perl (1962), assumed the blood flow to act in the following way: the blood enters the tissue at arterial temperature, attains the local tissue temperature and is then immediately lost in the venous part of the circulation without further heat exchange taking place. The blood flow in each blood vessel can therefore be considered as a heat sink and represented by a simple Fick's equation (see Chapter 3). It was assumed in this description that complete thermal equilibration between the tissue and blood is attained during the passage of the blood through each of the small, heat exchanging blood vessels.

Perl (1962) further showed that, by considering

only the collective effect of the large number of small blood vessels, it was possible to obtain an expression which described the total heat transfer in tissue due to the total blood supply. This model of the blood supply, which has been adopted extensively in recent studies and has been shown to provide fairly good agreement with experimental results (Shitzer and Kleiner, 1976; Chan et al, 1973; Cravalho et al, 1980) has, however, some deficiencies. As has been mentioned already in section 2.2 this type of model is reasonable only if heat exchange occurs in the capillary region alone and if temperature distributions are being assessed over distances much greater than the capillary size. The fact that heat exchange occurs in vessels much larger than capillaries has been shown previously (Bazett et al, 1948; Betz et al, 1966). Only Klinger (1974) and, very recently, Chen and Holmes (1980), have attempted to introduce this large vessel exchange into models of local heat distribution. The difficulty in modelling such a phenomenon is that the circulatory architecture is both extremely complex and variable with the blood vessels varying greatly in size both spatially and temporally. Although there is complete heat equilibrium between the tissue and blood at the capillary level this exchange becomes less and less complete as the vessel size increases.

Klinger (1974) attempted to produce a general analysis of this situation by invoking a complicated model involving a vector field of convection of the

blood. Although this in theory may provide more complete solutions to the problem it appears in practice that only very simple physical situations can be investigated with it.

An alternative approach is that of Chen¹ & Holmes (1980) who has preferred to investigate each part of the problem by a separate model. He investigated the loss of heat along the length of a cylindrical blood vessel and has shown the relative importance of blood vessels of varying sizes, stressing once again that heat exchange occurs also at vessels larger than capillaries.

In addition to conduction and blood flow several other factors must always be taken into account when modelling heat transfer in vivo (Bowman et al, 1975). In particular metabolic heat production (Bazett, 1948; Guy et al, 1974), the variation in blood flow in response to thermal regulation (Yang and Wang, 1979; Chan et al, 1973) and various boundary conditions on the skin surface such as radiation and convection have been described in the literature. These will be considered more fully in later chapters.

2.5 HEAT TRANSFER MODELS IN HYPERTHERMIA

The extensive interest in the effects of increased temperatures on biological tissues and the application of hyperthermia in clinical practice has been accompanied by surprisingly few studies of the temperature distributions produced in vivo and the factors affecting these distributions. This is in spite of evidence that

they may differ greatly from those previously expected (Hume et al, 1979).

Of the few papers which have attempted to model the temperature distributions more emphasis has been placed on the patterns produced by particular physical techniques than on the fundamental factors of heat transfer which may affect even an ideal heating modality (Chan et al, 1973; Guy et al, 1974; Yang and Wang, 1979; Hand et al, 1979).

Chan et al (1973) described a model based on the finite difference technique, which showed the temperature patterns obtained with both ultrasound and microwave heating. The model consisted of tissue layers, representing a pig thigh, and a cooling function described the collective effect of the capillary blood supply. Although variations in this function, reflecting variations in blood flow, were demonstrated the effect of each of the individual physical processes was lost in the complexity of the diagrams. A comparison with experimental results in a human thigh showed fairly good agreement indicating that such a model undoubtedly forms the basis for such investigations. No account, however, was taken of the effect of large blood vessels.

Yang and Wang (1979) presented a similar model of tissue layers heated by shortwave and microwave diathermy. They attempted to show the location of the maximum and minimum temperatures within the tissue layers but although the effect of blood flow was included

as part of the model it was not discussed in the results. The effect of changing the thickness of the tissue layers and hence showing the importance of conduction was similarly omitted. Therefore, although this paper is again of use in assessing a particular heating modality it did not treat the fundamental processes which may alter the heating patterns produced by these techniques.

Cravalho et al (1980) used a different approach and tried to calculate the heating pattern which would be required to produce a uniform temperature distribution within a circular tumour which had concentric shells of differing characteristics. Both the thickness of these shells and the blood flow, represented again by a single Fick's equation, within them was varied. In particular it was assumed that as a tumour grew it developed a larger area in the central core which had little or no blood flow. The paper showed that to produce uniform heating in such a solid tumour the heating pattern would have to be moulded to suit each particular tumour. A serious omission, however, was a consideration of the change in temperature profile with time caused by conduction of the heat. No indication of the time at which the profiles were obtained was given and therefore again they failed to demonstrate the relative importance of conduction and blood flow.

The first paper introducing the possible role of large blood vessels in hyperthermia has only recently been published (Chen and Holmes, 1980). By assuming a

blood vessel to be a simple long cylinder the authors show the relative heat exchange which occurs through the walls of blood vessels of various sizes. They show that even fairly large arterioles and venules will be involved in such exchange. However, although Hume et al (1979) have shown experimentally that there are localised reduced temperatures around large blood vessels this feature is not considered in Chen and Holmes' paper.

CHAPTER 3MATHEMATICAL MODELS OF HEAT AND MATTER TRANSFER

3.1 INTRODUCTION

3.2 GENERAL THEORY

3.3 THERMAL CONDUCTION AND DIFFUSION

3.3.1 Boundary conditions

3.3.2 Analytical solutions of conduction and
diffusion equations

3.4 TRANSPORT BY BLOOD FLOW

3.4.1 The capillary model

3.4.2 Large vessel exchange

3.5 NUMERICAL SOLUTION OF THE HEAT AND MATTER
TRANSFER EQUATIONS

3.5.1 The finite difference approximations

3.5.2 Finite difference approximation of the heat
and matter transfer equations

3.5.3 Choice of distance and time steps

3.5.4 Finite difference form of the boundary
conditions for conduction and diffusion

3.5.5 Calculation of points near the boundary

3.5.6 Evaluation of the accuracy of finite
difference solutions

3.1 INTRODUCTION

The complexity of living biological tissue presents a challenge to any attempt to model its behaviour. Clearly the only true model of tissue is tissue itself. In developing the mathematical models of heat and matter transfer in this chapter simplifying assumptions, as to the composition and properties of tissue and the geometrical arrangement of different tissues, are necessary. Such simplifications do, of course, restrict the scope of the model but it is clear that while a complex model will produce more accurate results, in contrast a simple model is more likely to allow practical solutions to be obtained. The general mathematical formulation of heat and matter transfer is outlined in section 3.2 together with some of the simplifying assumptions required to develop the model further. The theory is based on the laws of conservation of energy and mass and involves transport both by blood flow and the conduction/diffusion process. Each of these is then treated separately and in more detail in sections 3.3 and 3.4 and simple analytical solutions discussed. In section 3.4 blood flow is considered at two levels - one in which it is considered as a diffuse process describable by Fick's principle and the other on a larger scale where the effects of single blood vessels are evaluated. However only some of the characteristics of blood flow and the conduction/diffusion process can be examined separately and by analytical means and section 3.5 introduces a

flexible numerical computer technique, which allows more complex situations to be investigated. This finite difference technique is described fully in this section and a comparison with known analytical solutions, to assess the accuracy of the numerical technique, is outlined.

3.2 GENERAL THEORY

Consider a representative volume of a single tissue as shown in Figure 3.1. To satisfy the laws of conservation of energy or mass within this volume the following equation can be formulated.

$$\begin{aligned}
 & \left[\begin{array}{l} \text{increase in} \\ \text{heat energy} \\ \text{(or mass)} \\ \text{within the} \\ \text{tissue} \\ \text{volume} \end{array} \right] = \left[\begin{array}{l} \text{net amount of} \\ \text{heat energy} \\ \text{(or mass)} \\ \text{entering the} \\ \text{volume across} \\ \text{its surface} \\ \text{due to con-} \\ \text{duction (or} \\ \text{diffusion)} \end{array} \right] + \left[\begin{array}{l} \text{heat energy (or mass)} \\ \text{generated in the} \\ \text{tissue volume by} \\ \text{metabolism} \end{array} \right] \\
 & + \left[\begin{array}{l} \text{heat energy (or mass)} \\ \text{deposited in the} \\ \text{tissue by other} \\ \text{physical processes} \end{array} \right] + \left[\begin{array}{l} \text{net amount of heat energy} \\ \text{(or mass) entering the} \\ \text{volume across its surface} \\ \text{via the blood flow} \end{array} \right]
 \end{aligned}$$

The term on the left hand side of the equation represents the rate at which energy (or mass) accumulates within the volume as a result of the physical processes on the right hand side. This manifests itself in the case of heat as an increase in temperature within the volume and in the

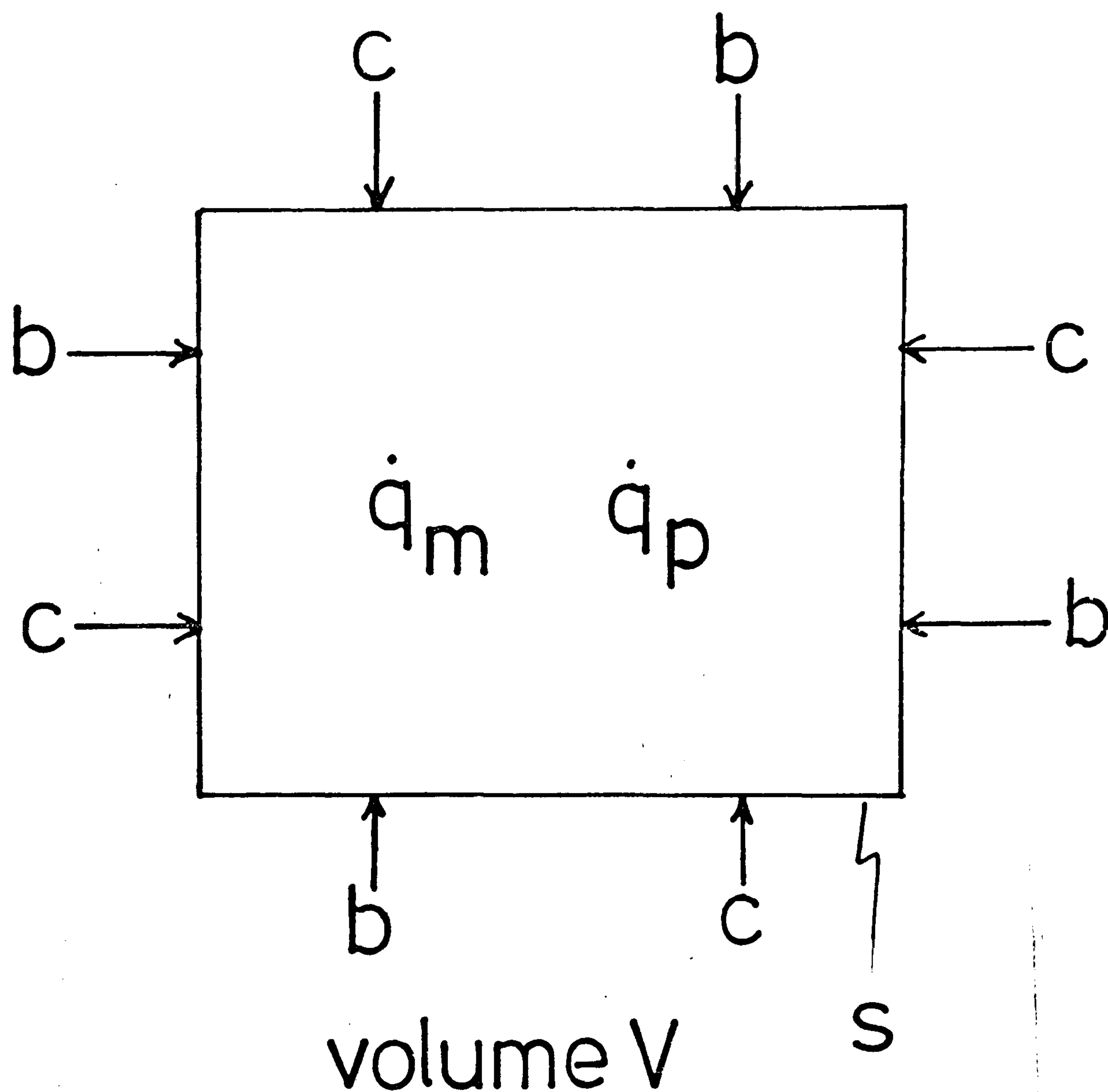


Figure 3.1 Heat and matter transfer processes in a representative volume of a tissue
 c - conduction or diffusion process
 b - transport by blood flow
 \dot{q}_m - metabolism
 \dot{q}_p - other physical processes as discussed in text.

case of matter as an increase in concentration; or more correctly, in the case of an inert gas, as an increase in the partial pressure of the gas. The first term on the right hand side represents the net rate at which heat energy or mass is entering the volume through the whole of its surface due to conduction or diffusion and can be obtained from Fourier's law (equation 1.1) or Fick's law (equation 1.2) as (Luikov, 1968)

$$-\int_S k \frac{\partial T}{\partial n} \bar{n}_0 \, dS \quad \text{for heat and}$$

$$-\int_S s_T D \frac{\partial P}{\partial n} \bar{n}_0 \, dS \quad \text{for an inert gas}$$

where the integration is performed over the surface S and k is the thermal conductivity of the tissue

T is the temperature at the surface

s_T is the solubility of the inert gas in the tissue

D is the diffusion coefficient of the inert gas in the tissue

P is the partial pressure of the inert gas at the surface

\bar{n}_0 is the unit vector normal to the surface in the direction of decreasing temperature or partial pressure

$\frac{\partial T}{\partial n}$ and $\frac{\partial P}{\partial n}$ are the temperature derivative and partial pressure derivative, respectively, along the normal to the surface.

The second and third terms in the equation represent

a direct input to the volume. These are due to metabolism, which can be omitted in the inert gas case, or some other physical process such as ultrasound or microwave heating in the heat equation and direct injection in the case of the inert gas equation. It may also include loss of heat energy by radiation or convection. These terms will be discussed in more detail in the specific models described in later chapters.

Transport of heat or inert gas by the blood flow is included in the fourth term. For heat, the total energy deposited in the volume is equal to the heat energy brought to the volume minus the heat taken away from it. This can be summed up most easily as

$$\int_s \rho_b c_b T_b \dot{f} dS \quad \text{for heat}$$

where ρ_b is the density of blood

c_b is the specific heat of blood

T_b is the temperature of the blood crossing
the surface

and \dot{f} is the blood flow rate at each point of the
surface.

Again the integral is taken over the whole surface and \dot{f} is positive when flow is into the volume and negative when out of the volume. When the tissue temperature equals the arterial blood temperature the above expression will, of course, be zero. A similar expression is used

for transport of an inert gas

$$\int_S s_b P_b \dot{f} dS$$

where S_b is the solubility of the inert gas in blood and P_b is the partial pressure of the inert gas in blood.

Taking volume integrals of the other terms the two general equations can be summarised as follows

$$\frac{d}{dt} \int_V \rho c T dV = - \int_S k \frac{\partial T}{\partial n} \bar{n}_0 dS + \int_V \dot{Q}_m dV + \int_V \dot{Q}_p dV + \int_S \rho_b c_b T_b \dot{f} dS \quad (3.1)$$

for heat and

$$\frac{d}{dt} \int_V s_T P dV = - \int_S s_T D \frac{\partial P}{\partial n} \bar{n}_0 dS + \int_V \dot{Q}'_p dV + \int_S s_b P_b \dot{f} dS \quad (3.2)$$

for an inert gas

where \dot{Q}_m , \dot{Q}_p and \dot{Q}'_p are input rates as discussed above.

These equations give a general formulation of the rate of change of temperature and partial pressure, respectively, within the representative volume of tissue. These will be expanded in the following sections but before doing so it is worth considering the simplifications which can be included in the analysis by examining the size of the volumes involved. For example, in the investigation of temperature distributions in hyperthermia, tissues of the order of 10 cm in length are involved. In much the same way that the individual effects of atoms can be ignored, it is therefore possible

to consider only the collective effects of other structures whose dimensions are small compared to the tissues involved - viz. cells and blood vessels. In this respect, then, the tissue can be considered homogeneous and only a bulk term used to describe any particular characteristic. A bulk value of the thermal conductivity and diffusion coefficient of ^{133}Xe in each tissue is therefore adopted. In addition for some of the investigations it will be shown that the blood supply can be treated in this way, and the effects of individual blood vessels ignored. Of course in other cases, where effects over smaller distances are being examined this is not the case and individual blood vessels assume greater importance.

It is also assumed that the tissue is isotropic, except in one case with respect to blood flow as will be detailed later, although anisotropy even over a large scale has been reported with respect to thermal conductivity of a tissue (Bowman et al, 1975).

3.3 THERMAL CONDUCTION AND DIFFUSION

By ignoring the effects of blood flow the transport of heat or matter through a tissue reduces, of course, to a problem of conduction or diffusion. The basis of the solution is then given by the first terms in equations 3.1 and 3.2 as,

$$\frac{\partial}{\partial t} \int_V \rho c T dV = - \int_S k \frac{\partial T}{\partial n} \bar{n}_o dS \quad \text{for heat}$$

and similarly for an inert gas. These equations can then be simplified (Luikov, 1968) to give

$$\frac{\partial T}{\partial t} = a \nabla^2 T \quad (3.3)$$

for heat

and
$$\frac{\partial P}{\partial t} = D \nabla^2 P \quad (3.4)$$

for an inert gas

where $\nabla^2 = \left(\frac{\partial^2}{\partial x^2} + \frac{\partial^2}{\partial y^2} + \frac{\partial^2}{\partial z^2} \right)$ in Cartesian co-ordinates

and a is the thermal diffusivity given by $\frac{k}{\rho c}$

These equations are known as the partial differential heat conduction or diffusion equations (3.4 is known as Fick's second law) and their solution allows the variation in temperature or partial pressure throughout the tissue at any time to be obtained.

3.3.1 Boundary conditions

Where more than one tissue is present, with different conduction or diffusion properties, then although equations 3.3 and 3.4 will hold within each of the media further conditions are necessary at the boundary between them. There are two of these boundary conditions.

(a) In order to satisfy the conservation laws at the boundary the flux on one side must equal the flux on the other side. This is expressed as

$$k_1 \left. \frac{\partial T_1}{\partial n} \right|_B = k_2 \left. \frac{\partial T_2}{\partial n} \right|_B \quad \text{for heat}$$

$$\frac{D_1}{s_1} \left. \frac{\partial P_1}{\partial n} \right|_B = \frac{D_2}{s_2} \left. \frac{\partial P_2}{\partial n} \right|_B \quad \text{for an inert gas}$$

where the subscripts 1 and 2 refer to the two tissues
 n is the direction normal to the boundary
 and each expression is assessed at the boundary B.

(b) Both temperature and partial pressure must be continuous functions and therefore

$$T_1)_B = T_2)_B \quad \text{for heat}$$

$$P_1)_B = P_2)_B \quad \text{for an inert gas}$$

where the expressions are again evaluated at the boundary.

3.3.2 Analytical solutions to conduction and diffusion equations

Exact analytical solutions to equations 3.3 and 3.4 for an enormous number of albeit fairly simple geometrical arrangements, obtained using a variety of mathematical techniques, have been reported (Crank, 1975; Jost, 1960; Carslaw and Jaeger, 1959; Luikov, 1968). No attempt has been made in the present study to develop a new analytical solution to any of the problems to be investigated since it would appear from the massive literature that if no solution has been previously reported then the problem is too complex to obtain such a solution. Where necessary in the present study analytical solutions are simply quoted and the appropriate reference should be consulted for details of its derivation.

3.4 TRANSPORT BY BLOOD FLOW

The terms in equations 3.1 and 3.2 describing transport by blood flow are essentially a restatement of a

principle first attributed to Fick in 1870. Traditionally this principle has come to be regarded in the following way (Kety, 1951; Perl, 1962); heat or matter transported by the blood enters a tissue within the arterial blood vessels. Branching of these vessels occurs several times until small capillary vessels are reached after which rejoining occurs and the venous side of the vascular network is formed. The structure and function of this vascular tree is assumed to be such that perfect exchange occurs between the tissue and the blood in the capillaries, and within all other vessels the blood has no interaction whatsoever with the tissue. In addition the length of these capillaries is assumed to be small compared to the dimensions of the representative tissue volume. This representation of transport via the blood will be termed the capillary model and a detailed examination of it follows in section 3.4.1.

Both Fick's original principle and the reality of the situation are, however, more subtle than this. A more general description is obtained by reference to Figure 3.2. Within the tissue volume several different parts of the blood vessel architecture are present, the most numerous clearly being where the blood enters in an artery, passes through a capillary bed and leaves in the venous system. However, there are also arterial and venous vessels of various sizes which do not terminate in a capillary bed within the tissue volume. If passive exchange is possible between these vessels and

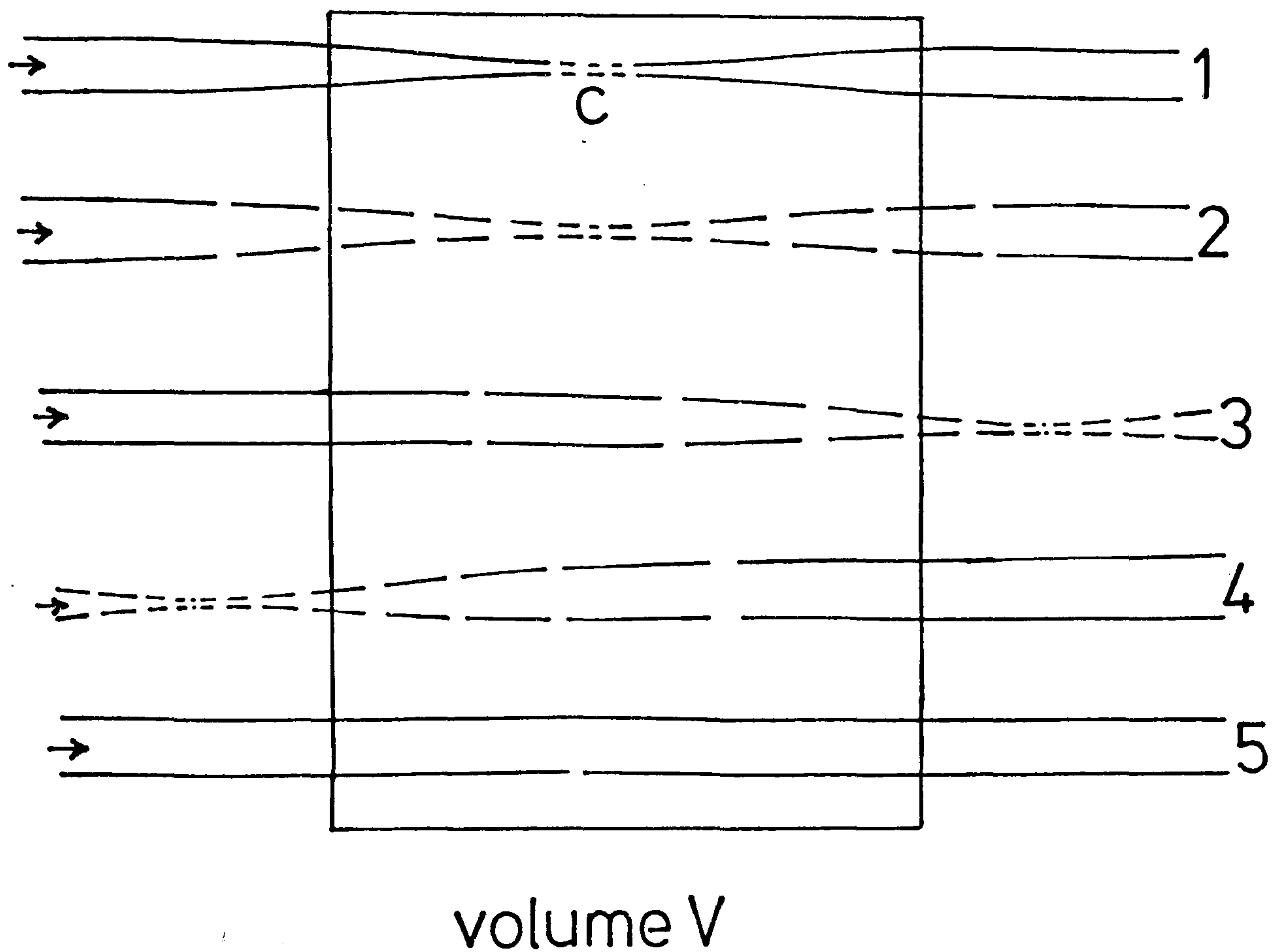


Figure 3.2 Schematic representation of blood vessels in a tissue volume. The ability to exchange heat or matter is depicted by the number of gaps in the vessel walls. 1 - ideal blood vessel with exchange confined to capillary, c , which is small compared to tissue dimension. 2 - more realistic picture with gradual change in exchange properties. 3,4 - exchange occurs within tissue volume but capillary lies outside it. 5 - only limited exchange occurs in vessels much larger than capillaries.

the tissue then they will be capable of depositing or picking up heat or matter as they pass through the tissue. A more realistic, gradual change in the passive exchange properties of vessels larger than capillaries (see chapter 2), compared with the abrupt change postulated in the capillary model, means that there will be circumstances where the effect of large vessels will be of some importance. The description of the exchange of heat and matter between large blood vessels and tissue is examined in section 3.4.2.

3.4.1 The capillary model

Making the assumptions mentioned above, and deriving the equation for an inert gas first, the change in the amount of an inert gas in a tissue with time is proportional to the amount flowing in to the tissue in the arterial blood minus the amount flowing out in the venous blood, or,

$$\frac{dQ_i}{dt} = F_a C_a - F_v C_v$$

where Q_i is the amount in the tissue

F_a and F_v are the arterial and venous blood flows, respectively

and C_a and C_v are the concentrations in the arterial and venous blood, respectively,

which, if the arterial and venous blood flows are equal, gives

$$\frac{dQ_i}{dt} = F_i (C_a - C_v)$$

F_i is the tissue blood flow.

Now if the amount of the inert gas which recirculates to the area under investigation is negligible, which is true in the present study due to the removal of ^{133}Xe in the lungs, and if there is no other input in the arterial blood, then

$$C_a = 0 \quad \text{and}$$

$$\frac{dQ_i}{dt} = -F_i C_v$$

Because there is complete diffusion equilibrium between blood and tissue at the capillaries and no further exchange takes place within the venous vessels, the concentration in the venous blood draining the tissue, C_v , is proportional to the concentration in the tissue itself,

$$\text{i.e. } C_v = \frac{C_i}{\lambda_i}$$

where λ_i is a constant, for a particular tissue, known as the partition coefficient and is the ratio of the solubility of the inert gas in tissue to the solubility in blood when these are in complete equilibrium.

Thus

$$\frac{dQ_i}{dt} = -\frac{F_i C_i}{\lambda_i}$$

which since $C_i = \frac{Q_i}{V_i}$, where V_i is the tissue volume, gives

$$\frac{dQ_i}{dt} = -\frac{F_i}{\lambda_i V_i} Q_i \quad (3.5)$$

Equation 3.5 shows that the rate of change of the amount of an inert gas in a tissue is proportional to the amount in the tissue at that time, the constant of proportionality being dependent on the tissue blood flow. Of course it should be noted that in the present study the amount detected by the radiation detectors equals the amount in the tissue plus the amount in the blood within the tissue. Although the volume of blood in skin is negligibly small (Mapleson, 1963), and therefore equation 3.5 can be used to describe the detected signal, this is not always so.

Equation 3.5 is the differential form of an exponential function

$$Q_i(t) = Q_0 \exp \left(- \frac{F_i}{\lambda_i V_i} \cdot t \right)$$

where Q_0 is the amount in the tissue at time $t = 0$.

A similar expression can be used to describe the partial pressure of the gas

$$P_i(t) = P_0 \exp \left(- \frac{F_i}{\lambda_i V_i} \cdot t \right) \quad (3.6)$$

This means that if a single homogeneous tissue with a blood flow, F_i , has a partial pressure, P_0 , of an inert gas at time zero then, assuming that the inert gas is removed from the tissue only by the capillary blood flow, the clearance is characterised by a single exponential function. The rate constant, k_i , of this exponential function is related to the tissue blood flow by

$$k_i = \frac{F_i}{\lambda_i V_i}$$

It is the usual practice to express tissue blood flow, f_i , in ml of blood per 100g of tissue per minute.

Thus

$$f_i = \frac{F_i}{\rho_i V_i} \times 100$$

where ρ_i is the density of the tissue g ml^{-1}

and from above this gives

$$f_i = \frac{100 \times k_i \times \lambda_i}{\rho_i}$$

If the partition coefficient, λ_i^0 , is then expressed in terms of the amount of ^{133}Xe per g of tissue relative to the amount of ^{133}Xe per ml of blood (see section 5.4) then

$$f_i = 100 \times k_i \times \lambda_i^0 \quad (3.7)$$

In other words, if the partition coefficient is known, the blood flow within a tissue can be determined from the exponential rate constant of the clearance of ^{133}Xe from the tissue.

The corresponding equation for the change in temperature of a tissue with time due to the capillary blood flow is given by

$$(T_i(t) - T_b) = (T_0 - T_b) \exp\left(-\frac{F_i}{\lambda'_i \rho'_i V_i} \cdot t\right) \quad (3.8)$$

where T_b is the arterial blood temperature = 37°C

and in this case λ'_i is the ratio of specific heats of tissue: blood

ρ'_i is the ratio of densities of tissue: blood.

Equation 3.8 describes the change in "excess temperature" of the tissue with time if the tissue has been raised to a temperature T_0 at time zero.

3.4.2 Large vessel exchange

The basis of the problem here is to calculate the heat or matter transfer which occurs when blood in a single blood vessel enters a volume of tissue which is at a different temperature or has a different partial pressure of a gas. This type of problem was originally tackled, for heat, by Graetz in 1885 and the solution rediscovered by Nusselt in 1910 (Jakob, 1959). It has since been used by Teorrel and Nilsson (1978) to evaluate the influence of large veins on temperatures at the skin surface in thermography.

Fluid of specific heat c_b and thermal conductivity k_b enters a pipe, of length L , at a temperature T_{in} and leaves at a temperature T_{out} . The flow in the pipe is assumed laminar so that the velocity distribution is parabolic, with zero velocity at the wall and maximum at the centre. The thermal conductivity is assumed uniform and heat is transferred by conduction in the radial direction only. As in most analytical solutions a fairly simple boundary condition must be used and Graetz assumed that the temperature at the inner surface of the pipe wall, T_s , was uniform and constant. With these assumptions Graetz obtained the following solution

$$\frac{T_{\text{out}} - T_{\text{in}}}{T_s - T_{\text{in}}} = 1 - 8 \phi(n) \quad (3.9)$$

in which $\phi(n)$ represents the convergent infinite series (Drew, 1931; Teorrel and Nilsson, 1978).

$$\begin{aligned} \phi(n) = & 0.10238 \exp(-14.6272 n) + 0.01220 \exp(-89.22 n) \\ & + 0.00237 \exp(-212 n) + \dots \end{aligned}$$

and n is given by

$$n = \frac{k_b L}{4r^2 \bar{v} \rho_b c_b}$$

where \bar{v} is the mean flow velocity

r is the radius of the pipe

k_b is the thermal conductivity of blood

Substituting the appropriate values of L , \bar{v} and r , equation 3.9 can therefore be used to predict the axial variation in temperature for pipes of different sizes and different velocities of flow. A plot of this, with $\frac{L}{\bar{v} r^2}$ as one axis is given in Figure 3.3, for a value of $k = 0.49 \text{ Wm}^{-1} \text{ } ^\circ\text{C}^{-1}$.

Teorrel and Nilsson (1978) discussed the validity of the assumptions used in obtaining equation 3.9 and concluded that by far the most important was that of uniform wall temperature. Since this clearly does not hold in a biological system they estimated the effect of this using an experimental model. Instead of plotting the data using T_s they used the value of the tissue temperature some distance from the pipe, a value which is more likely to be known in practice. They showed that,

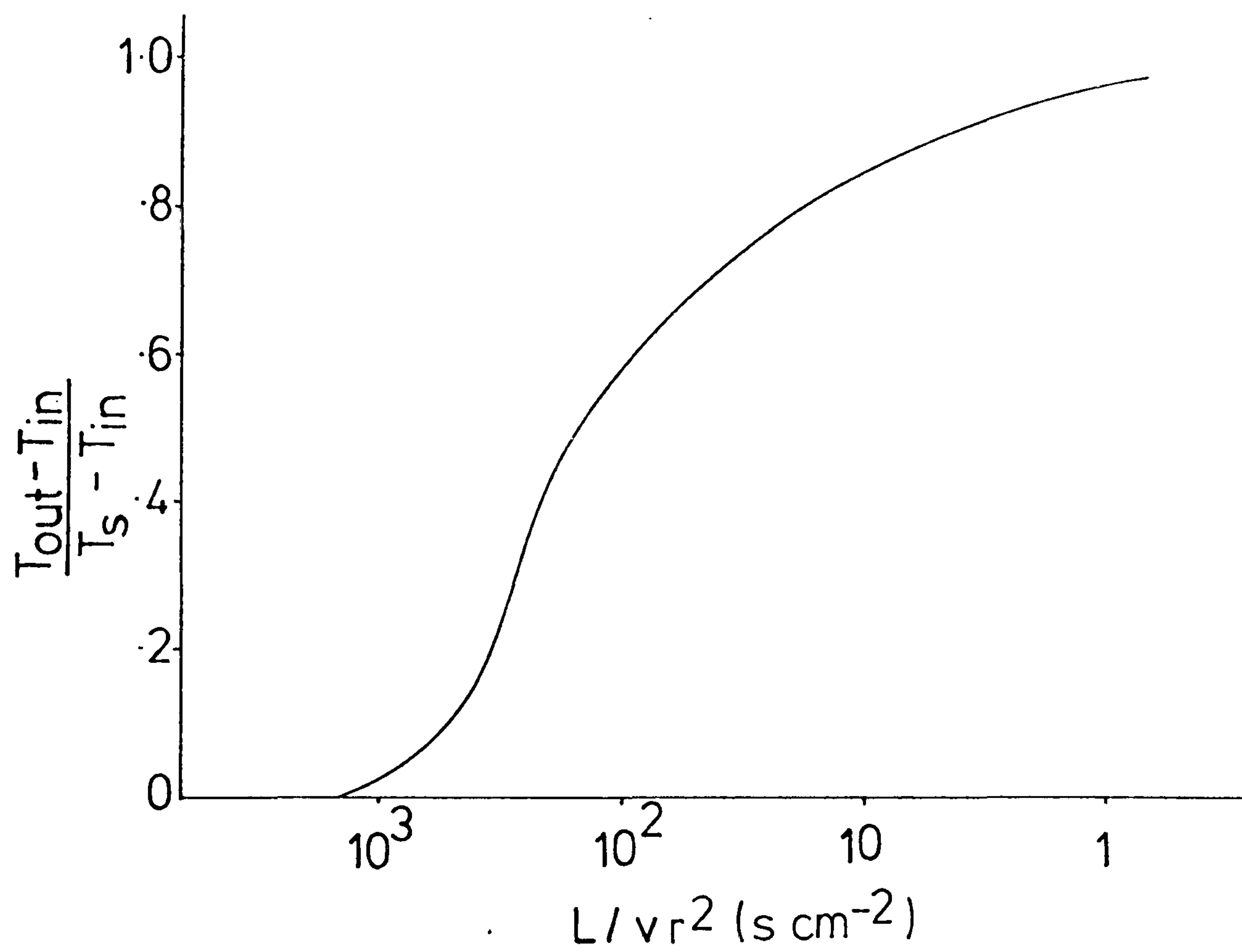


Figure 3.3 Graphical representation of Graetz equation. The ratio of temperature differences is plotted as a function of $\frac{L}{v r^2}$, where L is the length of the vessel, \bar{v} the flow velocity and r the vessel radius.

while the experimental data did not coincide exactly with Graetz's theory, the signoid form of the graph was the same. In other words they found that their experimental data could be expressed in the same way as equation 3.9 but with a correction factor, i.e.

$$\frac{T_{\text{out}} - T_{\text{in}}}{T_{\text{tissue}} - T_{\text{in}}} = 1 - 8 \phi(n) \quad (3.10)$$

where T_{tissue} is now the temperature in the tissue away from the vessel

and n is now given by

$$n = \frac{\beta k L}{4r^2 \bar{v} \rho_b c_b}$$

where β is a correction factor which allows for the use of T_{tissue} rather than T_s .

From Teorrel and Nilsson's data, allowing for differences in thermal conductivity, it is estimated that

$$\beta = 0.05$$

The corresponding equation for inert gas diffusion will be of a similar form,

$$\text{i.e. } \frac{P_{\text{out}} - P_{\text{in}}}{P_{\text{tissue}} - P_{\text{in}}} = 1 - 8 \phi(n) \quad (3.11)$$

$$\text{where } n = \frac{\beta D L}{4r^2 \bar{v}}$$

D is the diffusion coefficient of the inert gas.

Equations 3.10 and 3.11 are clearly approximate solutions to a very complex problem. They were derived assuming conduction in the radial direction only and are therefore strictly applicable only when axial conduction

or diffusion can be neglected, i.e. where the length of a vessel is large compared to its radius, and where the gradient in the tissue in the direction of the vessel is small. In addition the use of the temperature or partial pressure value at some distance from the vessel assumes that the tissue has similar characteristics to the blood. In one case in particular this is not true and the significance of this will be discussed (section 6.2). However equations 3.10 and 3.11 have been used to provide an estimate of the relative importance of the blood vessels in exchanging heat or matter with a tissue. Numerical evaluation is carried out in chapters 6 and 8.

The above solutions give only the axial temperature or partial pressure distributions but it is possible to obtain the radial distributions by remembering that these are, in fact, steady state solutions. In other words a situation has been achieved where, at any section of the pipe, there is a cylindrical source or sink whose surface temperature or partial pressure is constant with time. By making use of the finite difference numerical method, to be described in the next section, the radial distribution can be obtained for such a situation. The particular models used are described in later chapters.

For a specific situation, where the temperature or partial pressure is also held constant at a radius R_0 from the blood vessel, and where no other processes, e.g. heat generation, involved then analytical solutions have been described (Luikov, 1968 p.153). The radial

distribution is then given by

$$T(R) = \frac{T_b \ln\left(\frac{R_0}{R}\right) + T_{\text{tissue}} \ln\left(\frac{R}{r}\right)}{\ln\left(\frac{R_0}{r}\right)} \quad (3.12)$$

$$\text{or } P(R) = \frac{P_b \ln\left(\frac{R_0}{R}\right) + P_{\text{tissue}} \ln\left(\frac{R}{r}\right)}{\ln\left(\frac{R_0}{r}\right)} \quad (3.13)$$

where r is the radius of the blood vessel

T_b and P_b are the temperature and partial pressure of the blood

and T_{tissue} and P_{tissue} are the constant values at a distance R_0

3.5 NUMERICAL SOLUTION OF THE HEAT AND MATTER TRANSFER EQUATIONS

Where possible analytical solutions to the diffusion/conduction processes and to the equations representing blood flow have been used. However in most situations, particularly where the boundary conditions are other than very simple, it is not possible to obtain an exact solution to a differential equation by analytical methods. It is therefore necessary to resort to an approximate numerical method to provide a solution and in the present study a finite difference method has been adopted (Luikov, 1968). This method is based on the replacement of the derivatives of a continuous function by their approximate values at discrete points in time and space known as nodal points.

3.5.1 The finite difference approximations

Consider a continuous function $y = f(x)$ as plotted in Figure 3.4 and which in the present study may be related to either the one dimensional temperature distribution or partial pressure distribution in a tissue. An approximate value of the first derivative $\frac{dy}{dx}$ at the point M, whose co-ordinates are x_i and y_i , is given by

$$\frac{dy}{dx} = \frac{Y_{i+1} - Y_i}{h}$$

In other words the derivative has been replaced by the gradient of the chord through the point M and another adjacent point P whose co-ordinates are (x_{i+1}, Y_{i+1}) . The distance between the two points, known as the distance step, h is equal to $x_{i+1} - x_i$. Clearly the smaller the value of h the more closely will the finite difference expression relate to the exact derivative. The above expression is known as the forward difference operator and alternative expressions representing the backward, central or average difference may also be used (Croft and Lilley, 1977).

In a similar way the second derivative can be obtained by subtracting the finite difference approximations of the derivative on each side of point M and is given by

$$\frac{d^2y}{dx^2} = \frac{Y_{i+1} - 2Y_i + Y_{i-1}}{h^2}$$

Both temperature and partial pressure are, of course, functions of both time and space and an approximation of

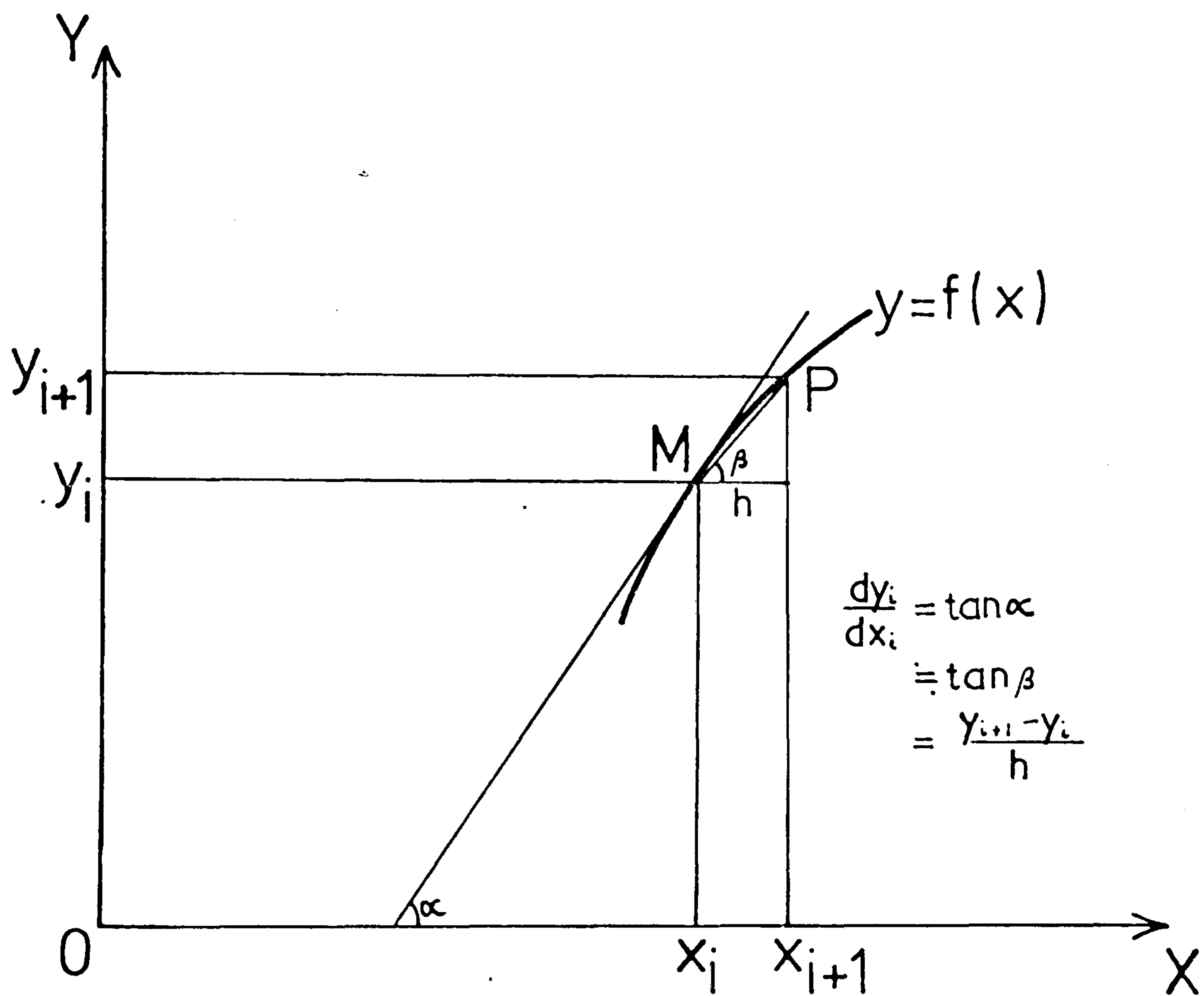


Figure 3.4 Determination of the finite difference relationship.

the time derivative is given by

$$\frac{dy}{dt} = \frac{Y_{k+1} - Y_k}{1}$$

where k now relates to the time axis and 1 is the time step.

The function can thus be represented by a rectangular network of nodal points with the time axis being the ordinate and the spacial dimension the abscissa (Figure 3.5), the axes being divided into equal steps of 1 units and h units respectively. Substituting the above expressions, for the appropriate derivatives in a partial differential equation, then allows the value of the function at a time $t + 1$ to be obtained. For the particular finite difference formulae used here, the value at a point x and time $t + 1$ is completely defined by the values at points $x - h$, x and $x + h$ at a time t . This is known as an explicit method (Cross and Lilley, 1977). An alternative scheme, known as an implicit method, involves defining the second derivative in terms of the values at the time $t + 1$. The result of this is that the value of the function at time $t + 1$ must be obtained from the solution of three simultaneous equations and therefore the computational procedure is much more complicated. Explicit methods are normally associated with speed and simplicity while implicit methods are associated with accuracy and stability (see section 3.5.3). In the present study the accuracy of the explicit method has been found to be acceptable (see section 3.5.6) and has been adopted here.

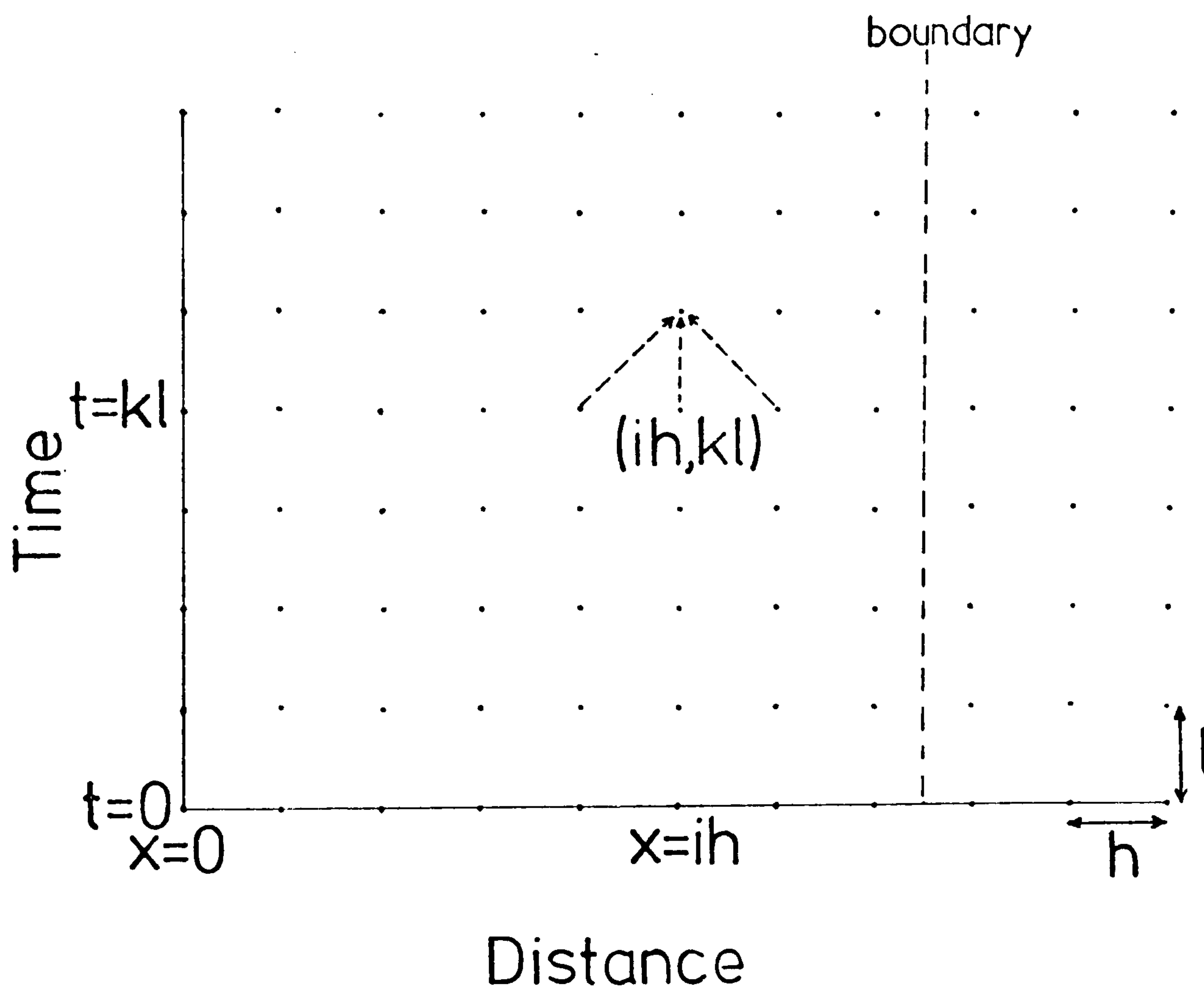


Figure 3.5 The finite difference network of nodal points. Each nodal point occurs at a value of $x = ih$ and $t = kl$ where h is the distance step and l the time step. A boundary is shown lying between the nodal points.

3.5.2 Finite difference approximation of the heat and matter transfer equations

Each process involved in the transfer of heat or matter in a tissue can now be described in terms of a finite difference approximation. First of all, the partial differential equations 3.3 and 3.4, representing diffusion and conduction, can be written as (using the diffusion coefficient D)

$$\frac{Y_{i,k+1} - Y_{i,k}}{\Delta t} = D \left(\frac{Y_{i+1,k} - 2Y_{i,k} + Y_{i-1,k}}{h^2} \right)$$

which on rearranging gives

$$Y_{i,k+1} = \left(1 - \frac{2\Delta t D}{h^2} \right) Y_{i,k} + \frac{\Delta t D}{h^2} (Y_{i+1,k} + Y_{i-1,k}) \quad (3.14)$$

Thus the values of temperature and partial pressure at a specific time, due to conduction or diffusion, can be obtained from the values at a preceding time step and therefore by successive application of equation 3.14 the full distribution at any time can be calculated.

The effects of other terms in the heat and matter transfer equations are also to be included in the finite difference computation. In all cases, however, it is sufficient to make a constant correction for these effects at each time step. For example a particular heating modality can be allowed for by increasing the temperature at each point by a constant amount each time interval, the value of this constant varying throughout the tissue according to the particular characteristics of the heating modality. Similarly it will be seen that blood flow

can be allowed for by decreasing the temperature by a constant fraction each time step. These terms will be described more fully in each particular model.

3.5.3 Choice of distance and time steps

It is a peculiarity of the explicit method that in order to produce a solution to the equations the value of R which is given by

$$R = 1D/h^2 \quad (3.15)$$

must be less than one-half. This is known as the stability condition (Luikov, 1968). The choice of distance and time steps is therefore limited by this and also by the practical limit of the time taken to compute a solution, which increases greatly as the time step or distance step is reduced. The smaller the distance step used, the more closely the finite difference solution will relate to the exact value and therefore for a particular value of h the maximum allowable time step can be obtained from (3.15).

3.5.4 Finite difference form of the boundary conditions for conduction and diffusion

As detailed in section 3.3.1, where two or more tissues are involved two conditions must be satisfied at the interface between them. These conditions are

$$P_1 = P_2 \quad \text{and} \quad \frac{D_1}{S_1} \frac{\partial P_1}{\partial x_1} = \frac{D_2}{S_2} \frac{\partial P_2}{\partial x_2} \quad \text{for diffusion}$$

$$T_1 = T_2 \quad \text{and} \quad k_1 \frac{\partial T_1}{\partial x_1} = k_2 \frac{\partial T_2}{\partial x_2} \quad \text{for conduction}$$

where all the expressions are evaluated at the boundary point.

For diffusion, substituting the finite difference relation for the partial derivative gives

$$\frac{D_1 P_{i,k}}{h} - \frac{D_1 P_{i-1,k}}{h} = \frac{D_2 \lambda P_{i+1,k}}{l} - \frac{D_2 \lambda P_{i,k}}{l}$$

The $P_{i,k}$ on the left side of this equation is the value on one side of the boundary while the $P_{i,k}$ on the right side of the equation is the value at the other side of the boundary. The first boundary condition, however, requires that these are equal, and so further rearrangement leads to

$$P_{i,k} = \frac{D_2 \lambda P_{i+1,k} h + D_1 P_{i-1,k} l}{D_1 l + D_2 h \lambda} \quad (3.16)$$

For thermal conduction the corresponding expression is

$$T_{i,k} = \frac{k_2 T_{i+1,k} h + k_1 T_{i-1,k} l}{D_1 l + D_2 h}$$

Note that the values at the boundary are therefore evaluated after all the other points within the tissue at a time t .

3.5.5 Calculation of points near the boundary

An improvement in the accuracy of the boundary values is obtained by assuring that the boundary lies, not at one of the nodal points, but between two nodal points as shown in Figure 3.5. With this arrangement the values of temperature and partial pressure at the points adjacent to the boundary must be calculated from modified expressions which take account of the reduced

distance between them and the boundary.

3.5.6 Evaluation of the accuracy of finite difference solutions

The finite difference method, by definition, provides only an approximate solution to a differential equation. The accuracy of this solution depends on a large number of factors including the thermal conductivity or diffusion coefficient values being used, the distance step, time step and total time for which the solution is evaluated. It is important, of course, to estimate the magnitude of the error in any specific model in order to assess whether it affects the conclusion obtained from the model. The simplest way to achieve this is by using a set of initial conditions and a geometric arrangement for which an analytical solution is known and comparing this solution with the one obtained using the finite difference method. This is carried out under the same conditions of distance step, etc., as is used in the model being assessed.

The results of such an assessment are presented in later chapters for each of the models used.

CHAPTER 4SKIN BLOOD FLOW - TECHNIQUES AND RADIATION DOSE

4.1 INTRODUCTION

4.2 CHOICE OF TRACER

4.3 INTRODUCING ^{133}Xe INTO THE SKIN

4.3.1 Intra-arterial injection

4.3.2 Intra-dermal injection

4.3.3 Epicutaneous diffusion

4.4 RADIATION DETECTION

4.4.1 Instrumentation

4.4.2 Collimation

4.4.3 Distance of detector from skin

4.5 DESCRIPTION OF THE ^{133}Xe CLEARANCE CURVE4.6 ANALYSIS OF ^{133}Xe CLEARANCE CURVES

4.6.1 Monoexponential clearance curves

4.6.2 Multiexponential clearance curves

4.7 RADIATION DOSE IN THE USE OF ^{133}Xe

4.1 INTRODUCTION

Although McLure and Aldrich recognised in 1923 that skin blood flow could be assessed by observing the rate of disappearance of a locally injected substance from the skin their method was completely subjective. No quantitative technique was available to monitor the amount of a substance within a tissue. It was not until 1948 that Kety reported the use of a radioactive isotope of sodium, ^{24}Na , which, after injection into the skin, could be detected by external radiation counters. This provided not only a convenient but also a highly sensitive way of measuring the clearance rate. Since then radioactive isotopes have been used extensively in blood flow measurements in almost all organs and tissues of the body (Bain and Harper, 1968; Belcher and Vetter, 1969; Freeman and Blaufox, 1976; Woodcock, 1976). The theory behind such measurements has already been outlined in chapters 2 and 3.

This chapter describes the techniques involved in assessing skin blood flow using a radioactive inert gas, Xenon-133, whose favourable characteristics, described in section 4.2, have led to it being adopted almost universally for tissue blood flow measurements (Lassen, 1964; Hoedt-Rasmussen, 1966; Sejrsen, 1966; Nielsen, 1972). The ^{133}Xe is introduced into the skin as described in section 4.3 and on being removed by the blood flow is carried through the vascular system to the lungs. There, greater than 90% of the ^{133}Xe is transferred to the air in the alveoli

(Ladefoged, 1964) and is removed from the body. This results in little build up of ^{133}Xe within the body. The detection of the ^{133}Xe remaining in the skin is outlined in section 4.4. A typical clearance curve and its mathematical description and analysis are then described in sections 4.5 and 4.6. Finally, in all investigations involving the administration of radioactive substances a radiation dose is delivered to the tissues and this is discussed in section 4.7.

4.2 CHOICE OF TRACER

Kety's (1951) original analysis of tissue clearance assumed the use of an inert gas, whose properties were discussed in chapter 3. The use of an inert gas also allows the analogy between heat and matter transfer to be conserved. However, for mainly practical reasons, other radioactive materials have been used in tissue blood flow measurements and it is worthwhile to consider them here as well as the properties of Xenon-133 which was used in the present study.

The radioisotopes which have previously been used in tissue blood flow measurements can be separated into two groups, those that are hydrophilic or water soluble and those that are lipophilic or lipid soluble. Hydrophilic molecules, using, for example, isotopes of sodium, iodine and technetium, are generally chemically active substances, charged, and pass through the capillary endothelium mainly by the narrow clefts or pores between the endothelial cells (Renkin, 1964). Because of this it has been

Table 4.1Characteristics of Xenon-133

Type of decay - β^- decay

Half-life - 5 days

<u>Emission</u>	<u>Abundance</u>	<u>Energy</u>
γ	35%	0.081 MeV
β^-	100%	0.34 MeV
conversion electrons	65%	

β particle range in tissue - 1.2 mm

γ ray half distance in tissue - 4 cm

suggested that their rate of clearance from a tissue is determined mainly by their rate of passage through these pores (Braithwaite et al, 1951). It has, however, been claimed that this limitation to tracer transport is only important at high rates of blood flow (Trap-Jensen et al, 1967). In contrast, lipophilic molecules such as ^{133}Xe , ^{85}Kr and antipyrone readily dissolve in the capillary endothelium and thereby pass through by diffusion (Renkin, 1952). Their rate of transport across the capillary endothelium will therefore be proportional to the concentration difference across it. This property also means that lipophilic molecules can pass easily through capillary endothelium and can even pass through cell layers in which no pores exist - for example in the brain and the layers of cells making up the epidermis, in the latter case, however, with some difficulty (see section 4.4.3).

The radioactive inert gas, Xenon-133, fulfils Kety's original assumptions of not being metabolised and not being limited by diffusion, while at the same time possessing suitable radiation characteristics (Table 4.1). Its five day half-life means that no significant decay of the isotope occurs during the course of an investigation. Its 81 keV gamma ray has a tissue half-distance of 4 cm which means that there will be little effect on the detected signal due to small movements (diffusion) of the ^{133}Xe in the skin and the signal will only reflect complete clearance of the isotope from the detector field of view. Its 340 keV β particle is easily stopped in tissue and particu-

larly in the aluminium cover of the scintillation crystal preventing contamination of the gamma ray signal. In addition ^{133}Xe is commercially available and relatively cheap.

4.3 INTRODUCING ^{133}Xe INTO THE SKIN

Sejrsen (1966) suggested three ways of introducing ^{133}Xe into the skin, each of which has its own advantages and disadvantages in specific situations. These will be discussed in relation to their use, clinically, in plastic surgery.

4.3.1 Intra-arterial injection

In this method the ^{133}Xe is injected into a local artery supplying the area of skin. Both clinically and theoretically this method is unsuitable - clinically because the artery must first be surgically exposed and theoretically because it is not always possible to identify an artery which supplies only the skin (McGregor, 1970). The detected gamma ray signal may then be a composite of the clearance rate from underlying muscle, and possibly other organs, as well as skin.

4.3.2 Intra-dermal injection

In this method the ^{133}Xe , which is supplied dissolved in isotonic saline, is introduced into the skin via a fine needle. A volume of about 0.02 ml (0.7-2.1 MBq of ^{133}Xe) is used, the needle being inserted a distance of about 1 cm along the skin parallel to the surface to prevent ^{133}Xe passing back along the needle track.

The main problem with this method is that of trauma

due to the injection, which has been shown to increase blood flow in an apparently unpredictable manner (Sejrsen, 1971; Challoner, 1973), a finding which has been contested by Veall (1968), who claims that if sufficient care is taken with the injection this will not happen. Veall did, however, report previously an initial interfering factor after injection into the skin of radioactive sodium (Barron, Veall and Arnott, 1951). This was, he felt, due to an increase in blood pressure attributable to psychological factors. The real cause of this initial reaction will, in most cases, be academic, since whatever the cause it will be difficult or impossible to control.

In an attempt to overcome this problem of variable injection response Sejrsen (1971) proposed adding 20 μ g of histamine per 1 ml of injected solution which, it was postulated, would produce a maximal hyperaemic reaction in the skin. This modification is therefore based on two assumptions; that the reaction to histamine is directly proportional to the resting blood flow, and that the reaction alters the steady state conditions for only the short time it takes to complete the test and any further tests are not influenced by a previous dose of histamine. Any measurement technique which radically alters the variable in question must obviously be viewed with suspicion and this is certainly true in this case. Lindbjerg (1965) has shown, in muscle, that the magnitude and duration of the reaction to the same histamine dose shows considerable variation although Amery et al (1973) claimed

that only by using histamine could he obtain reproducible results in skin. He did not, however, give results of this reproducibility. The duration of the effect of histamine was investigated by Holti (1955) who showed that the return to normal vascular responses takes about 20 days. Conway et al (1951) demonstrated that the flare reaction is dependent on an intact sympathetic nerve supply. This is an important fact in the study of skin flaps which, after raising, may contain areas of complete denervation (Grabb and Smith, 1973). Any test with histamine may then be a measure of the degree of innervation of the flap as well as its resting vascular state.

From a clinical point of view the intra-dermal injection method is unsuitable because of the dangers involved in direct injection into a delicate piece of skin, with the resultant hazard of introducing infection. Anything which may further compromise an already reduced blood supply must be viewed with caution.

Finally, from a practical point of view it is difficult to give an intra-dermal injection due to the mobility of the skin. Because of this, and the fact that the needle has to pass along the dermis for some distance, it is difficult to deposit the ^{133}Xe at the same depth every time, especially since the dermis varies greatly in thickness from one area of the body to another (Southwood, 1955). Challoner (1973) emphasised the importance of constant injection depth and demonstrated that injections deposited at the base of the dermis gave a considerably

slower clearance of ^{133}Xe .

4.3.3 Epicutaneous diffusion

To combat the artefacts detailed above Sejrson (1971) suggested a method whereby ^{133}Xe is allowed to diffuse through the epidermis and into the dermis. This is achieved by forming a small chamber on the surface of the skin which is then filled with ^{133}Xe , dissolved in saline. By leaving this on the skin for a period of three minutes a small fraction (approximately 1%) of the ^{133}Xe is able, by diffusion, to enter the epidermis and pass through into the dermis. In the present study the chamber is formed in one of two different ways (Fig. 4.1).

- a) A small ring is cut from double sided adhesive skin tape (Stomaseal, 3M Company) and a piece of melinex membrane is applied to one side of it. Using the other adhesive side the ring is stuck to the skin surface.
- b) A syringe, filled with Vaseline, is used to form a ring of Vaseline on the skin surface much the same way as decorating a cake. The melinex membrane is applied to the top of this.

In both cases ^{133}Xe , in a concentration of 35-100 MBq/ml, is injected into the chamber, which is normally between one and two cm in diameter but can be larger if required. After the three minute diffusion period the ^{133}Xe is sucked back out, the chamber removed and any excess ^{133}Xe wiped away. After a further 30 seconds monitoring of the activity left in the skin is begun,

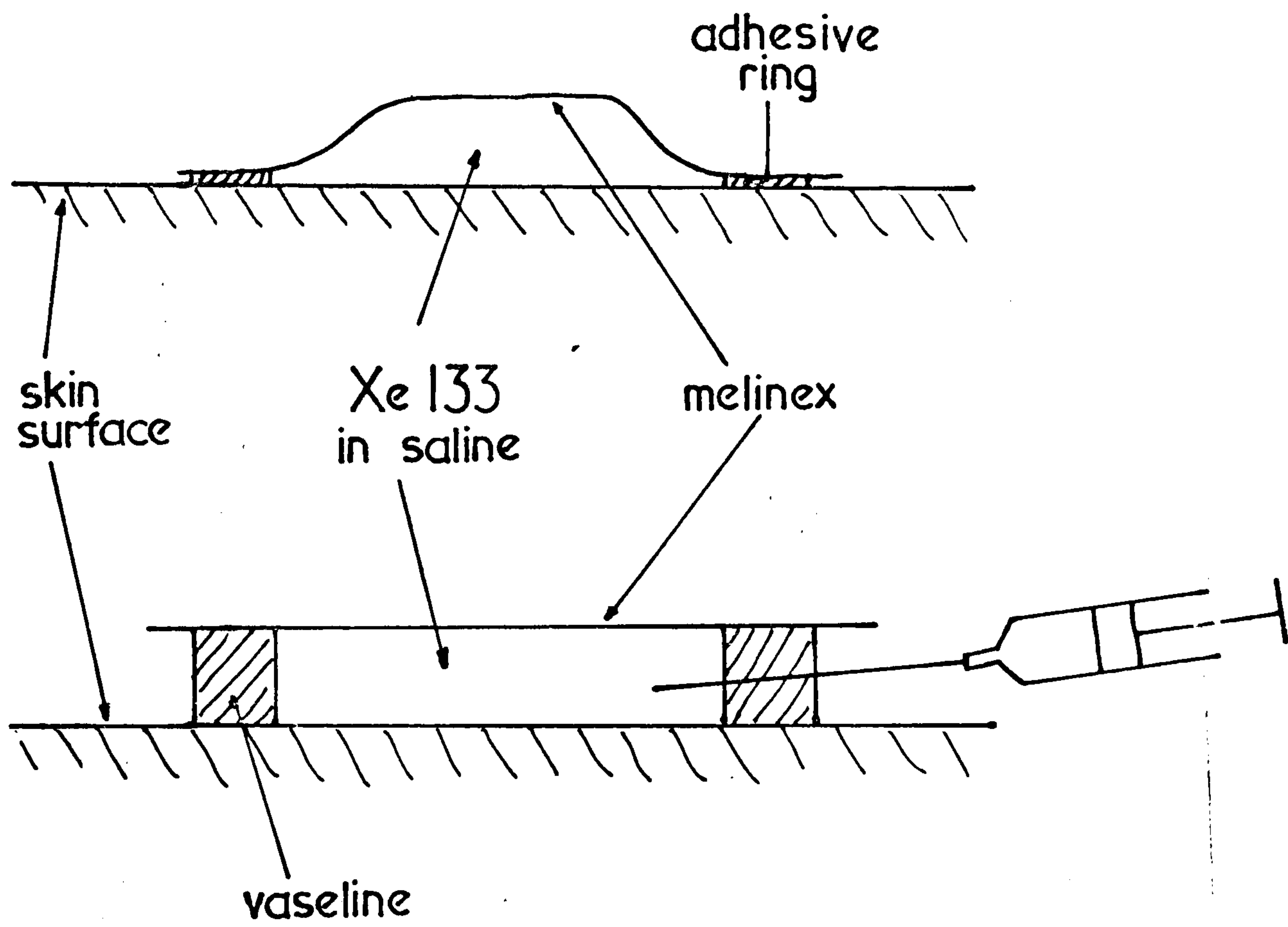


Figure 4.1 Epicutaneous application of ^{133}Xe .

and the start of the clearance curve is taken 30 seconds later.

This technique is completely atraumatic and because of this considerable advantage in the clinical situation it was adopted for use in assessing skin blood flow in the present study. A model representing the transport processes involved in this technique is presented in later chapters.

4.4 RADIATION DETECTION

The purpose of the radiation detection system is to accurately reflect the rate of clearance of the ^{133}Xe from the skin. To do this it must not only be able to detect the ^{133}Xe within the skin but also to reject any unwanted radiation and must not be influenced by any factors such as movement of the ^{133}Xe source.

4.4.1 Instrumentation

A block diagram of the equipment used to detect ^{133}Xe is given in Figure 4.2. It comprises four units - the detector, the amplifier and energy analyser, the ratemeter and the chart recorder. The detector consists of a 1" diameter sodium iodide (T1) scintillation crystal with a photomultiplier tube mounted behind it (P1062 Rank Precision Industries). The signals from this are fed into an amplifier/energy analyser/ratemeter unit (Nuclear Enterprises SR3). The energy discriminator of the analyser is set to detect only the photopeak of the ^{133}Xe spectrum and all radiation of a higher or lower radiation is rejected. In this way the amount of

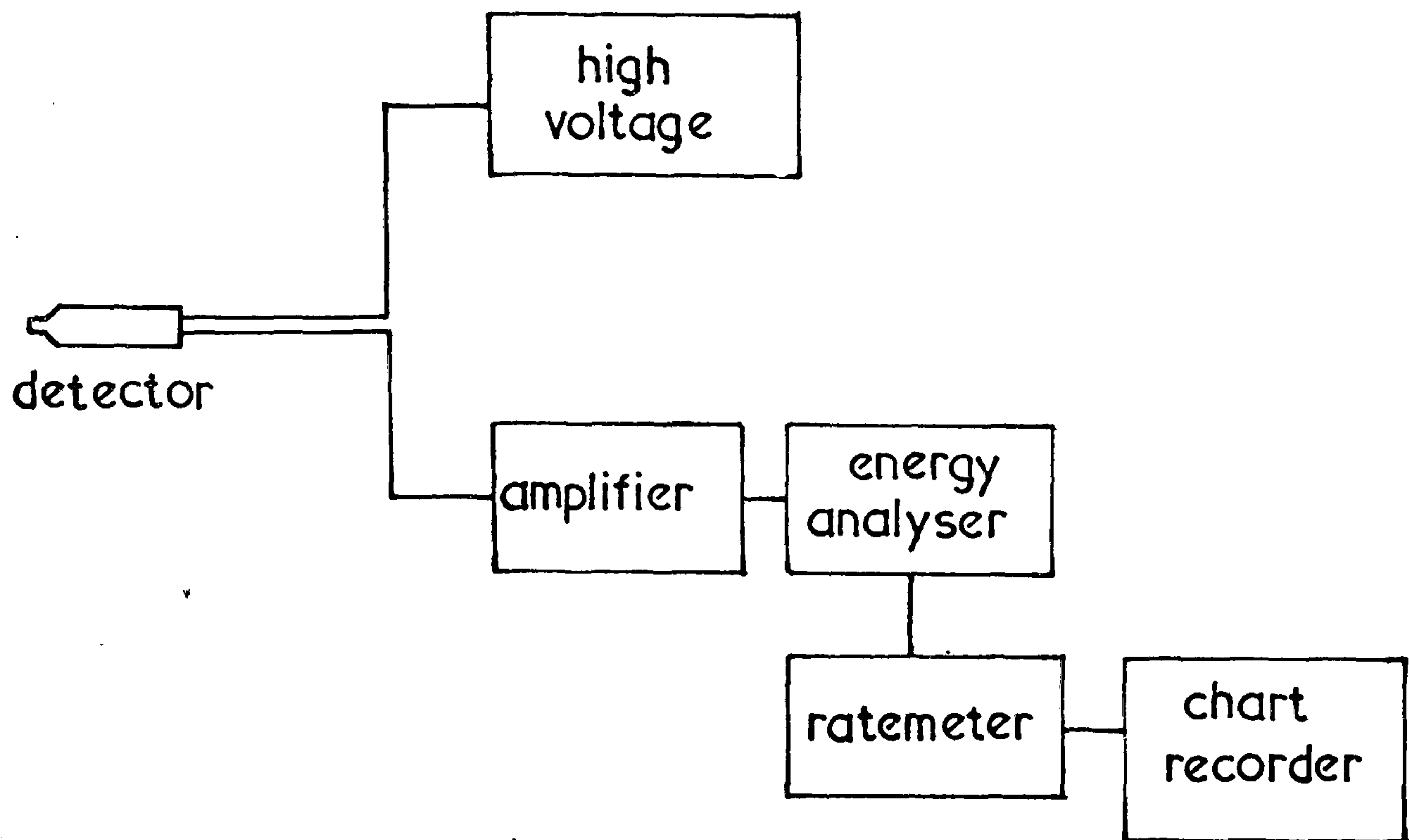


Figure 4.2 Block diagram of radiation detection system.

background radiation within the signal is reduced to a minimum. The accepted pulses from the energy analyser are then passed to the ratemeter to be counted. The ratemeter produces a signal of the number of counts per second which is then displayed on the chart recorder.

4.4.2 Collimation

The purpose of collimation of a radiation detector is to define the area from which the detector will accept radiation, i.e. its field of view. In the present study ^{133}Xe is deposited in a small area of skin about 1 cm in diameter. As will be discussed later it can then be transported locally over distances of a few millimetres or else be carried by the blood stream to the lungs. The diffusion over small distances requires that the detector's field of view be greater than the size of the original deposit, to ensure that this ^{133}Xe still forms part of the signal. The ^{133}Xe transported by the blood stream to the lungs should be shielded from the detector after it leaves the skin. This, in theory, sets a maximum limit on the detector's field of view. In the present case, however, since most of the ^{133}Xe is removed from the lungs to the atmosphere, where it is quickly dispersed, and the small fraction recirculated is, of course, redistributed to the whole body, very little of the removed ^{133}Xe will be seen even with very wide collimation. The lead collimator used in the present study is shown in Figure 4.3. It is unnecessarily heavy, since the half thickness of ^{133}Xe is only 0.17 mm

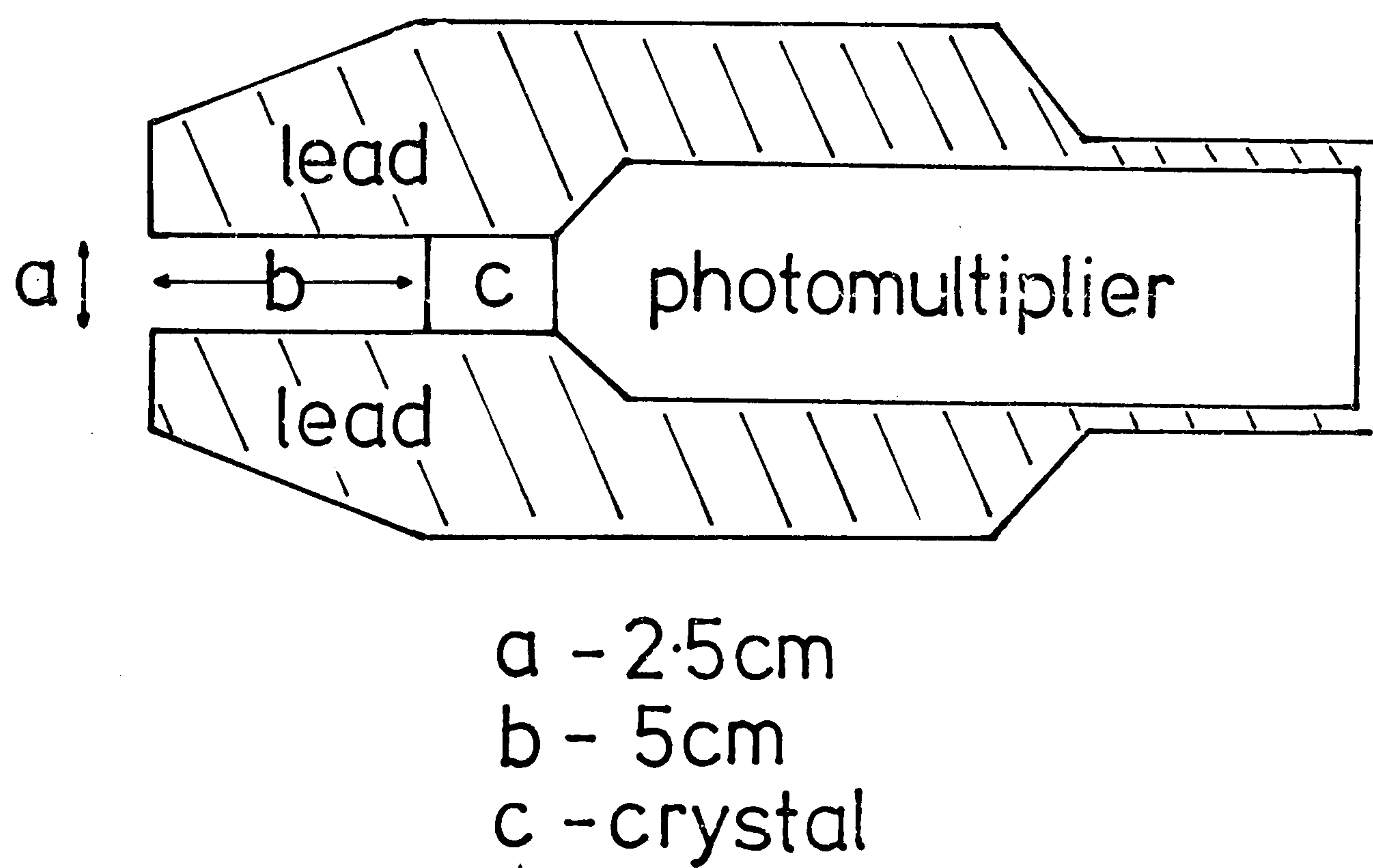


Figure 4.3 Radiation detector and lead collimator.

in lead and is unnecessarily narrow (Fig. 4.4), having an effective width of about 4 cm at a distance of 10 cm from the collimator face, in situations where a single area of skin is being tested. It is, however, necessary to have such collimation where two or more areas of skin close together are being tested simultaneously.

4.4.3 Distance of detector from skin

Because of patient respiration or restlessness it is possible that small movements of the ^{133}Xe deposit will occur relative to the detector. In addition the ^{133}Xe diffuses down into the subcutaneous tissue from the dermis (section 4.5) resulting in a change in geometry of the ^{133}Xe source. It is important that both of these processes have as little effect on the detected signal as possible. It is well known from the inverse-square law that small changes in distance have a greater effect the closer the source is to the detector. This is confirmed by the response of the present detector to a 1 cm diameter ^{133}Xe source, shown in Figure 4.5. As a result of this it was decided that the skin-detector distance should always be 10 cm which reduced the possible error in the signal to between 1-2% for a change in distance of 2 mm.

4.5 DESCRIPTION OF ^{133}Xe CLEARANCE CURVE

A typical clearance curve obtained from skin of the forearm is given in Figure 4.6. When replotted on a logarithmic scale (Fig. 4.7) it can be seen that the curve is characterised by a continually decreasing rate

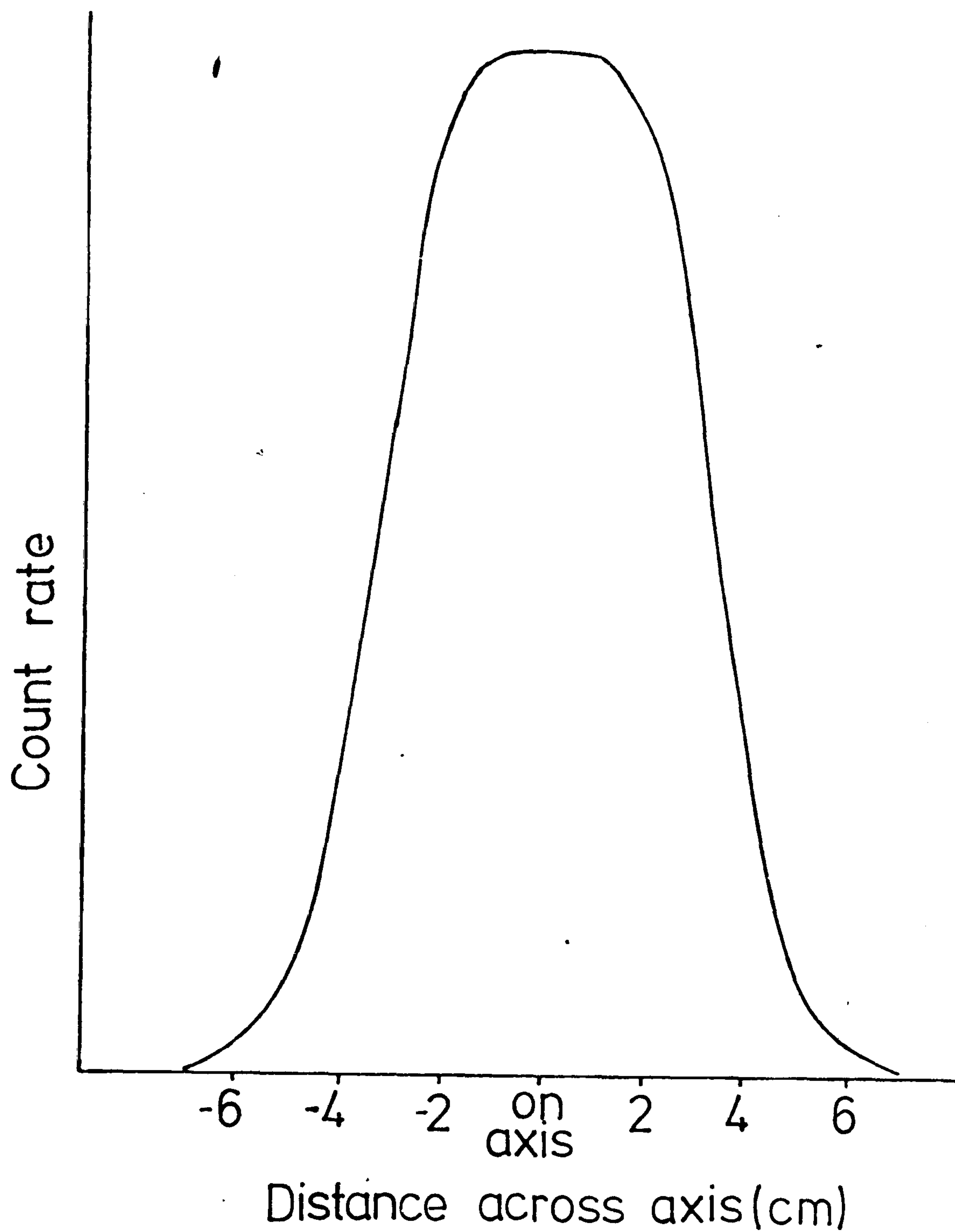


Figure 4.4 Response of collimated radiation detector to a point source of ^{133}Xe at a distance of 10 cm from the face of the collimator.

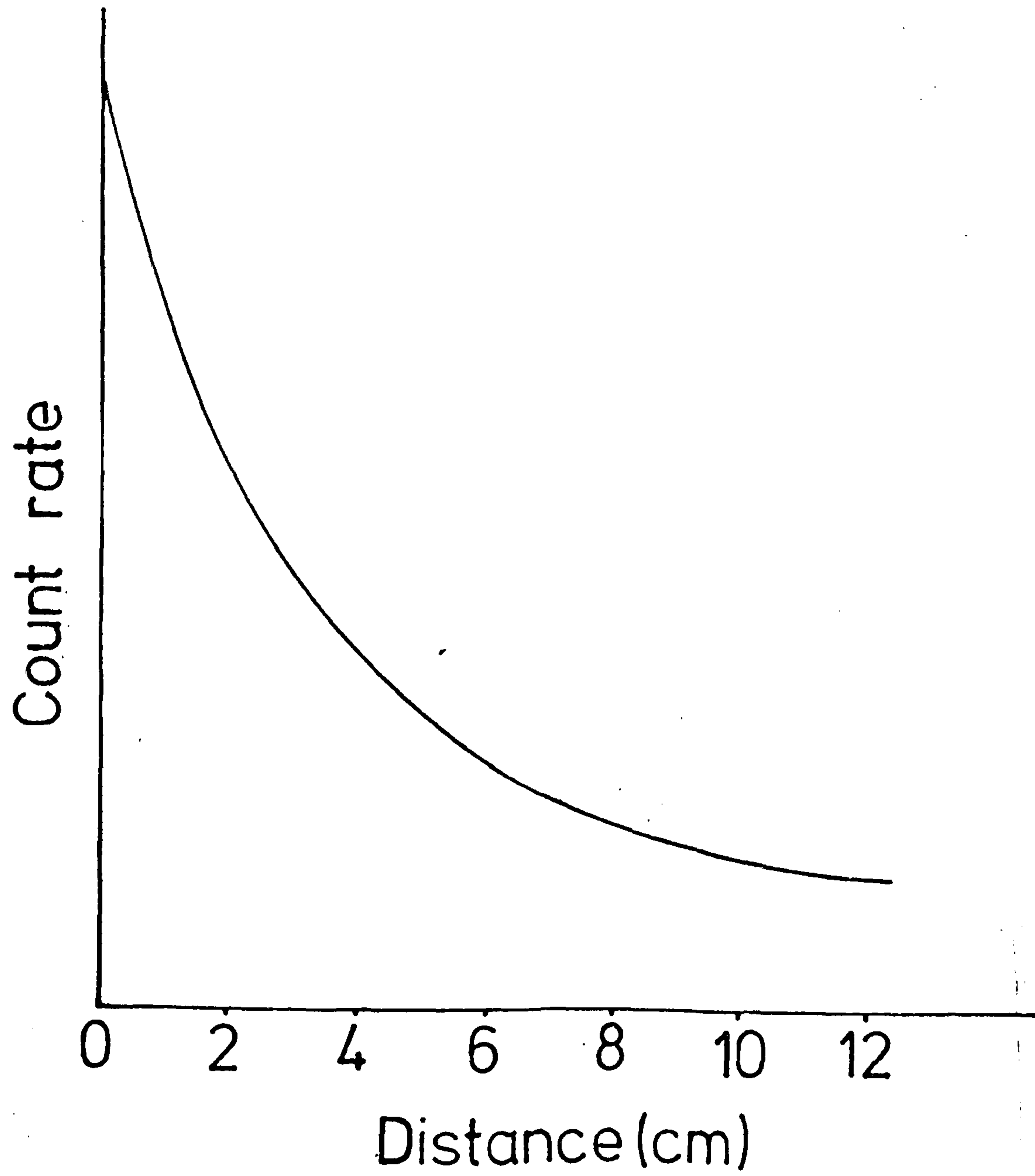


Figure 4.5 Response of radiation detector to a 1 cm diameter source of ^{133}Xe situated at a variable distance from the face of the collimator.

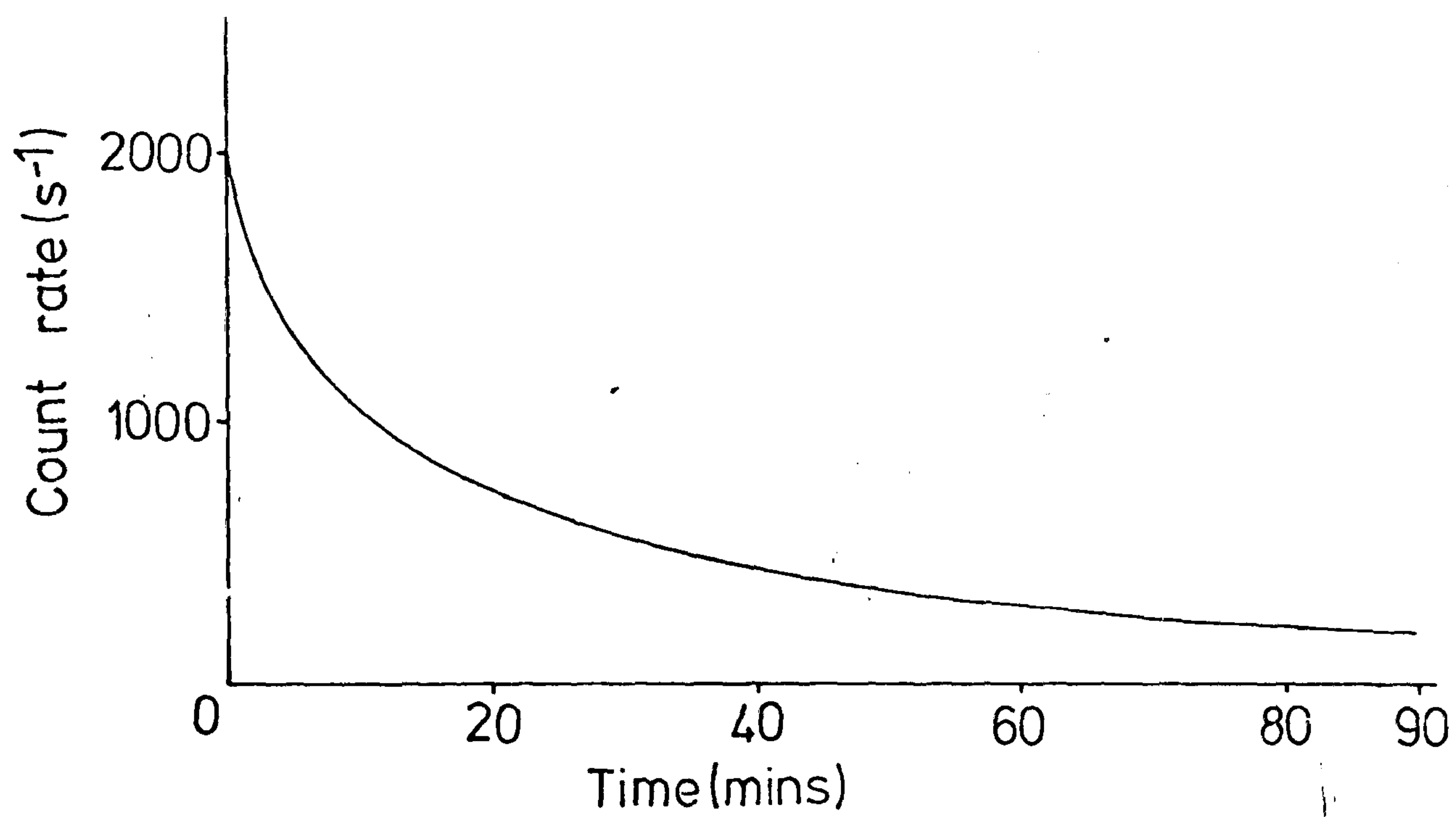


Figure 4.6 Typical clearance curve obtained after epicutaneous application of ^{133}Xe to the skin of the forearm.

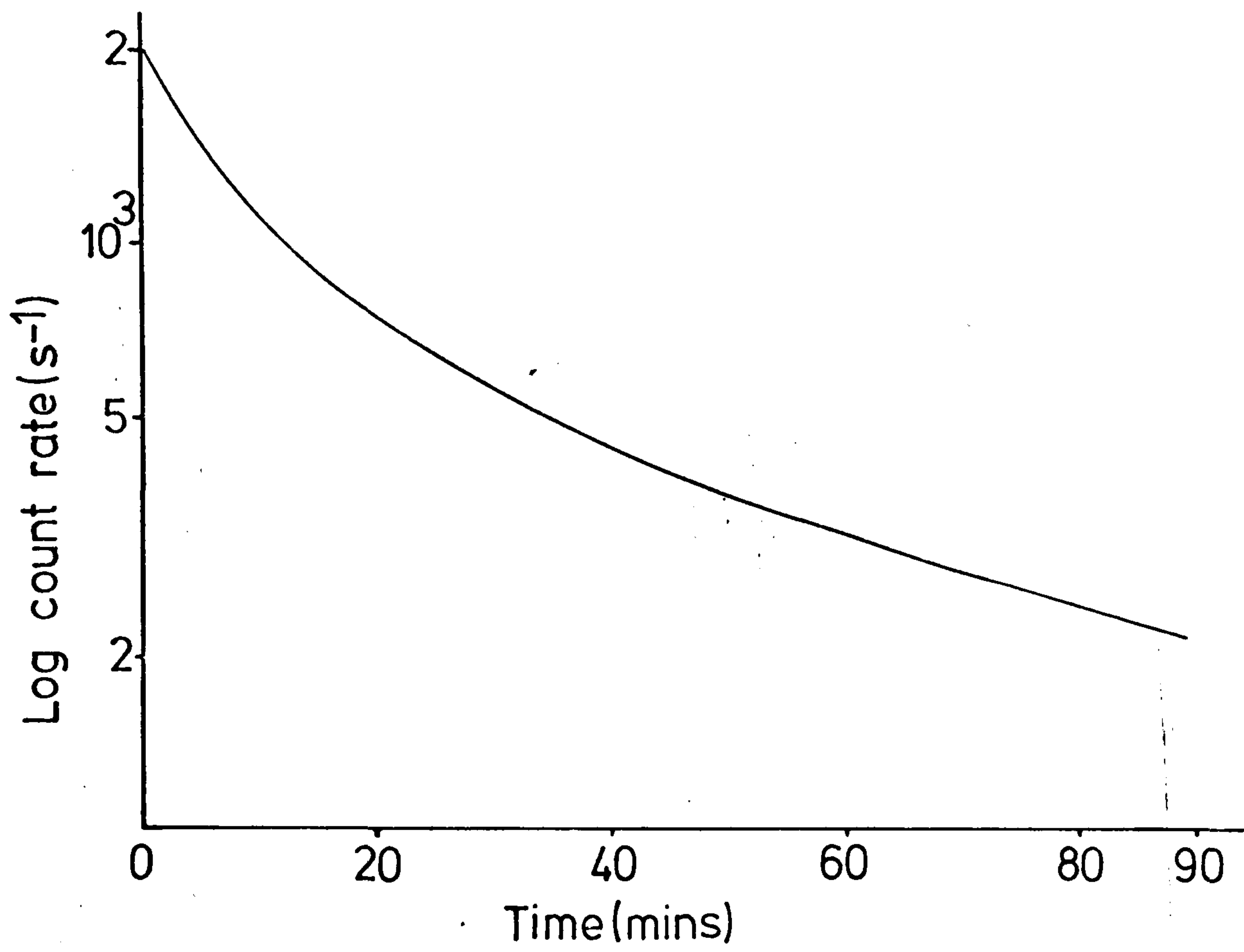


Figure 4.7 Typical clearance curve with the count rate plotted on a logarithmic scale.

of clearance, i.e. the beginning of the curve represents a fast exponential decrease in activity and the end of a slower rate of decrease. This, in itself, can give no indication of blood flow. Before this can be attempted all of the important processes contributing to clearance of ^{133}Xe from the skin must be known and their relative magnitudes in various situations assessed.

Sejrsen (1966) and, to a lesser degree, Challoner (1973) attributed the shape of the curve to the following factors, summarised in Figure 4.8. When the ^{133}Xe is introduced into the dermis it can be removed by the dermal blood flow, the lymph flow, sweating, diffusion into the subcutaneous fatty tissue and diffusion through the epidermis. Some of the ^{133}Xe removed by the dermal blood flow is deposited in the subcutaneous fatty tissue as the venous blood from the dermis passes through it. Together with this, the ^{133}Xe which diffuses down into the subcutaneous tissue is then removed by the subcutaneous blood flow. The relative importance of each of these, according to the previous literature, will now be discussed.

(a) Removal of ^{133}Xe by blood flow through the dermis

Sejrsen (1966) indicated that, except in cases of low blood flow, this is undoubtedly the major process of clearance from the dermis. In addition he showed that, by shielding the activity coming from the fatty tissue, the resulting clearance curve could be described by a single exponential. He attributed this to the fact

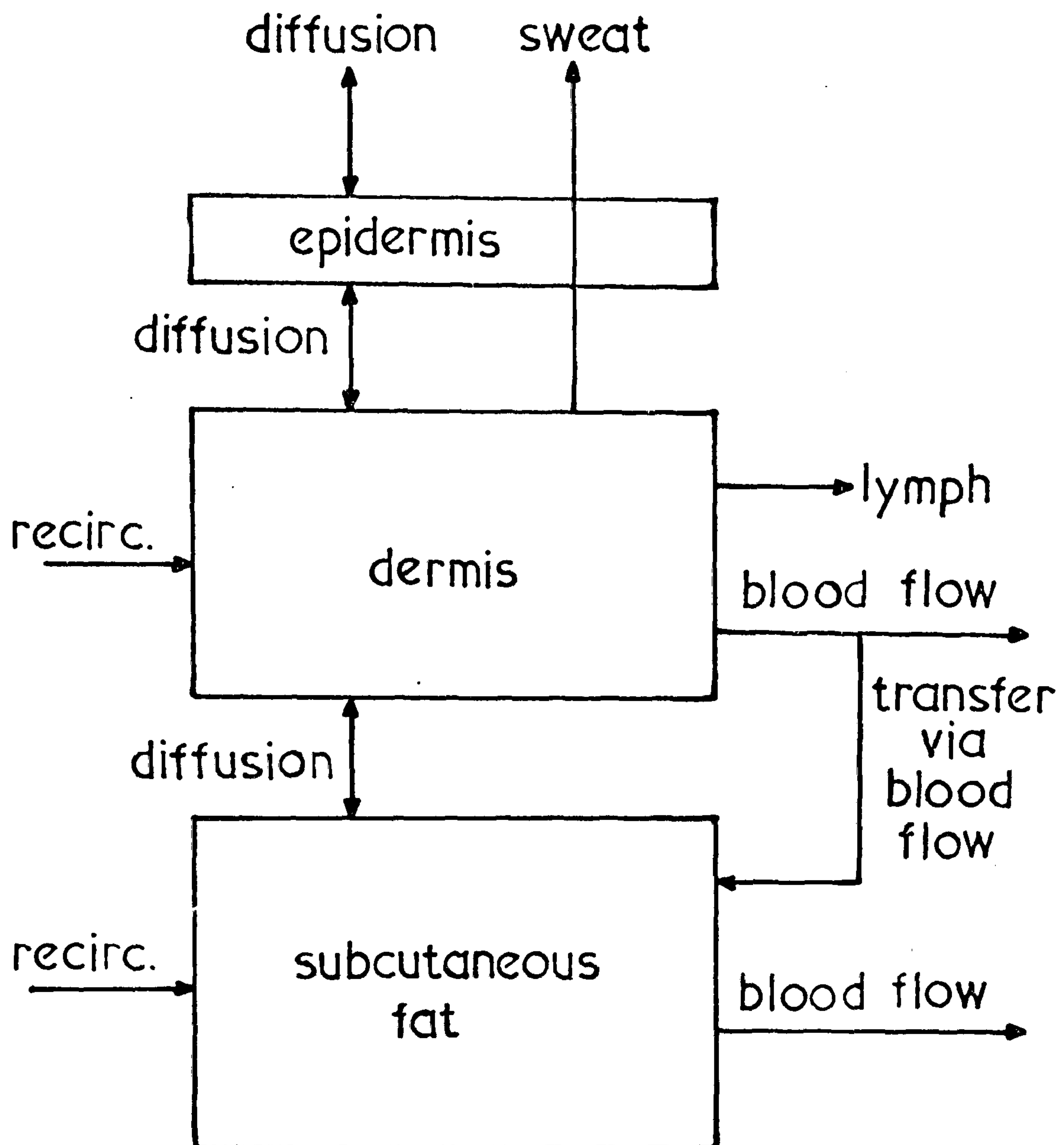


Figure 4.8 Summary of the processes involved in the clearance of ^{133}Xe from the skin.

that dermis above must behave like a single, homogeneous tissue and can therefore be characterised by the simple equations of section 3.4.1, producing a mono-exponential clearance rate.

(b) Removal by lymph

The flow of lymph is several orders of magnitude less than that of blood flow (Mayerson, 1963) and is therefore neglected in the clearance models.

(c) Removal by sweat

The rate of sweat production is also several orders of magnitude less than the rate of blood flow (Morimoto, 1978) at ambient temperatures less than 30°C. The effect of sweating can therefore be neglected for temperatures below 30°C but above 30°C, when sweating increases considerably, and particularly on areas of the skin such as forehead and palms, it may be necessary to consider this factor especially at low blood flows. In addition with regard to the present study it should be noted that sweating depends on an intact nerve supply which is present in a skin flap only to a variable degree.

(d) Diffusion into the subcutaneous tissue

In the absence of blood flow Sejrnsen (1966) showed, qualitatively, that only a small proportion of the ^{133}Xe had entered the subcutaneous tissue after one hour. When compared to the rate of clearance by blood flow he felt that this was insignificant and did not include it in his model of clearance.

(e) Diffusion through the epidermis

When the surface of the skin is intact the loss of

^{133}Xe , from an intradermal deposit, by diffusion through the epidermis is only of the order of 0.1% per minute (Sejrsen, 1968). This is due to the diffusion resistance existing in the compact, keratinised layer of the stratum corneum. Again, this was not considered a significant effect.

(f) Transfer of ^{133}Xe from effluent cutaneous blood to subcutaneous tissue

Although, as already discussed, only a very small amount of ^{133}Xe entered the subcutaneous tissue when there was no blood flow, it was also found (Sejrsen, 1966; Challoner, 1973) that a considerable proportion entered this tissue when blood flow was present. It was postulated that this occurred due to a transfer of ^{133}Xe from the venous blood, clearing the cutaneous tissue, as it passed through the subcutaneous tissue. Due to the size of these venous blood vessels a complete equilibrium would not, of course, be achieved between the blood and tissue and only a fraction of the ^{133}Xe would therefore leave these small veins.

(g) Blood flow through the subcutaneous tissue

The ^{133}Xe which enters the subcutaneous tissue due to the transfer process described above will then be removed by the subcutaneous capillary blood flow. Similar to the dermis, it has been shown (Larsen and Lassen, 1967) that the subcutaneous tissue also behaves as a single, homogeneous tissue which produces a clearance curve for this tissue alone which can be described by a single

exponential. However, because of the high solubility of ^{133}Xe in fat (see Chapter 5) this exponential is considerably slower than that characterising the dermis.

From the above processes Sejrnsen produced a model containing the most significant factors, which describes the clearance of ^{133}Xe from the skin using the epicutaneous diffusion technique. This simplified model is illustrated in Figure 4.9. The resulting clearance curve is made up of an initially fast exponential, representing blood flow in the dermis, plus a second, slower exponential representing blood flow in the subcutaneous tissue and is therefore similar to the typical experimental curve shown in Figures 4.6 and 4.7. The relative amplitudes of these component exponentials depend on the amount of ^{133}Xe transferred to the subcutaneous tissue due to process (f) above.

Sejrnsen (1969) was able to formulate a mathematical equation describing this clearance curve. This was a two exponential function given by

$$Q(t) = Q_0 \left(1 - \frac{E \cdot k_c}{k_c - k_s} \right) \exp(-k_c t) + \frac{E \cdot k_c}{k_c - k_s} \exp(-k_s t)$$

where $Q(t)$ is the amount of ^{133}Xe remaining in the detected field of view at time t

Q_0 is the amount of ^{133}Xe at time zero

k_c and k_s are the exponential rate constants for the cutaneous and subcutaneous tissues respectively

and E is the fraction of ^{133}Xe extracted from the dermal venous blood as it passes through the subcutaneous tissue.

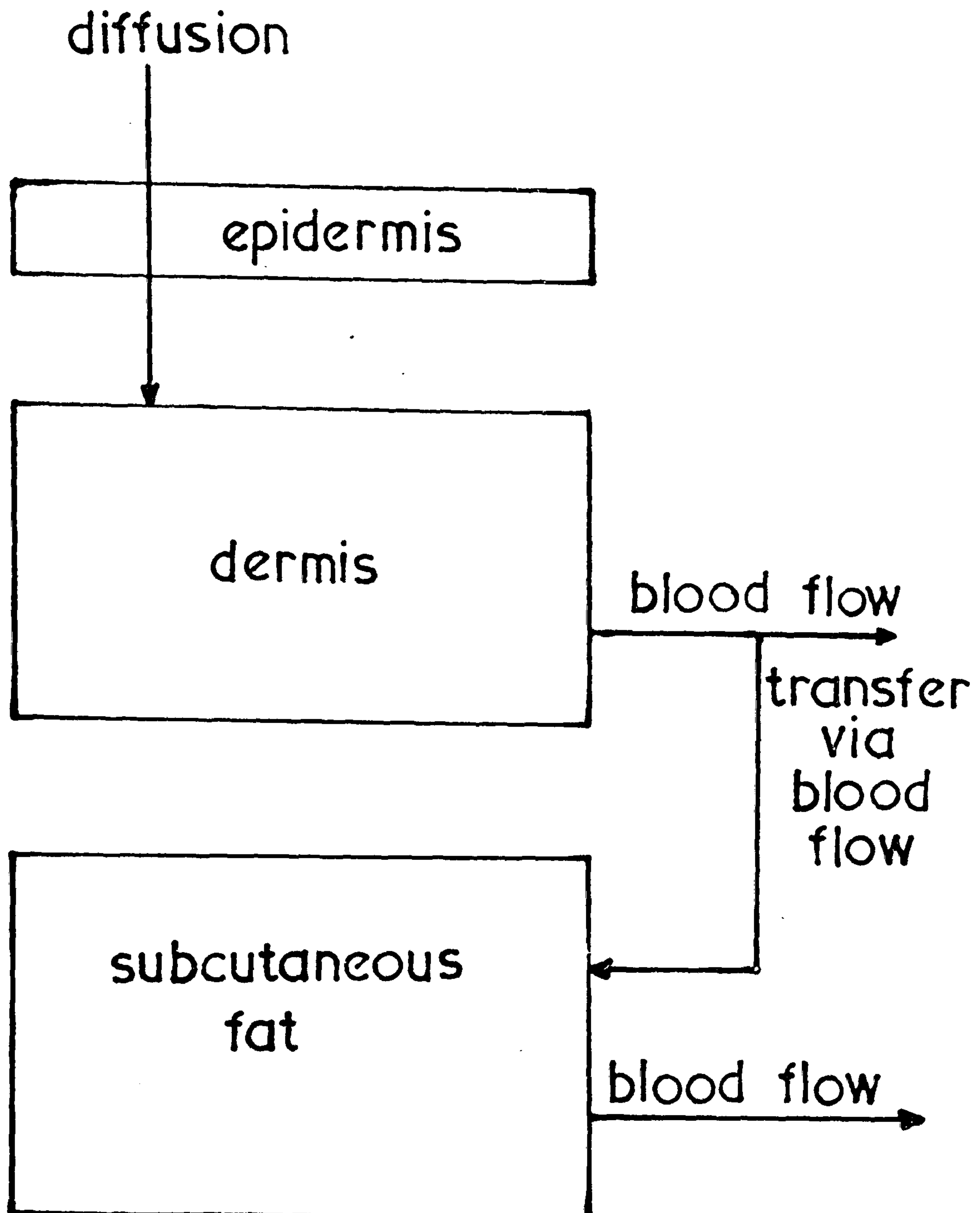


Figure 4.9 Summary of the processes adopted by previous authors to describe the clearance of ^{133}Xe from the skin, after epicutaneous application.

The above double exponential function is undoubtedly a possible fit to the experimental clearance curves. However, although this is a necessary condition for the use of this model it is not a sufficient one and does not necessarily prove that the model is the correct one. It is possible to invent almost any number of equations to fit a given curve (Zierler, 1965), but without direct confirmation of the validity of the results such models must always be open to doubt. No such direct method of measuring skin blood flow and hence of validating Sejr'sen's model exists.

Undoubtedly the major failure of the above model which was found in the present study (Chapter 6) is the inability to produce a zero rate of clearance in the absence of skin blood flow either in vivo or in excised tissue specimens. In addition although Sejr'sen largely ignores the role of diffusion of ^{133}Xe in the tissues he has previously noted that diffusion from dermis to subcutaneous tissue does in fact occur. By neglecting this he immediately introduces doubt as to the applicability of the technique in situations where the dermal flow is low, as in the present study, and thus where diffusion may be more significant. No consideration is given to the fact that, since ^{133}Xe is introduced into the dermis by diffusing it through the ^{epi-}dermis, then some of it must still be within this, albeit thin, avascular tissue at the end of the three minute epicutaneous diffusion period. Finally although the transfer from venous

blood to subcutaneous tissue forms an important part of the model the possibility that the same form of transfer occurs within the dermis itself is not considered.

The present study, using the epicutaneous diffusion method as an experimental base, provides a flexible model with which to assess the importance of all the above factors in different flow situations.

4.6 ANALYSIS OF THE ^{133}Xe CLEARANCE CURVES

Most inert gas clearance techniques for the measurement of tissue blood flow result in a clearance curve which can be described by a series of exponential functions. In order to obtain information on the blood flow within a particular tissue component it is necessary to resolve the composite clearance curve into its component parts and obtain the values of the exponential rate constants. Although the model to be described in the present study results in a much more complicated mathematical function, the method of analysing multi-exponential clearance curves is included here so that a comparison with Sejrsen's work is possible.

4.6.1 Monoexponential clearance curve

The simplest exponential function is, of course, the one in which only a single exponential is present. Although in practice this is rarely found to be an adequate description of a tissue it is often used, mainly for practical reasons, to provide a value of the blood flow which is a weighted mean value of all the tissues within the field of view (Paulson et al, 1969; Olesen

et al, 1971).

The exponential rate constant is most easily obtained by replotting the data on a semi-logarithmic scale (Fig. 4.10). A straight line can then be fitted to the initial part of the curve as shown. The rate constant is given by

$$k = \frac{\ln 2}{T_{1/2}} \quad 4.1$$

where $T_{1/2}$ is the time taken for the fitted line to fall to half its value at time zero.

This is then related to the flow by equation 3.7.

If the clearance curve is composed of only one exponential the straight line will provide a good fit to the plot for the full course of the curve. If it is not the data points and fitted line will gradually diverge.

4.6.2 Multiexponential clearance curve

In most situations more than one exponential component is present in a clearance curve. Many different techniques are available to separate the curve into these components but it should be noted that unless monitoring of a clearance curve is continued until each of the components has provided a substantial effect on the shape of the curve then it will always be very difficult to obtain some of these components. For example the initial part of a curve will be most affected by the fastest exponential and only minimally affected by very slow components. It will therefore be difficult to recognise these slow components at this stage and monitoring must be continued until they dominate the

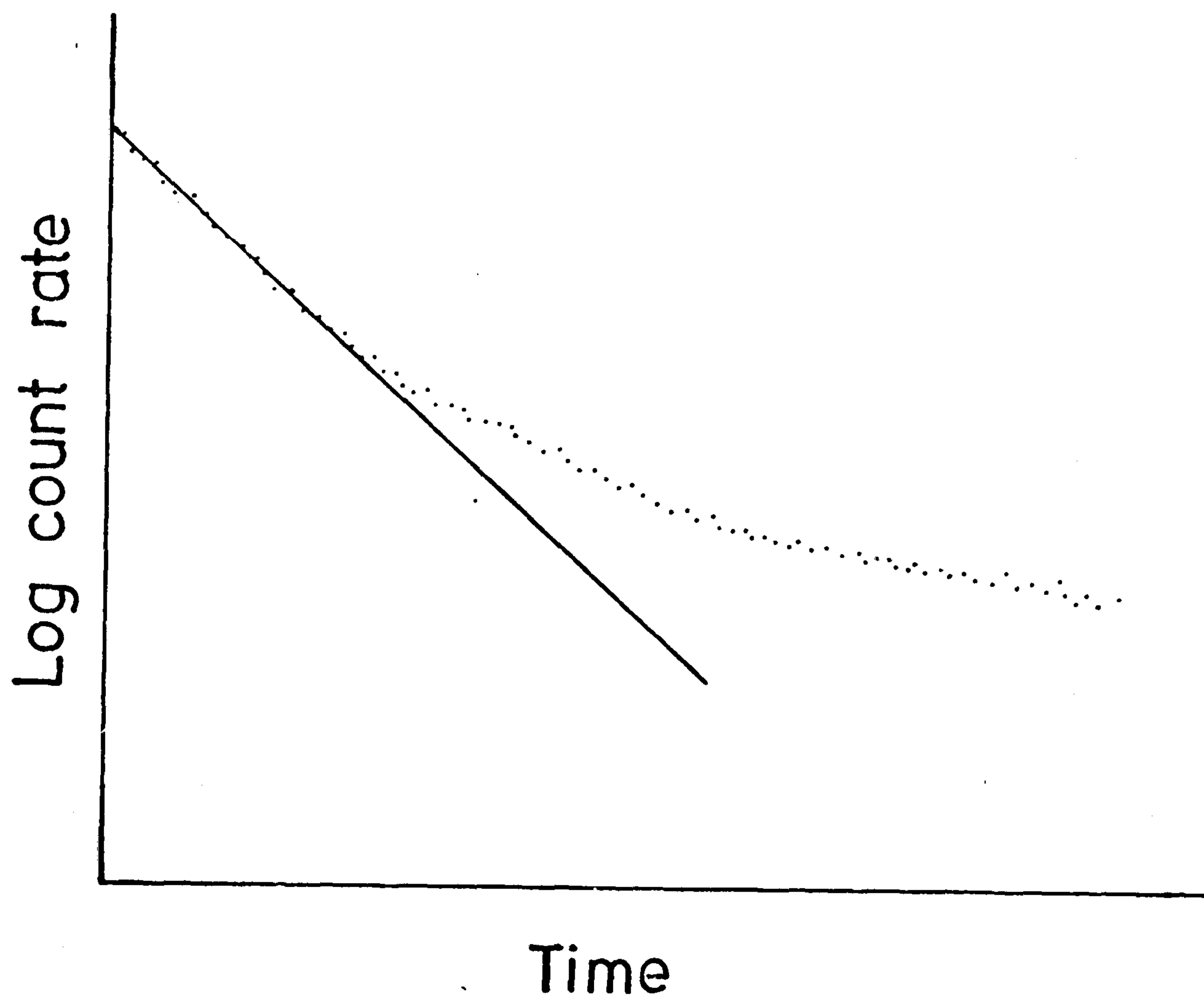


Figure 4.10 Fitting a straight line to the initial part of a clearance curve which is plotted on a logarithmic scale.

shape of the curve. This facet of exponential curve analysis and the errors involved in attempting to fit data from biological systems have been discussed by Glass and de Garreta (1971).

Two methods of curve fitting have been used in the present study.

(a) Graphical stripping of multiexponentials

This is the most popular method of separating exponential components and is illustrated in Figure 4.11. Again the data is first plotted on a semi-logarithmic scale, a straight line is drawn through the points at the end of the clearance curve and this then represents the slowest component. By extrapolating it back to time zero and subtracting from the original data a new set of data is formed. The process is repeated, by drawing a straight line through the slow component of the new set of data, until all components are obtained and the exponential rate constants calculated as in equation 4.1.

(b) Computer fitting of exponential functions

Many different methods of fitting a series of exponentials by computer techniques are available ranging from a computer version of the graphical stripping method (Perl, 1960) to analogue simulation (Abrams et al, 1969) to digital techniques by a least squares method (van Mastrigt, 1977). In the present study van Mastrigt's method has been used, providing an alternative to the graphical stripping method and also being similar to that used by Handel et al (1976) and therefore

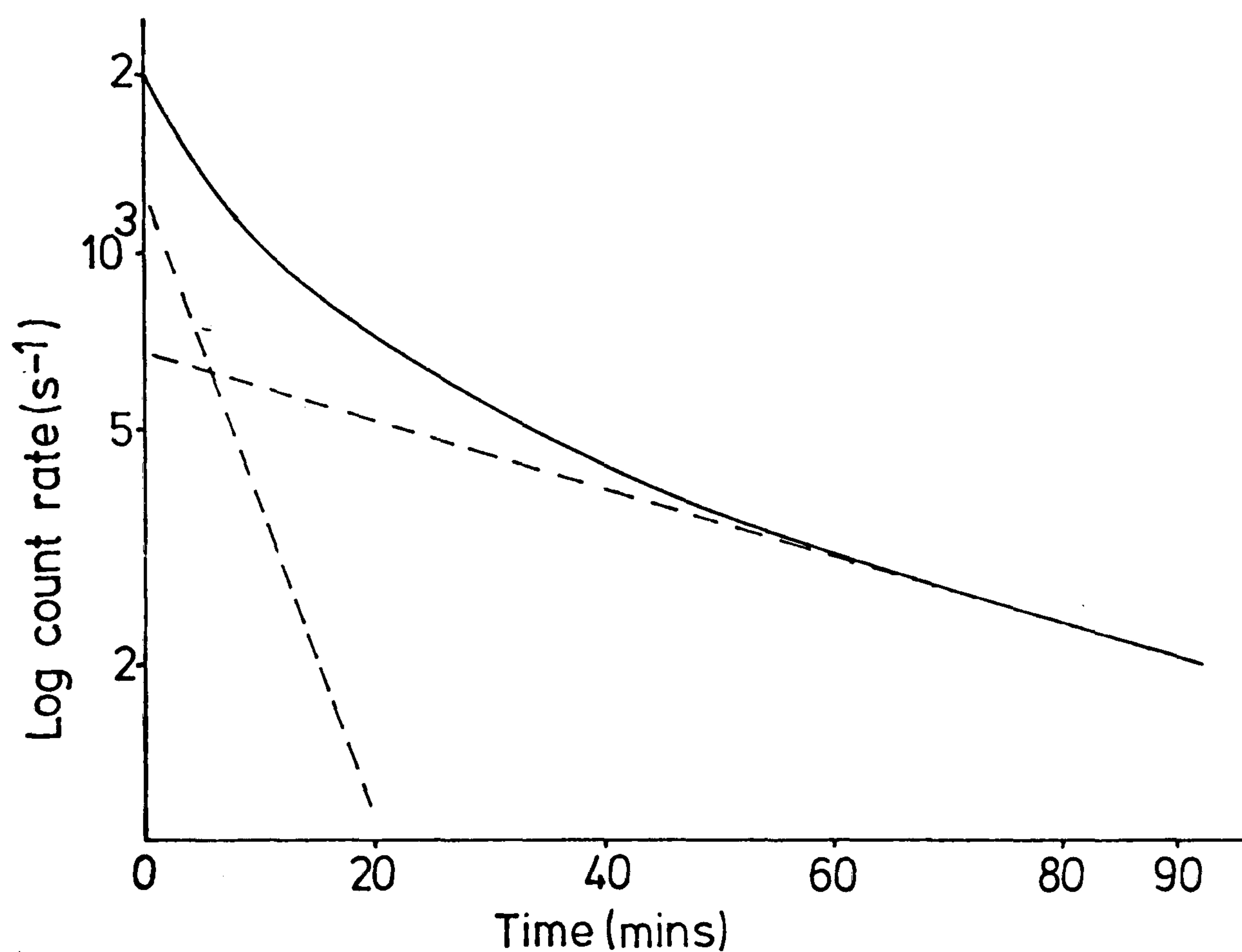


Figure 4.11 Graphical stripping of a clearance curve. A straight line is drawn through the tail of the curve, which is plotted on a logarithmic scale. This is extrapolated back to time zero and subtracted from the original curve, forming a second line which represents the faster exponential component.

suitable for direct comparison with their data.

The computer program is detailed in Appendix A but essentially it uses an iterative technique whereby an initial guess of the exponential rate constants is made, the sum of the square of the deviations of the data points from this function are calculated and then a new value of the rate constants is tried. This process is continued until the sum of squares is a minimum. The rate constants at this point are then the "least-squares" fit to the data points.

4.7 RADIATION DOSE IN THE USE OF ^{133}Xe

The fact that ^{133}Xe is generally listed as a low toxicity radionuclide (HMSO 1972) does not preclude the possibility of its posing a significant radiation hazard in any specific situation. It is important in any technique involving the administration of radioactive materials that prior assessment of the radiation dose delivered is made. Despite the fact that ^{133}Xe has been used in a very large number of studies of the skin circulation no proper estimate of the radiation dose has been made. A detailed assessment of the dose was therefore considered essential in this study.

Generally the radiation hazard from an isotope like ^{133}Xe which emits both β^- particles and gamma rays can be considered in three parts:-

- (a) When the source is some distance from the body the main hazard is due to the gamma rays.
- (b) As the source is moved closer to the body, or is in

direct contact with it, the role of the β^- particles, low energy photons and conversion electrons becomes more important. All of these are absorbed within a relatively short distance in tissue.

- (c) When the source is introduced into the body a localised radiation dose is produced at the site of entry. Thereafter as the source is circulated to other parts of the body the chemical and physiological properties of the radionuclide become important.

Normal precautions of providing lead shielding for the ^{133}Xe stock bottle are sufficient to prevent a significant dose occurring in the present application due to (a). In addition since Xenon transfers readily from blood to air in the lungs the radiation dose to the internal organs caused by the circulation of ^{133}Xe is small (ICRP 1966, ICRP 1971) - typically 0.007 mGy to the lungs in the present case.

However where a significant radiation hazard does exist it is due to the β^- particles and conversion electrons when the ^{133}Xe is in close contact with the skin. This will occur when the chamber is on the surface of the skin in the epicutaneous diffusion technique or when the ^{133}Xe is injected intradermally. Calculations of the dose in each of these cases are detailed in Appendix B.

To assess the significance of the radiation dose delivered in these techniques two questions must be answered (i) what is considered to be the critical layer

in the skin? and (ii) what level of radiation dose is considered to constitute a hazard? At the present time the critical layer of the skin is usually considered to be the reproductive basal cell layer of the epidermis. According to Whitten and Everall (1972) it has generally been agreed that this layer lies at an average distance of 0.04 mm below the surface of the skin, although this varies greatly from one site to another. With regard to question (ii) several organisations have published data on maximum permissible doses for workers occupationally exposed to radiation (FRC 1960, NCRP 1960, ICRP 1966) although no such recommendations exist in the case of patients and more particularly in the case of volunteer subjects. Although only very small areas are being irradiated in this study it is probably useful to compare the doses with that recommended by ICRP (1966) for occupationally exposed persons of 0.5 Gy to a small area of skin in 3 months.

From Figure A2 the dose rate to the basal layer of the epidermis using the epicutaneous diffusion technique with a ^{133}Xe concentration of 120 MBq/ml and a chamber thickness of 0.2 mm is 0.1 Gy/3 mins. Using the above criteria it would therefore seem acceptable to adopt such a technique for routine clinical use if useful information was being obtained from the investigation. However considerable repetition of such a test on the same area should always be avoided if possible.

It is interesting to note that if ^{133}Xe is intro-

duced into the chamber in the gaseous form rather than dissolved in saline then a different calculation is required. The reason for this is that since there is less absorption of the β^- particles by air than the ^{133}Xe can instead be represented as a very thin surface source. In this case data taken from Henson (1972, 1973), Figure 4.12, shows an increased dose rate within the skin. For example for the case quoted above the dose for a three minute period is now 0.5 Gy. It is important then, if practically acceptable, to use ^{133}Xe in saline rather than in the gaseous form since this will produce a lower radiation dose.

For comparison Figure A3 shows the dose obtained with the intradermal injection technique. In this case the radiation dose is entirely dependent on the blood flow within the tissue. This is unfortunate since it means that a prior assessment of dose is not possible because the test is designed to measure the blood flow. However a review of the literature shows that effective half-lives of ^{133}Xe in skin of greater than 30 minutes have been commonly quoted (Moore, 1973; Chimoskey, 1972; LeRoy, 1971). Reference to Figure A3 shows that doses of about 0.7 Gy for 40 MBq/ml ^{133}Xe and greater than 2 Gy for 120 MBq/ml ^{133}Xe are applicable in these circumstances. Repetition of tests in such low blood flow situations is clearly undesirable and the possible information to be gained from the test must be weighed against the possible radiation dose delivered.

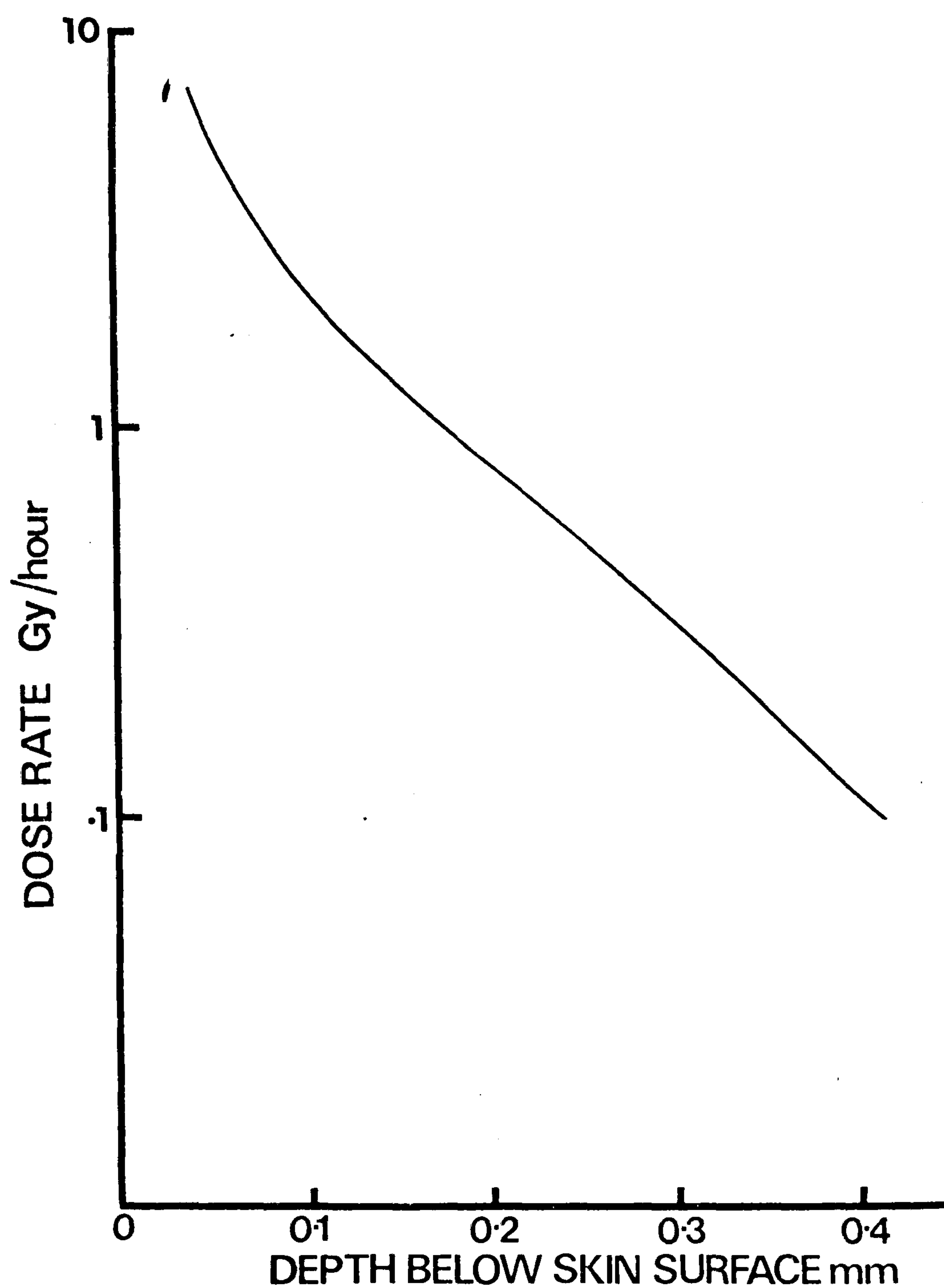


Figure 4.12 Variation of dose rate with depth below skin surface for an infinitely thin source of ^{133}Xe of 4.0 MBq cm^{-2} lying on the skin surface.

CHAPTER 5SKIN BLOOD FLOW - MODEL OF XENON-133 CLEARANCE

5.1 INTRODUCTION

5.2 MODEL GEOMETRY AND TISSUE LAYERS

5.3 THICKNESS OF THE TISSUE LAYERS

5.4 SOLUBILITY AND PARTITION COEFFICIENTS

5.5 DIFFUSION COEFFICIENTS

5.5.1 Method of measurement of diffusion coefficients

5.5.2 Diffusion coefficient in the epidermal barrier

5.5.3 Diffusion coefficient in dermis

5.5.4 Diffusion coefficient in subcutaneous fat

5.6 BLOOD FLOW TERM

5.7 SUMMARY OF THE COMPUTER PROGRAM

5.7.1 Evaluation of the accuracy of the program

5.1 INTRODUCTION

In the preceding chapters the mathematical equations describing heat and matter transfer and the practical techniques involved in the assessment of skin blood flow were presented. The present chapter now deals with the particular model used to represent the clearance of Xenon-133 from the skin. The tissue layers and their geometrical arrangement are outlined in section 5.2 and the derivation of the various parameters required to characterise each tissue follows in sections 5.3 to 5.5. These parameters, tissue thickness, solubility and diffusion coefficient of Xenon-133 are not, of course, constants but may vary between sites of the body and in particular in pathological conditions. The computer program into which these are introduced is detailed in section 5.6 and finally an assessment of the accuracy of the program is made.

5.2 MODEL GEOMETRY AND TISSUE LAYERS

Although it is possible to produce a three dimensional model of the skin it is, of course, preferable to use a simpler model if this will suffice. In the present context the skin is essentially made up of very thin layers. In addition in the application of ^{133}Xe by the epicutaneous diffusion technique a labelled region is produced which is also very thin compared to its diameter. Therefore, assuming that the skin is not highly anisotropic, diffusion in the direction normal to the skin surface will be the dominant process and a one dimensional

model, using the simple finite difference formulae of section 3.5, will be acceptable.

For application of the model four distinctly different layers can be identified (Figure 5.1); the external environment, the epidermal diffusion barrier, the dermis and the subcutaneous fatty tissue.

(a) the external environment - During application of the chamber to the surface of the skin this layer represents a saline solution, in which the ^{133}Xe is initially dissolved. After the chamber is removed this layer has the characteristics of air.

(b) the barrier layer of the epidermis - It is known (Berenson and Burch, 1951; Blank, 1953; Scheuplein and Blank, 1971) that a considerable resistance to the passage of materials exists within the epidermis. The location of this barrier layer has been shown to be the stratum corneum (Scheuplein and Blank, 1971), although this was disputed by Sejrsen (1968) who claimed that the resistance to ^{133}Xe existed within the middle third of the epidermis. This claim was based on his observations that, on successive removal of thin layers of the epidermis, its permeability remained almost constant until the middle one-third was removed. The same result has previously been reported by Blank (1951) but, as will be seen in the next chapter, such a conclusion is based on a misunderstanding of the mathematics of diffusion. In fact the barrier layer appears to be the stratum corneum and this is a uniformly good barrier.

<u>Air</u>	<u>Saline</u>	<u>Epidermal barrier</u>	<u>Dermis</u>	<u>Fatty tissue</u>
> 10 cm	2 mm	face, upper arm and leg	16 μ m	1.5 mm
		trunk	- 16 μ m	2.0 mm
		back of hand, lower arm and leg	- 30 μ m	1.5 mm
		palms, fingers, soles	- 100 μ m	1.5 mm
				> 2 mm

Fig. 5.1 Thickness of the layers used in the model

(c) the dermis - This layer includes not only the dermis but also the lower, viable part of the epidermis which has diffusion properties similar to dermis (Scheuplein, 1978). Although this part of the epidermis is avascular, its role will be minimal due to its small thickness and relatively high diffusion coefficient. The whole layer is therefore assumed to have uniform vascularity, as proposed by Sejrsen (1971).

(d) the subcutaneous fatty tissue - Although generally made up of fatty globules this layer is assumed to be homogeneous and credited with a uniform capillary blood flow as reported by Larsen and Lassen (1967).

5.3 THICKNESS OF THE TISSUE LAYERS

The thickness of each of the layers making up the skin varies according to age, sex, site of the body and from one individual to another (Southwood, 1955). In general, however, the values obtained from normal skin at a particular site fall within a particular range and the means of these are shown in Figure 5.1. The figures have been taken from several publications (Southwood, 1955; Whitton and Everall, 1972; Holbrook and Odland, 1974; Scheuplein, 1978c). Only normal skin is considered in the present study but a direct result of some pathological conditions is an alteration in the skin thickness (Rook et al, 1972) and this would need to be taken into account in the investigation of such situations.

By far the greatest thickness of the epidermal barrier occurs on the surfaces of the hands, fingers and

soles of the feet with regional variation in other areas being minor in comparison. In contrast, the dermis is thickest on the trunk, particularly the back but the range of variation is less than that found in the epidermis. The mean values quoted conceal a range of thicknesses, for example in the leg, of from one to two millimetres. The dermis is thicker in men than in women and the maximum value is achieved in middle age.

The subcutaneous fatty tissue is fairly evenly distributed in men but in women tends to be concentrated more in specific areas. For the purposes of the present model, however, a thickness in excess of two millimetres is presumed since variation in this has little effect on the overall result.

The solution of ^{133}Xe in saline is applied to the skin inside the chamber, the depth of which is two millimetres. After removal of this the surface of the epidermis is then in contact with the air which is effectively of infinite thickness.

5.4 SOLUBILITY AND PARTITION COEFFICIENTS

The Ostwald solubility coefficient of a gas is defined as

"the ratio of the volume of the gas absorbed to the volume of the absorbing material, at any specified temperature and pressure".

This is in reality an equilibrium constant and a comprehensive review for most biological gases has been published by Steward et al (1973). Its value for Xenon

has been measured for a variety of tissues and biological materials (Conn, 1961; Yeh and Peterson, 1963; Veall and Mallett, 1965; Ladefoged and Andersen, 1967; Andersen and Ladefoged, 1967) but it has not been determined for any of the layers of the skin. An alternative to direct measurement was described by Yeh and Peterson (1965) who showed that the solubility coefficient could be calculated from the amount of protein, lipid and water in the tissue and the solubility of Xenon in each of these components or, in equation form.

$$\begin{aligned}
 & \text{(solubility coefficient of } ^{133}\text{Xe in tissue)} \\
 & = \left(\begin{array}{l} \text{solubility coefficient} \\ \text{of protein} \end{array} \right) \times \left(\begin{array}{l} \text{fraction} \\ \text{of} \\ \text{protein} \end{array} \right) \\
 & + \left(\begin{array}{l} \text{solubility coefficient} \\ \text{of lipid} \end{array} \right) \times \left(\begin{array}{l} \text{fraction} \\ \text{of} \\ \text{lipid} \end{array} \right) \\
 & + \left(\begin{array}{l} \text{solubility coefficient} \\ \text{of saline} \end{array} \right) \times \left(\begin{array}{l} \text{fraction} \\ \text{of} \\ \text{saline} \end{array} \right)
 \end{aligned}$$

The values of the solubility coefficients for each of these components, obtained from the above papers, are shown in Table 5.1. The composition of most tissues of the body has also been well documented (Spector, 1956), and the constituents of the layers of the skin are shown in Table 5.2. Although only a single set of figures is quoted for the epidermal barrier, the water content of this layer decreases gradually towards the surface, while at the same time the lipid content increases (Schmidt-Nielsen, 1952; Reinerstron and Wheatley, 1959). Some variation in the fat content of the subcutaneous tissue

Table 5.1Solubility coefficients of tissue components

	<u>Saline</u>	<u>Blood</u>	<u>Lipid</u>	<u>Protein</u>
Ostwald solubility coefficient	0.078	0.14	1.8	0.15

Table 5.2Composition of the skin

	<u>Epidermal barrier</u>	<u>Dermis</u>	<u>Subcutaneous fat</u>
% protein	45	27	1
% lipid	15	1	80
% water	40	72	19

from one site of the body to another has also been suggested (Sejrsen, 1971) with the greatest amount being found on the abdomen. The figures shown are considered representative of most areas (Schmidt-Nielsen, 1952; Martinsson, 1967).

The resulting solubility coefficients for each layer of the skin, calculated from Yeh and Peterson's equation, are given in Table 5.3. Obviously the subcutaneous tissue, with its very high lipid content, has a much greater solubility than the other tissues. The reduced water content and increased lipid in the epidermal barrier means that this, too, has a higher solubility than the dermis.

The ability of blood, flowing through a tissue, to extract ^{133}Xe from it depends on the relative solubilities of ^{133}Xe in blood and tissue. In section 3.4.1 the partition coefficient λ_i was defined as "the ratio of the solubility of the inert gas in tissue to the solubility in blood when these are in equilibrium". In other words

$$\lambda_i = \frac{S_T}{S_b}$$

This produces the values shown in Table 5.4 and these are in close agreement with previously reported figures (Sejrsen, 1971). Since the epidermal barrier is avascular this term is not, of course, applicable to it. The partition coefficient is often modified in order to express the blood flow in ml/100g tissue/min (see equation

Table 5.3Solubility coefficients in the skin

	<u>Epidermal barrier</u>	<u>Dermis</u>	<u>Subcutaneous fat</u>
Ostwald solubility coefficient	0.37	0.11	1.4

Table 5.4Partition coefficients in the skin

<u>Epidermal barrier</u>	<u>Dermis</u>	<u>Subcutaneous fat</u>
not applicable	0.78	10.0

4.2) and strictly this requires that

$$\lambda^{\circ}_i = \frac{S_T}{\rho_T S_b}$$

where ρ_T is the density of the tissue.

In the present study, however, ρ_T will be assumed to be equal to one, which introduces a negligible error into the calculations (Spector, 1956).

5.5 DIFFUSION COEFFICIENTS

Although Scheuplein and Blank (1971) have shown that simple diffusion equations can be used to describe the passage of materials through the skin it is surprising how few direct measurements of diffusion coefficients in the skin have been made. Indeed despite the importance of diffusion of gases to the understanding of many biological processes, including tissue blood flow measurements, data on diffusion coefficients in any organ is rather sparse. The values, for ^{133}Xe , for a few tissues have been measured by a technique first described by Unsworth and Gillespie (1971; Evans et al, 1974; Strang, 1977). In this method a thin excised specimen of the tissue is firstly exposed to ^{133}Xe until it is saturated and then on exposure to fresh air the rate of clearance of the ^{133}Xe is monitored. From previously published diffusion equations describing such a situation, Unsworth and Gillespie showed how the diffusion coefficient could be obtained from the final steady exponential rate of clearance of the ^{133}Xe . However no studies of the diffusion of ^{133}Xe in skin have been re-

ported.

In the present study then it has been necessary to compute diffusion coefficients for each of the layers of the skin. In the case of the fatty tissue this has been extrapolated from previously published data on other inert gas systems and for the dermis and epidermal barrier these have been measured by an initial transient method. A summary of the diffusion coefficients is given in Table 5.5. The coefficients for water ($1.5 \times 10^{-5} \text{ cm}^2 \text{ s}^{-1}$) and air ($0.07 \text{ cm}^2 \text{ s}^{-1}$) have been taken from published results (Unsworth and Gillespie, 1971; CRC Handbook of Chemistry and Physics, 1972).

5.5.1 Method of measurement of diffusion coefficients

The method of Unsworth and Gillespie (1971) was unsuitable in the present study for two reasons. Firstly it requires an excised specimen of only a single tissue. Unfortunately the stratum corneum is both extremely thin and ridged and special chemical techniques are required in order to separate it from the dermis (Holbrook and Odland, 1974). It is doubtful whether the structural and functional integrity of this layer, particularly its diffusion properties, would be preserved following this separation process. Secondly Unsworth and Gillespie's (1971) method uses the rate of clearance of ^{133}Xe from the tissue once this has reached a steadily falling mono-exponential phase. However Scheuplein (1978) has shown that although the appendages of the skin, i.e. hair follicles, sweat glands, etc., have little effect on the overall rate of diffusion through the epidermis once a

TABLE 5.5Diffusion Coefficients of ^{133}Xe in the Skin

	<u>Diffusion Coefficient</u> <u>$\text{cm}^2 \text{s}^{-1}$</u>
Air	0.07
Water	1.5×10^{-5}
Epidermal barrier	
"thin" epidermis	1.3×10^{-9}
"thick" epidermis	1.0×10^{-8}
Dermis	0.4×10^{-5}
Subcutaneous fat	0.4×10^{-5}

steady state has been reached, in the initial stages their role is more significant. The time taken to reach a steady state for the epidermis is of the order of several minutes and since the epicutaneous application of ^{133}Xe takes only three minutes it was felt that perhaps a diffusion coefficient which was measured over this short time scale would be more relevant.

Thus, using the technique of the epicutaneous application of ^{133}Xe , with the gas dissolved in saline and contained in a chamber attached to the surface of the tissue, the solution was left in contact with either the epidermis or the dermis for periods of three minutes and five minutes. After these times the ^{133}Xe was sucked back out of the chamber and any excess wiped away. The activity remaining was measured and expressed as a percentage of the original depot. This was carried out on different skin areas using either excised full thickness skin samples or in vivo in limbs with the blood flow occluded by means of a tourniquet. The measurements on the dermis were, of course, carried out on excised samples with the epidermis stripped off. The finite difference computer model was then used to calculate the expected rate of transfer of ^{133}Xe into tissues for different values of the diffusion coefficient, using the same chamber thicknesses as in the experimental situation. A plot of this was produced and by comparing the experimental results with it, the true diffusion coefficient of the tissue was obtained.

5.5.2 Diffusion coefficient in the epidermal barrier

Figure 5.2 shows the percentage of ^{133}Xe which in theory will enter the skin from the ^{133}Xe solution for different thicknesses of the epidermis corresponding to the "thick" epidermis of the fingers (100 μm) and the "thin" epidermis (15 μm) found on most areas of the body (Fig. 5.1). For each of these areas five measurements were carried out and, for 3 minutes of diffusion from 0.9% to 1.6%, average 1.1%, was found to be retained in the skin in "thin" areas after removal of the chamber and from 2.8% to 3.5%, average 3.0%, in "thick" areas. This therefore corresponds to diffusion coefficients of $1.3 \times 10^{-9} \text{ cm}^2 \text{ s}^{-1}$ for areas covered by epidermis 15 μm thick and $1.0 \times 10^{-8} \text{ cm}^2 \text{ s}^{-1}$ for the thicker epidermal barrier found in the hands, fingers and soles. Thus the increased thickness of the barrier found in some areas is partly offset by a reduction in diffusion coefficient, which agrees with the observations of Scheuplein and Blank (1971) on the permeability of the epidermis to water.

Because the epidermis does not have a flat surface, particularly on the fingers, it might be expected that some of the ^{133}Xe left after the three minute labelling period was simply retained in the "grooves" and had not, in fact, diffused into the tissue. Such a process would result in a relatively large amount of ^{133}Xe being detected after very short labelling periods of only a few seconds. In addition such a background would

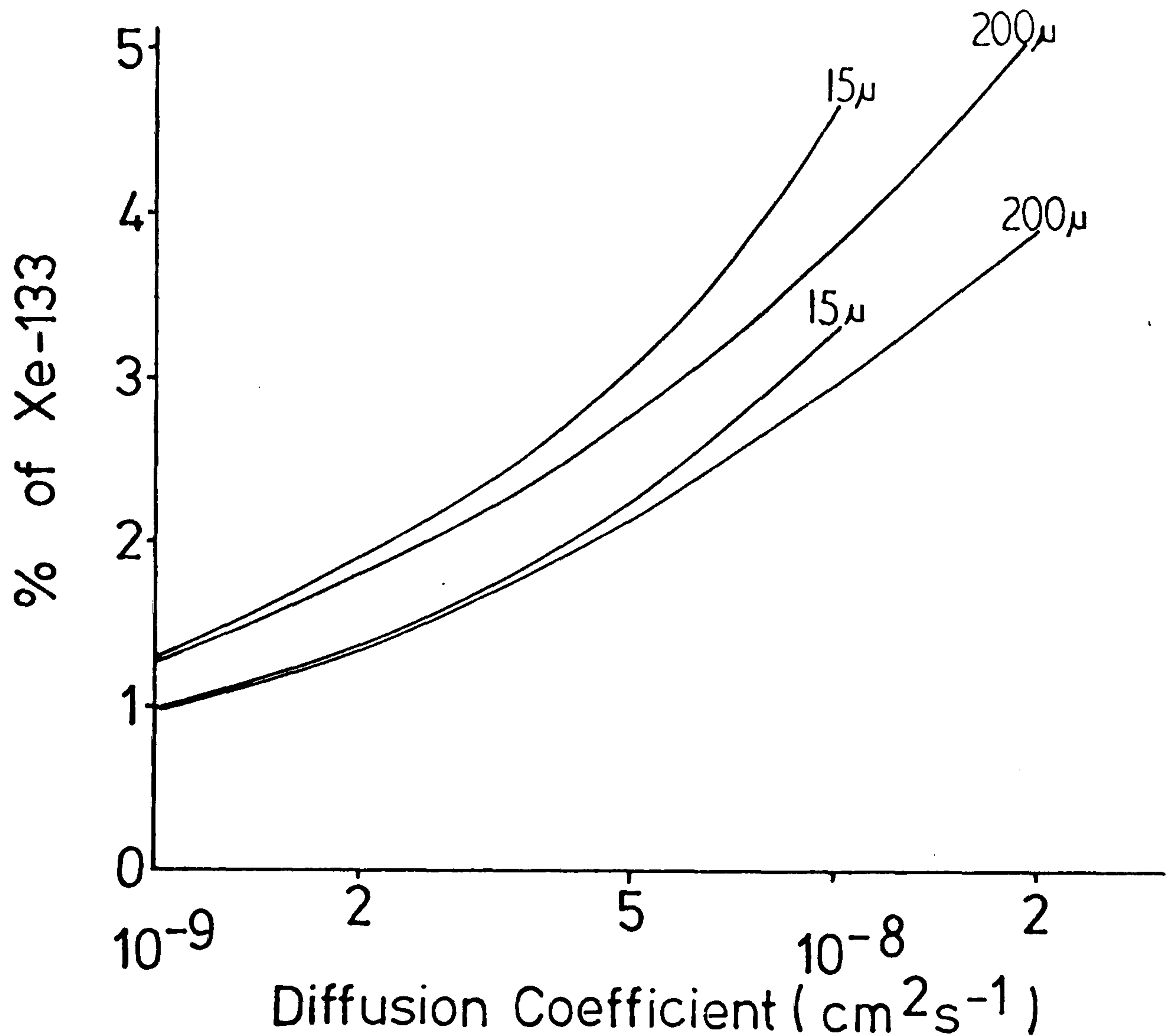


Figure 5.2 The amount of ^{133}Xe which enters the skin by diffusion as a percentage of the amount in a 2 mm thick chamber of ^{133}Xe in saline placed on the surface of the epidermis. The upper curves represent 5 mins. of application and the lower, 3 mins. The data is calculated for two thicknesses of epidermis, 15 μm and 200 μm . The diffusion coefficient of the epidermis is plotted on a log scale.

produce a higher value for the diffusion coefficient assessed at three minutes compared to that assessed at five minutes. That neither of the above are found in practice suggests that this retention of ^{133}Xe in the grooves of the skin is not significant. Even if it did occur it would result in an overestimate of the diffusion coefficient for the epidermis which, as will be seen in chapter 6, could only lead to ^{the} conclusions obtained in this study being an underestimate of the true effects.

An apparent anomaly was found when the amount of ^{133}Xe which enters the skin after five minutes of diffusion was considered. In this case 1.8% and 4.5% of the ^{133}Xe respectively was retained, which now corresponds to diffusion coefficients of $1.75 \times 10^{-9} \text{ cm}^2 \text{ s}^{-1}$ for "thin" areas and $2.0 \times 10^{-8} \text{ cm}^2 \text{ s}^{-1}$ for "thick" areas. This apparent increase in the diffusion coefficient is most likely to be due to the fact that the ^{133}Xe was dissolved in saline and therefore not only the gas but also water was diffusing into the dermis. Although the diffusion coefficient of water is at least an order of magnitude lower than that of Xenon (Scheuplein and Blank, 1971) this will still lead to increased hydration of the upper parts of the stratum corneum. This increased hydration in turn results in an increased diffusion coefficient (Blank et al, 1967).

Since a diffusion time of three minutes has been adopted in the present study as a compromise between the amount which enters the skin and radiation dose delivered

to it, the diffusion coefficients corresponding to this time have also been adopted.

5.5.3 Diffusion coefficient in dermis

Because of the greater thickness of the dermis the amount of ^{133}Xe which enters it in a three minute period is independent of any variation in this thickness over the typical range reported in section 5.3. Thus Figure 5.3 shows the percentage retained against diffusion coefficient for only one thickness of the dermis and therefore only a single value of the diffusion coefficient is used for all areas of the body. It was found that for the excised specimens, taken mainly from the groin and breast, on average 12% of the ^{133}Xe depot entered the dermis during the diffusion period. This corresponds to a diffusion coefficient of $0.4 \times 10^{-5} \text{ cm}^2 \text{ s}^{-1}$. This is in close agreement with the values obtained in other tissues of the body such as muscle (Unsworth and Gillespie, 1971; Sejrsen and Tonnessen, 1968).

5.5.4 Diffusion coefficient in subcutaneous fat

The measurement of this coefficient by the foregoing method is more difficult due to the globular nature of fat. However, Yeh and Peterson have shown that, for temperatures near body temperatures, the physical properties such as viscosity, density and solubility of animal fat are essentially the same as vegetable fats. Thus it is common practice to obtain data from a representative substance and to consider this applicable to

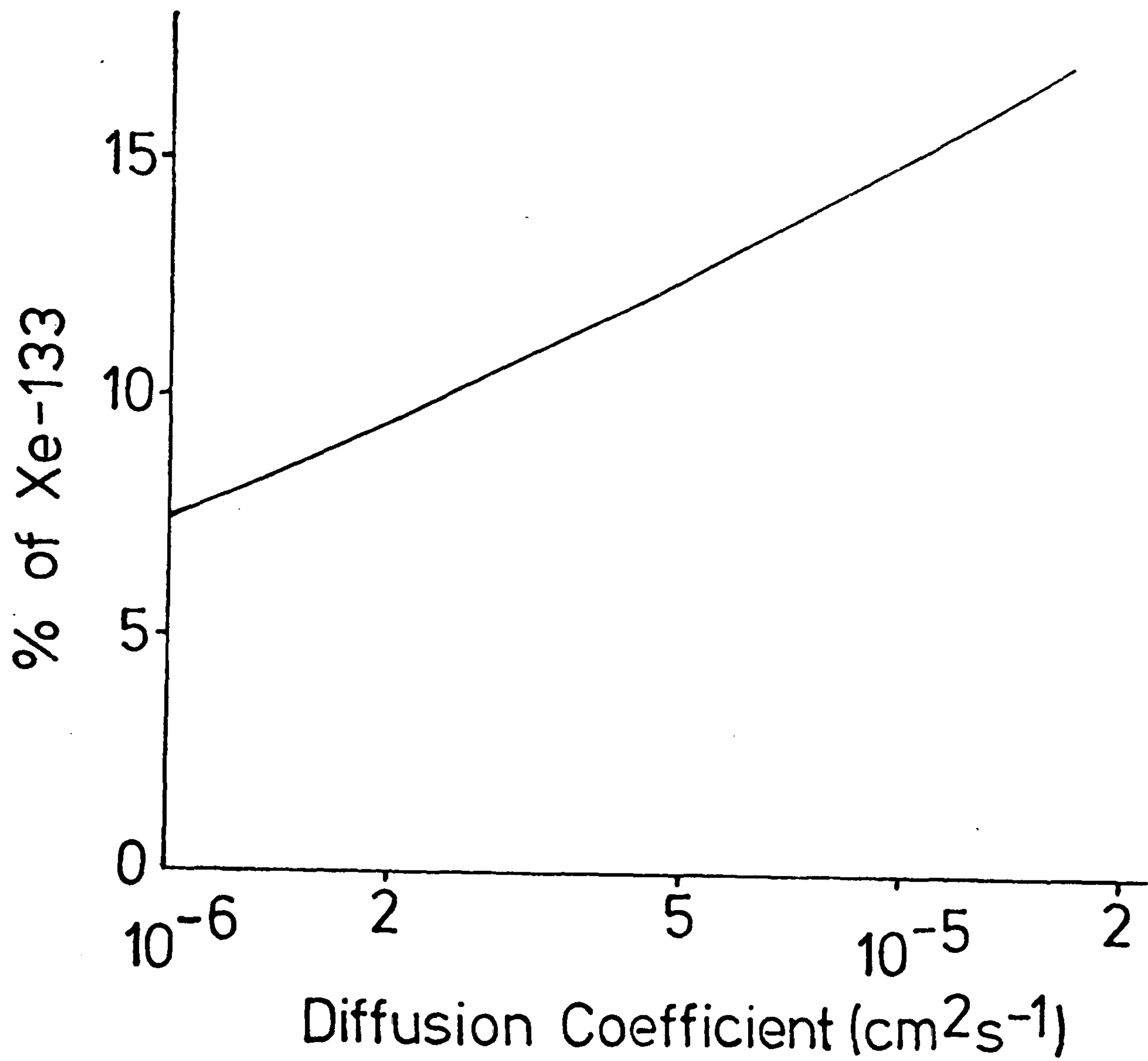


Figure 5.3 The percentage of ^{133}Xe which enters the dermis from a 2 mm depot placed on its surface for a diffusion time of 3 minutes, plotted against the diffusion coefficient of the dermis.

the corresponding fatty tissue material within the body. In studies of the inert gas system olive oil has been used almost exclusively (Osburn et al, 1969). For this reason Davidson et al (1952) measured the diffusion coefficient of several gases in this substance and for nitrogen, for example, found a value of $7.6 \times 10^{-6} \text{ cm}^2 \text{ s}^{-1}$ at 37°C . For inert, non-polar gases Unsworth and Gillespie (1971) have shown in tissue that Graham's Law, which states that the diffusion coefficient is proportional to the inverse square root of the molecular weight of the gas, is valid. On this basis a value of $0.37 \times 10^{-5} \text{ cm}^2 \text{ s}^{-1}$ for the diffusion coefficient of ^{133}Xe in olive oil can be obtained and hence in subcutaneous fatty tissue the same value as that of the dermis, i.e. $0.4 \times 10^{-5} \text{ cm}^2 \text{ s}^{-1}$ has been adopted. This value is consistent with the results of Perl et al (1965).

It is again stressed that all of the above values are bulk diffusion coefficients for the tissues and no attempt has been made to distinguish between intra- and extra-cellular diffusion. There have been widely conflicting reports concerning the magnitude of the diffusion coefficient of substances within cells as mentioned in section 2.2 but there is no doubt that such bulk diffusion coefficients adequately describe the diffusion of a gas in a tissue on a scale above the cellular level (Unsworth and Gillespie, 1971).

5.6 BLOOD FLOW TERM

The simulation of the removal of ^{133}Xe from the

dermis and subcutaneous tissue by their capillary blood flows is achieved using equation 3.6, which shows that at any time the rate of removal is proportional to the amount of ^{133}Xe remaining in the tissue. In other words at the end of each time step in the finite difference model the partial pressure is reduced by a constant fraction given by

$$k_i \Delta t$$

which is equal to

$$\frac{f_i l}{100 \lambda_i}$$

where l is the time step

f_i is the blood flow in ml/100g/min

and λ_i is the partition coefficient taken from Table 5.4.

In terms of the finite difference formulae the partial pressure is then written as

$$P_{i,k+1} = P_{i,k} - \frac{f_i l}{100 \lambda_i} P_{i,k} \quad (5.1)$$

Additionally in order to take account of the transfer of ^{133}Xe which it was suggested occurred between the venous blood, draining the dermis, and the subcutaneous tissue the partial pressure of the latter is increased at the end of each time step by an amount proportional to that removed from the dermis, i.e.

$$P_{i,k+1} \Big)_{sc} = P_{i,k} \Big)_{sc} + E \frac{S_D h_D}{S_{sc} h_{sc}} P_{i,k} \Big)_{D}$$

where E is the fraction of ^{133}Xe transferred

s_c and D relate to subcutaneous and dermis

respectively

h is the thickness of the tissue

s is its solubility

and ΔP is as described in the previous equation.

5.7 SUMMARY OF THE COMPUTER PROGRAM

With the characteristics of the tissue layers thus defined, substitution of the values into the computer program, based on the finite difference approximations, allowed the calculation of the partial pressure of ^{133}Xe at any time throughout the tissue. The steps involved in the computer program are summarised here.

(a) After input of the characteristic constants the initial values of the partial pressure of ^{133}Xe were attributed to each nodal point. In general the partial pressure was zero throughout except in one layer where the ^{133}Xe was initially deposited. For each situation investigated the particular initial conditions will be indicated.

(b) At a time equal to one time step later the partial pressure at each point was altered by a certain fraction corresponding to the effect of the capillary blood flow (equation 5.2).

(c) Using the finite difference approximations of the diffusion equation (equation 3.14) and boundary conditions (equation 3.16) the new partial pressure, due

to diffusion, at the points within each tissue, at points near the boundary and then at the boundary points were calculated in turn.

(d) The total amount of ^{133}Xe within each tissue was then computed and the amount detected by the radiation detector calculated.

(e) The above processes were then repeated for each time step until the required total time was reached.

A full listing of the program, which was written in FORTRAN, and run on PDP 11 and Data General NOVA mini-computers, is given in Appendix C.

5.7.1 Evaluation of the accuracy of the program

As mentioned in section 3.5.5 an evaluation of the accuracy of the finite difference approximation is desirable and this can be carried out by comparison with a known analytical solution. In the present case the following initial conditions were used

$$\begin{aligned} P &= P_0 \quad \text{for } x < 0 \\ P &= 0 \quad \text{for } x > 0 \end{aligned}$$

For $x < 0$ medium 1 had a solubility of 0.1 and diffusion coefficient $0.4 \times 10^{-5} \text{ cm}^2 \text{ s}^{-1}$ while for $x > 0$ medium 2 had a solubility of 0.3 and diffusion coefficient $1.0 \times 10^{-9} \text{ cm}^2 \text{ s}^{-1}$. These values were similar to those used in the model of skin as were the distance and time steps. The solution to this has been given by Crank (1975 p37) as

$$C_2 = \frac{\frac{S_2}{S_1} k C_0}{1 + \frac{S_2}{S_1} x (D_2/D_1)^{1/2}} \operatorname{erfc} \frac{|x|}{2 \sqrt{D_2 t}} \quad (5.2)$$

where C_2 is the concentration in medium 2

C_0 is the concentration in medium 1 at time zero.

This function is plotted in Figure 5.5 for a total time of 60 minutes. The percentage error in individual points was assessed from

$$\frac{\text{analytical value} - \text{finite difference value}}{\text{analytical value}} \times 100$$

and was found to be about 4% for points close to the boundary and less than 1% for points further away, but still within diffusion distance. Similarly, by differentiating equation 5.2 the flux over the boundary was calculated and the total amount which passed from medium 1 to medium 2 obtained. Comparison with the exact values showed the finite difference method to be in error by less than 1% after 30 minutes of diffusion and by 1.6% at 60 minutes.

It is unlikely in any biological investigation to be able to obtain data with uncertainty less than the above figures (Glass and de Garreta, 1967) and in the present study the statistical uncertainty of the data points of a clearance curve were at least this order of magnitude. It was therefore considered that the error introduced by the finite difference approximations was not sufficiently great to affect the results of the study.

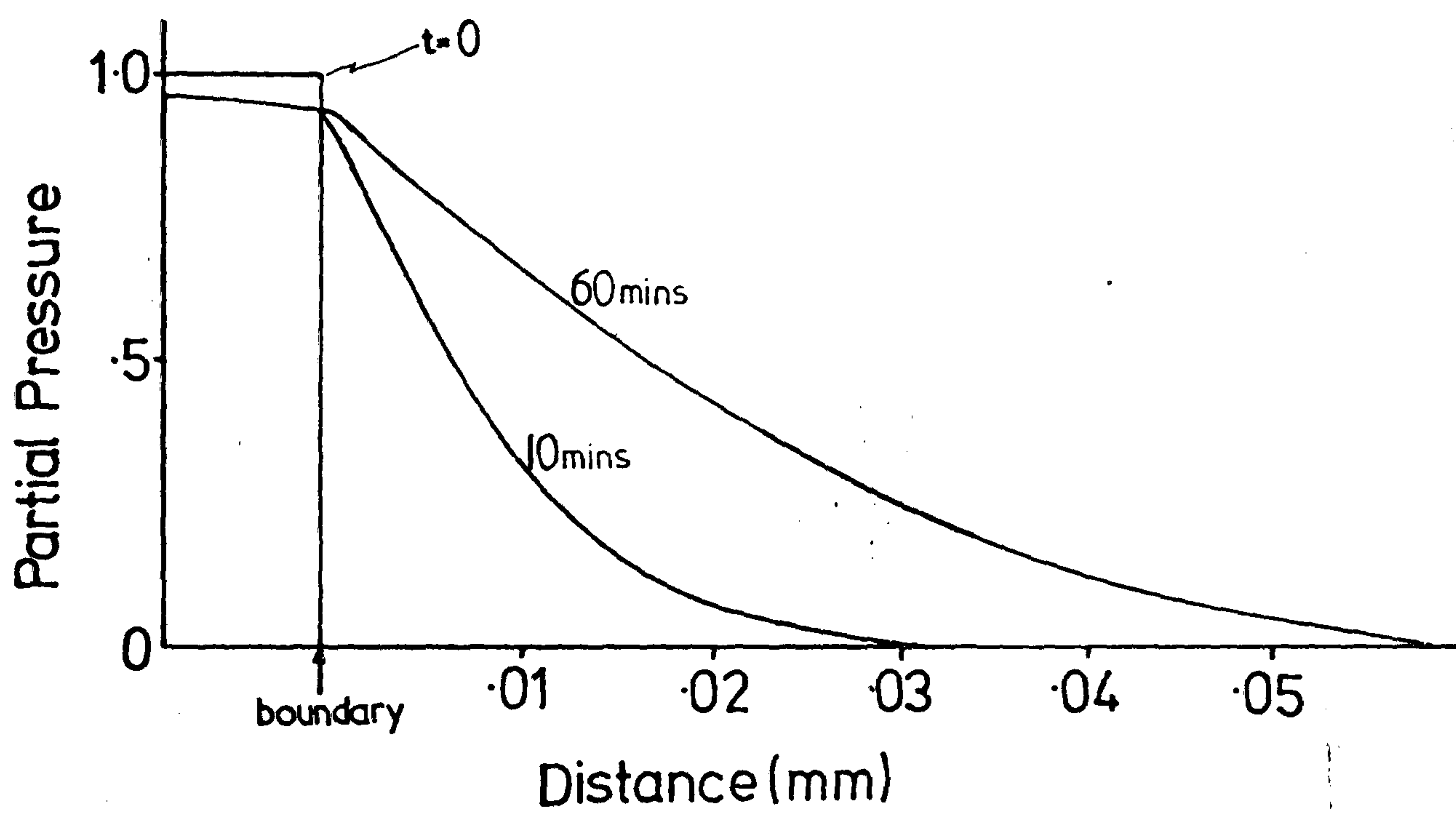


Figure 5.4 Model used to assess the accuracy of the finite difference computer program. The relative partial pressure is plotted against distance from the boundary between the two media, for the initial distribution and for 10 mins. and 60 mins. later.

CHAPTER 6SKIN BLOOD FLOW - RESULTS AND DISCUSSION

6.1 INTRODUCTION

6.2 EXCHANGE OF ^{133}Xe BETWEEN BLOOD VESSELS AND TISSUE

6.2.1 Model and results

6.2.2 Discussion

6.3 DIFFUSION OF ^{133}Xe IN SKIN6.3.1 Diffusion between dermis and subcutaneous
tissue

6.3.2 Diffusion within and through the epidermis

6.4 THE INFLUENCE OF BLOOD FLOW ON THE CLEARANCE CURVES

6.4.1 Relationship between blood flow and clearance
rate - intracutaneous labelling6.4.2 Relationship between blood flow and clearance
rate - epicutaneous labelling

6.5 CONCLUSIONS

6.1 INTRODUCTION

In this chapter the predictions of the mathematical models of ^{133}Xe transport within and out of skin are presented and are compared with the corresponding experimental results. The profiles of partial pressure in the skin layers are illustrated for various situations and, where necessary, the concentration profiles are also given. The concentration profiles are discontinuous at the boundaries between the layers, due to the different solubilities, but give a clearer picture of the relative amounts of ^{133}Xe in each layer. The predicted clearance curves, obtained by summing the amount of ^{133}Xe within all of the skin layers at each time, are also presented.

First of all, section 6.2 looks at the exchange of ^{133}Xe between the blood vessels and tissue and attempts to identify which blood vessels play an active part in the clearance of ^{133}Xe from the skin. In particular the role of blood vessels larger than capillaries is investigated. Various aspects of the bulk diffusion of ^{133}Xe within the skin layers are then considered, in the absence of blood flow, in section 6.3. In section 6.4 an overall model, including blood flow, is presented and an assessment of the relationship between clearance rate and blood flow is made. A discussion of the significance of the results is given as each model is presented and finally a summary of the findings is given in section 6.5.

6.2 EXCHANGE OF ^{133}Xe BETWEEN BLOOD VESSELS AND TISSUE

Both Sejrsen (1971) and Challoner (1973) have demonstrated that, after depositing ^{133}Xe in the dermis, the amount found within the subcutaneous fatty tissue at subsequent times is greater in the presence of blood flow than without it. They have postulated that this is due to the loss of ^{133}Xe from the venous blood draining out of the dermis and passing through the subcutaneous tissue. While this is compatible with the experimental findings of other workers in other tissues, as detailed in section 2.2, neither Sejrsen nor Challoner discussed the full implications of this transfer. In particular it is certainly conceivable that if this happens in the subcutaneous tissue then it might also take place in the small veins of the dermis. Thus any ^{133}Xe deposited in the upper layers of the dermis could be cleared from this area by the blood flow only to re-enter the dermis at a lower level. The rate of clearance of the ^{133}Xe monitored by a radiation detector would not then be related to the blood flow in the normal way since the ^{133}Xe would effectively be counted more than once. Since no mathematical treatment of this problem has been previously reported it was therefore felt necessary to attempt an assessment of the relative importance of different blood vessels in exchanging ^{133}Xe .

6.2.1 Model and results

The mathematical description of the exchange of ^{133}Xe between a blood vessel and tissue has been

discussed in section 3.4.2 and can be described by equation 3.10. In the present case P_{tissue} , which is the partial pressure away from the blood vessel, is assumed to be zero, which reflects the situation when blood draining from a labelled region passes through a tissue which is not initially labelled. It is evident that the assumption is also being made that the effect of other draining veins on the tissue concentration is negligible. In addition to this the model is applicable only to tissues whose characteristics are similar to those of blood, which is true for the dermis but not for fat, and this will be discussed later. Thus the ratio of $\frac{P_{\text{out}}}{P_{\text{in}}}$ is plotted in Figure 6.1 against $\frac{L}{\bar{v}r^2}$. Alternatively the ordinate is labelled to show the percentage loss of ^{133}Xe from blood as it passes down a blood vessel of radius r cm and length L cm at a mean velocity \bar{v} cm s⁻¹. The loss is 100% when the vascular parameters combine to produce a value for $\frac{L}{\bar{v}r^2}$ greater than 10^7 s cm⁻² and therefore for all such vessels complete exchange will take place between the blood and tissue. For values lower than this the loss drops gradually to zero.

In order to assess the significance of these results, typical blood vessel characteristics have been obtained from the literature (Whitmore, 1968; Folkow and Neil, 1971; Burton, 1972) and are shown in Table 6.1 along with the respective values of $\frac{L}{\bar{v}r^2}$ and hence the calculated loss of ^{133}Xe from such vessels. The reported characteristics of the small arteries and veins at the base of the

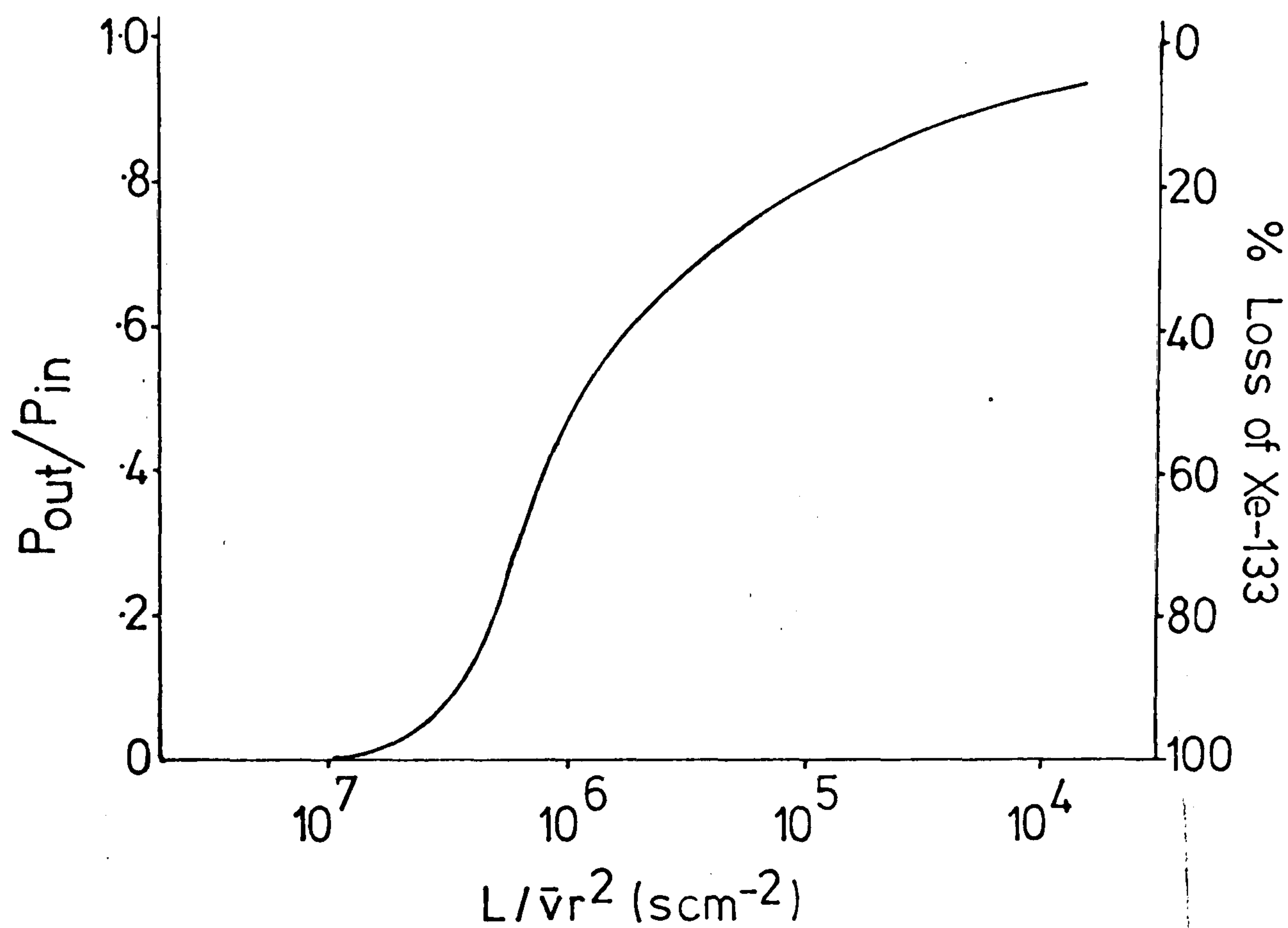


Figure 6.1 The ratio of the partial pressure of ^{133}Xe in the blood flowing out of a blood vessel to that flowing into the vessel plotted against $L/\bar{v}r^2$ where L is the length of the vessel, r the radius and \bar{v} the flow velocity. Alternatively the percentage loss of ^{133}Xe while passing through such a blood vessel is also shown. The tissue partial pressure is assumed to be zero.

dermis are also included (see section 1.4.4). It is emphasised that the values quoted are by no means an accurate representation of all tissues at all times but are simply average values taken from the literature and are an attempt to give a general impression of the relative sizes of the vessels. In particular, variation in the values is caused by changes in the blood flow. For example as the velocity of the blood, and hence the flow, decreases the loss of ^{133}Xe will consequently increase.

In addition the length of the smaller blood vessels (arterioles, capillaries and venules) does not necessarily represent the thickness of the tissue through which they pass, since these vessels are often very tortuous. For instance, most of the capillaries in the skin are formed into loops with the two arms of the loop travelling at 180° to each other.

6.2.2 Discussion

As expected the model predicts that, during passage of blood through a capillary, complete exchange of ^{133}Xe between the blood and the tissue will occur. This means that the concentration of ^{133}Xe in the blood, as it leaves the capillary, will be related to the concentration in the tissue by the partition coefficient, as detailed in section 3.4.1. However it is also seen that some exchange takes place in the arterioles and venules and, to a very limited extent, in vessels of a size corresponding to those found in the lower part of the dermis and the subdermal plexus. Each of these therefore

requires consideration in the overall analysis of the effects of blood flow.

Firstly considering the "sink" function of the blood vessels. The contribution of each type of blood vessel to the removal of ^{133}Xe from a labelled region depends on the exchange which can occur in each individual vessel multiplied by the total flow in vessels of that type within the region. To conserve matter the total flow in capillaries must obviously be equal to the total flow in arteries or any other vessels. The figures in Table 6.1 are therefore representative of the relative importance of each type of blood vessel in removing ^{133}Xe . This means that in a large, uniformly labelled region the exchange vessels are not just the capillaries, although the mathematical description of the clearance will still essentially be the same. The major significance of the above findings is in smaller, non-uniformly labelled regions where, for example, an arteriole may pick up some ^{133}Xe . This would then be deposited further along in the capillary bed, which may lie outside the original labelled region. A similar problem occurs when ^{133}Xe has entered the blood at the capillary level and the subsequent venous blood vessels now become potential "sources".

The magnitude of the above effects is dependent on the size of the labelled region but before discussing this it is worth reflecting on the particular arrangement of the blood supply in the skin (section 1.4.4),

TABLE 6.1

CHARACTERISTICS OF BLOOD VESSEL EXCHANGE

<u>Vessel</u>	<u>Length</u> cm	<u>Internal Radius</u> cm	<u>Velocity</u> cm s ⁻¹	$\frac{L}{vr^2}$ s cm ⁻²	<u>% loss of 133Xe over length of vessel</u>
Aorta	60	1	25	2.4	0
Large Artery	20	0.15	20	44	0
Small Artery	1	0.02	15	166	0
Dermal Artery	0.2	0.005	5	1600	1
Arteriole	<0.2	0.001	1	2x10 ⁵	25
Capillary	<0.05	0.0004	0.05	0.6x10 ⁷	100
Venule	<0.2	0.0015	0.5	1.7x10 ⁵	25
Dermal Vein	0.2	0.006	1	5.5x10 ³	5
Small Vein	1	0.05	2	200	0
Large Vein	20	0.25	5	64	0
Vena Cava	60	1.2	10	4.2	0

in which most of the small arteries, etc., lie at 90° to the surface except in well defined horizontal plexuses found at certain levels. This means that, with the labelling techniques used in the present study, it is unlikely that an arteriole or small artery will pass through a high partial pressure region, and then enter one with a lower partial pressure, at least in the initial stages. This however may be a possibility in the later stages of clearance when most of the ^{133}Xe is in the subcutaneous fatty tissue. For this reason the transfer by small arterial vessels has been neglected. In contrast the venous blood vessels will tend to pass from regions of high to those of low partial pressures.

The potential of the venous blood vessels to act as sources of ^{133}Xe can be envisaged in the following way. Consider a uniformly labelled region, A, situated next to a non-labelled region, B, as shown in Figure 6.2. If ^{133}Xe is removed from the tissue and enters the blood at point C within the labelled region it will be carried through the venous circulation and eventually cross the interface into region B. At that point it will be within a particular size of venous blood vessel and this size will essentially be determined by the distance of point C from the interface. Now it can be seen from Table 6.1 that for a loss of ^{133}Xe , from the vessel, to occur within the non-labelled region then the ^{133}Xe must either be in a capillary, a venule or a small dermal vein. The lengths of these vessels are <0.5 mm,

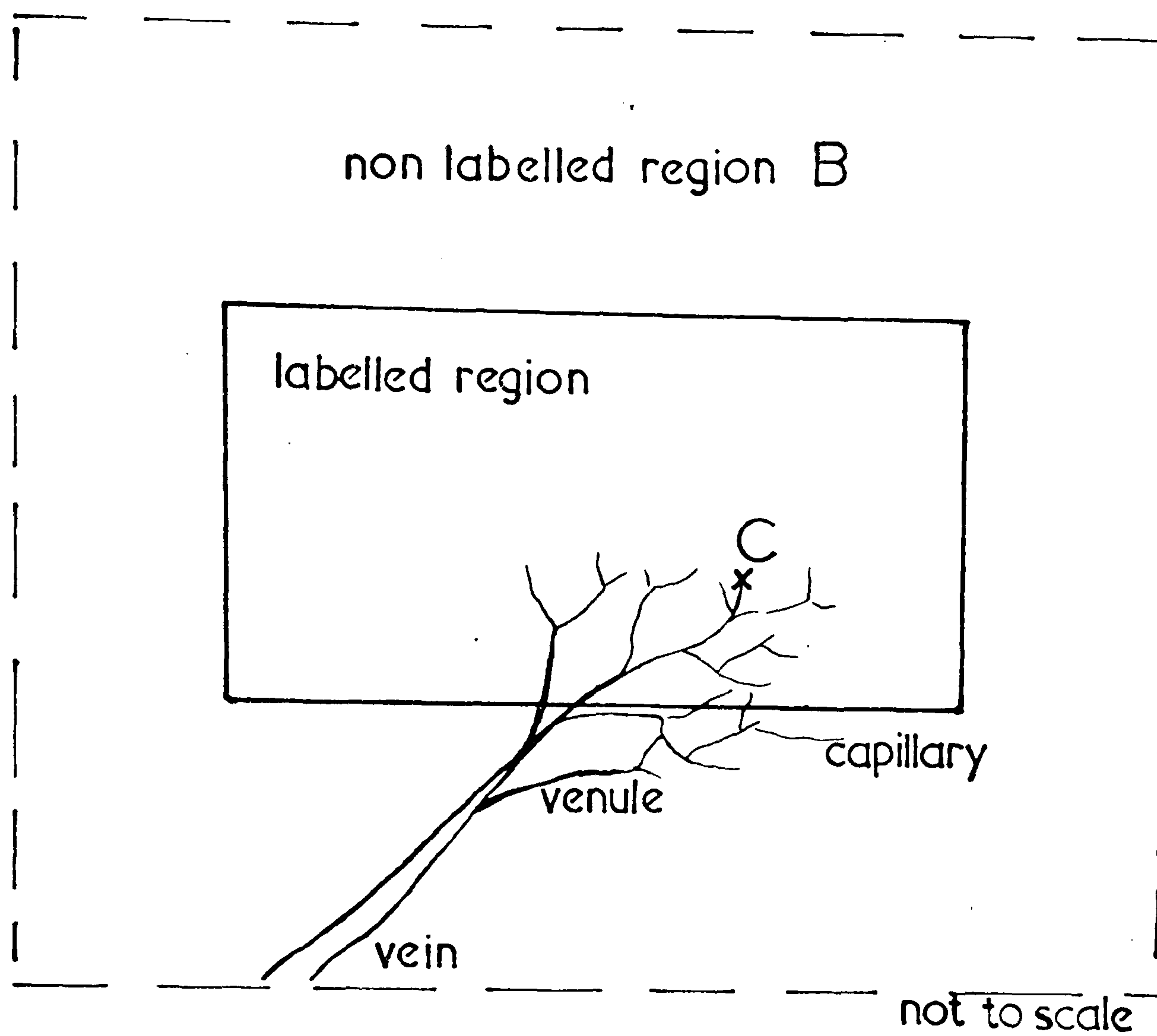


Figure 6.2 Diagram of the transport of ^{133}Xe within the venous circulation.

<2 mm and approximately 2 mm respectively although again it should be remembered that the capillaries, in particular, are often quite tortuous and randomly orientated (Bassingthwaite, 1970). The figures for the loss of ^{133}Xe given in Table 6.1 were calculated for the total length of the particular vessel. In the present example however only part of the vessel may, in fact, be within the non-labelled region and therefore for the venules and dermal veins the total loss would be less than that shown in Table 6.1. Thus, taking all of these factors into consideration, it is suggested that in order for any ^{133}Xe , which is picked up at point C, to be transferred by a capillary and re-deposited in region B, then point C must be within about 0.25 mm of the interface. Similarly for loss of ^{133}Xe from a venule to occur, then point C must be less than 1 mm from the interface and for a small dermal vein less than 2 mm. It is clear that in the case of capillaries, for such a transfer process to be significant then a significant proportion of the total volume of the labelled region must be within 0.25 mm of the interface, i.e. the labelled region must be this order of magnitude in size. Again similar conclusions can be drawn for the venules and small dermal veins where the labelled region must be of the order of 1 mm and 2 mm respectively. It should be stressed that the above figures relate to an idealised situation of a labelled tissue adjacent to a non-labelled one. In practice a smoother concentration gradient will be

achieved and so the transfer will be less than has been inferred above, particularly for capillaries.

For most tissue blood flow measurements by inert gas clearance methods the labelled volume has dimensions greater than those mentioned above and such a transfer process has, quite rightly, been ignored. Unfortunately this is not the case in the skin. For the intracutaneous technique, although uniform labelling throughout the skin is achieved this is only two millimetres thick. For the epicutaneous technique, diffusion through the epidermis results in a very thin layer, of about 0.3 mm, being labelled (see section 6.3.2).

In the case of intracutaneous labelling most of the ^{133}Xe will leave the dermis in the small dermal veins which, according to Table 6.1 allow only a small percentage ($\sim 5\%$) of the ^{133}Xe to be lost to the surrounding tissue. This is not consistent with the considerable transfer to subcutaneous fat described by Sejrsen and Challoner, and the reason for this is that, in the derivation of the equations given in section 3.4.2, differences in the solubility of the tissues were not taken into account. It can be shown (Crank, 1971) that the steady state rate of diffusion of material between two media with different solubilities is proportional to the ratio of the solubilities. Since the solubility of ^{133}Xe in the subcutaneous fat is about 10 times that of blood (Table 5.3) the loss of ^{133}Xe from blood vessels passing through the subcutaneous fat will be

correspondingly increased. The result of this is that the capillaries will equilibrate over a shorter distance and both the arterioles and venules will allow complete exchange of ^{133}Xe . More importantly for the present case the small veins draining the dermis will now lose about 50% of their ^{133}Xe on passing through the fatty tissue, which is now in agreement with the experimental findings. As mentioned before the exact figure will depend on the particular combination of L , \bar{v} and r for these vessels, but as the flow decreases this transfer to subcutaneous fat will increase.

The situation with epicutaneous labelling is much more complex. After three minutes of diffusion through the epidermis a layer effectively no thicker than 0.3 mm is labelled in the dermis (see 6.3.2). Again three generations of blood vessel deserve consideration a) the capillaries, b) the venules and c) the dermal veins. Because of their random orientation the capillaries are often considered very much as a diffuse sink (Bassingthwaite, 1970), lying mainly at the dermo-epidermal junction. The above figures suggest that, in the initial stages of the epicutaneous technique, the capillaries may be involved in transferring ^{133}Xe deeper into the dermis, until the labelled region expands to a size larger than the capillary lengths. The dermal veins will, as seen above, allow little loss of ^{133}Xe within the dermis itself but provide a considerable source in the subcutaneous tissue. The venules on the other hand

travel for about 1 mm through the dermis and will allow significant loss of ^{133}Xe ($\sim 25\%$) to areas within the dermis with a lower partial pressure. Thus with an initial labelling as produced by the epicutaneous technique some of the ^{133}Xe will enter the blood in the capillaries, be carried deeper into the dermis and will then re-enter the tissue where it will remain until picked up again by fresh blood. Experimental verification of such a process is difficult to achieve. Although this should produce an initially slower component to the clearance curves, diffusion processes, to be described in the following sections, make this difficult to detect. However Sejrsen (1969) has published autoradiographic findings which may be interpreted as providing evidence of this transfer. The effect of such a transfer will be to allow the ^{133}Xe to travel through the tissue at a rate much faster than that expected from its diffusion coefficient. Sejrsen has presented autoradiographic photographs which show (1969, Fig. 4d) that, after the three minutes of epicutaneous labelling and a further two minutes of clearance, ^{133}Xe has travelled down to a depth of 1.5 mm in the dermis. Indeed, as Sejrsen stated "after two minutes of clearance a diffuse labelling of the entire thickness of the cutaneous layer" is obtained. From the finite difference model of the epicutaneous labelling (see 6.3.2) no appreciable amounts of ^{133}Xe would be expected at depths greater than 0.6 mm. It would therefore appear that in practice some

process has allowed the ^{133}Xe to reach the lower parts of the dermis faster than could be expected from diffusion alone. It is not unreasonable to conclude that the same process which transports ^{133}Xe to the subcutaneous fat is responsible for this.

In summary the rather semi-quantitative model presented here has predicted the considerable transfer of ^{133}Xe to the subcutaneous fatty tissue from the small veins passing through it. In addition it has also shown that such a transfer may occur in the dermis itself, when the epicutaneous labelling technique is used, although in this case the smaller venules are responsible. This results in ^{133}Xe effectively "rolling" through this tissue which initially will produce a clearance rate not directly related, in the traditional way, to the magnitude of the blood flow.

In the further models presented in the following sections it is assumed that the capillaries are the dominant blood vessels with regard to the removal of ^{133}Xe from a particular area, and equation 3.6 is used to describe this for each nodal point. However after this removal has occurred the ^{133}Xe may be deposited again in other layers, and for the subcutaneous tissue Sejrsen's model of this has been used. This means that a constant fraction (E in equation 4.1) of the ^{133}Xe removed from the dermis is re-deposited in the subcutaneous tissue. As far as transfer by blood within the dermis itself is concerned because of the difficulty

of verifying this experimentally and in fact the difficulty in modelling it, this has not been included in further models. This allows these models to concentrate on the other processes involved in the overall clearance of ^{133}Xe . It does not, however, detract from the importance of such a transfer process.

6.3 DIFFUSION OF ^{133}Xe IN THE SKIN

Previous descriptions of the clearance of ^{133}Xe from the skin have neglected the role of diffusion. This section assesses the magnitude of the effects of diffusion in each layer of the skin. In order to highlight these processes it is assumed for the present that the blood flow is zero, and this is achieved in practice either by using excised tissue or by the use of a tourniquet to occlude blood flow in vivo.

6.3.1 Diffusion from the dermis to the subcutaneous tissue

(a) Model and results

In order to assess only the rate of diffusion from the dermis to the subcutaneous tissue it is assumed that the ^{133}Xe is directly introduced into the dermis, as it would be with the intracutaneous injection technique. The model uses the values of solubilities and diffusion coefficients derived in chapter 5 and is made up of four layers - the air, the epidermal barrier, the dermis and the subcutaneous fat. Initially the ^{133}Xe is uniformly distributed in the dermis or in part of

the dermis. Three thicknesses of the dermis, one, two and three millimetres are used, being representative of most of the body.

Figure 6.3 shows the partial pressure profiles at times 0, 10 and 30 minutes after uniform labelling of the entire thickness of a 2 mm thick dermis. To appreciate more clearly the relative amounts in each layer Figure 6.4 gives the concentration profiles for the same situation. Note that in each case the epidermal barrier is too thin to be properly visualised on the same distance scale but this is not important in the present model. In addition the loss of ^{133}Xe through the epidermis can be neglected. It can be seen that although the partial pressure in the fat does not rise quickly this is entirely due to its solubility and a substantial amount of the ^{133}Xe crosses over into it as evidenced by the concentration profiles. Most of the ^{133}Xe which does so, however, is localised in the top 1 mm of the fat, even at 30 minutes.

A slightly different picture is obtained if the ^{133}Xe is initially distributed in only the upper 1 mm of the dermis (Figure 6.5), which may reflect more accurately the labelling produced in practice. As expected much less of the ^{133}Xe is found in the fatty tissue especially at early times although again this is confined mainly to the top 1 mm.

The fraction of ^{133}Xe to be found at any time in the subcutaneous tissue is plotted in Figure 6.6 for various

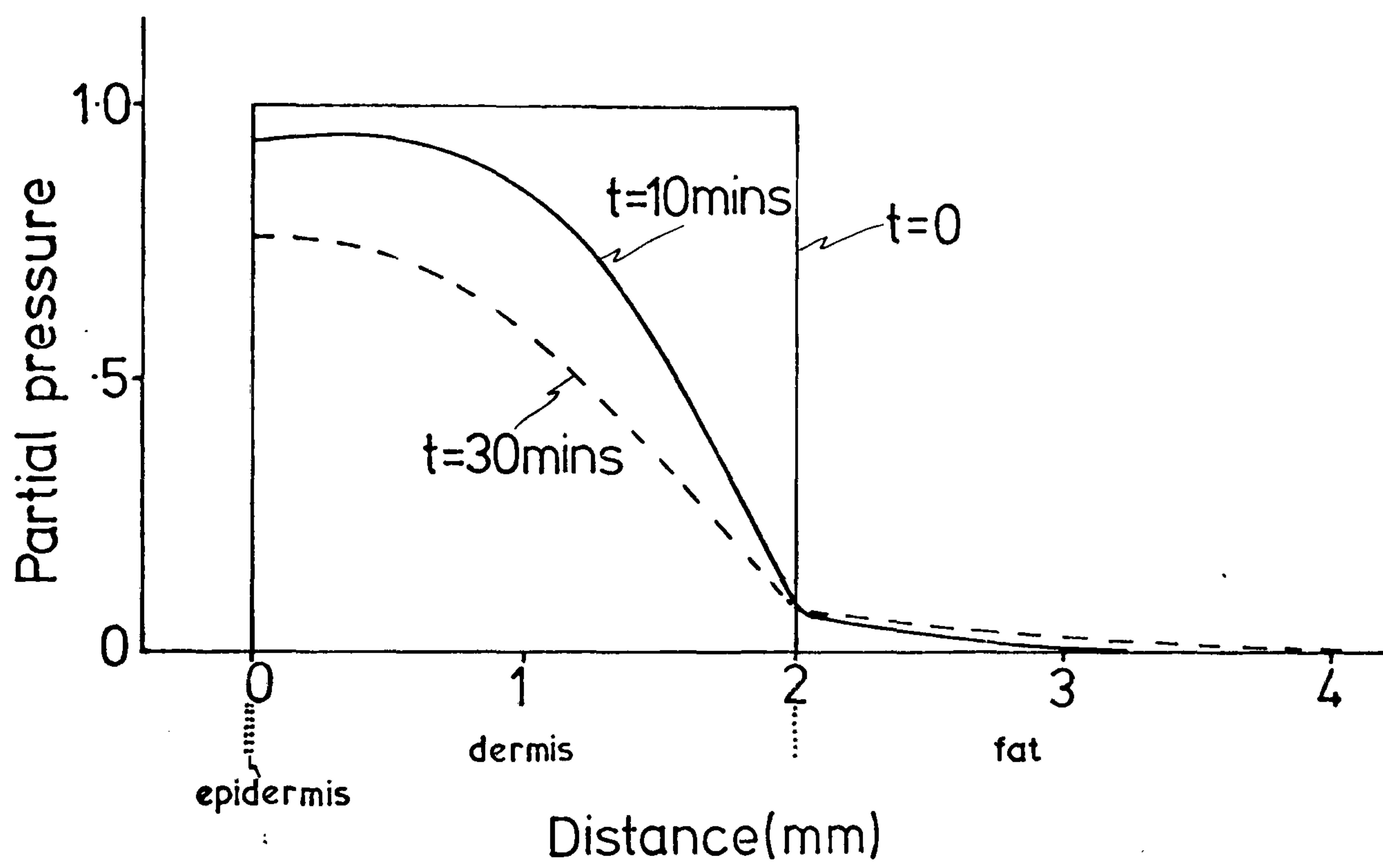


Figure 6.3 Relative partial pressure of ^{133}Xe within the skin at 10 mins. and 30 mins. after the uniform labelling of the entire thickness of the dermis (2 mm).

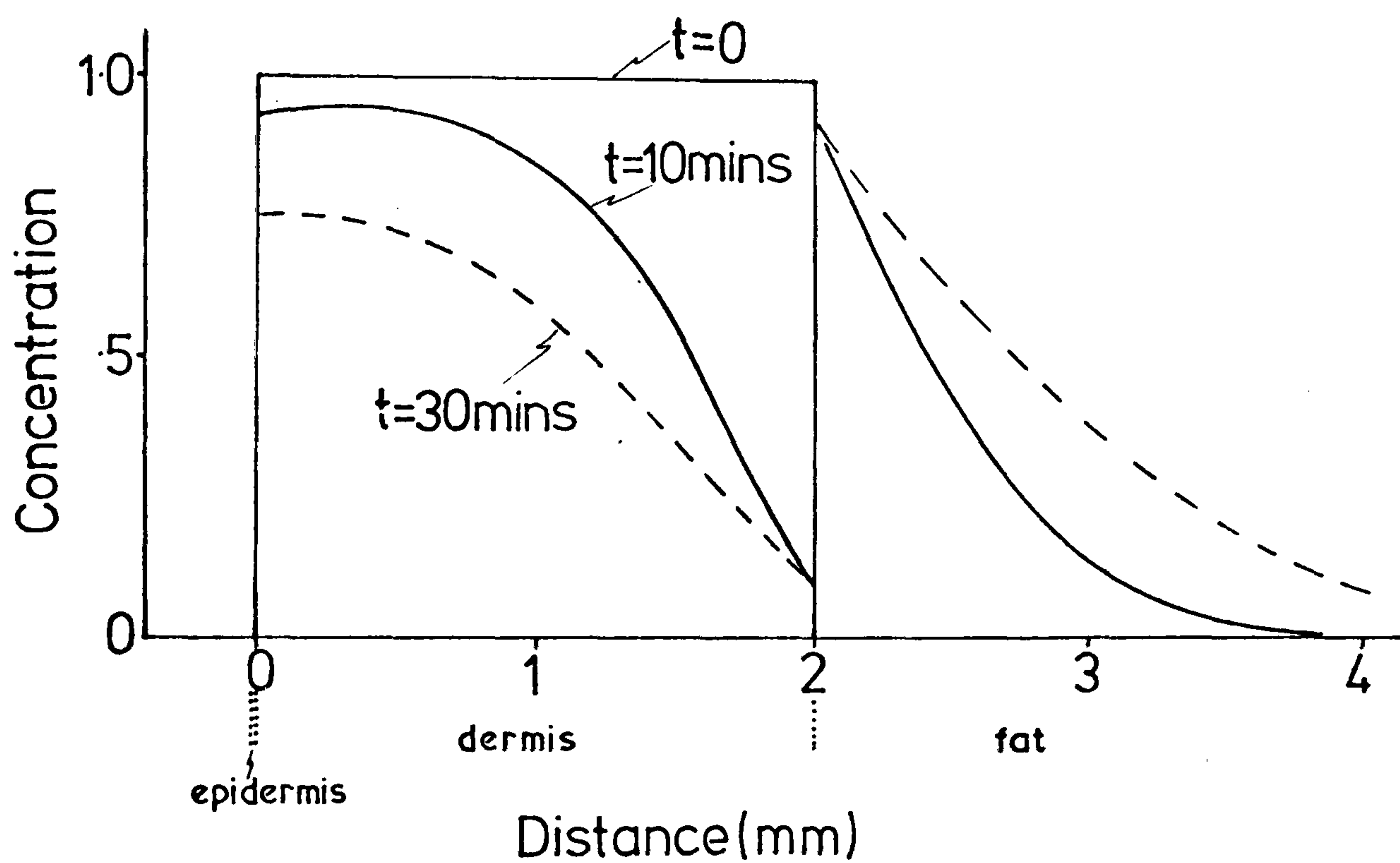


Figure 6.4 Relative concentration of ^{133}Xe within the skin at 10 mins. and 30 mins. after the uniform labelling of the entire thickness of the dermis (2 mm).

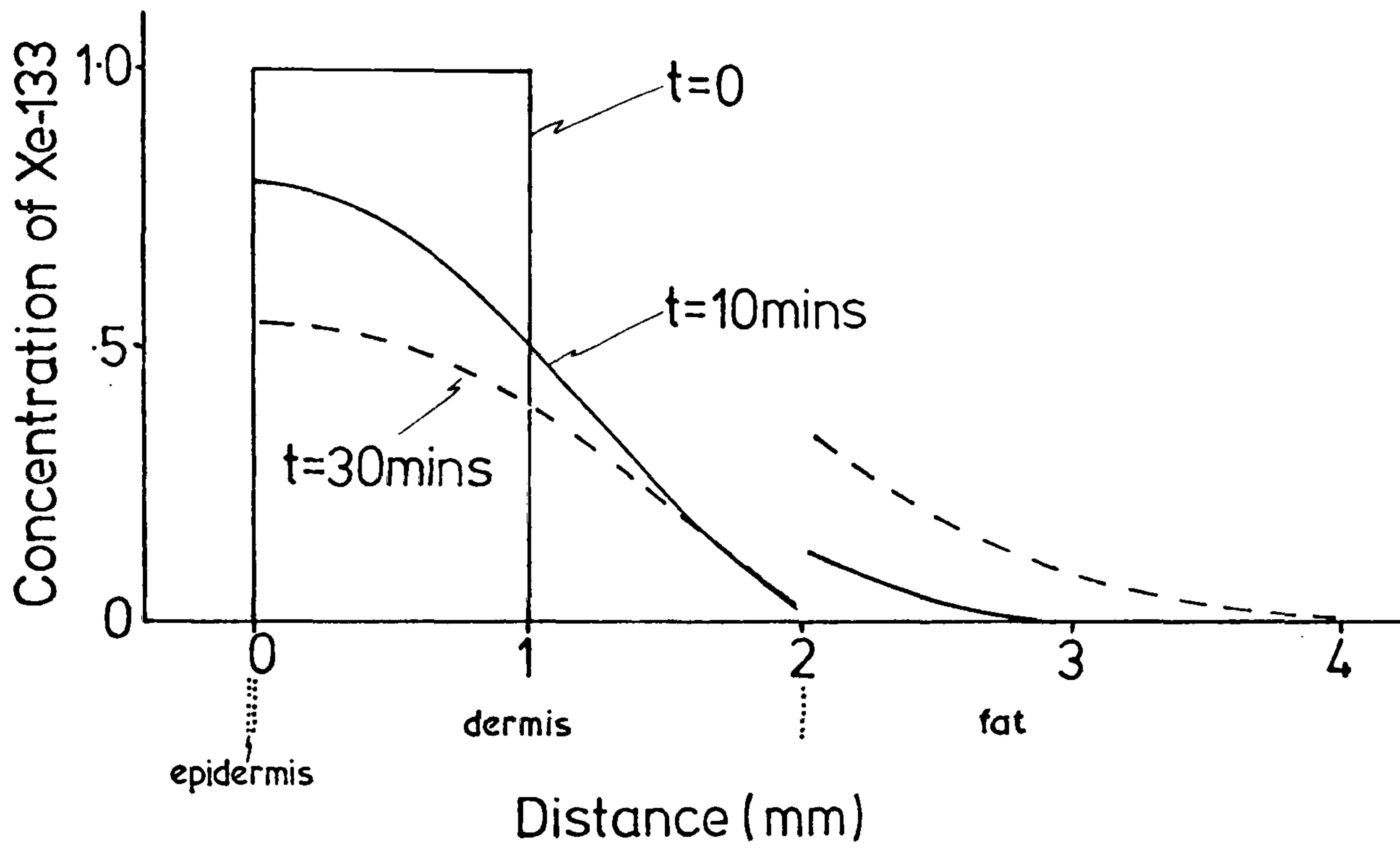


Figure 6.5 Relative concentration of ^{133}Xe within the skin at 10 mins. and 30 mins. after labelling of the top 1 mm of the dermis, whose thickness is 2 mm.

situations. Where the initial deposit labels the entire thickness of the dermis the ^{133}Xe can immediately begin to pass over into the fat. If, however, it labels only a part of the dermis, curves 4 and 5, there is a time lag before the build up of ^{133}Xe begins and, of course, this results in less of the ^{133}Xe appearing in the fatty tissue at a particular time.

Experimentally the diffusion from dermis to fat was assessed in the following way. Using full thickness, excised breast tissue an injection of 0.05 ml ^{133}Xe in saline was made directly into the dermis in the normal way. This produced a slight bleb in the skin expanding the dermis by 0.5 mm to 1 mm. Diffusion was allowed to take place for 30 minutes after which time the tissue was dissected and the dermis and fat separated. The activity in each component was then measured using the radiation detector. From five samples an average of 30% of the ^{133}Xe was found to have entered the fatty tissue during this time although it was difficult to obtain a precise value for this since much of the ^{133}Xe was situated at the interface between the two tissues. Taking into account the effect of the injection volume on the dermis it can be seen from Figure 6.6 that diffusion of this magnitude into the subcutaneous fat is consistent with the predictions of the finite difference calculations.

(b) Discussion

Both the experimental and calculated results are at odds with the findings of Challoner (1973) who claimed that no diffusion whatsoever occurred between the dermis

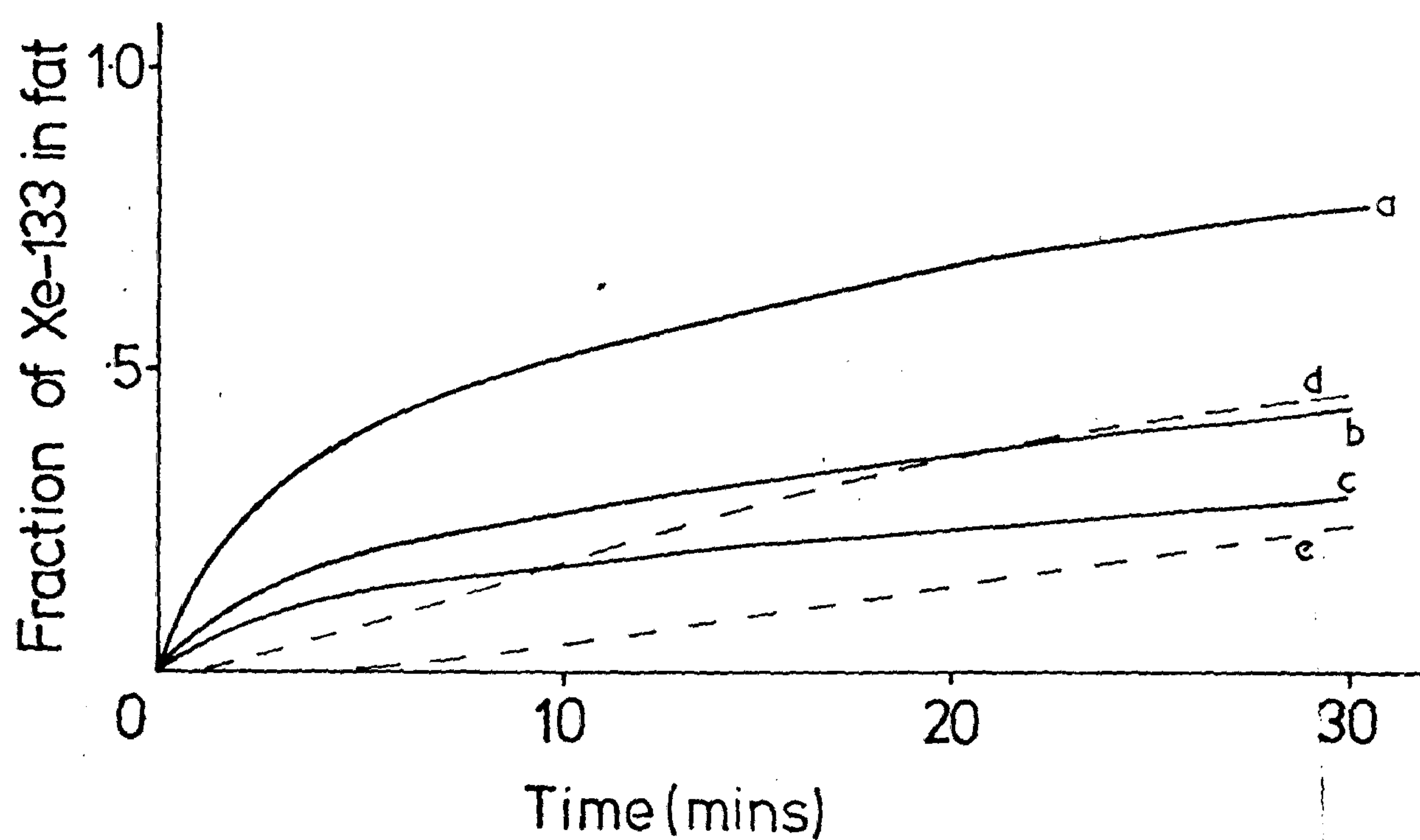


Figure 6.6 Fraction of ^{133}Xe to be found at any time, in the subcutaneous fatty tissue, after labelling of the dermis. Uniform labelling in 1 mm, 2 mm and 3 mm thick dermis - a, b and c respectively. Labelling of top 1 mm in 1.5 mm and 2 mm thick dermis - d and e.

and fat in a time of 30 minutes. This claim is surprising since it would imply, from the above calculations, that some sort of barrier to diffusion existed between the two tissues. No such barrier has been reported in the literature (Wells and Lubowe, 1964) and the most likely cause of the discrepancy between the present results and those of Challoner is that, as seen in Figure 6.4, most of the ^{133}Xe is localised to within 1 mm of the interface. Thus it is obviously important, when dissecting the tissue, to remove all of the fat although this is not easy to achieve and may be the reason for Challoner's failure to detect this diffusion. Although Sejrsen also ignored diffusion in his final model of ^{133}Xe clearance, his previous publications (Sejrsen, 1967, 1969) are in agreement with the present results.

The effect of diffusion from dermis to fat on the assessment of dermal blood flow will be presented in section 6.4, but clearly this process allows considerable transfer away from the dermis, even in the early stages, leading to poorer definition of the dermal component.

6.3.2 Diffusion within and through the epidermis

(a) Models and results

The first situation to be considered here is the diffusion of ^{133}Xe through the intact epidermis from the dermis and for this it is again assumed that the ^{133}Xe is introduced directly into the dermis. Using both the same finite difference model and the same experimental set-up as in the previous section the total diffusion of ^{133}Xe

through the epidermis and out of the skin was calculated and measured. The predicted loss of ^{133}Xe was 2.2% in 30 minutes compared to the measured value, in excised breast tissue, of 2.5%. Similar observations reported by Sejrnsen (1968) in the skin of the leg, with the blood flow occluded by a tourniquet, showed a loss over 30 minutes of from 1.2% to 4.2%. Further insight into the diffusion of ^{133}Xe through the epidermis was obtained by calculating the diffusion loss for different thicknesses of the epidermis and this is shown in Figure 6.7. It can be seen that the percentage lost is non-linearly related to the thickness and gives the appearance of being almost constant until the thickness is reduced below a certain value. This figure is, in fact, remarkably similar to one published by Sejrnsen (1968) which was based on his observations of clearance curves from excised tissue, in which the layers of the epidermis were gradually removed by stripping with adhesive tape. Sejrnsen, however, concluded that since the outer layers of the epidermis could be removed with relatively little change in the amount of ^{133}Xe lost then these layers were not part of the diffusion barrier. On this basis, he therefore reported that the barrier was situated in the middle third of the epidermis. From Figure 6.7 it can be seen that, in fact, a uniform barrier, including the outer layers, produces a graph of the same form as Sejrnsen's experimental curve.

The above results are representative of the

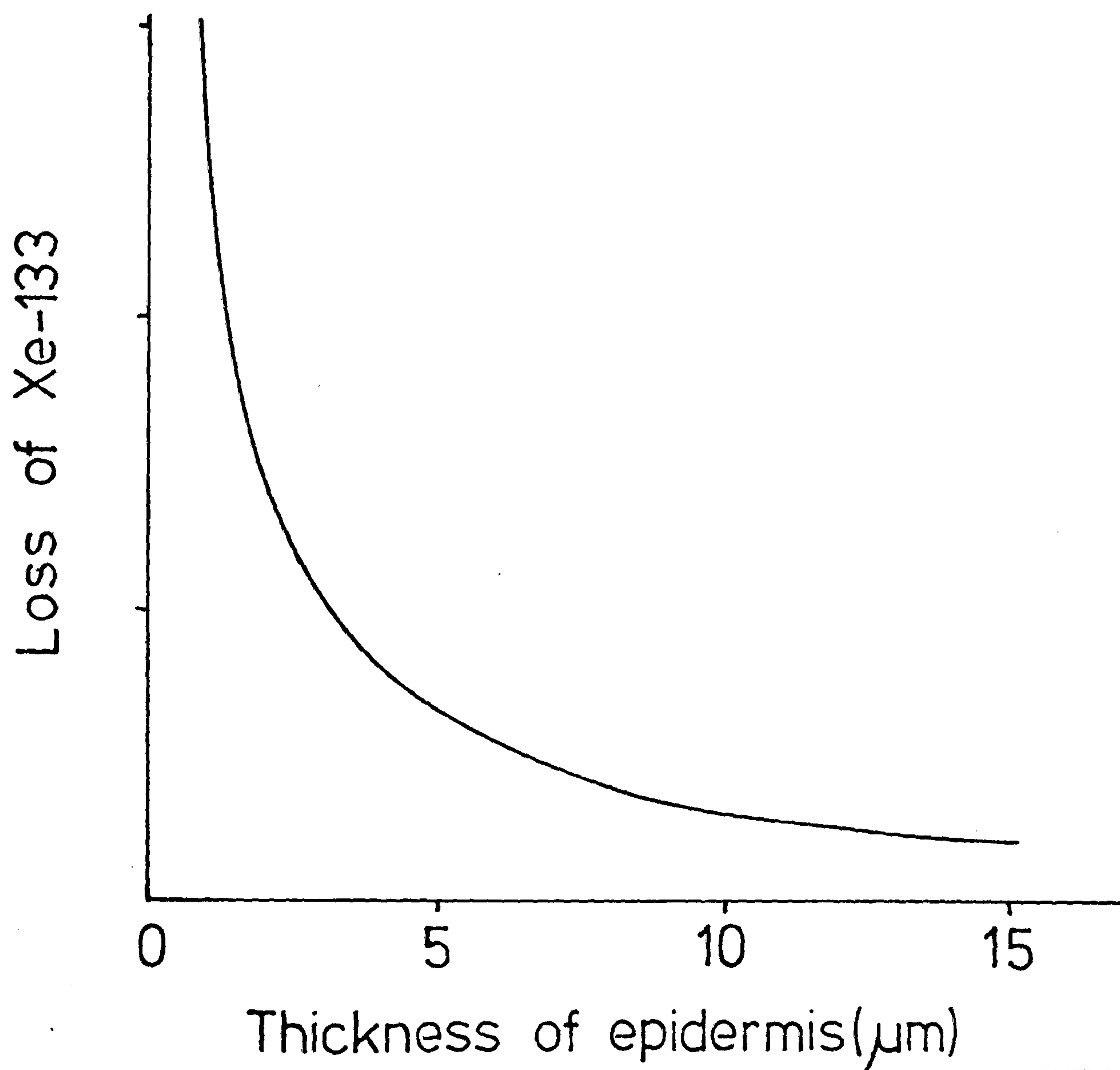


Figure 6.7 Variation of the rate of loss of ^{133}Xe through the epidermis with its thickness.

intracutaneous labelling technique but for epicutaneous labelling a different aspect of diffusion requires consideration. Using the finite difference model based on this technique, with an initial three minutes of diffusion from a ^{133}Xe in saline solution on the surface of the skin, Figure 6.8 shows the resulting partial pressure profiles in the skin layers for a thin ($15\ \mu\text{m}$) epidermal barrier. Note that for each time the curves are normalised to the maximum value of the partial pressure and also that the distance scales are different for each tissue. It can be seen that at the end of the three minute labelling period almost all of the ^{133}Xe remaining in the skin is contained within the epidermal barrier and not in the dermis. After this time the ^{133}Xe begins to leave the epidermal barrier both by diffusion back into the air and also forward into the dermis. A plot of the amount of ^{133}Xe in each layer with time is given in Figure 6.9 for thin epidermis and in Figure 6.10 for thick epidermis. No ^{133}Xe whatsoever is found in the dermis until about 3 minutes and 10 minutes, respectively, after the start of labelling. As the amount in the epidermal barrier decreases the dermal content increases and an equal amount is found in both tissues after 7 minutes, for the thin epidermis. However this does not occur for the thick epidermis until 36 minutes. Within the time scales illustrated the amount which has diffused to the subcutaneous tissue is negligible.

The resulting "clearance" curves for both cases are

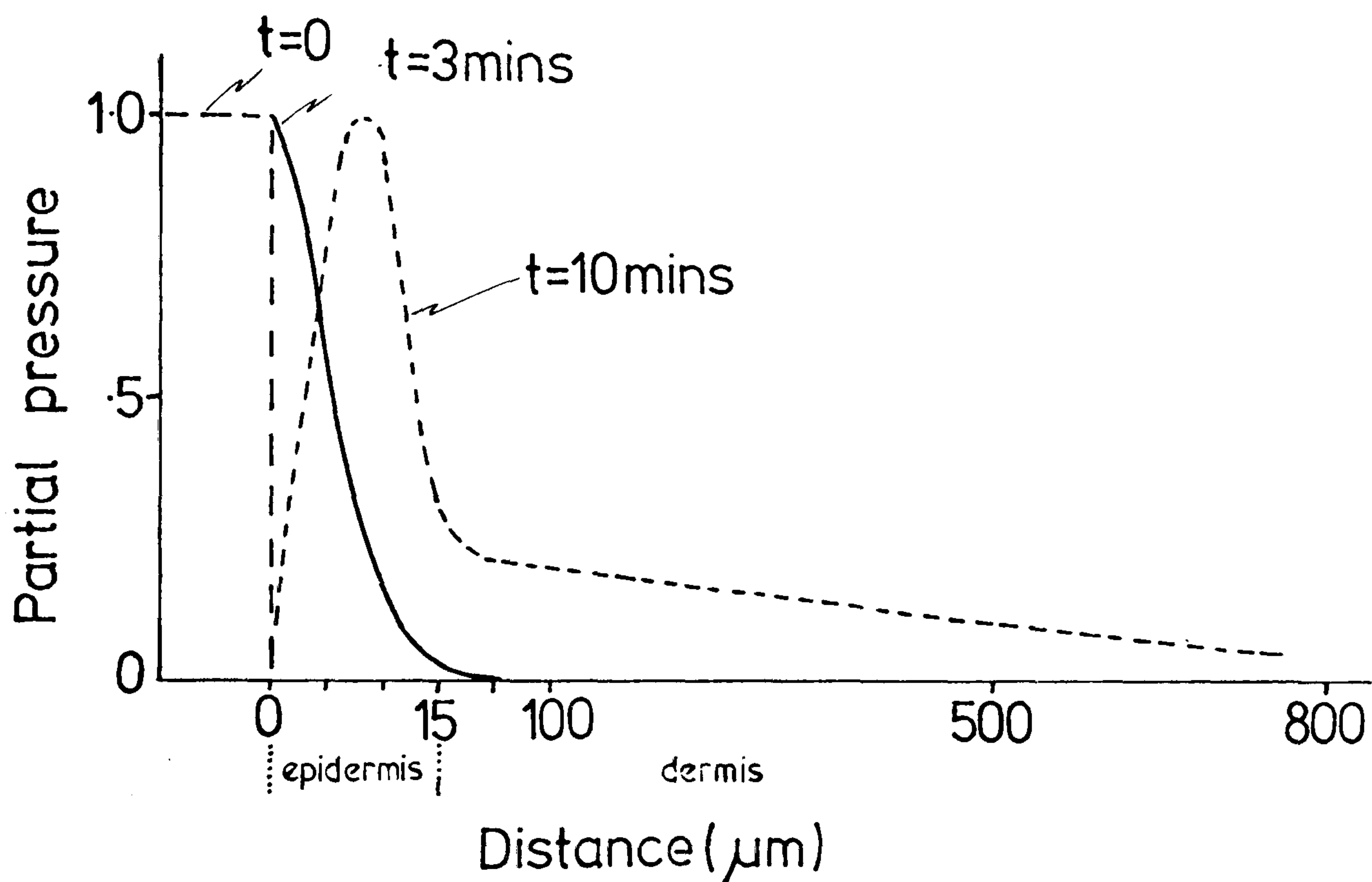


Figure 6.8 Epicutaneous labelling - relative partial pressure of ^{133}Xe within the epidermal barrier and dermis at the end of the epicutaneous labelling period ($t = 3$ mins.) and at 10 mins. Curves are normalised to the maximum value of partial pressure at each time. Different distance scales are used for epidermis and dermis.

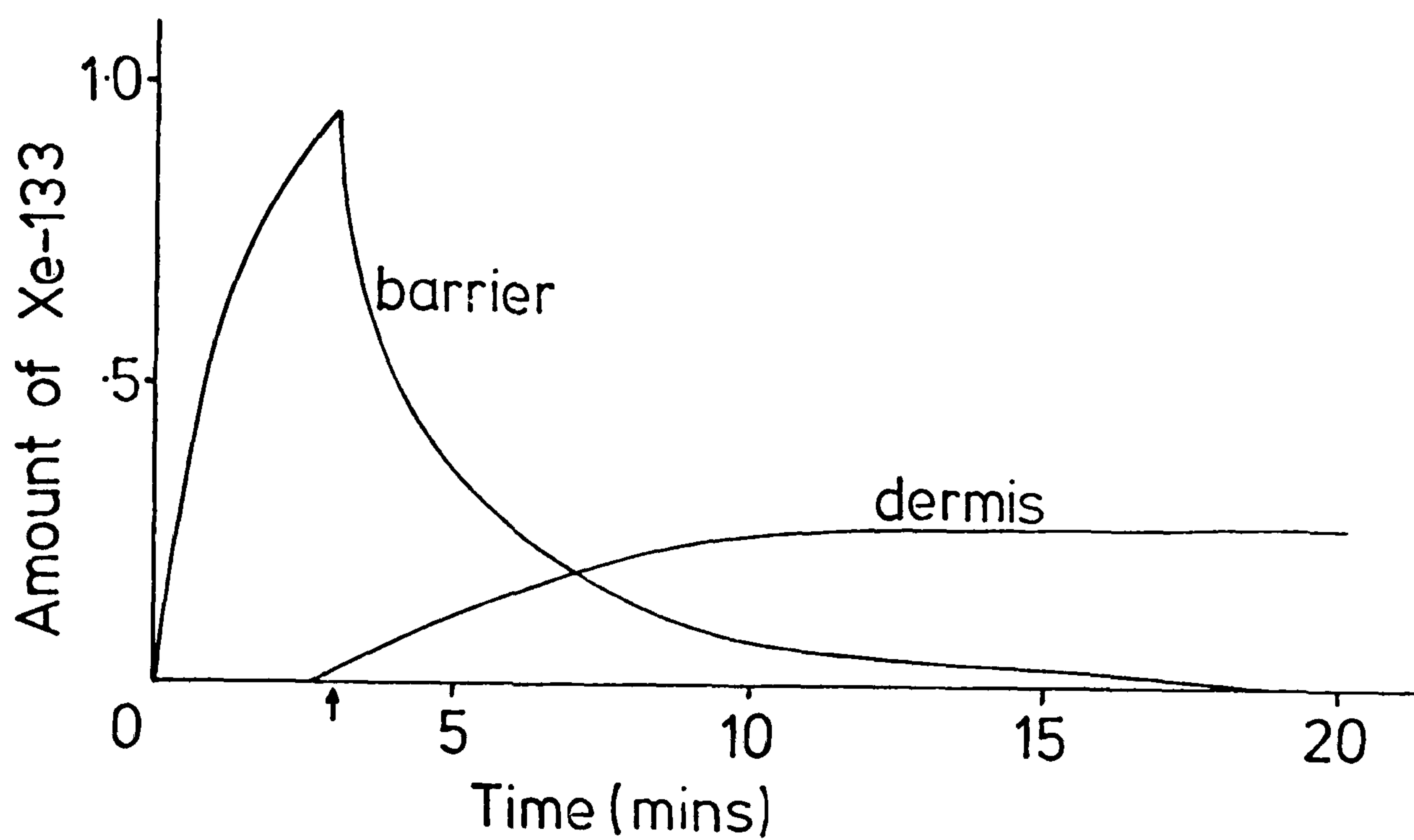


Figure 6.9 The amount of ^{133}Xe found within the epidermal barrier and dermis, for a $15\ \mu\text{m}$ thick barrier, at times after the start of the spicutaneous labelling period. The end of the labelling period is indicated by an arrow.

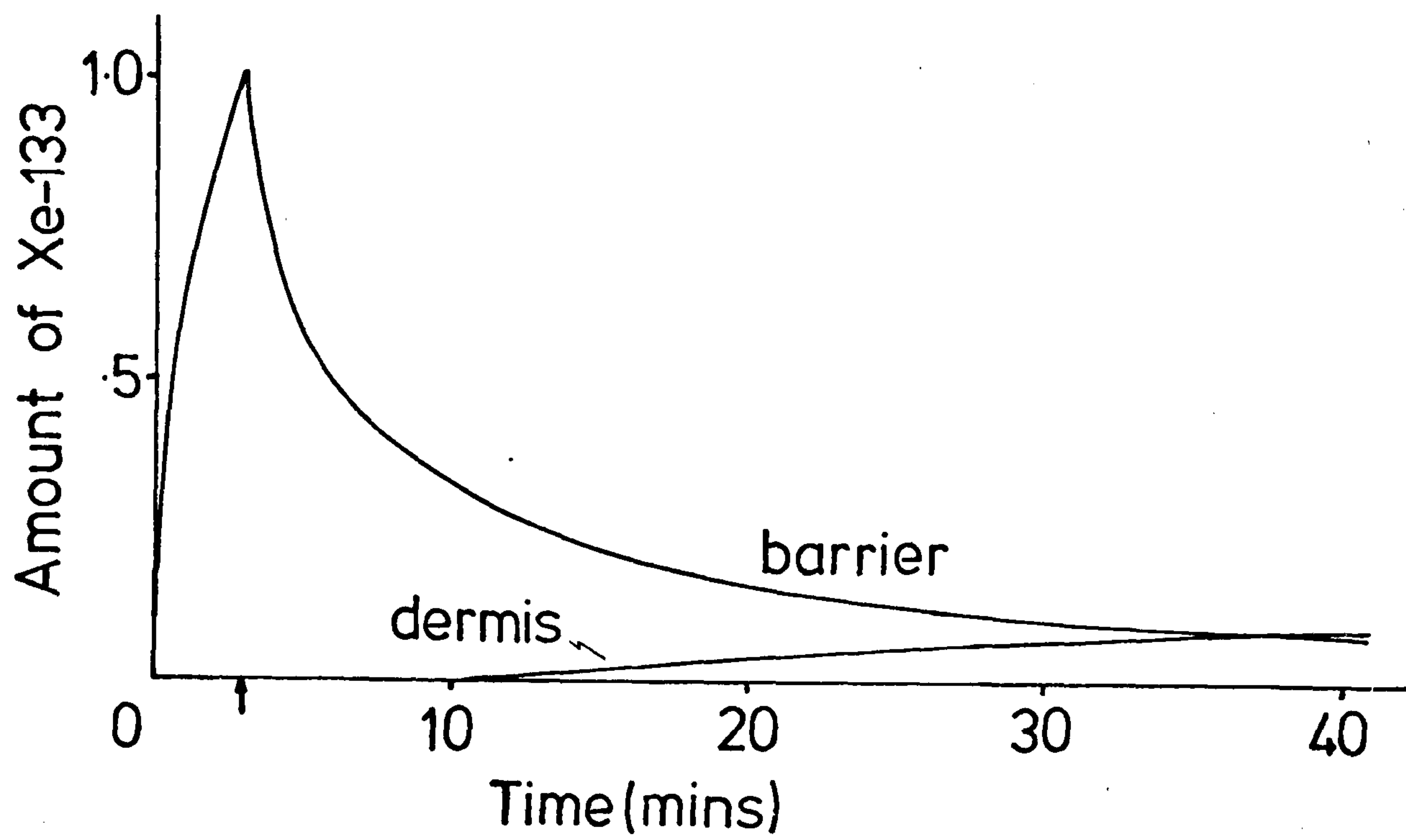


Figure 6.10 The amount of ^{133}Xe found within the epidermal barrier and dermis, for a $100\ \mu\text{m}$ thick barrier, at times after the start of the epicutaneous labelling period. The end of the labelling period is indicated by an arrow.

shown in Figures 6.11 and 6.12 respectively. Initially there is a rapid loss of ^{133}Xe as a proportion of it diffuses back out into the air. Eventually an equilibrium level is attained at which time all of the remaining ^{133}Xe has passed completely through the epidermis into the other skin layers, and the clearance rate is then dependent on diffusion back through the epidermis as in the previous section. To show the possible variation from one piece of skin to another Figure 6.11 gives the "clearance" curves obtained for different values of the diffusion coefficient, but still considering the barrier to be 15 μm thick. These represent the range of values calculated in section 5.5.2. As the diffusion coefficient increases, the amount of ^{133}Xe which diffuses back out of the skin decreases. A greater fraction of the ^{133}Xe is then available for clearance by blood flow.

Three ways of investigating the above model experimentally were utilised. Firstly epicutaneous labelling was performed in the normal way on excised skin and, after removal of the chamber, the amount of ^{133}Xe left in the skin at subsequent times was monitored. Secondly the above procedure was carried out in vivo in a limb with the blood flow occluded using a tourniquet. It was not, of course, possible to use this for periods much longer than 15 minutes or so. The third method could be used on any area of skin and involved smearing a layer of Vaseline over the labelled area one minute after the

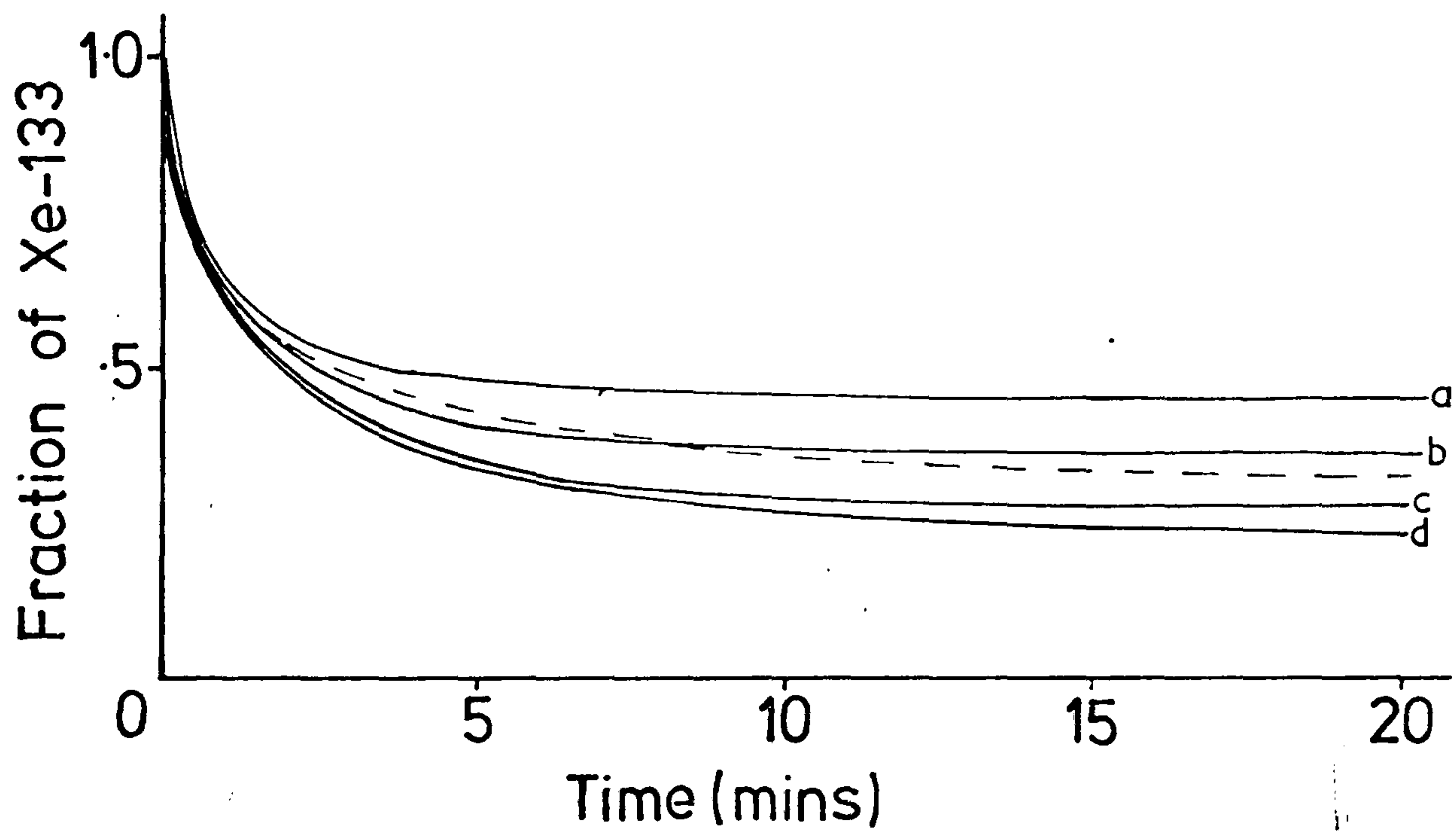


Figure 6.11 The amount of ^{133}Xe detected at any time within the skin as a fraction of the amount at the end of the labelling period, for different values of the epidermal diffusion coefficient. a) $4 \times 10^{-9} \text{ cm}^2 \text{ s}^{-1}$, b) $2.5 \times 10^{-9} \text{ cm}^2 \text{ s}^{-1}$, c) $1.3 \times 10^{-9} \text{ cm}^2 \text{ s}^{-1}$, d) $0.8 \times 10^{-9} \text{ cm}^2 \text{ s}^{-1}$. The epidermal barrier is $15 \mu\text{m}$ thick and there is assumed to be no blood flow in the dermis. Dotted line - the corresponding clearance curve obtained from excised tissue.

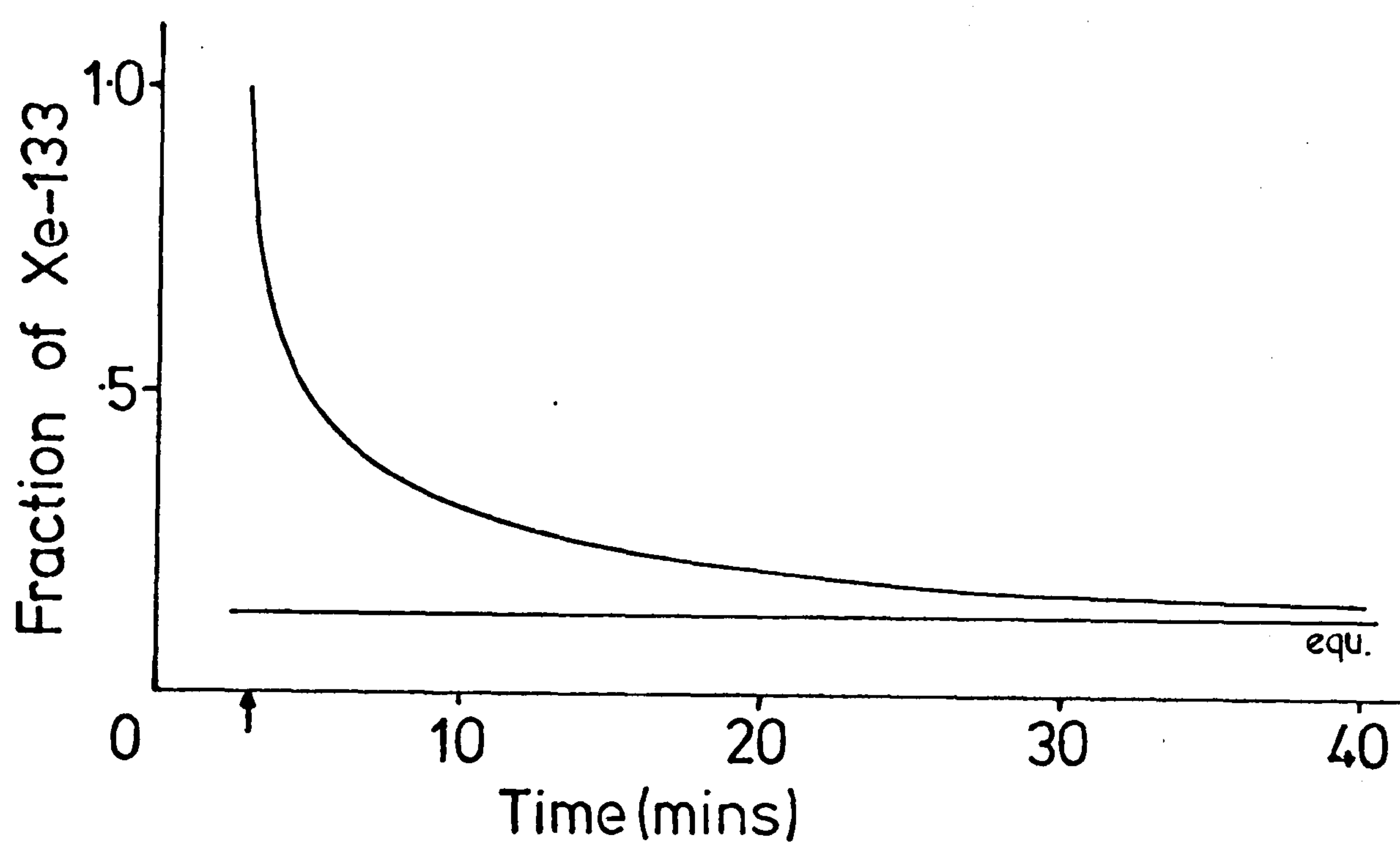


Figure 6.12 The amount of ^{133}Xe detected at any time within the skin as a fraction of the amount at the end of the labelling period, for a $100\ \mu\text{m}$ thick epidermal barrier. There is assumed to be no blood flow in the dermis.

^{133}Xe chamber had been removed. By then removing this layer and re-applying it at regular intervals the amount of ^{133}Xe which diffused back out of the skin, and was trapped in the Vaseline, could be measured by noting the decrease in counts as the Vaseline was removed. With this third option blood flow was present and, if anything, this would lead to an underestimate of the amount of ^{133}Xe which could diffuse back out in the absence of flow. In addition the effect of Vaseline on the diffusion properties of the barrier was uncertain but the results obtained using this method agreed well with those obtained in other ways. In all cases the "clearance" curves were plotted from one minute after the chamber was removed, which is in line with most reported studies and allows for initial transients and the positioning of detectors. A free flow of air over the labelled areas was arranged in order that any ^{133}Xe which diffused out of the skin was quickly removed from the area.

Figure 6.11 shows (dotted line) the average clearance curve obtained from excised tissue and this is similar to the predicted curves. The total percentage of ^{133}Xe which diffused back out of a labelled area was obtained, for a variety of sites as

$$\frac{\text{activity at 1 min} - \text{activity at equilibrium}}{\text{activity at 1 min}} \times 100\%$$

and these values are shown in Table 6.2, along with the predicted values. Although mean values for the measured loss are again quoted it should be realised that this

TABLE 6.2

Loss of ^{133}Xe back out of skin
after epicutaneous labelling

<u>Region</u>	<u>No. of Obs.</u>	<u>Thickness of epidermal barrier</u>	<u>Calculated Loss</u>	<u>Measured loss (mean values)</u>
Breast	3	15 μm	49%	45% (excised tissue)
Face, trunk	3	15 μm	49%	25% (in vivo)
Forearm	10	15 - 30 μm	49 - 65%	48% (in vivo, occluded flow)
Finger	5	100 μm	78%	75% (in vivo, occluded flow)

represents a wide range and, for example in the forearm, two studies gave a loss of less than 20%. This most probably reflects individual variations in the diffusion parameters of solubility, thickness and diffusion coefficient. The figures show a good agreement between the predicted and measured values and suggest that, in general, the back diffusion increases with epidermal barrier thickness.

(b) Discussion

The above results have confirmed that once ^{133}Xe has penetrated the epidermal barrier and entered the dermis its rate of diffusion back through the epidermis is very small and can be neglected in the presence of blood flow. However the results have also shown that, contrary to the practice in previous studies, this cannot simply be extended to the epicutaneous labelling technique. Because of the very low diffusion coefficient of ^{133}Xe in the epidermal barrier the time taken for ^{133}Xe to penetrate this is such that only a small fraction of it is within the dermis after the labelling period. Most of the ^{133}Xe is still contained within the epidermal barrier and subsequently some of it diffuses back out into the air. This apparent clearance of ^{133}Xe , in the absence of blood flow, has not previously been reported in the literature even though it was easily demonstrated both in vivo and in excised tissue in the present study. However a review of the literature has revealed that

although zero clearance with no blood flow has been inferred in many studies it has not been specifically confirmed for the epicutaneous labelling technique. Most authors have only demonstrated zero clearance for the intracutaneous labelling (Nyfors and Rothenborg, 1970; Leroy et al, 1971; Chimoskey, 1972) which, from the above results, is certainly true, or else have referred to Sejrsen's work (Greeson et al, 1973; Handel et al, 1976; Kristensen and Wadskov, 1976) which was also based on zero clearance in the intracutaneous technique. The effect of this clearance on the assessment of blood flow will be examined in the next section.

With epicutaneous labelling it was also found that diffusion down into the subcutaneous fat was negligible. In other words, with the particular labelling close to the skin surface, diffusion on its own cannot account for accumulation within the subcutaneous fatty tissue. The transfer of ^{133}Xe by blood flow, either directly to the fatty tissue or into the deeper parts of the dermis and then by diffusion, must be responsible for this.

6.4 THE INFLUENCE OF BLOOD FLOW ON THE CLEARANCE CURVES

The relationship between blood flow and the rate of clearance of ^{133}Xe from the skin will now be examined. A uniform flow is assumed in both the dermis and the subcutaneous fat and the magnitude of the transfer between the venous blood and the fat is indicated for each investigation.

6.4.1 Relationship between blood flow and clearance rate - intracutaneous labelling

(a) Results

In order to illustrate some of the difficulties in extracting information on individual components, from a composite curve, the simpler case of intracutaneous labelling will be considered first. It is assumed that the blood flow is constant, which is not, of course, true in practice since the injection alters the flow in a transient way.

Terms corresponding to various values of blood flow in the dermis, f_D , and fat, f_{sc} , were inserted into the finite difference model along with different values of the constant E which represents the transfer from venous blood to fat. The resulting predicted clearance curves were analysed using the methods described in section 4.6 and either the initial slope of the curve or the magnitude of the first exponential component in a bi-exponential analysis was obtained. In all cases the clearance curves were continued for a sufficient time so that the subcutaneous component was precisely defined.

The first exponential component was found to be an accurate reflection of the true dermal blood flow (Figure 6.13) except at low flows and this correlation was essentially independent of the values of E or the subcutaneous blood flow. The effect of both the diffusion of ^{133}Xe from the dermis to the fat and also the transfer by blood flow to the fat was to reduce the relative

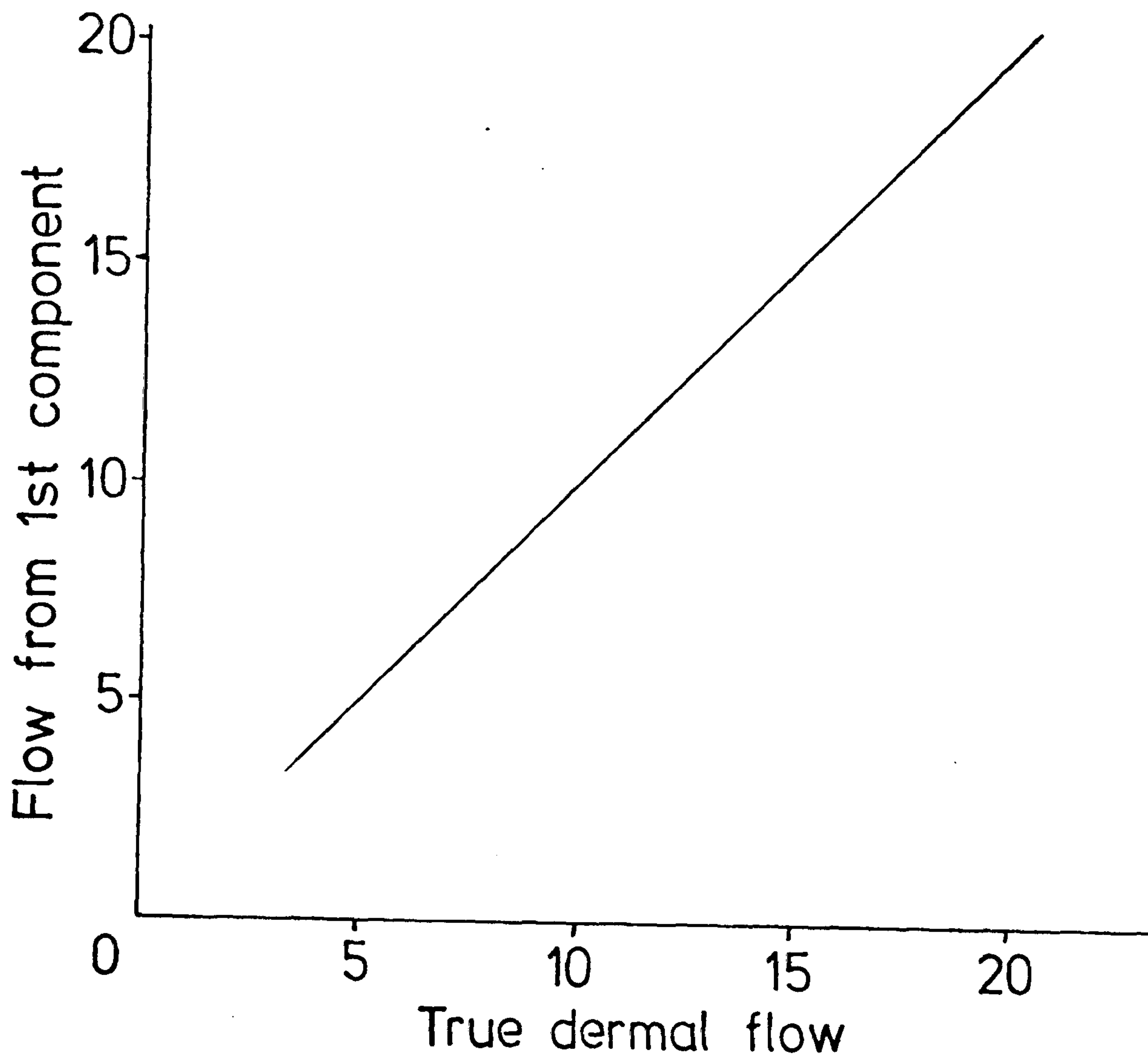


Figure 6.13 Intracutaneous labelling - the relationship between the blood flow, calculated from the first exponential component of the predicted clearance curve, and the true value of the dermal blood flow used in the model.

amplitude of the first component. As Glass and de Garreta (1967) have reported in some detail this eventually results in the inability to resolve the curve into two components especially in the presence of biological noise. Since both of the above processes become more significant at low flow values it was therefore found that, at true dermal flows less than about 3 ml/100g/min, it was not possible to define the first exponential component. The exact value at which this occurred depended to some extent on the value of E and also on f_{sc} .

Figure 6.14 shows the relationship between the initial slope of the curve and the true dermal flow. It can be seen that, for particular conditions, the initial slope increases with the dermal flow but at all stages underestimates it. However it is clear that the initial slope is also greatly affected by the values of f_{sc} and E but only minimally by the position within the dermis of the initial labelling. In other words in any particular situation the measurement of initial slope is dependent on a variety of factors and not just the true dermal flow.

Figure 6.15 again presents the initial slope of the curve but this time it is plotted against the average of the flows in the dermis and fat. Again, although there is a general correlation between them there is considerable scatter of the points, with different initial slopes being possible for the same average flow.

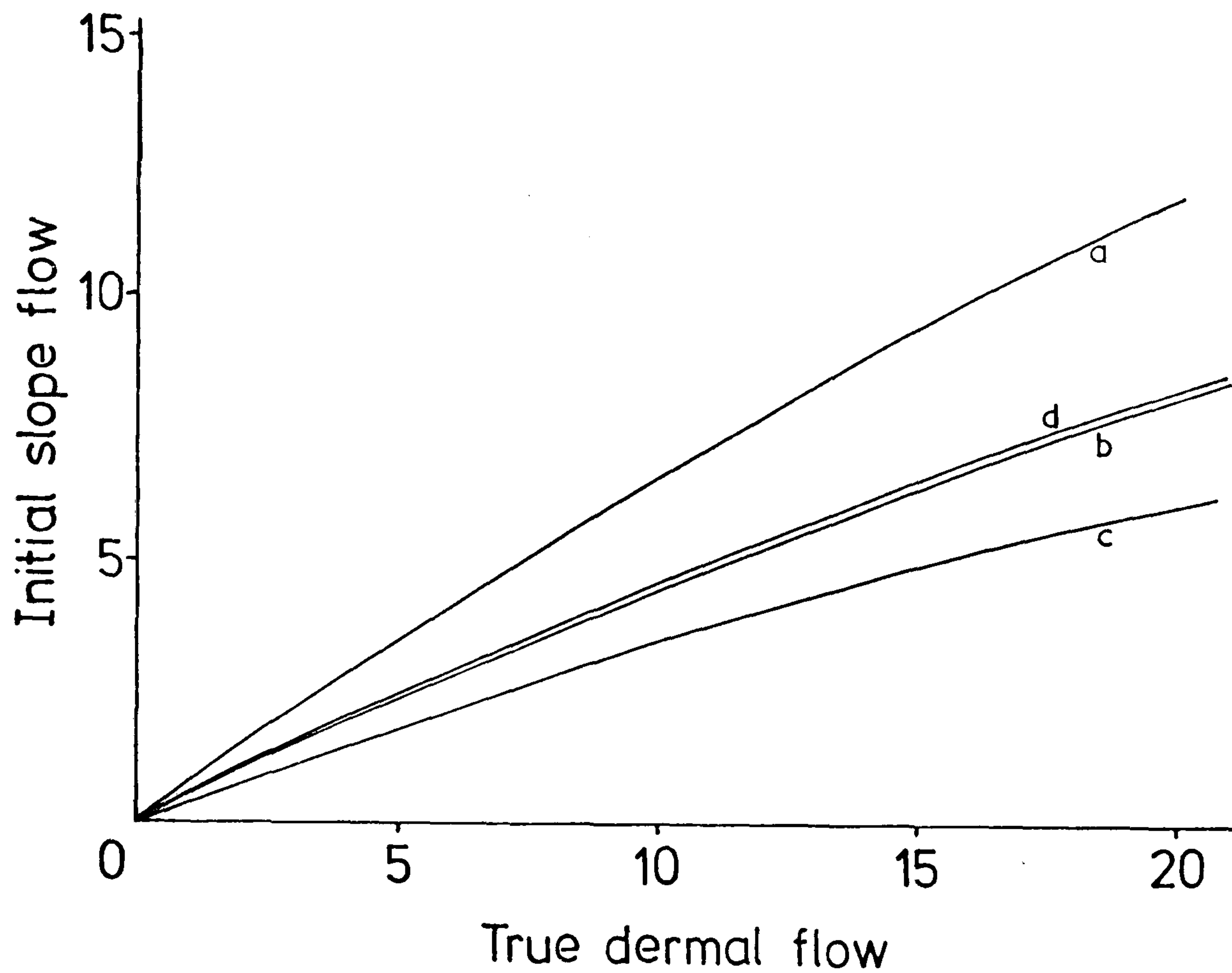


Figure 6.14 Intracutaneous labelling - the relationship between the blood flow, calculated from the initial slope of the predicted clearance curve, and the true value of the dermal blood flow used in the model. Different values of the subcutaneous blood flow and fraction E transferred from the blood to the fatty tissue:- a) $f_{SC} = 6$, $E = 0.2$, b) $f_{SC} = 6$, $E = 0.5$, c) $f_{SC} = 2$, $E = 0.5$, d) $f_{SC} = 6$, $E = 0.5$, label at top 1 mm of dermis.

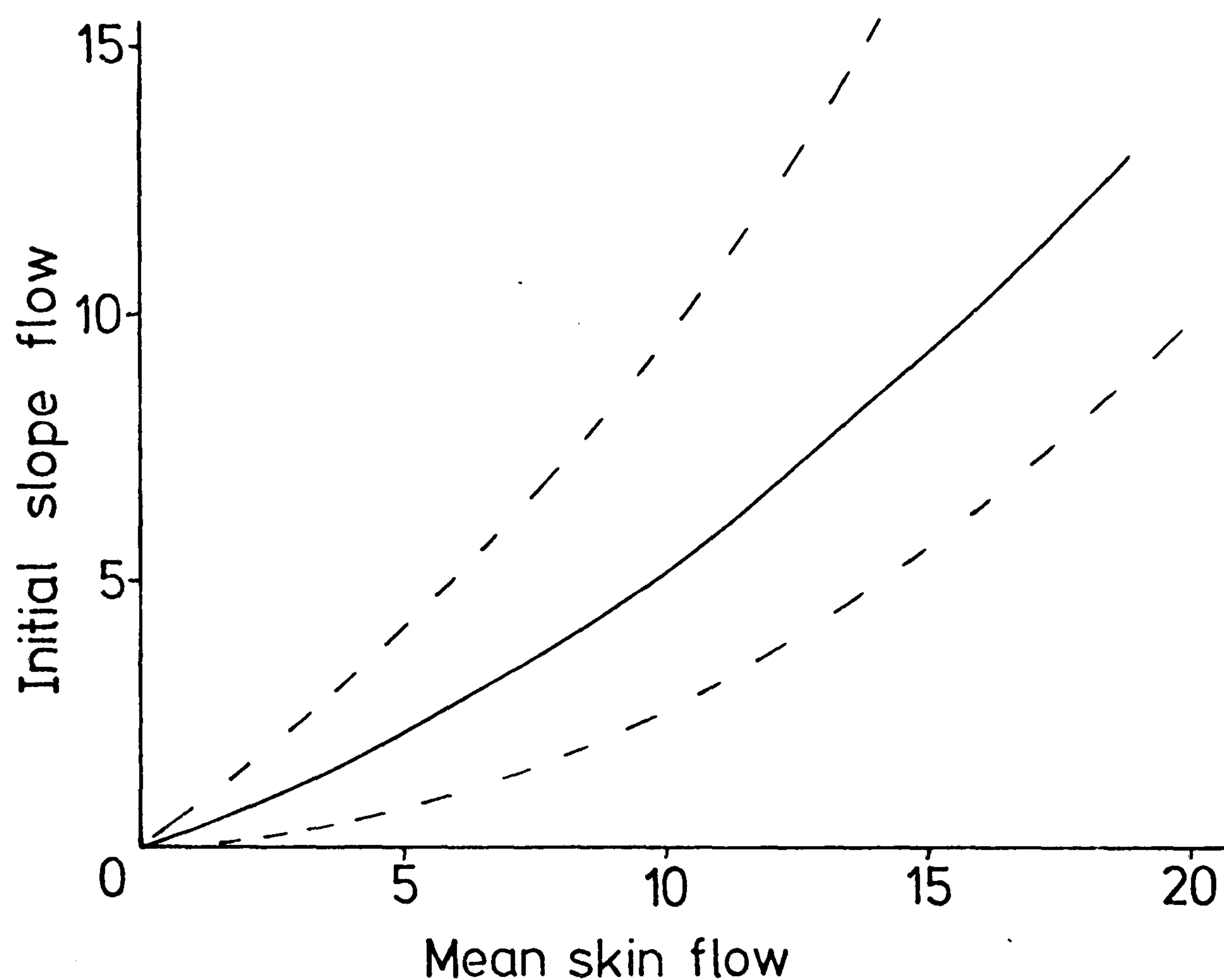


Figure 6.15 Intracutaneous labelling - the relationship between the blood flow, calculated from the initial slope of the predicted clearance curve, and the mean value of the dermal and subcutaneous blood flows used in the model. The dotted lines show the variation in slope produced by varying the values of the subcutaneous flow from 2 to 10 ml/100g/min and E from 0.2 to 0.6

(b) Discussion

The results of the above model have shown that, despite the transfer of ^{133}Xe from the dermis to the subcutaneous tissue by the two processes described previously, after direct labelling of the dermis the blood flow in it is represented by the first component of a bi-exponential analysis of the clearance curve. This, however, is only true for blood flows greater than a certain value and, where low flows are involved, which is unfortunately the case in many clinical situations, it is not possible to obtain the value of this component. An alternative measurement is the initial slope of the curve and this has been used in previous studies using intracutaneous labelling and involving low flows (Moore, 1973; Kostuik et al, 1976). The above results have shown that there is some dependence of the initial slope on the dermal flow and in particular on the average flow. Figure 6.15 is consistent with the results of Chimoskey (1972) who compared the initial slope with the average flow obtained using venous occlusion plethysmography. However both Figures 6.14 and 6.15 and Chimoskey's results show that the initial slope is a complex measurement dependent on several factors including transfer from venous blood to fat and the relative magnitudes of the dermal and fat flows. Whether this measurement is acceptable in any particular study will ultimately depend on the use to which this measurement is to be put and an assessment of the possible effects

of changes in the factors indicated above. Clearly however it is dubious to base clinical decisions on a single measurement which is not, in fact, entirely blood flow dependent as Moore and Kostuik et al have done.

6.4.2 Relationship between blood flow and clearance rate - epicutaneous labelling

(a) Results

Predicted clearance curves, after three minutes of epicutaneous labelling and a further one minute waiting period, are shown in Figure 6.16 for $D = 1.3 \cdot 10^{-9} \text{ cm}^2 \text{ sec}^{-1}$, $E = 0.4$, $f_{sc} = 4 \text{ ml/100g/min}$ and for dermal blood flows of 5, 10 and 20 ml/100g/min. The curves are plotted on a logarithmic scale and, while it is clear that an infinite combination of the above variables and hence clearance curves is possible, in all cases they are characterised initially by a continually decreasing rate of clearance followed by a constant exponential rate at later times. The influence of the dermal blood flow on the curves is clearly visualised.

Experimentally considerable variation in the clearance curves was, of course, also found, depending on the site of the body and various other factors. Since no direct method of measuring skin blood flow is available the dependence of clearance rate on blood flow is often verified by plotting the curves before and after giving a stimulus which is known to alter blood flow. In the present study this was assessed in the following way. In four patients the clearance rate after epicutaneous

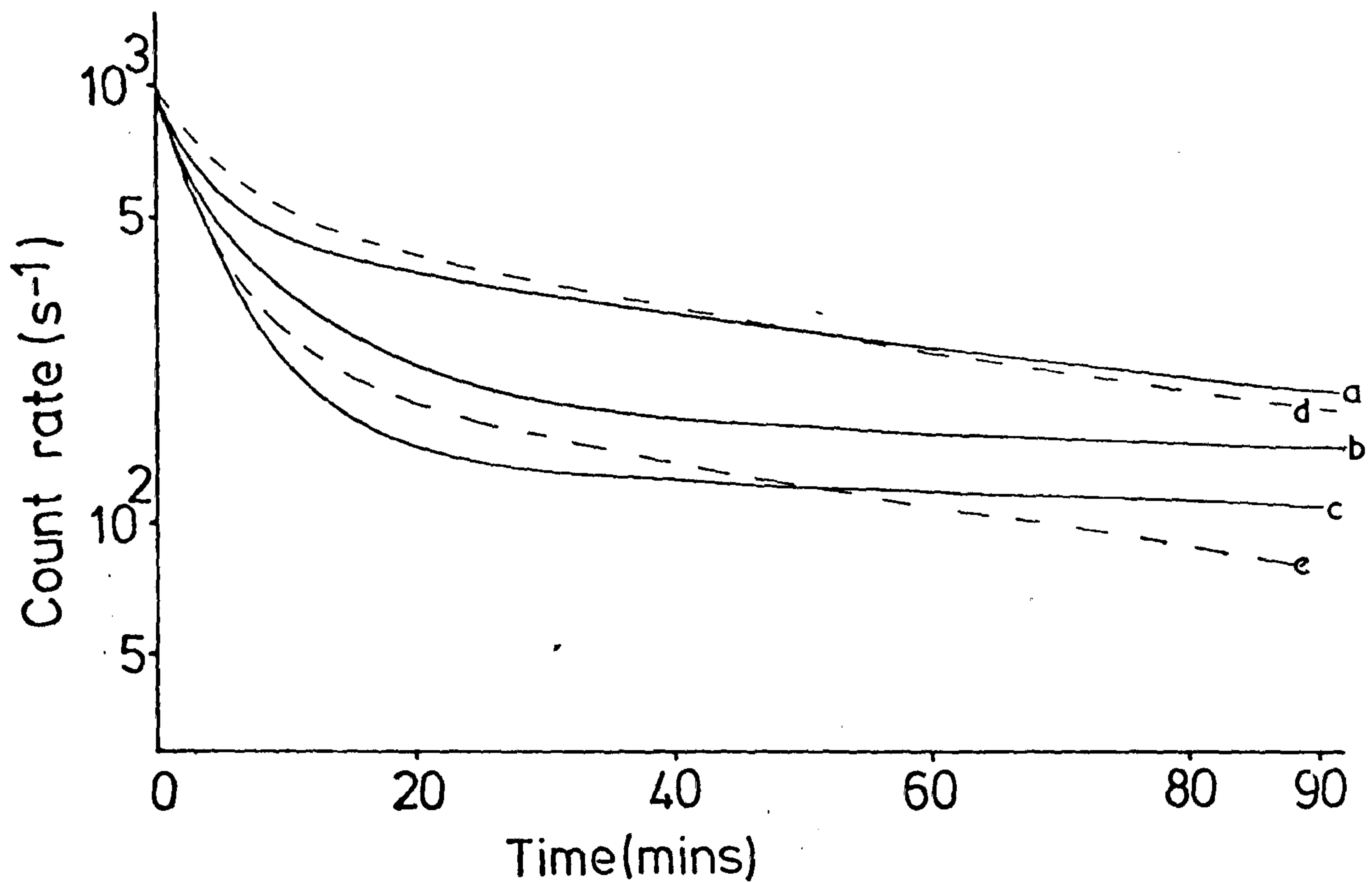


Figure 6.16 Epicutaneous labelling - the predicted clearance curves (starting 1 min. after the end of labelling) obtained for dermal blood flows of a) 5 ml/100g/min, b) 10 ml/100g/min, c) 20 ml/100g/min and for the thin epidermis with diffusion coefficient $1.3 \times 10^{-9} \text{ cm}^2 \text{ s}^{-1}$. In each case the subcutaneous flow is 4 ml/100g/min and $E = 0.4$. The dotted lines show the experimental curves obtained from skin of the forearm at rest (d) and after release of a tourniquet (e).

labelling was measured in the skin of the forearm. A cuff was then put on the opposite arm and blown up above arterial blood pressure, occluding the blood flow for ten minutes. Four minutes before the cuff was removed epicutaneous labelling was carried out on the skin distal to the cuff. On releasing the cuff a reactive hyperaemia is produced and the clearance rate in this situation is compared to the clearance rate at resting conditions on the other arm. The average clearance curves obtained at rest and with increased blood flow are shown in Figure 6.16 as dotted lines. These show a similarity to the predicted curves and again give a visual impression of the increase in clearance caused by blood flow.

Although the above results show that the dermal blood flow affects the clearance rate they do not indicate how the clearance rate is related to the flow in particular situations. Figures 6.17 and 6.18 show different series of clearance curves obtained for thin epidermis with $D = 4.0 \cdot 10^{-9} \text{ cm}^2 \text{ sec}^{-1}$ and thick epidermis with $D = 1.0 \cdot 10^{-8} \text{ cm}^2 \text{ sec}^{-1}$. For comparison Figure 6.17 includes the curve obtained for $D = 1.3 \cdot 10^{-9} \text{ cm}^2 \text{ sec}^{-1}$ and a dermal flow of 10 ml/100g/min. Therefore it is seen that although the dermal flow affects the curve, considerable variation is introduced by changes in the diffusion coefficient of the epidermis.

The predicted clearance curves were resolved into two exponential components using both the least squares fitting method and graphical stripping. The relationship

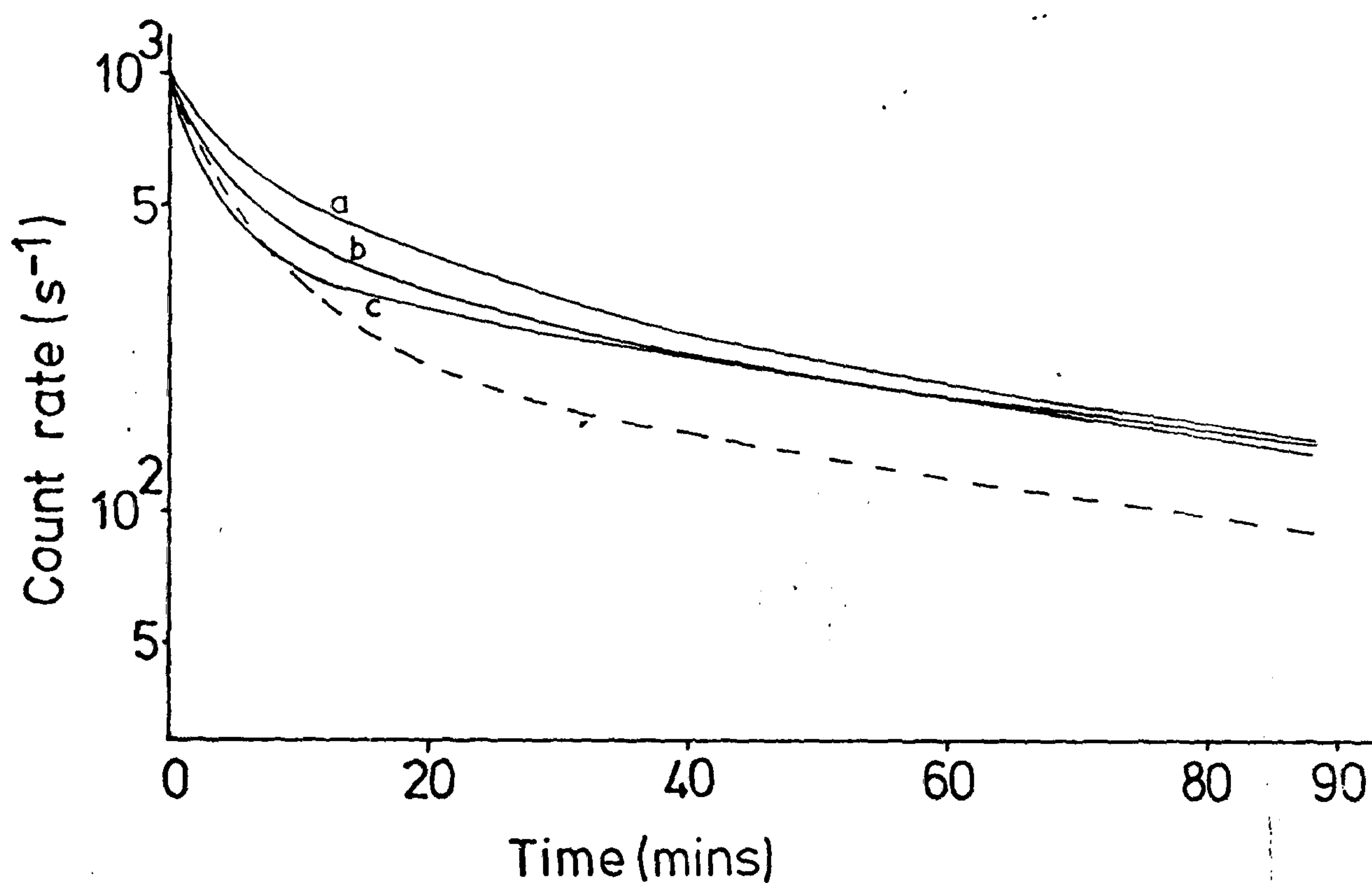


Figure 6.17 Epicutaneous labelling - the predicted clearance curves obtained for dermal blood flows of a) 5 ml/100g/min, b) 10 ml/100g/min and c) 20 ml/100g/min, for thin epidermis with a diffusion coefficient of $4.0 \times 10^{-9} \text{ cm}^2 \text{ s}^{-1}$. For comparison the dotted line shows the corresponding clearance curve for $D = 1.3 \times 10^{-9} \text{ cm}^2 \text{ s}^{-1}$ for a dermal blood flow of 10 ml/100g/min.

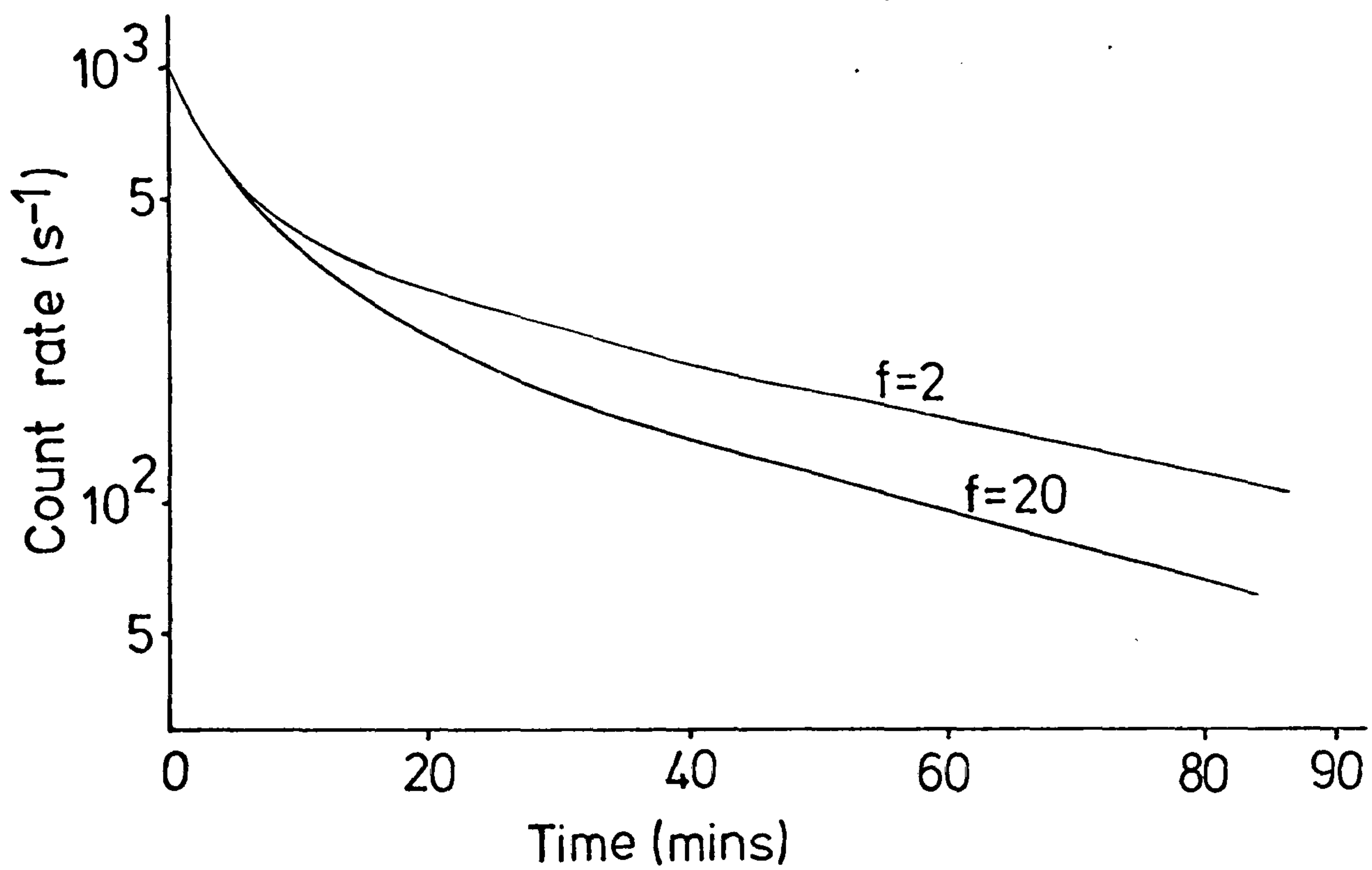


Figure 6.18 Epicutaneous labelling - the predicted clearance curves obtained for dermal blood flows of 2 ml/100g/min and 20 ml/100g/min, for thick epidermis with a diffusion coefficient of $1.0 \times 10^{-8} \text{ cm}^2 \text{ s}^{-1}$. The subcutaneous blood flow is 4 ml/100g/min and $E = 0.4$.

between the first exponential component and the true dermal flow is shown for each of these cases in Figure 6.19 for $D = 1.3 \cdot 10^{-9} \text{ cm}^2 \text{ sec}^{-1}$ and $D = 4.0 \cdot 10^{-9} \text{ cm}^2 \text{ sec}^{-1}$. The two fitting techniques differ in that with graphical stripping the subcutaneous component is precisely defined and the first component is then obtained from the rest of the data whereas the least squares method results in the errors being shared between the two components. The graphical stripping method produces lower values of the first component than the least squares method. It can be seen that there is no correlation between the first component and the dermal flow for $D = 1.3 \cdot 10^{-9} \text{ cm}^2 \text{ sec}^{-1}$ and only minimal correlation between them for $D = 4 \cdot 10^{-9} \text{ cm}^2 \text{ sec}^{-1}$. This, of course, is not surprising since it has previously been shown that much of the initial clearance is due to diffusion back out of the dermis.

It may be expected that since the predicted curve from the epicutaneous method is made up of a much more complex function than just the two exponentials proposed in other studies then this would be recognised by a poor fit of the curve. One way to test the goodness of fit is to plot the residual value, i.e. the actual value at a point minus the value predicted by fitting the curve, against time. A poor fit should yield high residual values and show a systematic deviation at long times. The percentage residual value is plotted against time for a typical predicted curve in Figure 6.20 and the levels for a typical experimental curve ($\pm 5\%$) are also

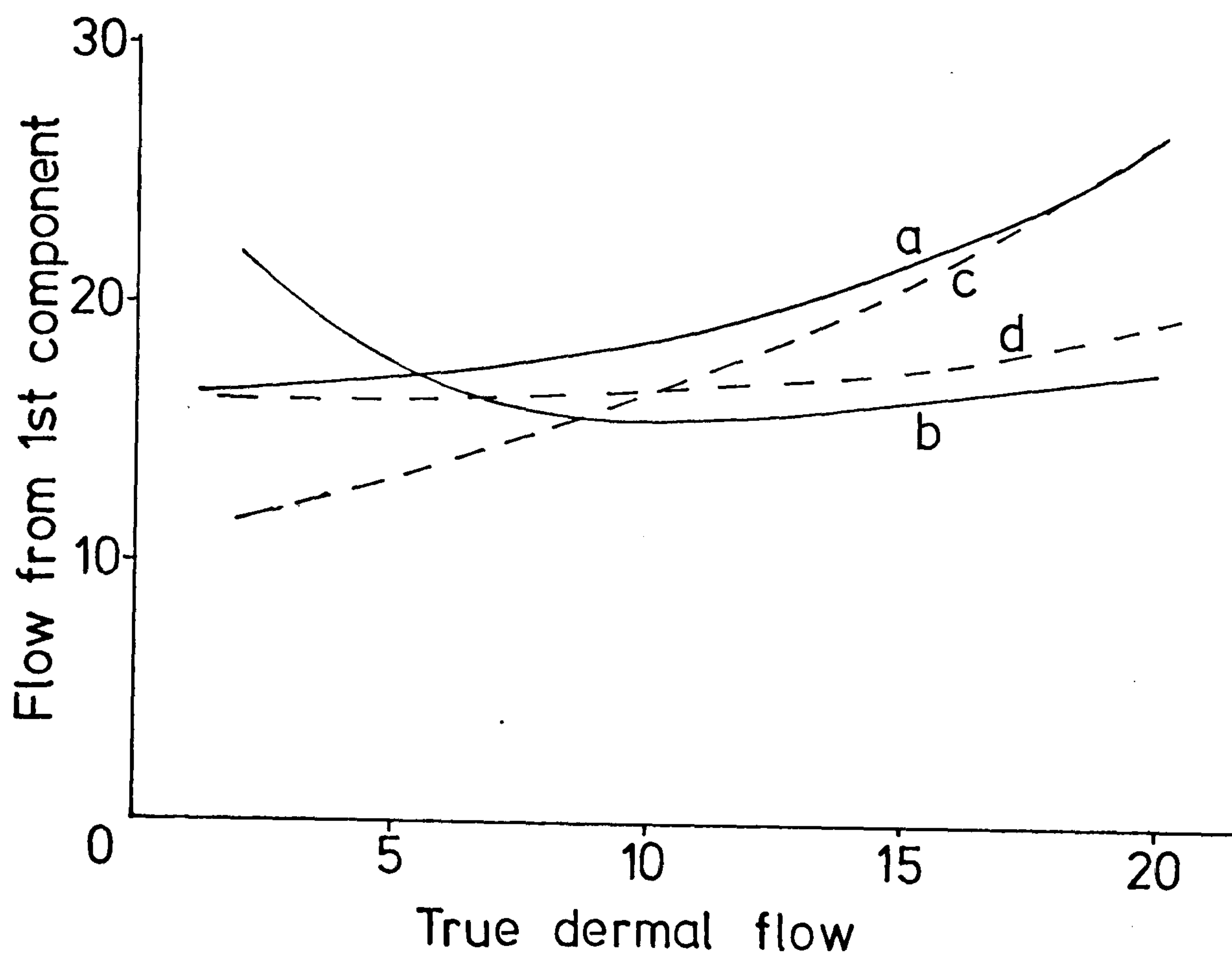


Figure 6.19 Epicutaneous labelling - the relationship between the blood flow, calculated from the first exponential component of the predicted clearance curve, and the true value of the dermal blood flow used in the model, for thin epidermis of diffusion coefficient $1.3 \times 10^{-9} \text{ cm}^2 \text{ s}^{-1}$ (b and d) and $4.0 \times 10^{-9} \text{ cm}^2 \text{ s}^{-1}$ (a and c). The first exponential component is calculated using the graphical stripping technique (dotted lines) and the least squares technique (solid lines).

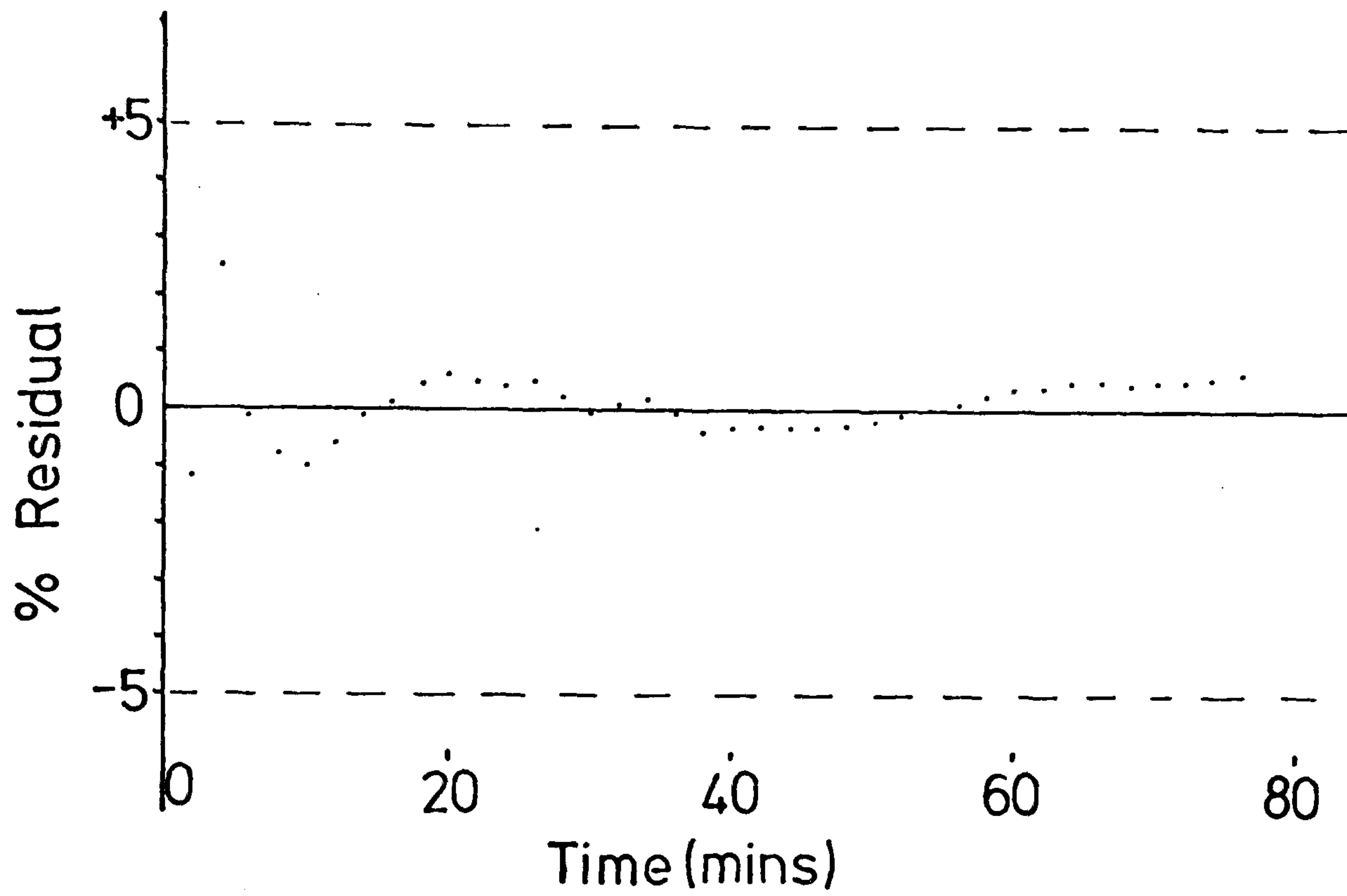


Figure 6.20 % residual value plotted against time for the fit of a double exponential function to a typical predicted clearance curve. The limits of the residual values found in experimental curves are shown by the dotted lines.

shown. It can be seen that the residual values for the predicted curve are well within the limits found experimentally. This, once again, stresses the fact that fitting a curve by a certain function does not prove that this function is the correct one.

Since most of the diffusion from the epidermis occurs in the early stages of clearance Figure 6.21 shows the relationship between the first component and the true dermal flow but neglecting the first five minutes of the curve. This results in an improved correlation between them, particularly for the higher value of the diffusion coefficient. However the correlation is still poor at low flows and variations in the epidermal diffusion coefficient are clearly of major importance. Any further delay in analysing the clearance curves only results in greater errors in determining the first component since its relative amplitude is reduced.

The curves in Figures 6.16 - 6.18 show obvious changes in initial slope with blood flow and it may be felt that this would provide a useful measurement. However, as in the previous section this slope is dependent on E and f_{sc} . Figure 6.22 shows the slope after the first five minutes of clearance, plotted against blood flow, for different values of the diffusion coefficient. Again, although the 5 minute slope of the clearance curve increases with blood flow, it underestimates the flow, and there is considerable variation with the epidermal diffusion coefficient.

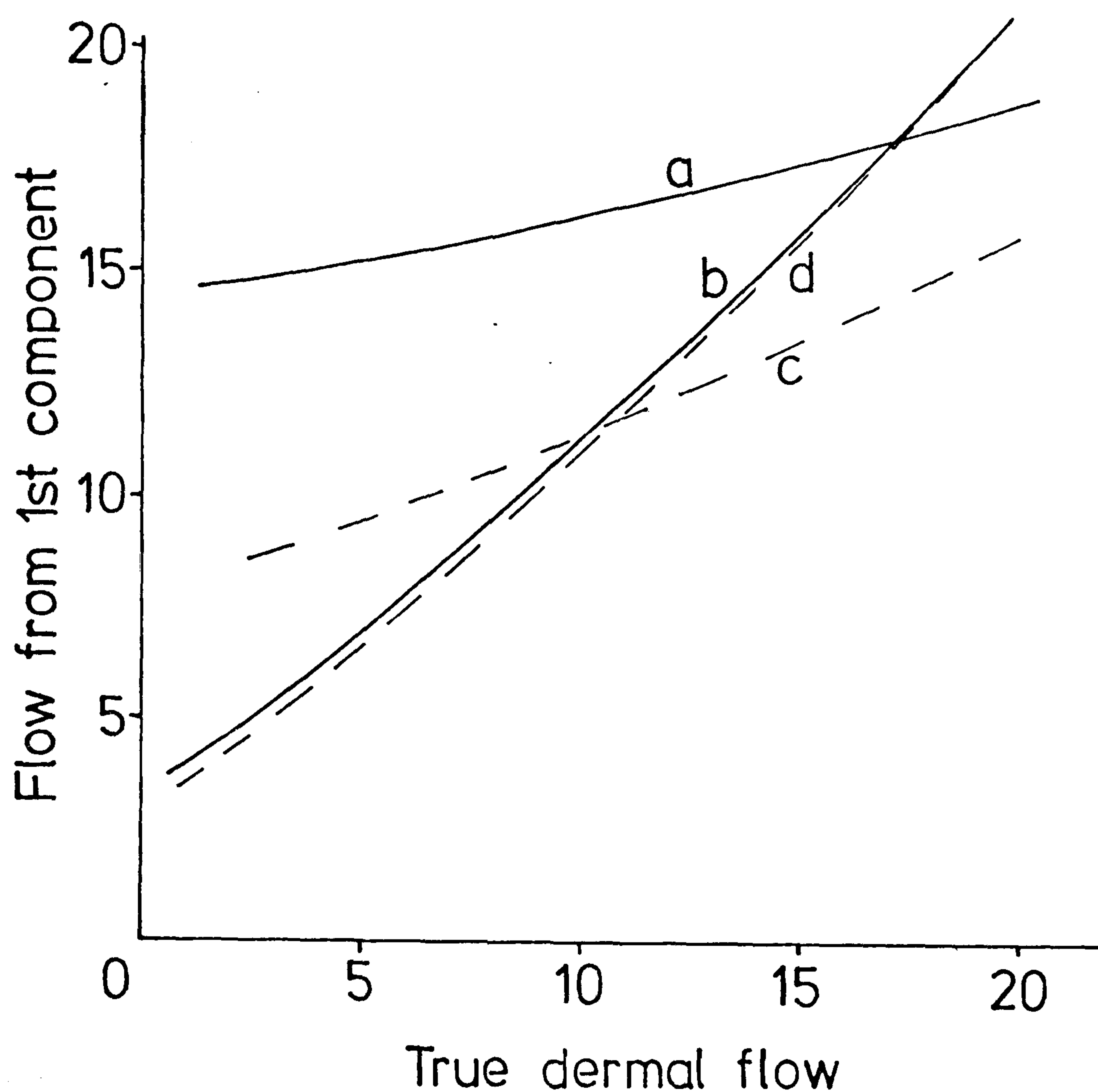


Figure 6.21 Relationship between the blood flow calculated from the first component of the predicted clearance curve, neglecting the first 5 minutes of this curve, and the true dermal blood flow. a) and c) represent thin epidermis with $D = 1.3 \times 10^{-9} \text{ cm}^2 \text{ s}^{-1}$; b) and d) represent $D = 4.0 \times 10^{-9} \text{ cm}^2 \text{ s}^{-1}$. The solid lines are again obtained using the least squares fit and the dotted lines using graphical stripping.

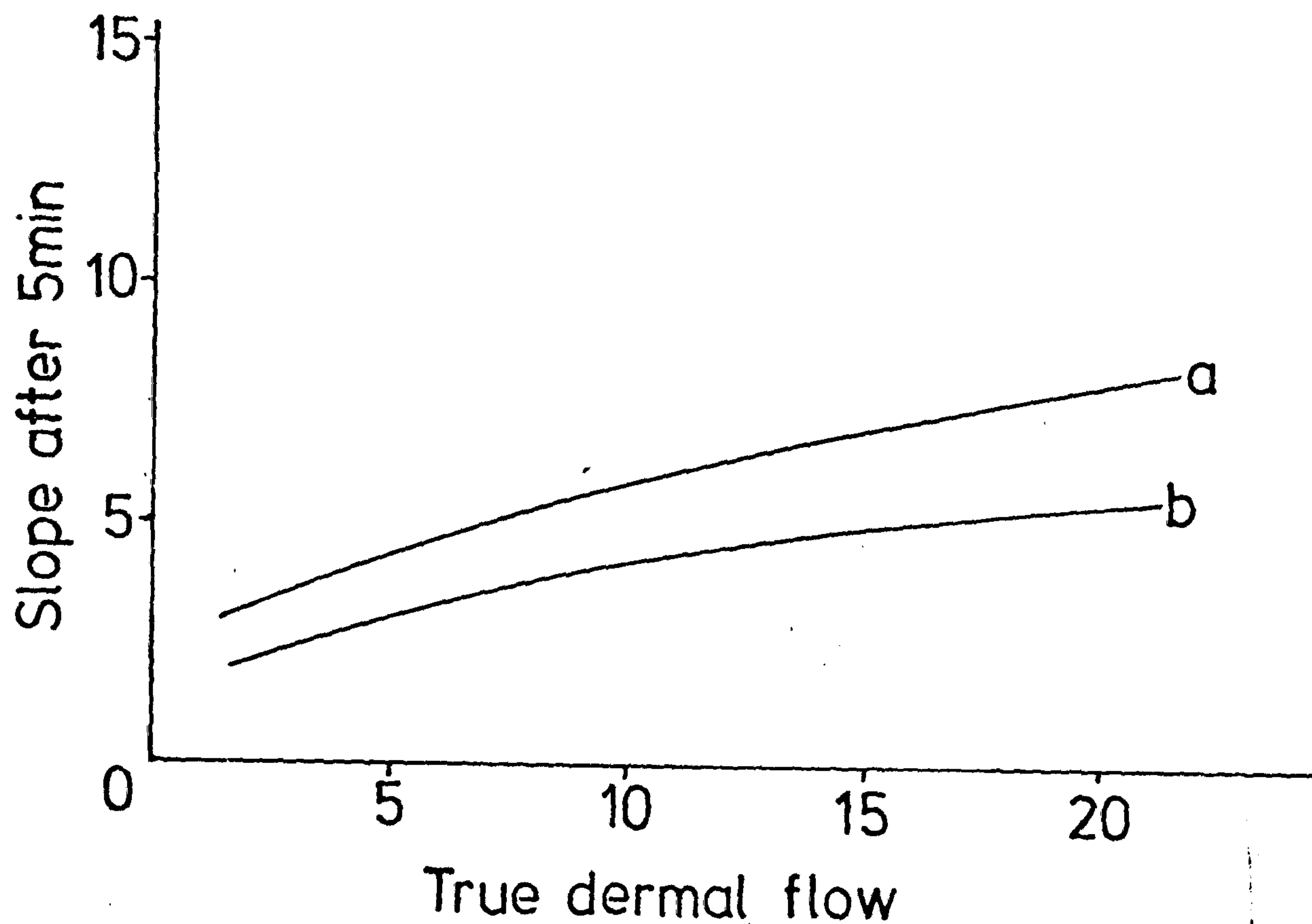


Figure 6.22 Relationship between the blood flow, calculated from the initial slope of the predicted clearance curve, neglecting the first 5 mins. of the curve, and the true dermal blood flow. a) epidermal diffusion coefficient = $1.3 \times 10^{-9} \text{ cm}^2 \text{ s}^{-1}$, $E = 0.4$, $f_{\text{SC}} = 4 \text{ ml}/100\text{g}/\text{min}$, b) $D = 4.0 \times 10^{-9} \text{ cm}^2 \text{ s}^{-1}$, $E = 0.4$, $f_{\text{SC}} = 10 \text{ ml}/100\text{g}/\text{min}$.

(b) Discussion

The model of the epicutaneous labelling technique has shown that the various indices which may be used to characterise the clearance rate of the ^{133}Xe are all poorly correlated with the dermal blood flow and, instead, are more dependent on the diffusion characteristics of the epidermis. Despite this the clearance curves from skin, which are dominated by diffusion of ^{133}Xe back out of the epidermis and also forward into the dermis, are adequately described by double exponential functions. The errors involved in fitting the predicted curves with such functions are, as shown in Figure 6.20, within the errors obtained from experimental curves. Handel et al (1976) also used the least squares method and for their experimental data obtained a plot of residual values similar to Figure 6.20. They therefore accepted this as justification of the two exponential, blood flow dependent model. Their measurements in control subjects, in the forearm, showed a mean value of 20.4 ml/100g/min which is remarkably similar to the value of the first component in Figure 6.19. However in the present case this has been shown to be due to diffusion and not, in fact, related to blood flow. The apparent reduction in flow in skin flaps, reported by Handel et al may instead have reflected the change in diffusion properties of the epidermis as the skin became necrotic. A similar conclusion may be drawn from the study of Kostuik et al (1976), who investigated the clearance rate in patients with poor

circulation due to peripheral vascular disease. The relevance of their measurement of initial slope to blood flow has certainly been shown to be questionable. Greeson et al (1973) attempted to show the effect on blood flow of the application of drugs to the skin surface. Again the possibility of the drugs causing changes in diffusion properties must be considered as the cause of the resulting changes in clearance rate.

6.5 CONCLUSIONS

It has been shown with the aid of simple mathematical models that the clearance of ^{133}Xe from the skin is a complex process dependent on the interaction of diffusion and blood flow, both of which allow the transfer of ^{133}Xe within and away from the skin. The variability of the skin in terms of its composition, thickness, diffusion properties, vascular architecture, etc., particularly in pathological conditions, means that the number of ways in which these processes can interact is virtually limitless. The present study has been confined to a model of clearance from what is generally considered as normal skin.

The following particular results of the models have been shown to be consistent with experimental data.

(a) Exchange of ^{133}Xe can occur between the tissue and blood vessels larger than capillaries and this allows ^{133}Xe to be picked up in one part of a tissue and then deposited again in a different part as the venous blood passes through it. While this process is more readily

demonstrated in the subcutaneous fat it may also occur in the dermis with the particular labelling technique used in the present study. This means that the ^{133}Xe will "roll" through a tissue, producing a clearance rate which is not directly related to blood flow.

(b) With intracutaneous labelling, diffusion of ^{133}Xe occurs from the dermis to the fat. At low flows this, along with process (a), makes it difficult to determine the exponential component related to blood flow.

(c) The initial slope of the curve, while often used as a measure of the dermal blood flow, is only poorly correlated with this and is also dependent on the subcutaneous flow and the magnitude of the transfer from blood to fat.

(d) Diffusion within and out of the epidermis is the dominant process in the initial stages of the clearance of ^{133}Xe after epicutaneous labelling. For this reason dermal blood flow cannot be measured by the first exponential component of the curve. Other indices calculated from later parts of the curve are only poorly correlated with this flow.

Although the clearance of ^{133}Xe from the skin is undoubtedly affected by blood flow the processes summarised above mean that it is not possible to obtain a reliable measurement of the blood flow. In any specific situation it would always be questionable whether the changes seen are due to blood flow or these other factors and this is particularly true at low flows.

To base clinical decisions on an individual result requires a technique with exceptional accuracy.

Unfortunately the epicutaneous labelling of ^{133}Xe has been shown to be incapable of providing this and it is therefore unsuitable for use in the clinical setting of plastic surgery.

CHAPTER 7LOCALISED HYPERTHERMIA - TECHNIQUES
AND TISSUE CHARACTERISTICS

7.1 INTRODUCTION

7.2 TECHNIQUES OF LOCALISED HYPERTHERMIA

7.2.1 Water bath or conduction heating

7.2.2 Localised current field heating

7.2.3 Microwave heating

7.2.4 Equilibration point

7.2.5 Finite difference approximation of heating
terms

7.3 TISSUE GEOMETRIES

7.3.1 Finite difference forms of the conduction
equations

7.4 TISSUE CHARACTERISTICS

7.5 METABOLIC HEAT PRODUCTION

7.6 TISSUE BLOOD FLOW

7.6.1 Finite difference form of blood flow term

7.7 CALCULATED PROCEDURES

7.7.1 Summary of the computer programs

7.7.2 Evaluation of the accuracy of the programs

7.1 INTRODUCTION

Localised hyperthermia involves the heating of a limited volume of the tissues of the body by means of an external heating modality. The temperature distributions produced by this depend on the heating pattern of the particular modality itself and also on the heat transfer processes which exist within the tissue. Calculation of these temperature distributions, using the mathematical models described in chapter 3, requires knowledge of specific characteristics of both the techniques and the tissues, and these are detailed in the present chapter. Firstly, although it is not the purpose of the present study to compare heating techniques, the three modalities which are used in order to illustrate the effects of blood flow and conduction are described in section 7.2. The arrangement of tissues is then discussed in section 7.3 and in particular the modifications to the conduction equation, to take account of specific geometries, are detailed. In section 7.4 the properties of various tissues, which determine their thermal characteristics, are given. Heating of a tissue by its own metabolism is then considered in section 7.5 and, in section 7.6, typical values of the blood flow in various tissues are tabulated. Following this some specific aspects of the blood flow in a tumour are discussed. Although many of the problems in localised hyperthermia, to be presented in the next chapter, are open to solution by simple analytical methods, the more complex arrangements require

the use of the finite difference numerical method. In each of the above sections the finite difference approximations are therefore detailed and in section 7.7 a summary of the computer program based on these is given.

7.2 TECHNIQUES OF LOCALISED HYPERTHERMIA

The temperature distributions produced in tissue obviously depend primarily on the physical technique used to deposit heat within it. Three techniques giving widely differing heating patterns have been modelled in the present study. The aim of this was not to assess the relative merits of each technique but to provide heating patterns which would best allow the effects of blood flow and conduction to be assessed.

7.2.1 Water bath or conduction heating

The simplest way of heating a tissue is by direct conduction of the heat from the surrounding medium and this is most commonly carried out on small animals. The tissue is immersed in a hot water bath, which is kept well stirred and whose temperature is kept constant (Crile, 1963). Variations in this technique involve the infusion of hot fluid into a body cavity, for example the bladder (Hall et al, 1974) or the perfusion of hot fluid through the body's vascular network (Cavaliere et al, 1967). One advantage of this technique is that, if the temperature of the fluid is carefully monitored, this will equal the value within the tissue and thus there will be no possibility of producing local "hot" spots at temperatures above this value.

7.2.2 Localised current field heating

This heating technique involves passing a high frequency (100 kHz - 1 MHz) alternating current through the tissue by means of two electrodes placed, most usually, on opposite sides of the tissue. The advantage of this technique is that it most closely represents an ideal heating modality since, with the above arrangement, an almost uniform heat generation is produced (Doss and McCabe, 1976). Its disadvantage is that the different tissues of the body vary greatly with regard to their resistivity (Geddes and Baker, 1967) and hence there is a considerable difference in the heat produced within each of them. For the present study this technique is considered in two forms; one in which the heating is assumed completely uniform within each tissue treatment volume and the second in which the above is true but in addition a heating penumbra is present due to which heat is also generated outwith the treatment volume, the heating falling to 50% at 0.5 cm outwith the volume.

7.2.3 Microwave heating

Microwaves are absorbed exponentially with depth in a homogeneous tissue (Schwan, 1967) and hence the temperature rise, ΔT , produced is given by

$$\Delta T = E_0 \exp(-2x/d) \quad (7.1)$$

where x is the depth from the surface of the tissue

d is the depth of penetration of the electric field

E_0 is a constant dependent on the power of the source. The depth of penetration of the electric field, d , is a function of the electrical properties of the tissue, which in turn varies with the frequency of the microwaves. A value of $d = 1.7$ cm corresponding to the absorption of 2450 MHz microwaves in muscle was used here.

Therefore within a single tissue the temperature produced will fall exponentially with distance from its surface. In some cases it may be possible to heat the tissue from more than one side and so reduce the temperature gradient.

7.2.4 Equilibration point

It is essential in the practical application of hyperthermia that some indication of the tissue temperature is available. In some cases, involving conduction heating, this has simply been assumed to bear a direct relationship to the temperature of the heated fluid (Robinson et al, 1974; Hall et al, 1974) but doubts have been raised about this (Robinson et al, 1978; Hume et al, 1979) particularly where complex geometries are involved. For all other techniques it is the practice to monitor the tissue temperature by means of a small thermister or thermocouple probe inserted into it (Overgaard and Overgaard, 1972; Marmor et al, 1977). Heating of the tissue continues until the temperature at this point, known as the equilibration point, reaches the desired

level at which time the heating source is then switched off. The output of the heating modality is therefore controlled by feedback from this sensor, the power being switched on as the tissue loses heat due to blood flow or conduction and off again when the equilibration temperature is reached. In general the temperature at other points in the tissue are not monitored.

7.2.5 Finite difference approximation of heating terms

The simulation of heat input, either by the localised current field (LCF) method or by microwaves, is achieved in the finite difference model by increasing the temperature, at each nodal point, by a constant value at each time step. For the LCF heating all points within the treatment volume are increased by the same value which is given by

$$\Delta T = \frac{W_0 l}{c} \quad (7.2)$$

where W_0 is the power delivered per unit mass of tissue ($J g^{-1} s^{-1}$).

l is the time step (s)

and c is the specific heat ($J g^{-1} ^\circ C^{-1}$)

The points within the penumbra of the field are increased by a fraction of the above value, the fraction depending on the position from the edge of the treatment volume.

For microwaves a similar expression is used for the points at the surface of the tissue while, at depth, allowance is made for the exponential fall off given by

Equation 7.1

equation 7.1.

7.3 ARRANGEMENT OF TISSUES

The aim of this part of the study is to investigate the general effects of blood flow and thermal conduction in hyperthermia and not to consider any specific situation. Thus, unlike chapter 5, a specific arrangement of tissues is not used here and, instead, different arrangements are described in the next chapter as they are used. For example in assessing the effect of blood flow each tissue is effectively considered in isolation and with no particular dimensions. Different tissue geometries are, however, considered in assessing the effects of conduction and the modifications required to deal with these are now discussed.

7.3.1 Tissue geometries

The regions of the body can be thought of in a variety of forms; for example a leg can be considered as a cylinder, while many tumours are essentially spherical. This means that it is simpler to consider such tissues using different coordinate systems and consequently different forms of the conduction equations are required. The general form of the equation is

$$\frac{\partial T}{\partial t} = a \nabla^2 T$$

where the terms are as described for equation 3.3.

It has already been shown that for a one dimensional system this can be written as

$$\nabla^2 T = \frac{\partial^2 T}{\partial x^2}$$

and clearly this can be extended to two or three dimensions.

$$\nabla^2 T = \frac{\partial^2 T}{\partial x^2} + \frac{\partial^2 T}{\partial y^2} + \frac{\partial^2 T}{\partial z^2} \quad (7.3)$$

For a cylindrical tissue where conduction in only the radial direction is being considered this is then given by

$$\nabla^2 T = \frac{\partial^2 T}{\partial r^2} + \frac{1}{r} \frac{\partial T}{\partial r} \quad (7.4)$$

and similarly for a spherical region

$$\nabla^2 T = \frac{\partial^2 T}{\partial r^2} + \frac{2}{r} \frac{\partial T}{\partial r} \quad (7.5)$$

7.3.2 Finite difference forms of the conduction equations

As in section 3.5 the finite difference forms of the above equations can be calculated and, for equation 7.4, this becomes

$$T_{i,k+1} = iPT_{i-1,k} + P(1+i)T_{i+1,k} - \left((1+2i)P-1 \right) T_{i,k} \quad (7.6)$$

Similarly the spherical form of the diffusion equation 7.5 is given by

$$T_{i,k+1} = iPT_{i-1,k} + P(2+i)T_{i+1,k} - \left((2+2i)P-1 \right) T_{i,k} \quad (7.7)$$

where $P = \frac{lD}{ih^2}$

the radius is given by $r = ih$

h is again the distance step and l is the time step

7.4 TISSUE CHARACTERISTICS

The thermal characteristics of the tissues of the body have been thoroughly investigated and the values used in the present study (Table 7.1) as taken from the literature (Hatfield and Pugh, 1951; Minard, 1970; Nevins and Darwish, 1970; Bowman et al, 1975). The thermal conductivity values correspond to those found in excised specimens. It has been shown (Bowman et al, 1975) that the apparent thermal conductivity of a tissue is higher in vivo due to the blood flow, as will be seen in the next chapter.

For comparison with chapter 5, the thermal diffusivity values are also included, using the same units as in that chapter. The greater than 10^2 difference in diffusivity between heat and ^{133}Xe clearly results in a much more significant transfer of heat by this process.

7.5 METABOLIC HEAT PRODUCTION

Heat is continually being produced within the body by metabolism. Typical values of the basal metabolic heat production are given for several tissues in Table 7.2 (Draper and Boag, 1971; Guy et al, 1974). For the range of increased temperatures considered in the present study the metabolic heat rate varies according to van't Hoff's law (Newburgh, 1968), producing values approximately 65% higher at 42.5°C . Taking into account that a minimum value of heat generation by external means of $50\text{--}100 \text{ mW g}^{-1}$ is used in hyperthermia (see chapter 8) the effect of metabolism is therefore minimal in most

TABLE 7.1TISSUE CHARACTERISTICS

	<u>Density</u> (gcm^{-3})	<u>Specific heat</u> ($\text{J g}^{-1} \text{ } ^\circ\text{C}^{-1}$)	<u>Thermal conductivity</u> ($\text{Wcm}^{-1} \text{ } ^\circ\text{C}^{-1}$)	<u>Thermal diffusivity</u> ($\text{cm}^2 \text{s}^{-1}$)
Fat	0.94	2.3	0.079×10^{-2}	3.7×10^{-4}
Muscle	1.07	3.5	0.39×10^{-2}	1.0×10^{-3}
Bone	1.79	1.3	1.5×10^{-2}	6.4×10^{-3}
Blood	1.056	3.9	0.49×10^{-2}	1.2×10^{-3}

TABLE 7.2BASAL METABOLIC HEAT PRODUCTION

<u>Organ</u>	<u>Heat Production</u> (W g^{-1})
whole body	1.3×10^{-3}
fat	0.4×10^{-3}
muscle	0.7×10^{-3}
skin	1.0×10^{-3}
liver	4.0×10^{-3}
brain	11×10^{-3}
kidney	15×10^{-3}

situations, but may have to be considered in specific organs such as the kidney.

7.6 TISSUE BLOOD FLOW

Values of the blood flow in different tissues and organs in man are given in Table 7.3 and illustrate the substantial variation, not only from one tissue to another, but also between the resting and maximum flows found in the same tissue. It is known that the blood flow in skin increases considerably with temperature and that this occurs through a variety of mechanisms (Hertzman, 1961) including a direct effect of temperature on tissues, local nervous control, central control through the hypothalamus and the release of chemical vasodilators. However the interactions of such mechanisms do not always produce this result and in contrast the blood flow to the intestine and kidney appear to decrease during body heating (Shepherd and Webb-Peploe, 1970). The actual effect in any tissue will depend on the above mechanisms and also on the volume of tissue heated and the time of heating, i.e. on whether the heating can be described as local, regional or body heating. Although most studies in hyperthermia have used a function which describes the increase of flow with temperature (Chan et al, 1973; Guy et al, 1974; Yang and Wang, 1979) this contrasts with recent evidence which shows a decrease in flow within a tumour (Song et al, 1980; Bicher et al, 1980). It is evident that our knowledge of the change in blood flow with temperature is incomplete and for this

TABLE 7.3

BLOOD FLOW IN TISSUES AND ORGANS IN MAN

<u>Tissue</u>	<u>Resting blood flow</u> (ml/100g/min)	<u>Maximum blood flow</u> (ml/100g/min)	<u>References</u>
Muscle	1.6	60	1,2
Fat	3.3	30	2,3,4
Liver	30	180	2
Kidney			
- cortex	400	500	
- juxtamed zone	100		2,5
- medulla	20		
Adrenals	500		6
Thyroid	400		6
G.I. tract	35	275	2
Skin	5	170	2,7
Myocardium	70	400	2
Human Lymphoma	18	60	8
Anaplastic carcinoma	3	20	8

References: 1. Lassen et al, 1965. 2. Mellander and Johansson, 1968. 3. Nielsen, 1972.
4. Nielsen, 1973. 5. Hollenberg, 1973.
6. Mapleson, 1963. 7. Sejrsen, 1971.
8. Mantyla et al, 1976.

reason the present study makes no allowance for such variations during the treatment time. What is clear is that these changes will only serve to enhance the importance of blood flow in hyperthermia treatment.

In the next chapter it is assumed that in general the blood flow within a tissue is homogenous. The exceptions to this are where individual blood vessels are being considered and also where a particular pattern for a solid tumour is being examined. It has been suggested (Straw et al, 1974; Jain and Wei, 1977) that a solid tumour has a central core in which the blood flow is very low and the tissue necrotic. Outwith this area the flow is much higher and indeed in the outside shell of the tumour the flow may be several times higher than the surrounding normal tissue (Endrich et al, 1979). Although such a pattern is examined in the next chapter it should be emphasised here that this is in no way characteristic of all tumours.

7.6.1 Finite difference form of blood flow term

As in section 5.6 the simulation of the removal of heat by the capillary blood flow, in the computer model, is achieved by reducing the temperature by a constant fraction at each time step, i.e.

$$\Delta T = - \frac{f_i \rho l}{100 \lambda'_i} (T_{i,k} - 37^\circ\text{C}) \quad (7.8)$$

where l is the time step

f_i is the blood flow in ml/100g/min

λ'_i is the ratio of specific heat of tissue: specific

heat of blood

ρ is the density of tissue

It is assumed that the temperature of the blood arriving at each nodal point is 37°C . This will be discussed fully in chapter 8.

7.7 CALCULATION PROCEDURES

With the characteristics of both the tissues and techniques thus defined in the above sections, substitution of the appropriate values into the mathematical models of chapter 3 allowed the calculation of the effects of conduction and blood flow in hyperthermia. For each situation the particular constants, geometry and initial conditions are indicated in the next chapter. The flexible computer programs based on the finite difference approximations are capable of providing a solution to all of the situations investigated but in some cases simpler analytical solutions have been used, and these are described where necessary.

7.7.1 Summary of the computer programs

Although more than one computer program was used a general summary of the steps involved is given below and an example is listed in Appendix D. The program was again written in FORTRAN and run on Digital PDP-11 and Data General Nova minicomputers.

(a) Following input of the tissue characteristics the initial values of the temperature were attributed to each nodal point. In most cases the points were at

normal body temperature, 37°C .

(b) At one time step later the new temperatures throughout the tissue and at the boundaries, due to conduction, were calculated. For one dimensional, cylindrical and spherical geometries this involved the use of equations 3.14, 7.6 and 7.7 respectively and an equation of the form 3.16 for the boundary where necessary. In most cases the boundary condition was satisfied by holding the temperature constant at an end point.

(c) The temperature was then reset to the relevant value for any points within the tissue which were to be constant.

(d) Using equation 7.8 the temperature at each point was altered by a certain amount to allow for the effect of blood flow. Different corrections were used if the flow was different in various regions of the tissue.

(e) The temperature at the equilibration point was then examined and if this was less than the desired value, it was increased by an amount determined by the particular heating modality (see section 7.2.5). If the desired temperature had been reached no further heat was deposited in the tissue.

(f) These processes were repeated each time step until the required total time had been reached.

7.7.1 Evaluation of the accuracy of the programs

The programs were evaluated as in section 5.7.1, using known analytical solutions for conduction in plane, cylindrical and spherical geometries (see Luikov pp. 97,

131 and 119). In each case the comparison between the finite difference computer model and the analytical solution showed an error of less than 0.1°C for times up to 45 minutes. The finite difference model was therefore considered acceptable for the present study.

CHAPTER 8LOCALISED HYPERTHERMIA - RESULTS AND DISCUSSION

8.1 INTRODUCTION

8.2 EXCHANGE OF HEAT BETWEEN BLOOD VESSELS AND TISSUE

8.2.1 Determination of the heat exchange vessels

8.2.2 Axial temperature distribution

8.2.3 Radial temperature distribution

8.2.4 Discussion

8.3 ROLE OF THE "CAPILLARY" BLOOD FLOW

8.3.1 Model of the removal of heat by the capillary
blood flow

8.3.2 Results

8.3.3 Discussion

8.4 THE EFFECTS OF THERMAL CONDUCTION

8.4.1 Models of thermal conduction

8.4.2 Results

8.4.3 Discussion

8.5 INTERACTION OF BLOOD FLOW AND CONDUCTION

8.5.1 Models

8.5.2 Results

8.5.3 Discussion

8.6 CONCLUSIONS

8.1 INTRODUCTION

This chapter now looks at the predictions of the mathematical models with regard to the ways in which both blood flow and thermal conduction can modify the temperature distributions produced during heating of a localised region of tissue. In order to emphasise their individual effects each process is dealt with separately, starting in section 8.2 with an examination of the exchange of heat between the tissue and the blood flowing in individual blood vessels. The importance of the different generations of blood vessels in cooling the tissue and in transporting heat to other parts of the tissue is investigated. An ideal view of the blood flow, as a diffuse heat sink, is then adopted in section 8.3 to describe its overall effects. The ability of thermal conduction to smooth out temperature gradients is analysed in section 8.4 and following this the way in which blood flow and thermal conduction interact in specific situations is examined in section 8.5. Finally section 8.6 presents a summary of the roles played by the above processes in localised hyperthermia. The limitations and possible benefits introduced by them is discussed and the prospects for clinical use of localised hyperthermia examined.

Throughout this chapter the importance of any temperature non-uniformity within the treatment volume is assessed by referring to section 1.5.2. From that it should be remembered that the difference in temperature

required to produce 100% necrosis in a normal tissue compared to virtually no necrosis is only 0.5°C (Field and Bleehen, 1979; Dickson and Calderwood, 1980). Alternatively the percentage difference in heating times to produce such effects is only 20%. The implications of these figures depend on the specific arrangement of the tumour and normal tissue. In an ideal situation the tumour would form a well demarcated region surrounded by normal tissue, and the temperature field could, in theory, be shaped so that the temperature in the normal tissue would be at least 0.5°C below that of the tumour. In relation only to the heating effect, the upper limit of temperature at the centre of the tumour would not be crucial, provided conduction to the normal tissue did not result in its temperature rising above the critical level. In practice few techniques are available to provide accurate localisation of even well defined tumours. Furthermore many tumours infiltrate the normal tissue and thus have no definite edges. For these reasons the treatment volume will necessarily contain both normal and tumour tissue and clearly in these circumstances, to prevent an unacceptable level of normal tissue damage, the temperature within such a volume must be closely controlled. Again, however, a high temperature, confined to the tumour bearing area itself, may be acceptable. On the basis of the above observations two criteria have been formulated for the present study in order to assess the temperature distributions.

- a) Accepting Dickson and Calderwood's (1980) recommendations of the optimum treatment temperature and time, although different temperatures are used by other investigators, minimal normal tissue damage will be produced in areas at a temperature of less than 42°C or in other words an ineffective thermal dose will be delivered at this level. At temperatures above 42.5°C almost complete destruction of the tissue would be expected.
- b) Assuming an optimum treatment time of one hour at 42°C then a reduction in this time of about 10 mins ($\sim 20\%$) for a particular region will again lead to an ineffective dose. In other words if the temperature in part of the volume is increased immediately to the desired level (42°C) while that in another part takes 10 minutes to achieve, considerable difference in hyperthermal effect will be produced.

8.2 EXCHANGE OF HEAT BETWEEN BLOOD VESSELS AND TISSUE

The approach here is similar to that of chapter 6 in that the first step is to define which blood vessels play a significant part in the exchange of heat between the blood and tissues. However it is clear that in hyperthermia not only the total exchange, but also the temperature distributions along and around the vessels, are required. Although the temperature may be reduced for only a small distance around a blood vessel this may, of course, still be significant with regard to the re-growth of a tumour. The analysis therefore includes

the axial and radial temperature distributions around the blood vessels.

8.2.1 Determination of the heat exchange vessels

Again as described in section 3.4.2 the heat lost or gained by blood as it flows through a tissue with a higher or lower temperature can be described by equation 3.10. If it is assumed that the tissue away from the blood vessel is maintained at body temperature, i.e. $T_{\text{tissue}} = 37^{\circ}\text{C}$ and the blood enters the tissue at a higher temperature than this, then by taking all temperatures relative to 37°C the equilibration of the blood with the tissue can be illustrated as in Figure 8.1. A similar graph is obtained for the passage of "cold" blood through a heated tissue. It can be seen that for values of $\frac{L}{vr}$ greater than about $5 \times 10^4 \text{ scm}^{-2}$ the temperature of the blood flowing out of the tissue is the same as that of the tissue itself or, in other words, total exchange of heat has occurred. Table 8.1 thus shows the heat exchange which can be expected in the typical blood vessels previously described in chapter 6. A comparison of the above figures with those reported in section 6.2 for ^{133}Xe clearly shows the effect of the greater than 10^2 difference in diffusivities of heat and ^{133}Xe . Heat exchange extends well beyond the capillary level and occurs to some extent even in large arteries and veins, although in these cases the length of the vessel over which this occurs is of the order of 20 cm. While each generation of blood vessel is

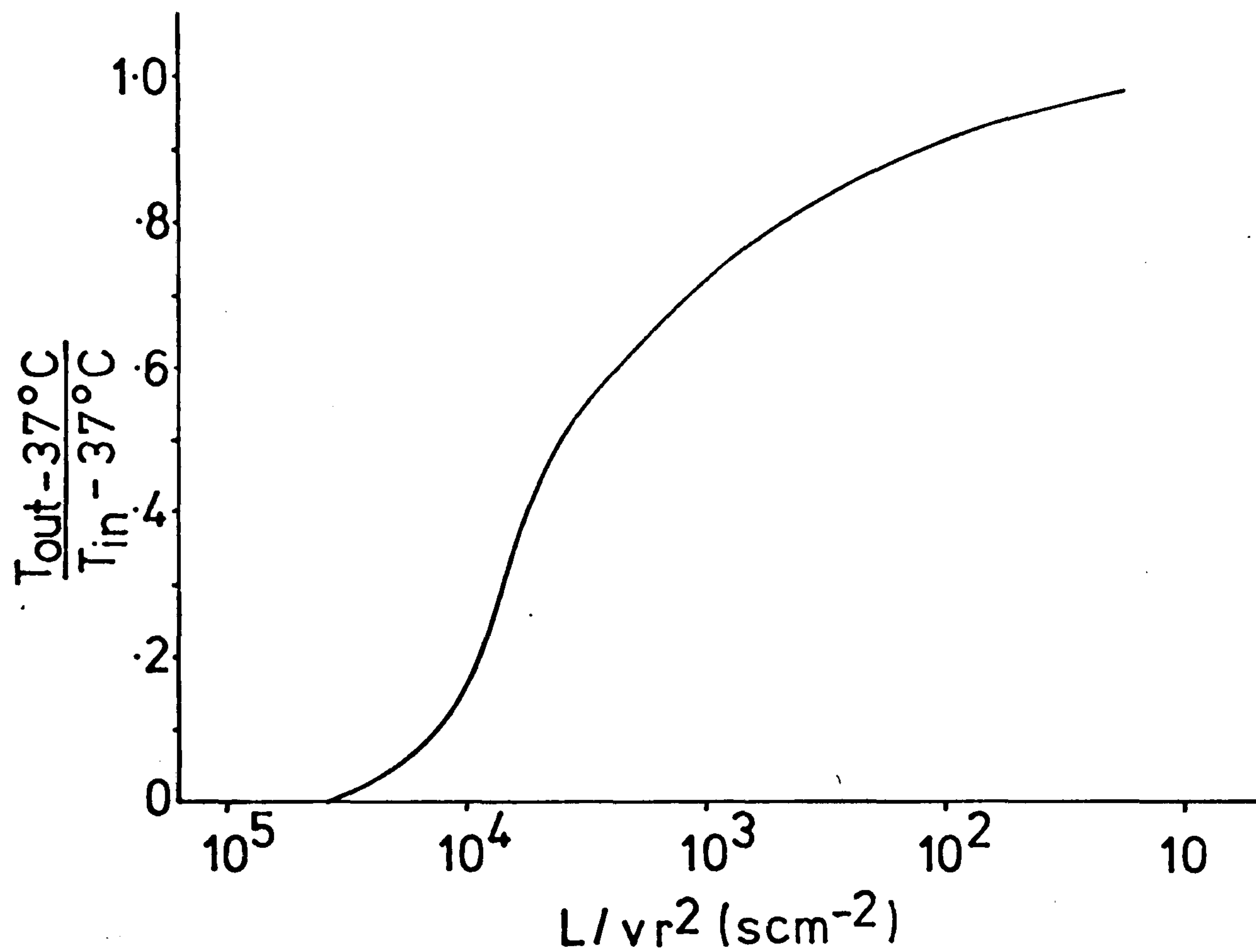


Figure 8.1 The ratio of the temperature of the blood flowing out of a blood vessel to that flowing into the vessel plotted against $L/\bar{v}r^2$, where L is the length of the vessel, \bar{v} the flow velocity and r the radius. The vessel passes through a tissue whose temperature is 37°C , with the blood temperature higher than this.

TABLE 8.1

CHARACTERISTICS OF HEAT EXCHANGE BY BLOOD VESSELS

<u>Vessel</u>	<u>Length</u> cm	<u>Radius</u> cm	<u>Velocity</u> cm s ⁻¹	$\frac{L}{vr^2}$ s cm ⁻²	% equilibration of temperature over length of vessel
Aorta	60	1	25	2.4	0
Large artery	20	0.15	20	44	5
Small artery	1	0.02	15	166	10
Arteriole	<0.2	0.001	1	2x10 ⁵	100
Capillary	<0.1	0.0004	0.05	1.2x10 ⁷	100
Venule	<0.2	0.0015	0.5	1.7x10 ⁵	100
Small vein	1	0.05	2	200	10
Large vein	20	0.25	5	64	5
Vena Cava	60	1.2	10	4.2	0

attributed with specific values of L , \bar{v} and r in Table 8.1 it is again emphasised that in reality a range of values will exist, depending on the particular tissue and, of course, the blood flow itself.

8.2.2 Axial temperature distribution

The temperature profile along a blood vessel, as it passes through a hotter or colder tissue, can also be obtained from equation 3.10 and is illustrated in Figure 8.2 for different vessels. As has been seen from Table 8.1 the arterioles, capillaries and venules allow complete heat exchange and therefore come to equilibrium with the tissue within their own lengths of 0.5 - 2 mm. The small arteries do not achieve this and, if they were long enough, would take several centimetres to reach the tissue temperature. The larger arteries travel long distances through the tissue without their temperature being appreciably affected.

8.2.3 Radial temperature distribution

As discussed in section 3.4.2 simulation of the temperature distribution around a blood vessel, during hyperthermia, has been achieved using the finite difference computer program in cylindrical coordinates (equation 7.6). The model has essentially two boundary conditions. Firstly, accepting that the axial temperature distribution is given as in the previous section and remembering that this represents a steady state solution, the temperature at the surface of the blood vessel was therefore kept constant.

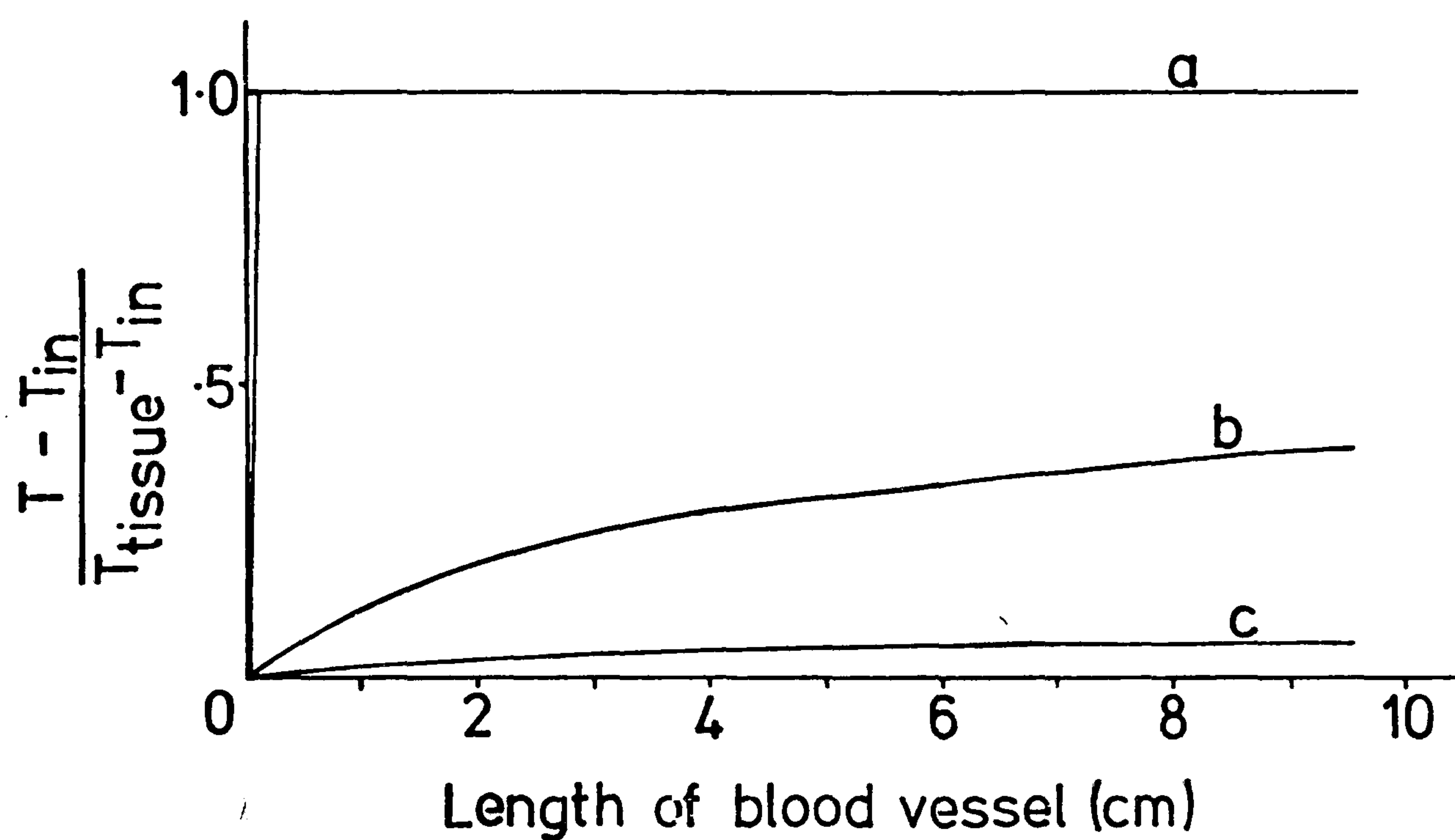


Figure 8.2 The equilibration of blood temperature, T , with the tissue temperature plotted against the length of blood vessel. a - arterioles, capillaries and venules. b - small arteries and veins. c - large arteries and veins.

$$\text{i.e. } T(r) = T_a \quad t \gg 0$$

where r is the radius of the vessel.

In addition once the temperature at the equilibration point reached the desired level it, too, was effectively kept constant.

$$T(R_0) = T_q \quad t \gg t_q$$

where R_0 is the radial position of the equilibration point
 t_q is the time to achieve equilibration

Within the tissue volume uniform heating was allowed for as in section 7.2.2, with the heat input being controlled by the temperature at the equilibration point. In addition it was assumed that a diffuse "capillary" blood flow existed outwith the blood vessel and thus cooling of the tissue occurred as given by equation 7.8.

The solution to this approached a steady state in only a few minutes and an example of the radial temperature distribution is given in Figure 8.3 for a vessel of radius $400 \mu\text{m}$ carrying blood at a temperature T_b . This shows the relative drop in temperature at a radius R , from the centre of the vessel, for three positions of the equilibration point. The capillary flow for these three curves is $30 \text{ ml}/100\text{g}/\text{min}$ and also shown is the curve which would be obtained if no capillary flow was cooling the tissue (equation 3.12).

Taking the particular example of the blood entering the tissue at 37°C , the equilibration temperature

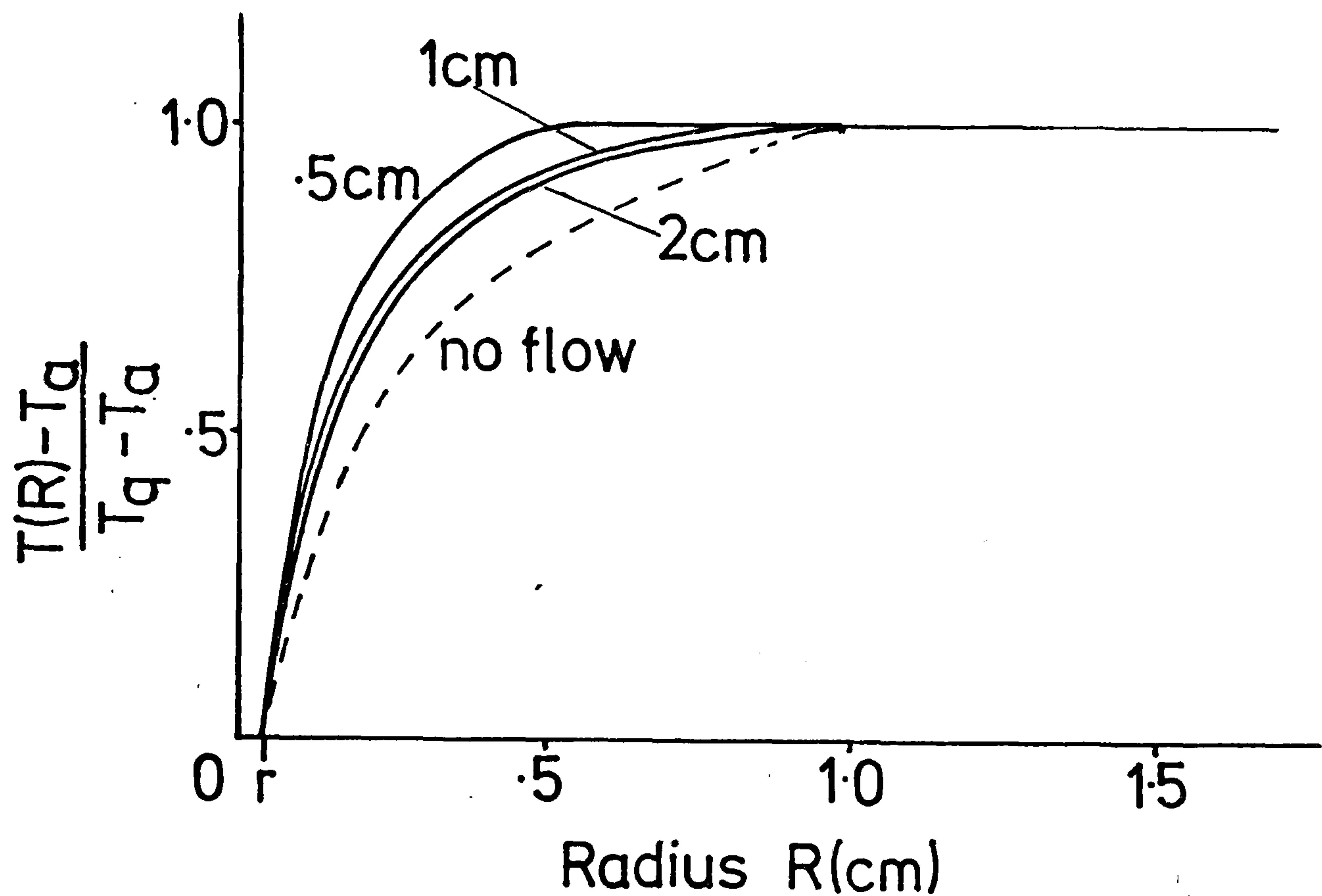


Figure 8.3 The temperature within a tissue, $T(R)$, plotted against radius from the centre of a blood vessel, whose radius is r . Within the tissue a diffuse capillary blood flow of 30 ml/100g/min is assumed and the tissue is uniformly heated such that the equilibration point is maintained at a constant temperature T_q . Various positions of the equilibration point, at radii of 0.5, 1 and 2 cm are shown. The dotted line shows the temperature for an equilibration point of 2 cm and no capillary blood flow.

$T_q = 42.5^{\circ}\text{C}$ and the equilibration point being at 2 cm, it can be seen that the region of tissue within 4.7 mm of the vessel is at a temperature lower than 42°C . Therefore this region of tissue would not satisfy the criteria given in section 8.1.

The exact volume of tissue which comes under the influence of the cold blood in the blood vessel, is determined by the position of the equilibration point and the value of the "capillary" blood flow. The closer the equilibration point is to the blood vessel, the smaller the volume of tissue which will be underheated. In the extreme situation, with the equilibration point at the surface of the vessel, no tissue will be underheated but, in fact, the opposite will occur and the tissue away from the blood vessel will be at a higher temperature than expected. The "capillary" blood flow also influences the temperature distribution with the maximum volume of underheated tissue occurring when this flow is zero. In practice, of course, this flow will almost certainly be related to the flow through the large blood vessel.

Similar curves can be obtained to describe the temperature around a blood vessel which is carrying blood from a heated region through an unheated region.

8.2.4 Discussion

Two aspects of the exchange of heat between blood vessels and tissue are illustrated by the above results. Firstly, the process has been considered from the point

of view of the total heat exchange which occurs and its resulting effect on blood temperature. Secondly, consideration has also been given to the alteration in tissue temperature around a blood vessel, even when only limited heat exchange is possible. The significance of both of these to hyperthermia will now be examined.

As expected, from Table 8.1 the model predicts that complete exchange of heat occurs between the blood in a capillary and the surrounding tissue. Furthermore, as in chapter 6, it is again seen that such exchange may also take place in other generations of blood vessels and, in the case of heat, this extends even to fairly large arteries and veins. These results are similar to those recently reported by Chen and Holmes (1980) and are consistent with the experimental observations of Bazett et al (1948) and Betz et al (1966). An increase in the above figures is obtained when heat is exchanged between blood vessels, such as when an artery and vein run parallel to each other, forming a countercurrent arrangement (Bazett et al, 1948).

The significance of these results is best appreciated by looking at the change in blood temperature, in each part of the circulation, as the blood first approaches, and then leaves, a region of tissue at a higher temperature. Note that reference is made to the excess temperature, which is the difference between the arterial blood and tissue temperatures. Starting in a vessel with the characteristics of the aorta no significant heat

exchange occurs and blood passes rapidly through it into the smaller branching networks with essentially the same temperature. In the next stage, the large arteries, the blood temperature may increase by about 5% of the excess temperature but, of course, for such vessels this requires a length of several centimetres. A further 10% increase in temperature may occur in the small arteries, which are about one centimetre in length and, after this, complete equilibration with the tissue temperature is produced and maintained during passage through the arterioles, capillaries and venules. The opposite picture can now be drawn for the venous side of the circulation. If the tissue temperature remains constant until the blood reaches the small veins then only a small decrease in blood temperature will occur, in the small and large veins, before the blood re-circulates back to the vena cava. If, however, the tissue temperature decreases between the venules and small veins then a considerable loss of heat to the surrounding tissue may occur.

The above analysis has several implications.

a) Traditionally heat transfer models have assumed that the exchange of heat between blood and tissue takes place only at the capillary level (Perl, 1962; Chan et al, 1973; Cravalho, 1980). In contrast the above results suggest that the equilibration of the tissue and blood temperatures does in fact occur between the small arteries and arterioles and that this equilibration is maintained until the venules and small veins are reached. Thus, for

heat, the "effective" capillaries are possibly of the order of one centimetre long. However, if a uniform temperature is present in the tissue and if the dimensions of the heated region are much larger than one centimetre then it clearly makes no difference which vessels actually exchange the heat and the traditional concept of the blood flow as a diffuse heat sink (section 3.4.1) will still be acceptable. Thus the major effects of blood flow on temperature distributions are examined on the basis of this "capillary" description and are presented in section 8.3.

b) Although it has been suggested that the capillary description may not be sufficient in all situations (Priebe, 1970; Klinger, 1974; Cravalho et al, 1980; Chen and Holmes, 1980) no estimate of when it may be inadequate has been made. The above results suggest that the extra-capillary heat exchange may become particularly important when the relevant tissue volume is of the order of one centimetre or less in size or if significant temperature gradients occur over this length. Its effects can be expressed in three ways: (i) the effective input temperature of the blood to the tissue may be higher than 37°C due to the blood picking up heat while passing through adjacent tissue, (ii) the tissue may be cooled by arterioles and venules which pass through it but do not terminate in a capillary bed within it. Thus for heat, and for particular temperature distributions, the effective blood flow at a point in a

tissue may be higher than expected from its capillary blood flow, (iii) heat may be carried from a region of high temperature to one of low temperature, by the blood flow, in the same way as ^{133}Xe was transported to the subcutaneous fat in chapter 6.

It is evident that the calculation of the effect of the above processes is extremely complex, as has been previously realised by Klinger (1974), and requires data on the specific vascular architecture of the tissue, which does not exist. Processes (i) and (ii) will cancel to some extent, particularly if the blood vessels are randomly orientated. Process (iii) will result in an increase in the effective thermal conductivity of the tissue. This is consistent with experimental data (Nevins and Darwish, 1970; Bowman et al, 1975) which show the thermal conductivity of living tissue to be about 1.5 to 2 times the value in excised specimens. Since heat exchange increases as the blood flow decreases, the greatest change in thermal conductivity is likely to be detected at low blood flows.

In conclusion, in terms of the overall heat exchange, the "capillary" model is sufficient to describe the effects of blood flow for large tissue volumes. For tissues smaller than a certain size, or where temperature gradients are present over a certain distance, an alternative model may be necessary. It is suggested from the results that the size referred to here is less than one centimetre but it is again emphasised that this

is dependent on the particular values of the vascular characteristics used.

A further consequence of the flow of blood through a tissue, which is at a different temperature, is that not only does an overall exchange of heat occur but a localised "hot" or "cold" region may be produced around the blood vessel. The smaller vessels, with their combination of low flow, large number and small diffusion distances, allow rapid equilibrium to be achieved between the blood and tissue as shown above. Thus the effect of such vessels is to produce a uniform cooling of the tissue. As has been seen, however, the larger vessels do not come to equilibrium but travel for some distance through the tissue at a different temperature. Although the exchange of heat which occurs may have a negligible effect on the blood temperature, the tissue temperature around the vessel is still altered. Thus the results in section 8.2.3 show, for one example, the protection afforded to tissue within about 4 mm of a blood vessel whose blood is at a temperature of 37°C. This represents a considerable volume of tissue which in turn would contain a large number of tumour cells, leading to the possibility of regrowth from this site (Robinson et al, 1978; Hume et al, 1979). Although the smaller arteries travel only a small distance through a tissue, and their temperature increases more rapidly than the large arteries, they are of course more numerous. Consequently a significant amount of tissue around the

periphery of a heated region may be protected from the hyperthermic dose (Storm et al, 1980). It may therefore be necessary to allow for this by extending the volume of the heated region.

It should be noted that the flow in a blood vessel, particularly in the middle of a heated region, may decrease due to the damage being produced in the tissue. This would lead to improved heat exchange in the vessel and therefore reduce the volume of tissue underdosed by the heat.

Figure 8.3 also represents the analagous situation of "hot" blood passing through a "cold" tissue. Therefore in this way the venous blood draining from a heated region may deliver a damaging heat dose to blood vessels and tissue outwith the treatment volume. This may place a constraint on the maximum temperature acceptable within a heated region, even if that temperature is present only in tumour tissue. Because of the arrangement of the venous circulation, however, it is likely that the "hot" blood will be diluted by blood draining from other unheated regions.

8.3 ROLE OF THE CAPILLARY BLOOD FLOW

The overall ability of blood flow to remove heat from a tissue is best described by the "capillary" model presented in section 3.4.1, although it has been recognised in the previous section that it is not just the capillaries that are involved in heat exchange. The

specific influence of blood flow on tissue temperature has not been studied before and is examined here by considering each tissue effectively in isolation and assuming that no other processes are responsible for removing the heat. In terms of the thermal conduction this means that the tissue is considered to be large enough that the effects of conduction are essentially negligible. The assumptions made in deriving equation 3.8 are again accepted here and, where necessary, will be discussed later. For simplicity the heating of the tissue is assumed to be uniform as in section 7.2.2 but the basic principles derived here will still be applicable to other techniques.

8.3.1 Model of the removal of heat by the capillary blood flow

It has been shown in section 3.4.1 that if an amount of heat, Q_0 , is deposited in a tissue then at subsequent times after this the amount left will follow an exponential course, i.e.

$$Q(t) = Q_0 \exp(-kt)$$

where t is the time after the heat is deposited and k is the exponential rate constant given by

$$k = \frac{F}{\lambda' \rho' V}$$

where F is the tissue blood flow (ml min^{-1})

λ' is the ratio of specific heats tissue: blood

ρ' is the ratio of densities tissue: blood

V is the tissue volume

This can be expressed as (see equation 3.7)

$$k = \frac{f \rho_b}{100 \lambda} \quad (8.1)$$

where ρ_b is the density of blood

and f is now the tissue blood flow in ml/100g/min

As in equation 3.8 the change in temperature of the tissue can similarly be written as

$$\Delta T = \Delta T_0 \exp(-kt) \quad (8.2)$$

where the temperatures are measured relative to the arterial blood temperature, which is normally 37°C for example $\Delta T_0 = (T_0 - 37^\circ\text{C})$.

Now if, instead of a single instantaneous input of heat to the tissue, the heat is delivered at a constant rate I per unit mass of tissue the temperature rise at any time is then given by

$$\Delta T = \frac{I}{kc_t} (1 - e^{-kt}) \quad (8.3)$$

c_t is specific heat of the tissue.

It is now possible to simulate a hyperthermia treatment which involves the application of heat, at an input rate I_1 , until the equilibration temperature is achieved at a particular point, and then a reduced input I_2 which is necessary to maintain a constant temperature at the equilibration point. Thus

$$\Delta T = \Delta T_0 e^{-kt} + \frac{I_2}{kc_t} (1 - e^{-kt}) \quad (8.4)$$

where time zero is taken when the equilibration temperature

is reached.

ΔT_0 is the temperature change at the end of the initial heating period which, for the tissue containing the equilibration point represents, of course, the equilibration temperature. For other tissues

$$\Delta T = \frac{I_1}{kc_t} (1 - e^{-kt_0})$$

where t_0 is the time taken to achieve the equilibration temperature.

8.3.2 Results

Using the values of the densities, specific heats and blood flows tabulated in chapter 7 the above equations were used to calculate the effects of blood flow on tissue temperatures. First of all, Figure 8.4 shows the rise in temperature of a single tissue, with the properties of muscle, for a constant heat input rate and when no blood flow is present. The different values of the heat input correspond to those used in practice (Storm et al, 1980). The temperature of the tissue steadily increases with time, as would be expected since this model assumes that no other mechanism for loss of heat is present. In contrast Figures 8.5 to 8.7 show the rise in temperature, for different heat input rates, in the presence of blood flow. It is seen that the temperature of the tissue does not increase steadily but rises less and less rapidly with time until a constant, limiting value is obtained. This limiting value,

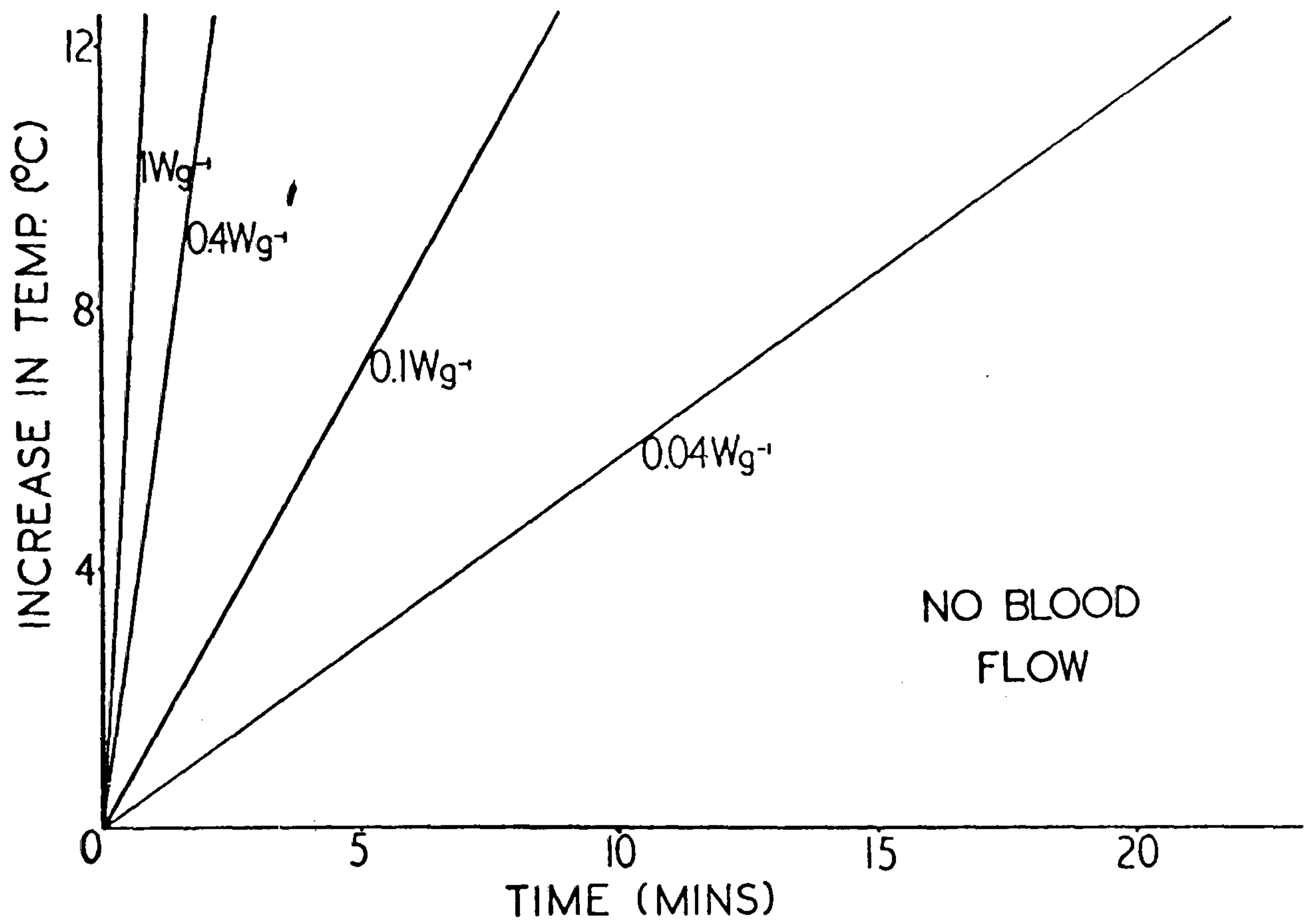


Figure 8.4 The increase in temperature with time for various heat input rates. There is no blood flow.

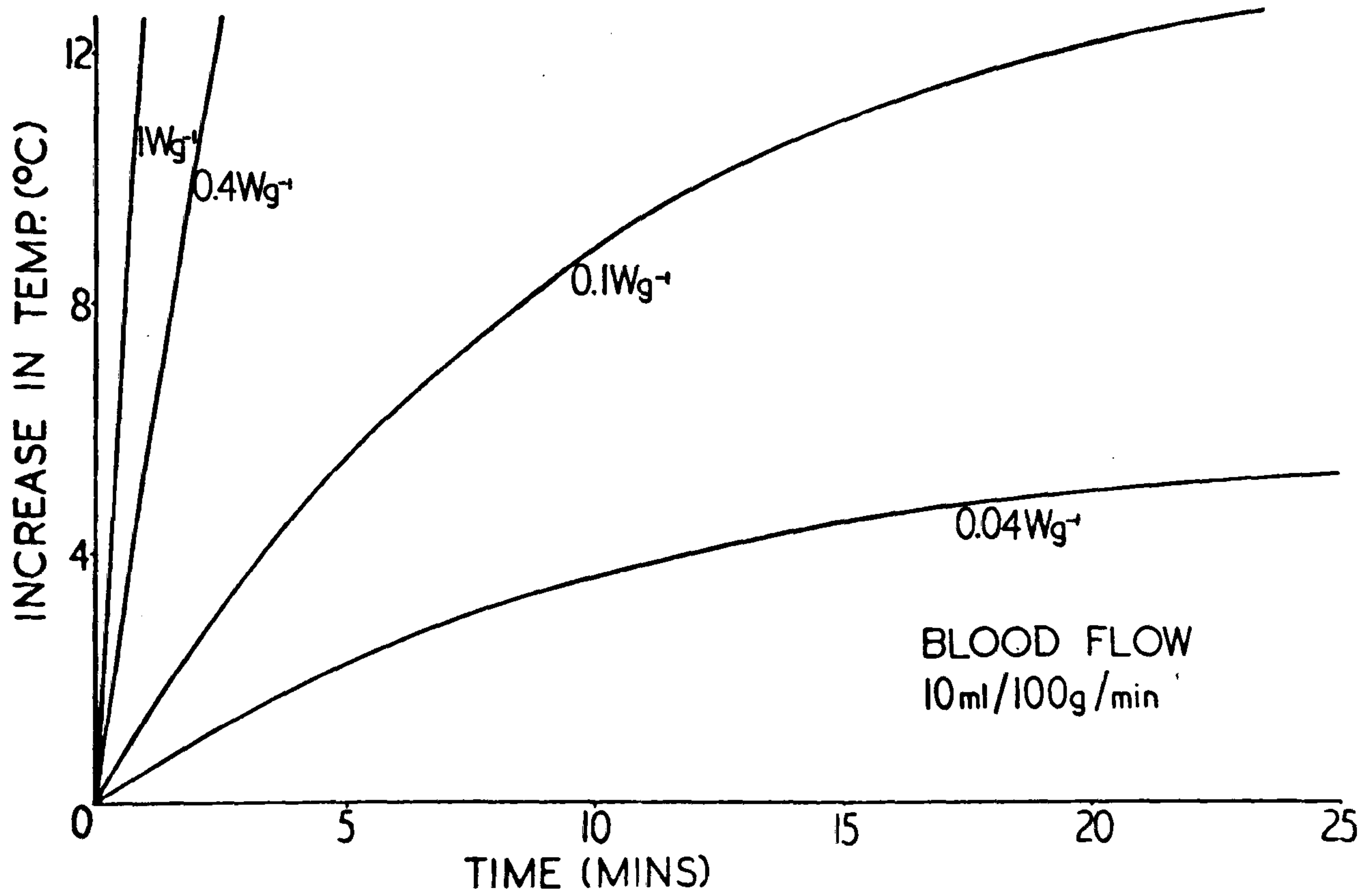


Figure 8.5 The increase in temperature with time for various heat input rates. Blood flow - 10 ml/100g/min.

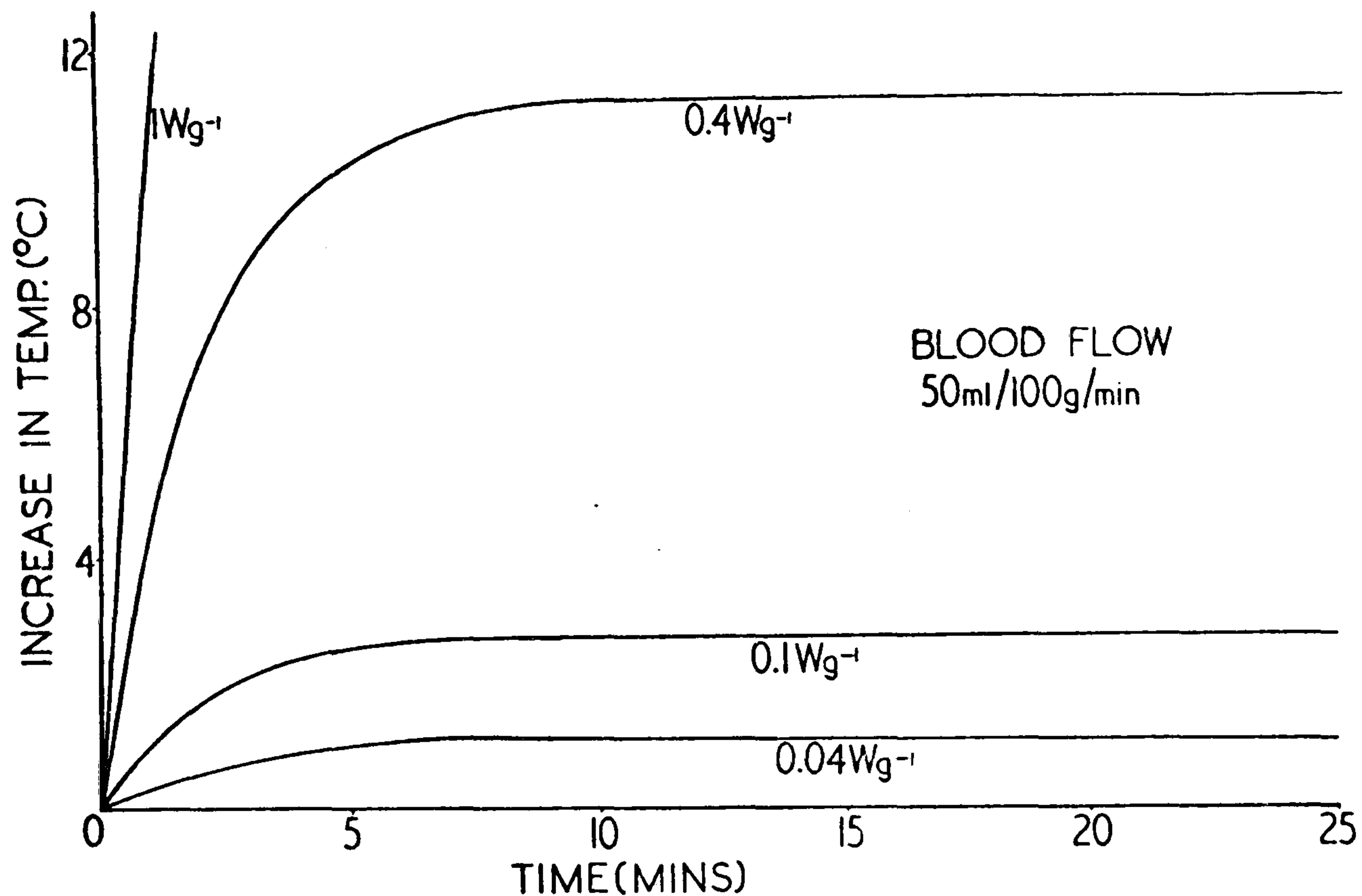


Figure 8.6 The increase in temperature with time for various heat input rates. Blood flow - 50 ml/100g/min.

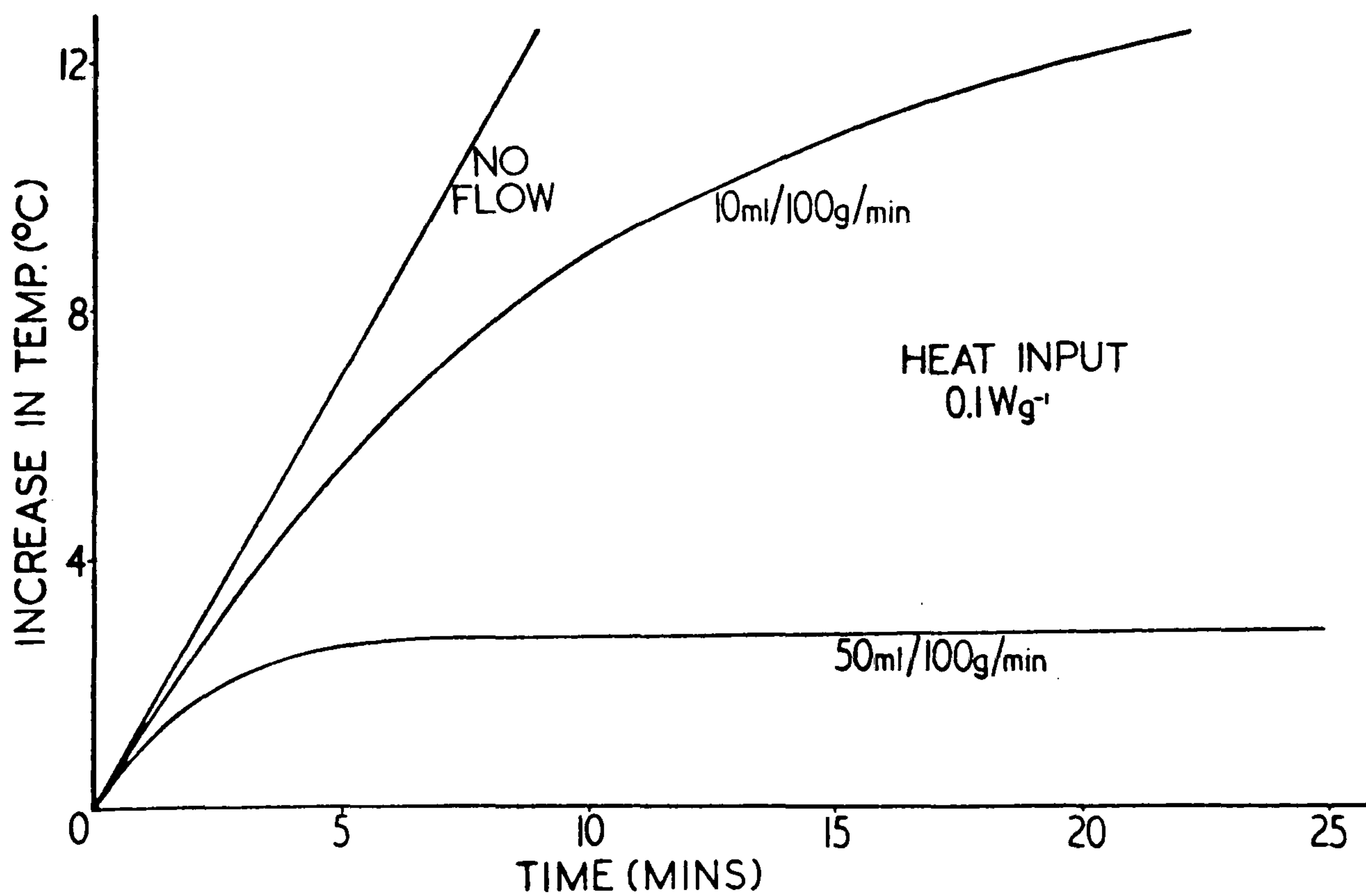


Figure 8.7 The increase in temperature with time for various blood flows. The heat input is $0.1 W g^{-1}$.

and the time taken to achieve a certain temperature, depend on the heat input and the blood flow. As the input decreases and the flow increases the time taken to achieve a specific temperature rise is increased.

The reason for the shape of these curves is evident from the derivation of equation 8.3. The amount of heat removed from a tissue at any time, by the blood flow, is a constant fraction of the amount of excess heat within it. As the temperature of the tissue increases, the absolute amount of heat removed will therefore also increase. At some time the amount of heat removed will then be equal to the constant amount which is supplied by the heating modality and, as a result, the temperature of the tissue will remain stable. It is clear from these results that it cannot be assumed that by simply applying heat to a tissue for a long enough time that a particular temperature rise will eventually be achieved. Instead the tissue will attain a maximum temperature which will depend on both the heat input rate and the blood flow. In these circumstances it is therefore essential that a measurement of tissue temperature is made; otherwise it may be questioned whether it is significantly elevated at all (LeVeen et al, 1976; Miller et al, 1977).

From equation 8.3 the limiting value of the temperature rise is given by

$$\Delta T = \frac{I}{kc_t}$$

Alternatively the heat input rate required to maintain

such a temperature rise is

$$I = kc_t \Delta T$$

and clearly this is also the minimum heat input rate which will be required to raise the temperature by this amount in the first place. The large range of heat inputs required for the different tissues of the body are therefore illustrated in Figure 8.8. It is again emphasised that the temperature rise produced is dependent not on the total amount of heat delivered to the tissue but on the power of the heating source.

In practice more than one tissue will be contained within a treatment volume. Again assuming that blood flow is the only heat transfer mechanism present and that the heating is uniform throughout the volume, Figure 8.9 shows the ratio of the temperature rises in two tissues whose blood flows are 5 ml/100g/min and 10 ml/100g/min. At short times the temperature rise is similar in both tissues but as time progresses the ratio increases. It can be seen from equation 8.3 that eventually a limit is obtained, given by

$$\text{Limit } \frac{\Delta T_1}{\Delta T_2} = \frac{k_2 c_{t2}}{k_1 c_{t1}}$$

In other words, if the tissues have the same specific heat, eventually the ratio of the temperature increments becomes equal to the inverse ratio of the tissue blood flows; in this case the tissue with twice the blood flow attains a temperature increase of one half of that in

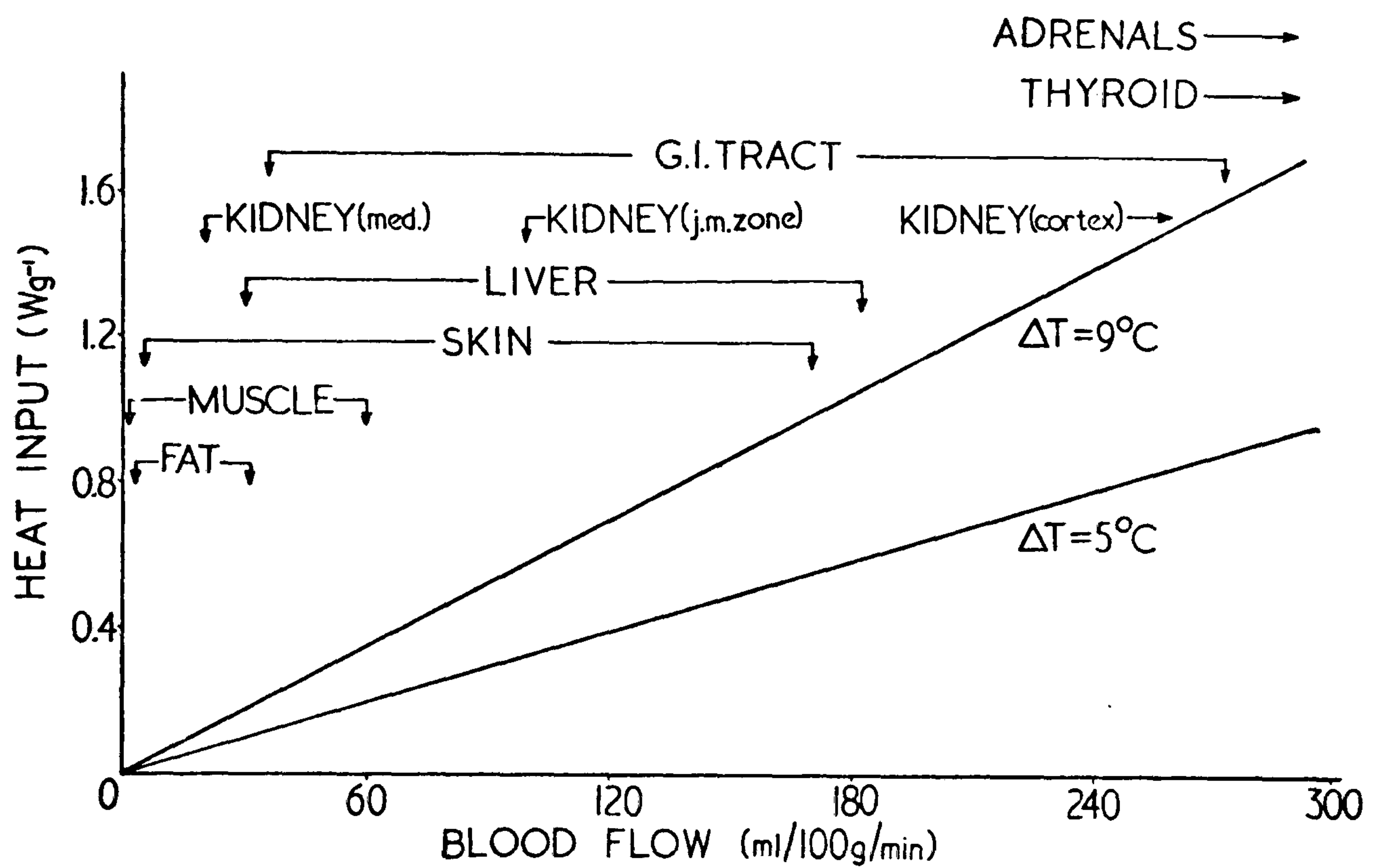


Figure 8.8 The heat input rate per g of tissue required to maintain the tissue temperature elevated by 5°C and by 9°C plotted against blood flow in the tissue. The tissue density is 1 g cm^{-3} and the specific heat is $4.2 \text{ J g}^{-1} \text{ }^\circ\text{C}^{-1}$. Also shown are the ranges of blood flows to be found in some tissues in man.

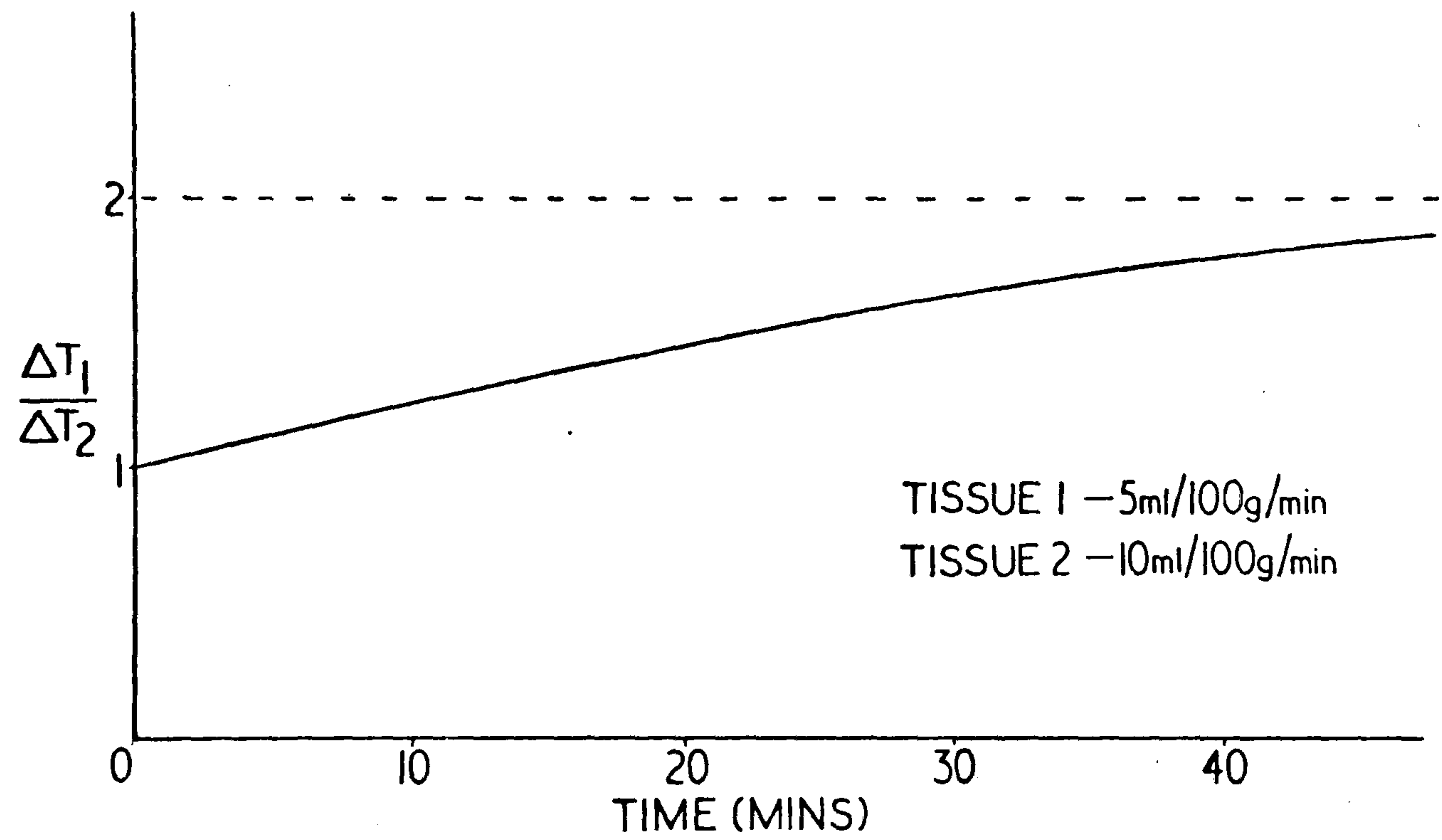


Figure 8.9 The ratio of the temperature increase in two tissues being heated simultaneously with the same heat input. Tissue 1 has a blood flow of 5 ml/100g/min and tissue 2 a flow of 10 ml/100g/min.

the other tissue.

While the above result might imply that the differential effects produced by blood flow might be avoided by using short heating times it should be realised that the above represents only the heating stage. This is followed either by cooling of the tissue or more usually by a reduced heat input such that the temperature at the equilibration point is kept constant. Figure 8.10 shows the temperature-time curves obtained if the two tissues are immediately raised to 42.5°C at time zero and are then allowed simply to cool down again by the blood flowing through them. It can be seen that tissue 1, with the lower blood flow, has a temperature higher than 42°C for twice as long as tissue 2. In other words the differential effect of the blood flow is still present.

Figures 8.11 and 8.12 simulate a specific hyperthermia treatment, where the same two tissues are again within the treatment volume. The equilibration temperature is again 42.5°C and this is maintained for 30 minutes. Firstly, with the equilibration point in tissue 1, the heat input required to maintain this at a constant temperature is insufficient to maintain the temperature in tissue 2, and this then falls as shown (Fig. 8.11). Alternatively, with the equilibration point in tissue 2, the temperature of tissue 1 continues to rise above 42.5°C (Fig. 8.12).

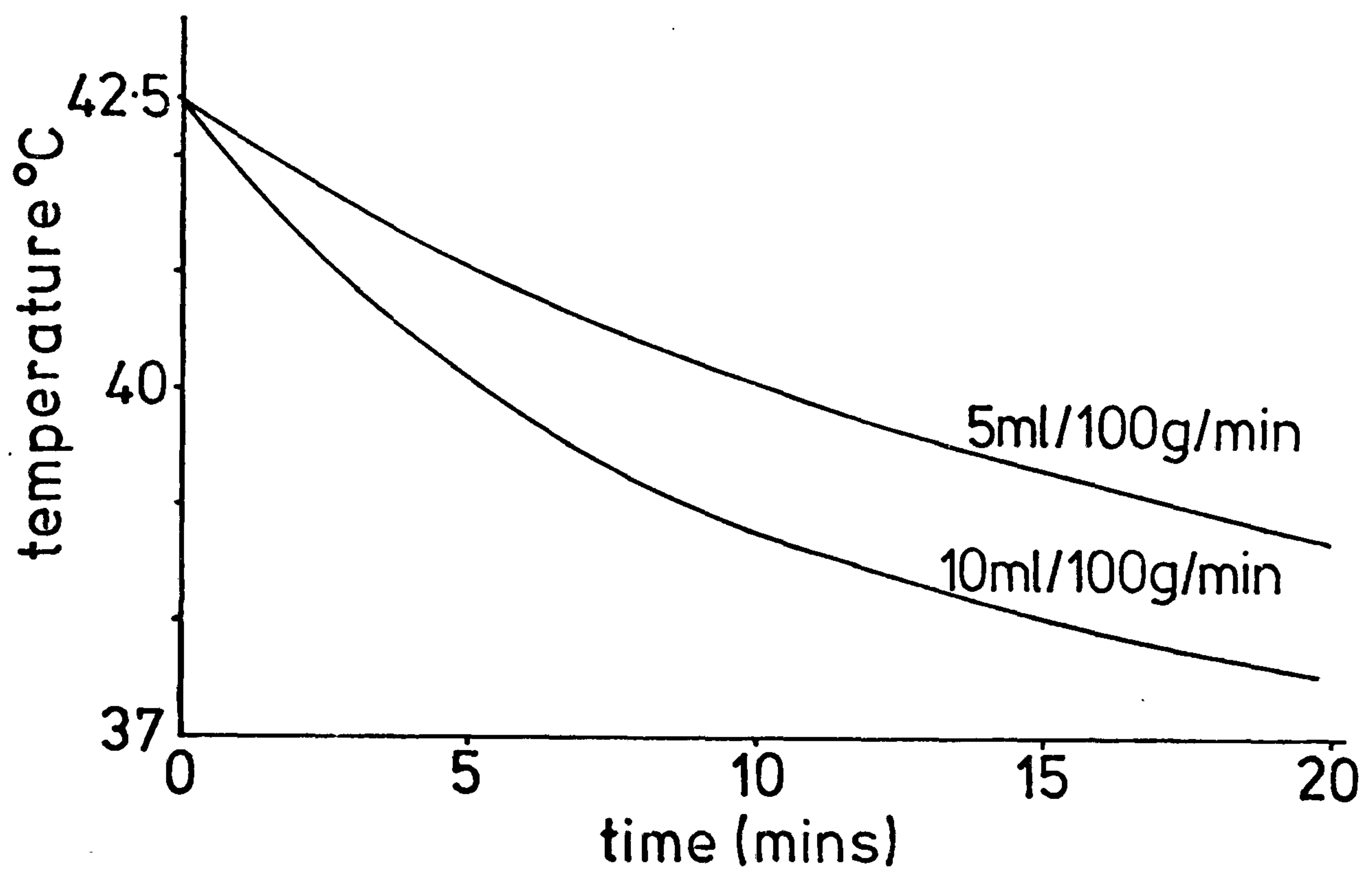


Figure 8.10 The variation in temperature with time for two tissues whose blood flows are 5 ml/100g/min and 10 ml/100g/min. Both tissues are immediately heated to 42.5°C at time zero and are then allowed to cool by their blood flow.

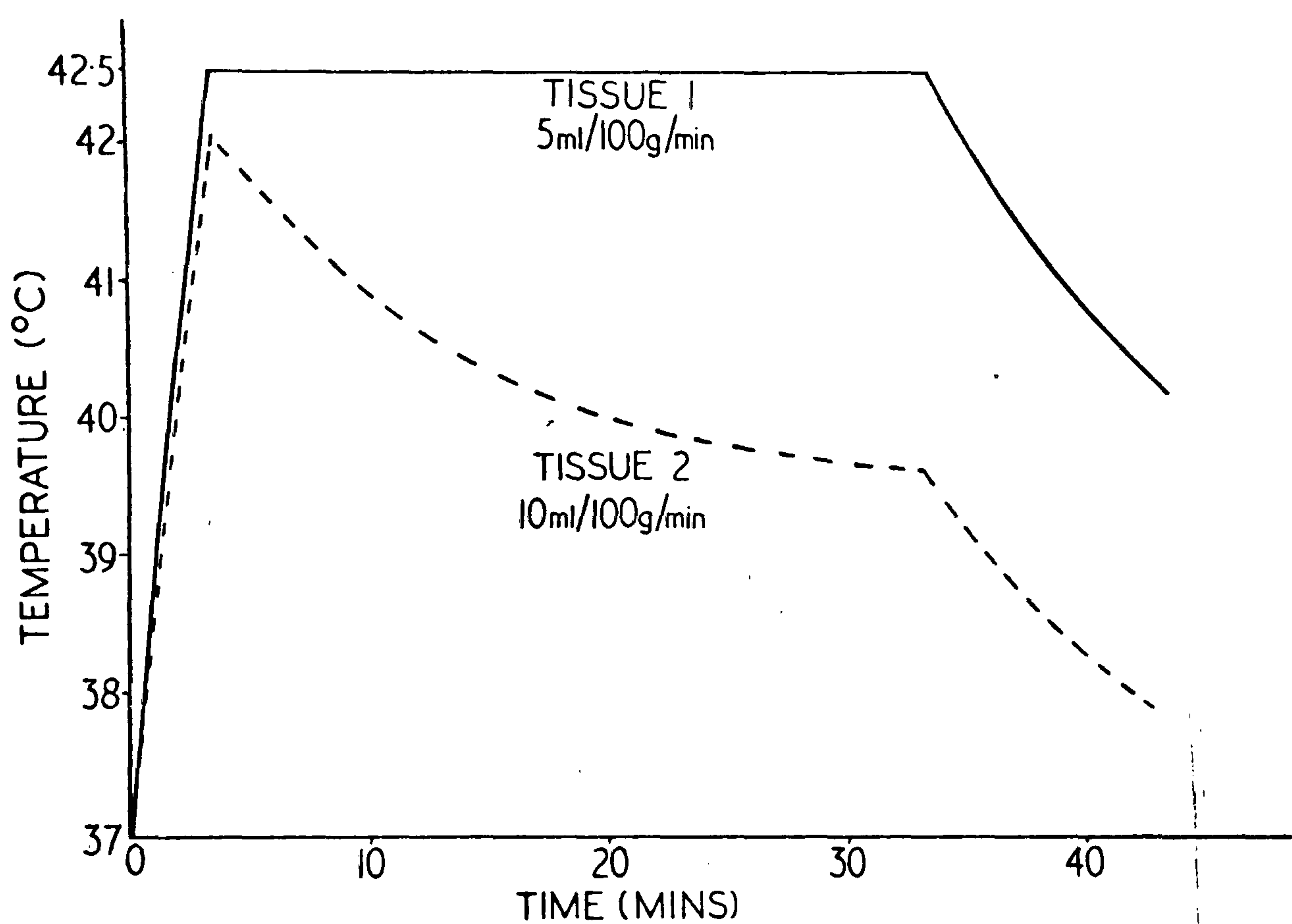


Figure 8.11 The variation in temperature with time for two tissues being heated with the same heat input. The temperature of tissue 1 is raised to 42.5°C and maintained there for 30 mins. During the initial stage the heat input is 0.2 W g^{-1} .

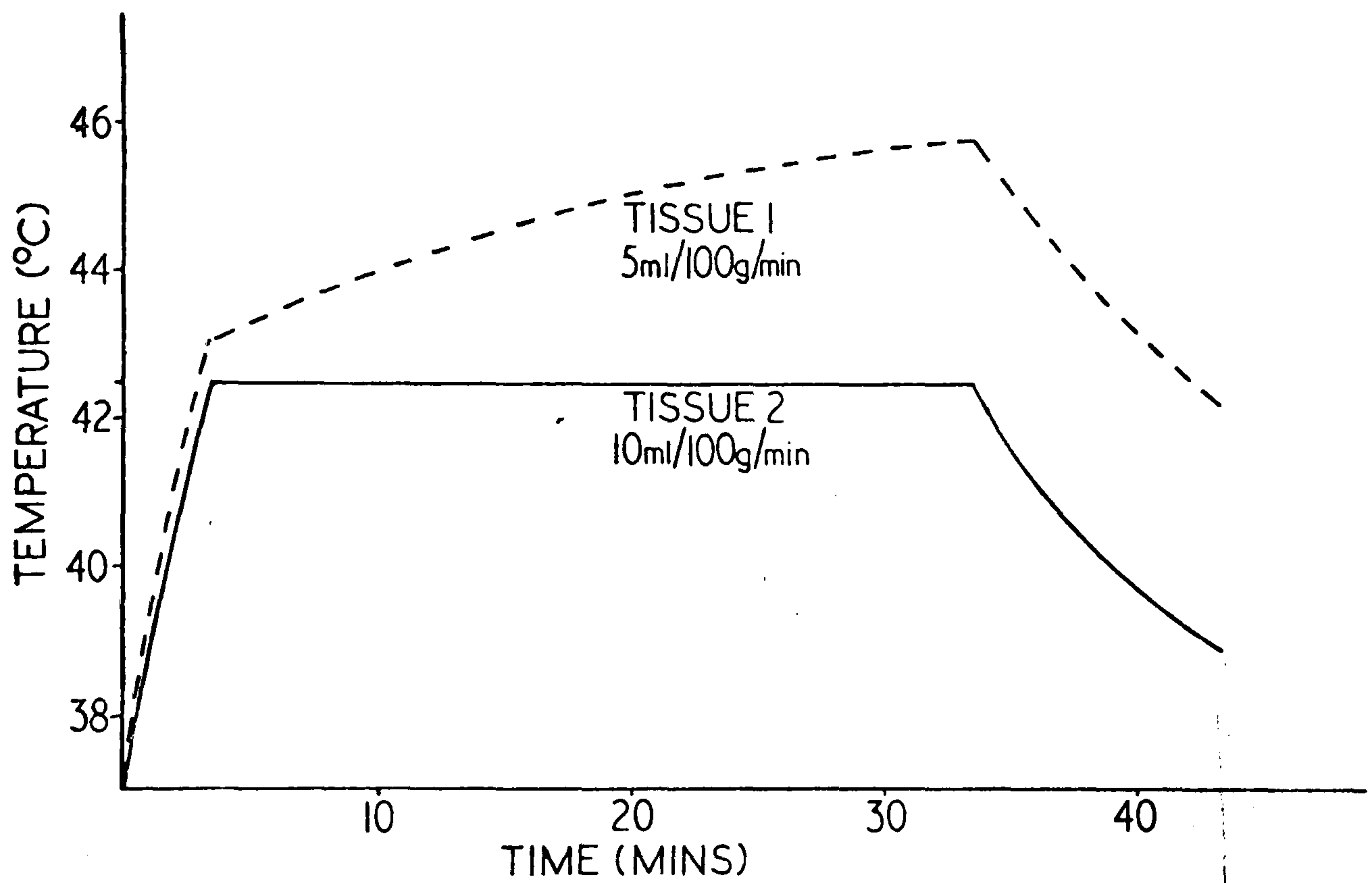


Figure 8.12 The variation in temperature with time for two tissues being heated with the same heat input. The temperature of tissue 2 is raised to 42.5°C and maintained there for 30 mins. During the initial stage the heat input is 0.2 W g^{-1} .

8.3.3 Discussion

As was detailed in section 3.4.1 several assumptions are made in order to allow equations 8.1 to 8.4 to be used to assess the removal of heat by the blood flow. These are: a) the blood and tissue are at thermal equilibrium and no limit to the exchange of heat between them is imposed by thermal conduction, b) the heat is removed from the tissue only by the blood flow, c) the blood flow is constant, d) there is no re-circulation of heat, e) the tissue is homogeneous.

Assumptions a), b) and e) have already been examined in this chapter and would appear to be justified in tissues above a certain size, and where the temperatures away from the edges and boundaries are considered. For assumption c) the variation of blood flow with temperature has been discussed in section 7.6 and would affect the above results. However the basic principle of the blood flow producing non-uniformities in temperature would, of course, still be equally applicable. The assumption of no re-circulation, i.e. that the temperature of the arterial blood entering the heated volume does not change, can be examined in the following way. When heat is removed from a tissue it will be carried by the blood in the venous system from where it will be directly deposited in other tissues or will pass to the arterial circulation to be re-distributed throughout all the tissues of the body. Thus the blood entering the heated tissue may in fact rise in temperature. An

estimate of this rise can be made by considering a volume of tissue to which 400w of heat are being delivered. If all of this heat is removed from the volume instantaneously and if it is re-distributed uniformly throughout the whole body then, in one minute, 70 kg of tissue, which is the average weight of a man, will increase in temperature by approximately 0.08°C . This represents the maximum increase in temperature of the arterial blood. Since the important thermoregulatory mechanism of the body has been ignored in this calculation, and loss of heat will take place through the lungs and by radiation, convection and sweating then in reality the increase in temperature will be considerably smaller. Thus it appears that this assumption may be justified in man but, where a large fractional volume is heated, and in small animals, this may have to be taken into account.

The capillary model has shown three distinct effects of blood flow in hyperthermia; a) it increases the time taken to achieve a desired temperature within a tissue, b) it puts a definite limit on the temperature achieved with a heating source of a certain power capability and c) it produces different hyperthermic doses in tissues with different blood flows by producing non-uniformities in temperature or in effective heating time. A direct comparison of the above results with published experimental observations is limited because allowance must be made for the particular heating patterns produced

and also for thermal conduction, since most studies have used small animals. More importantly, however, comparison is limited because very few measurements of temperature profiles in tissue have been made. Despite this the basic principles of the simple model presented above appear to be confirmed. Cook (1952) and Lehmann et al (1969) have shown the rapid increase in temperature of a tissue, during heating, when its blood flow is occluded. In addition their results illustrate the contrast between a linear rise in temperature in the absence of blood flow compared to an asymptotic curve obtained with flow, although neither author recognised the significance of this. The asymptotic behaviour of the temperature-time curve has also been illustrated in several other studies (Yerushalmi, 1975; Marmor et al, 1977; Hahn and Kim, 1980; Raymond et al, 1980; Storm et al, 1980) but again more complex reasons have been sought to explain it. Hahn and Kim (1980), for example, suggest that "at about 10 minutes into the heat treatment the temperature regulatory mechanisms are activated in tissue". While increased blood flow may result from heating of a tissue this will only accentuate the bending of the curve.

Storm et al (1980) have shown that, for the same power input of their heating source, considerable variation was obtained in the maximum temperature produced within different tumours. Several authors have also shown non-uniformity in temperature between a tumour

and the adjacent normal tissue. In most cases the tumour was hotter (LeVeen et al, 1976; Dickson and Calderwood, 1980; Raymond et al, 1980) but some reports also give examples of the normal tissue being hotter (Marmor et al, 1977; Storm et al, 1980; Hahn and Kim, 1980). It is highly likely that such temperature differences are caused by different blood flows but, of course, in the absence of simultaneous direct measurements of tissue blood flow and temperature it is not possible to verify this in every situation.

The equations presented in this section can also be used to study other hyperthermia situations. For example an alternative method of heating a tissue is by perfusion with heated blood (Cavaliere et al, 1967). The equilibration of the tissue with the heated blood can be described in a similar way to equation 8.2. The temperature will rise faster in regions with a high blood flow and therefore this technique may complement the external heating modalities where, as shown, the regions with a high flow will be cooler.

8.4 THE EFFECTS OF THERMAL CONDUCTION

This section now looks at the possible role of thermal conduction in modifying temperature gradients within a heated region. For the moment the blood flow is assumed to be zero but it should be realised that the effects of conduction are very much dependent on blood flow and this will be shown in the next section.

Three examples, illustrating different aspects of the conduction process, are presented. In each case the temperature distribution was calculated using the finite difference computer program and the characteristics detailed in chapter 7.

8.4.1 Models of thermal conduction

Model 1 - Thermal conduction as a heating modality

The use of thermal conduction as a means of heating a tissue has been described in section 7.2.1. In this type of situation the temperature gradient is maximised by maintaining a constant temperature on the surface of the tissue. In order to study the ability of conduction to supply heat in this way, models were developed in which the initial temperature throughout the tissue was 37°C and the outside temperature was held constant at 42.5°C. Three different geometries, spherical, cylindrical and a one dimensional slab were studied, as were three different types of tissue; muscle, fat and bone. Temperature profiles were calculated for periods up to one hour, across a diameter for the sphere and cylinder, and between the faces of the slab of tissue. This was carried out for several tissue sizes.

Model 2 - Microwave heating of a tissue

The non-uniform heating of a tissue by microwaves was modelled in order to study the effect of conduction in smoothing out a less extreme temperature gradient. It was assumed that a slab of muscle tissue was heated by parallel opposed microwave fields, switched from one

to the other to avoid interference effects. The temperature rise produced by each field is given by equation 7.1. The equilibration point was taken at the surface of the tissue and temperature profiles, along the direction of the microwave fields, were calculated for periods up to one hour and tissue thicknesses of one to 10 centimetres.

Model 3 - Conduction out of a heated region

Conduction of heat out of a heated volume was studied using a two dimensional tissue slab model based on the localised current field (LCF) heat sources described in section 7.2.2. At time zero the temperature throughout the tissue was taken as 37°C . The heat input term was then chosen so that the equilibration point, at the centre of the heated region, was raised to 42.5°C within 60 seconds, after which time it was maintained at this temperature. The temperature profiles in this case were then calculated perpendicular to the direction of the LCF fields in order to show conduction out of the region. This was done for both forms of the LCF fields (section 7.2.2) for times up to one hour and heated regions of width one to 10 centimetres.

8.4.2 Results

Model 1 - Thermal conduction as a heating modality

As an example, temperature profiles are shown in figure 8.13 for a 5 cm diameter sphere, for various times. The temperature throughout the sphere rises as heat is conducted from the outside into the tissue and

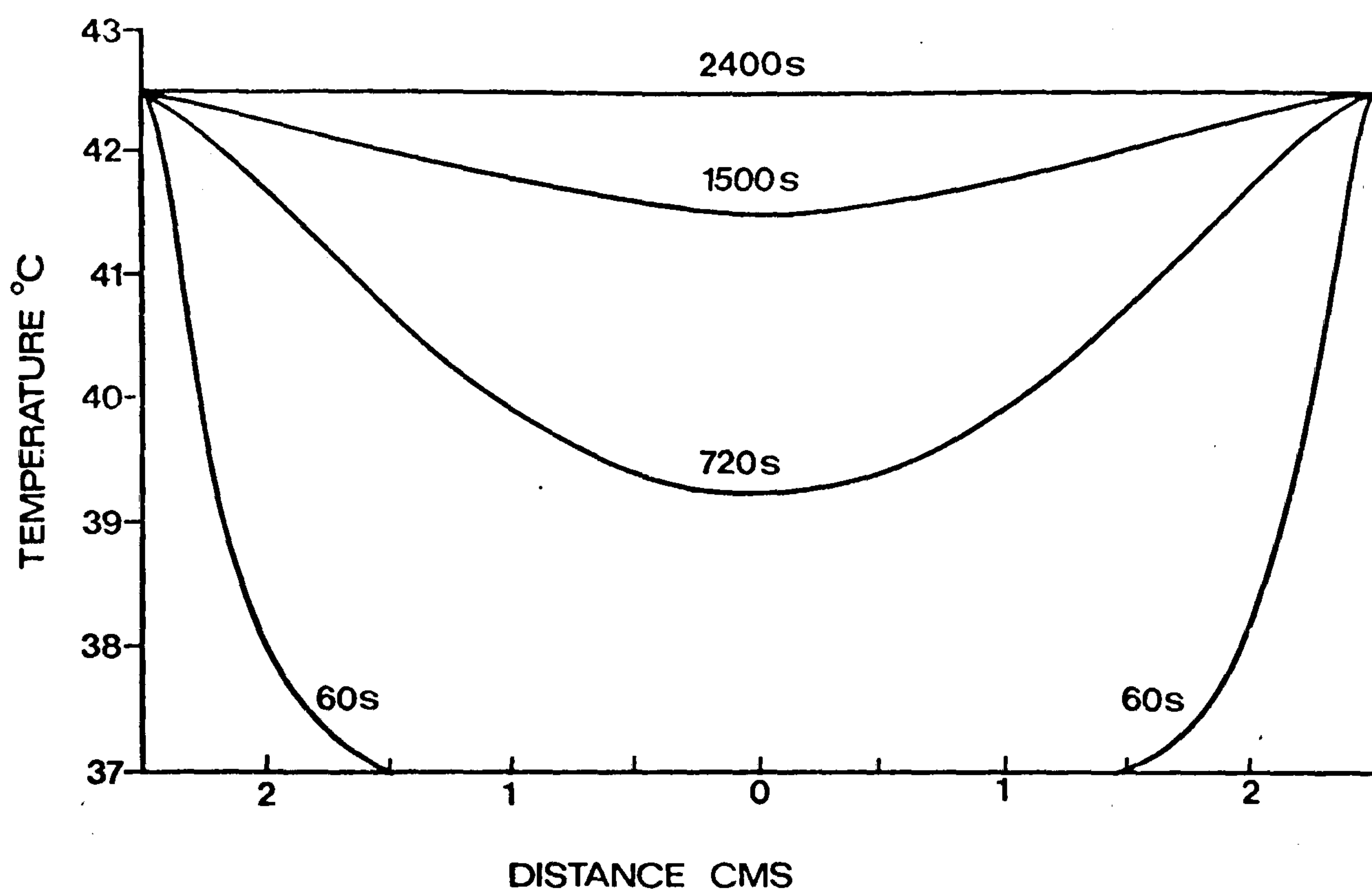


Figure 8.13 Heating by thermal conduction - temperature profiles across a 5 cm diameter sphere of muscle tissue. Surface temperature 42.5°C.

has reached 42.5°C by 40 minutes. The shape of the temperature profiles are similar for all sizes of tissue but, of course, the time scales involved vary considerably.

The ability of thermal conduction to deliver heat to a tissue can be evaluated on the basis of the criteria discussed in section 8.1, i.e. since the surface of the tissue is maintained at a temperature of 42.5°C then, for an effective thermal dose, the rest of the tissue must be raised above 42°C and this must be done within a period of about 10 minutes. The lowest temperature will, of course, be at the centre of the tissue and Figure 8.14 shows the time taken for this point to rise to 42°C , for tissue with the properties of muscle and for the various tissue geometries. As expected "all round heating", as in a sphere, is the most efficient modality. Similarly Figure 8.15 shows the time taken for different types of tissue, using spherical heating. The results of these two figures are summarised in Table 8.1 which shows the size of tissue which may be efficiently heated by thermal conduction alone, on the basis of the two criteria of section 8.1.

Model 2 - Microwave heating of a tissue

An example of microwave heating is shown in Figure 8.16 for a plane slab of muscle tissue of two centimetres thickness. Although the heating pattern is non-uniform, thermal conduction improves the temperature uniformity. However the hyperthermia criteria suggest that such an arrangement will be useful only in tissues up to two

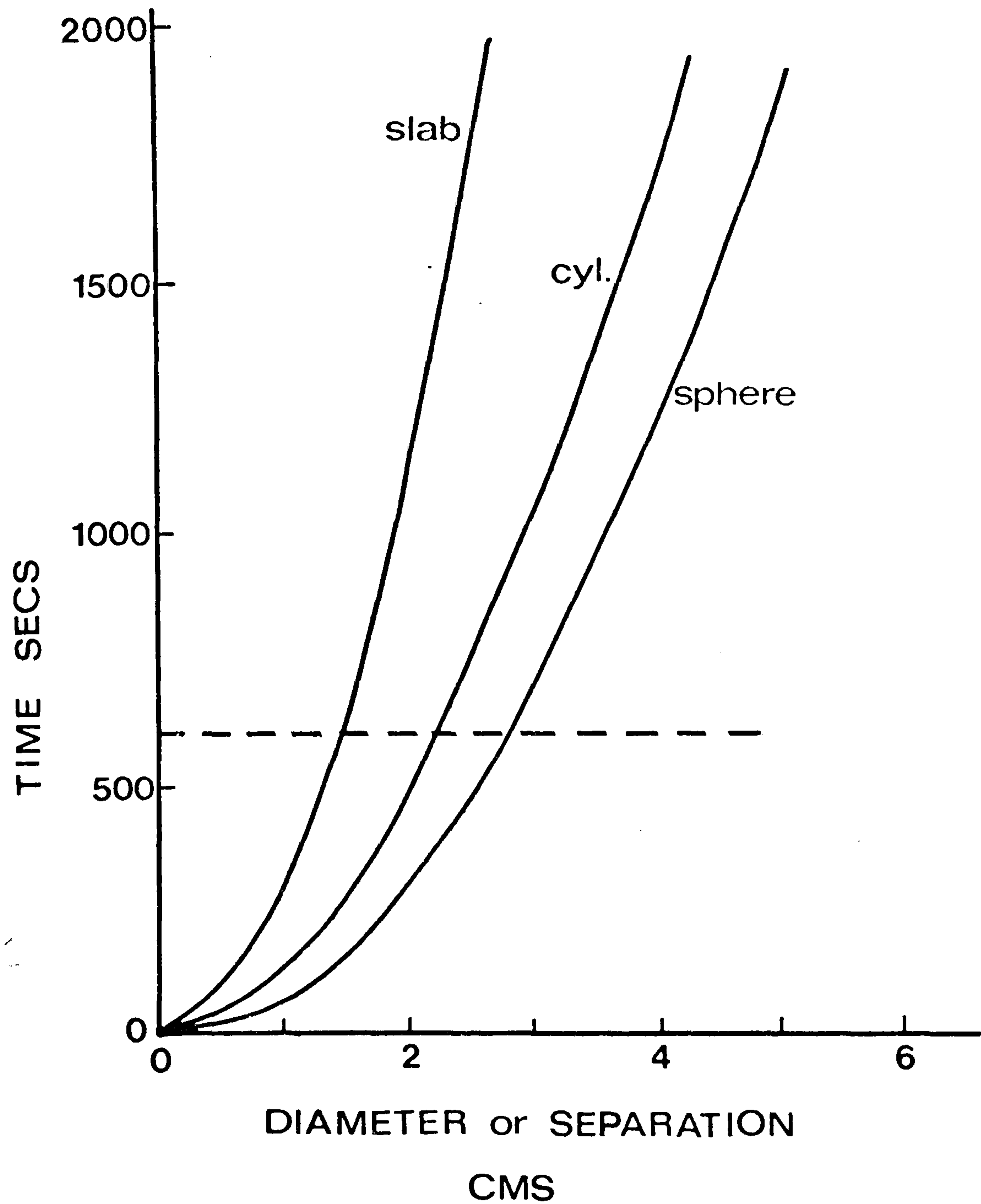


Figure 8.14 Heating by thermal conduction - time taken for centre of tissue to reach 42°C plotted against tissue size. Muscle tissue, surface temperature 42.5°C . Dotted line indicates sizes of tissues heated to 42°C in 10 minutes.

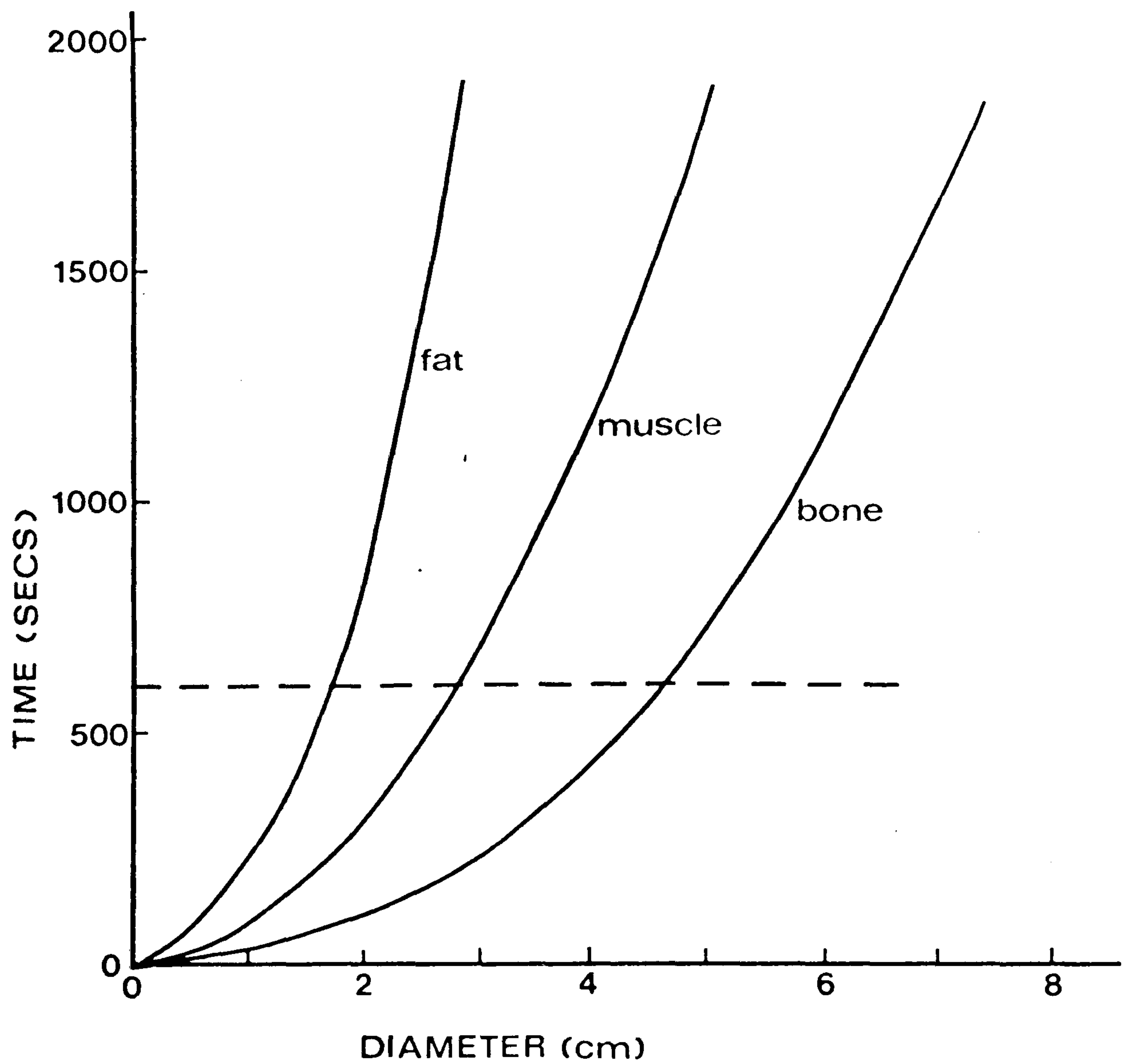


Figure 8.15 Heating by thermal conduction - time taken for centre of tissue to reach 42°C plotted against tissue size for tissues with thermal diffusivities corresponding to bone, muscle and fat. Dotted line indicates sizes of tissues heated to 42°C in 10 minutes.

TABLE 8.1

Size of tissues which are efficiently heated
by thermal conduction alone

<u>Tissue</u>	<u>Diameter or thickness (cm)</u>
Muscle - slab	1.5
Muscle - cylinder	2.2
Muscle - sphere	2.8
Fat - sphere	1.75
Bone - sphere	4.6

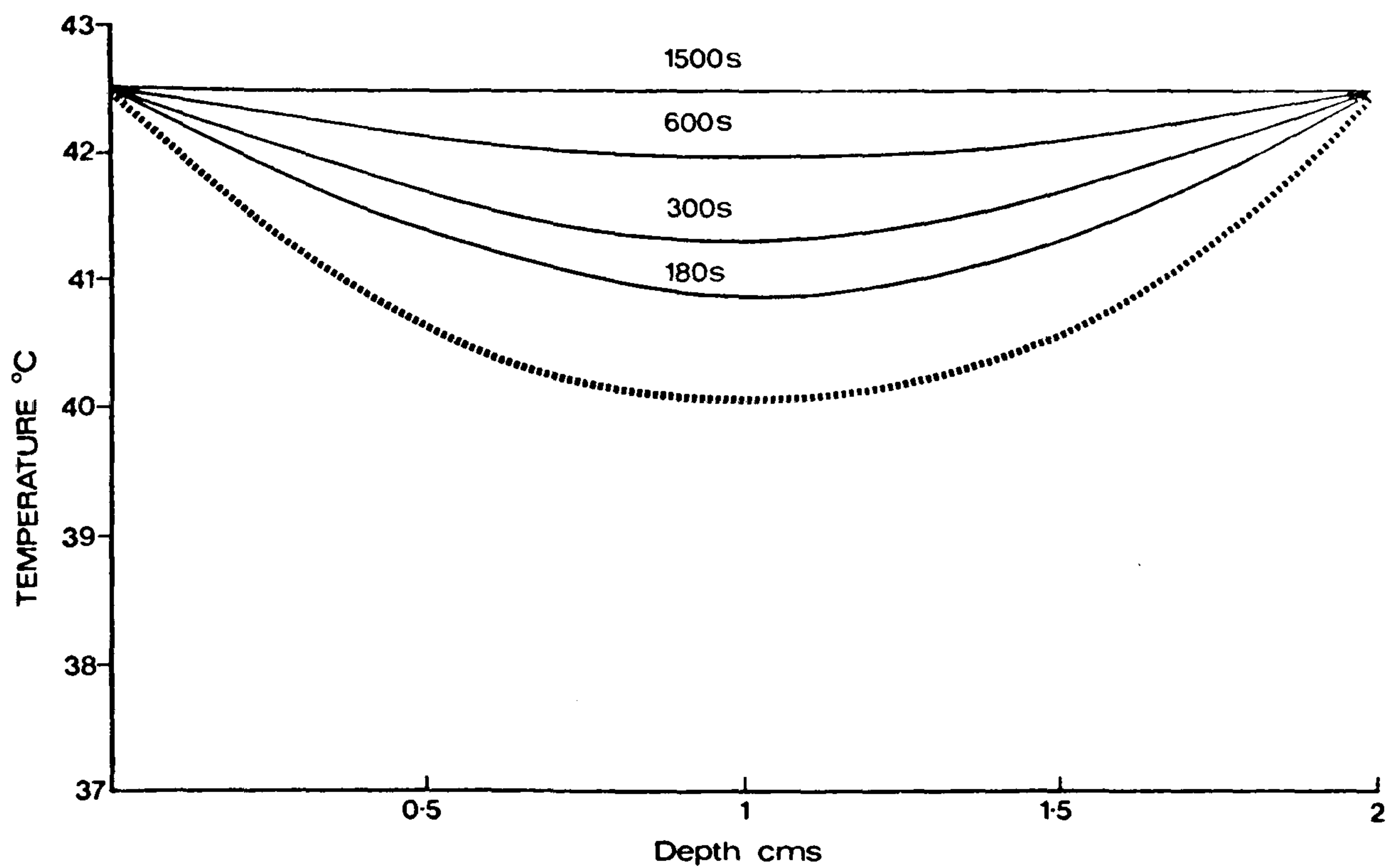


Figure 8.16 Microwave heating - temperature profiles, at various times, resulting from heating of muscle tissue (width 2 cm) by parallel, opposed, switched, microwave fields (2450 MHz). Broken line - no thermal conduction. Equilibration point at surface of tissue.

centimetres thickness, which is little improvement on simple conduction heating indicated in Table 8.1. Thus the non-uniform heating patterns produced by microwaves cannot be sufficiently smoothed out by thermal conduction in tissues greater than about two centimetres in size.

Model 3 - Conduction out of a heated region

Using the ideal LCF heating source, with no penumbra, Figure 8.17 shows the temperature profiles, at various times, across a heated region of width five centimetres. Thermal conduction continuously modifies the temperature distributions both within and out of the heated volume and reduces the size of the region which is above the therapeutic level of 42°C . The percentage volume of the heated region which is above 42°C , at any time, is indicated in Figure 8.18 for different sizes of tissue. The rather complex shapes of the curves are determined by the extent to which the equilibration point is affected by thermal conduction. For example, for an LCF field of width five centimetres, initially almost all of it is above 42°C . Over a period of ten minutes the effective volume falls to less than 50% as conduction carries away heat into the surrounding tissues. After this time, however, as conduction begins to influence the equilibration point more heat is added by the heat source and the effective volume increases again.

Because of the sharp boundary of the heat input

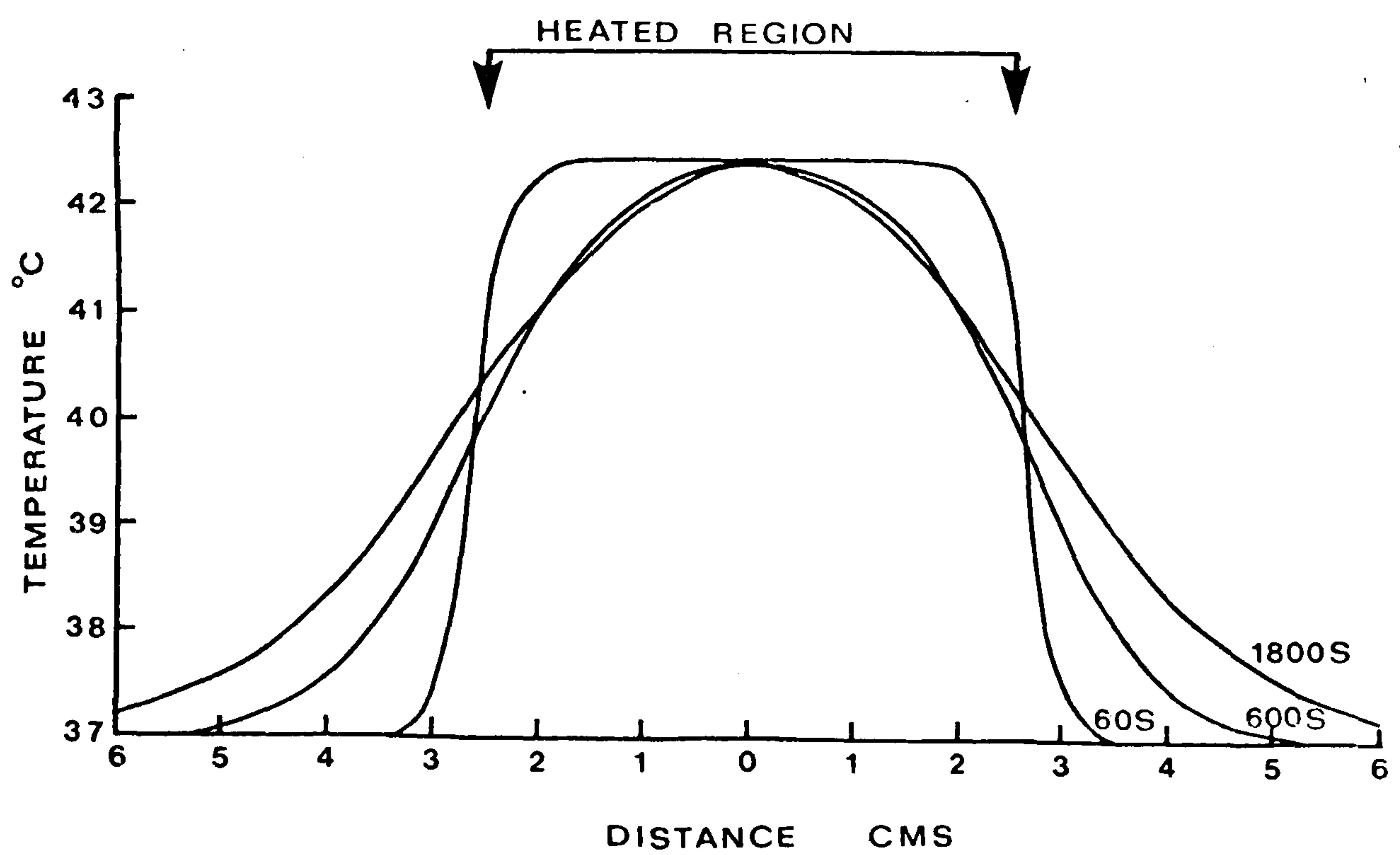


Figure 8.17 Localised current field heating - temperature distributions at various times across the heated region (idealised heat source, equilibration point in centre of heated region). Muscle tissue.

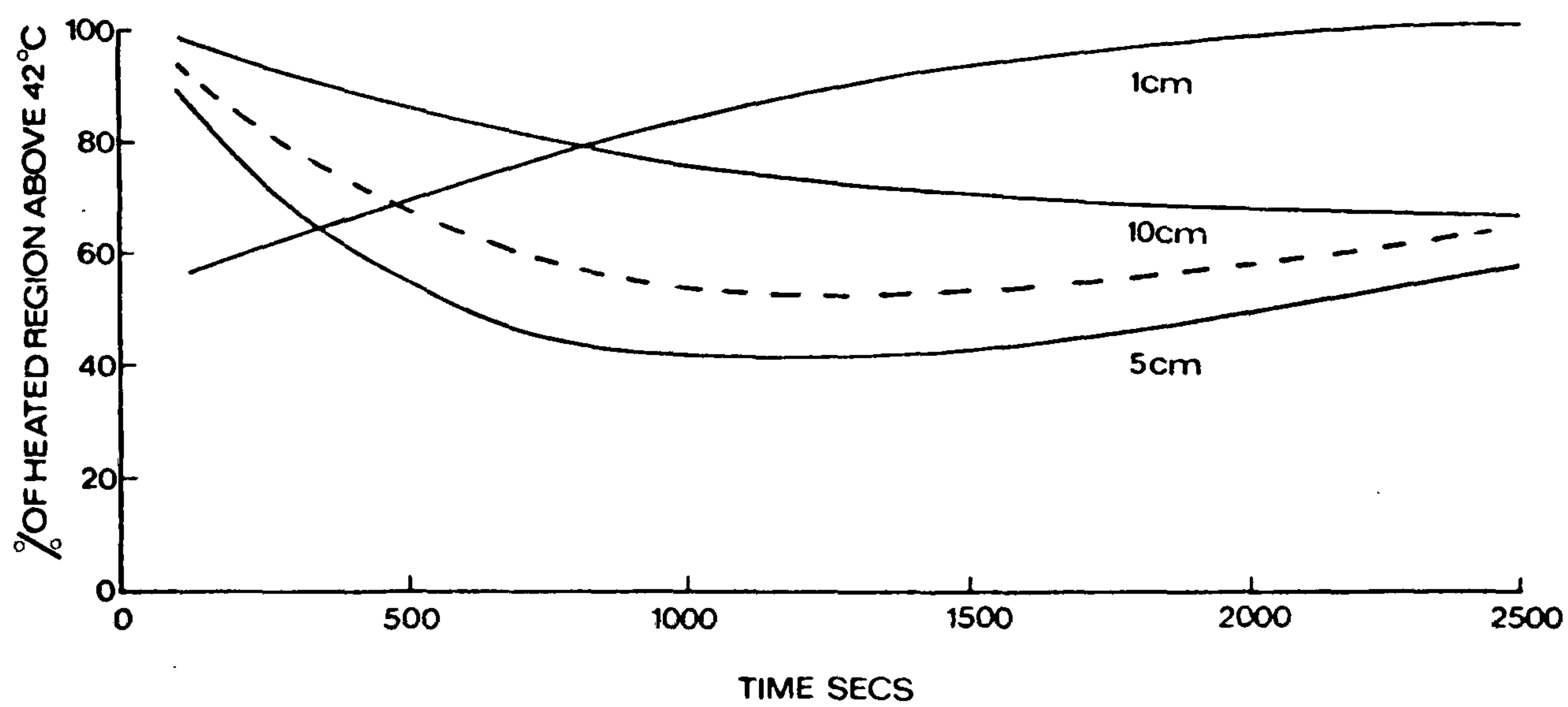


Figure 8.18 Localised current field heating - the variation of the percentage of the heated region above 42°C with time, for various widths of tissue. Equilibration point in centre of region. Solid lines - idealised field. Broken line - field of width 5 cm with penumbra.

of the idealised LCF source these results illustrate the maximum effects of conduction. Temperature distributions were also calculated for a more realistic LCF source, of width five centimetres, with a penumbra (section 7.2.2) and the percentage of the volume above 42°C is shown in Figure 8.18 by the dotted line. The heating penumbra reduces the effect of conduction out of the treatment volume, at the expense of an increased temperature in the surrounding tissue. However the volume which receives an effective thermal dose still falls to just over 50% during the treatment.

8.4.3 Discussion

The above results indicate the general magnitude of the effects of thermal conduction in hyperthermia but it is again stressed that they are strictly applicable only in the absence of blood flow. The following particular conclusions can be drawn.

a) Thermal conduction is efficient at smoothing out temperature gradients over distances of about two centimetres, the exact value being dependent on factors such as the steepness of the temperature gradient, the geometry of the tissue and the type of tissue (Table 8.1). It is therefore itself a viable form of heating for small tissues of this order of size and is of particular use in experimental animals. With larger tissues it provides heating to the superficial layers but does not produce satisfactory temperatures at depth. The results are not only applicable to water bath heating but are

also be important in other techniques involving perfusion or infusion of heated fluids.

b) Thermal conduction also provides a means by which heat may be lost from a region. The consequence of this is that the thermally effective volume may only be about 50% of the volume to which the external heat energy is being applied. Thus to be certain of effectively heating a tissue of a certain size requires that the surrounding tissues also be heated, which may result in undesirable effects if the blood flow is low in these areas.

8.5 INTERACTION OF BLOOD FLOW AND CONDUCTION

In the preceding sections some of the individual effects of thermal conduction and the flow of blood through a tissue have been described. This section now attempts to indicate how these effects may interact and in this way illustrate the type of problem which may be encountered in the practical use of hyperthermia. Two specific examples are considered; one which illustrates the way in which the effects of conduction may be dominated by blood flow and the other in which the effects of blood flow are influenced greatly by thermal conduction. Temperature distributions were again calculated using the finite difference computer program.

8.5.1 Models

Model 1 - Conduction heating of a perfused tissue

This model again involved the heating of a tissue

by conduction from its surrounding medium. The tissue was considered as a sphere, of muscle tissue, where initially the temperature throughout was 37°C , with the surface of the sphere being maintained at 42.5°C . In this case, however, a uniform blood flow was assumed to be present in the tissue and the effects of this have been simulated in two ways. First of all it was assumed that the blood flow simply removed heat from the spherical tissue according to the capillary model and at each time step of the computer program a correction was made for this as described in section 7.6.1. Secondly, however, it was suggested in section 8.2.4 that blood flow may also increase the effective thermal conductivity of tissue and therefore two different values of the conductivity were used. While it is accepted that conductivity may be a variable function of blood flow, for simplicity the general observations of Nevins and Darwish (1970) were used and the conductivity with flow was taken to be twice that without flow.

The temperature profiles across the diameter of the sphere were calculated for periods up to one hour, for flows of 5, 10 and 30 ml/100g/min and diameters of 2 cm and 5 cm.

Model 2 - A non-uniformly perfused tumour

The aim here was to examine the temperature distributions obtained when non-uniform blood flows are present over distances which are relevant to the practical use of hyperthermia. It was felt appropriate

to adopt a model based on a description of a solid tumour which has recently received considerable attention in the literature (see section 7.6). The model used is depicted in Figure 8.19 and is of spherical geometry. Within the central core of the tumour the blood flow is low or zero and in the surrounding shell the flow is higher than in the adjacent normal tissues. It was assumed that the initial temperature throughout the tumour and normal tissues, both of which had the thermal characteristics of muscle, was 37°C and that the volume was uniformly heated. The heating term was chosen such that the equilibration temperature, which was 42.5°C , was reached within one minute. The equilibration point was positioned in either the central core or in the normal tissue. The effect of changing the thermal conductivity, when blood flow was present, was again examined.

Temperature profiles were calculated across the volume for periods up to one hour and for two combinations of the tissue component dimensions and blood flows. Clearly the number of possible combinations is limitless but the values used were consistent with the reported general descriptions of a small and a fairly large tumour (Straw et al, 1974; Endrich et al, 1979) and are shown in Table 8.2.

8.5.2 Results

Model 1 - Conduction heating of a perfused tissue

In contrast to the temperature profiles obtained in

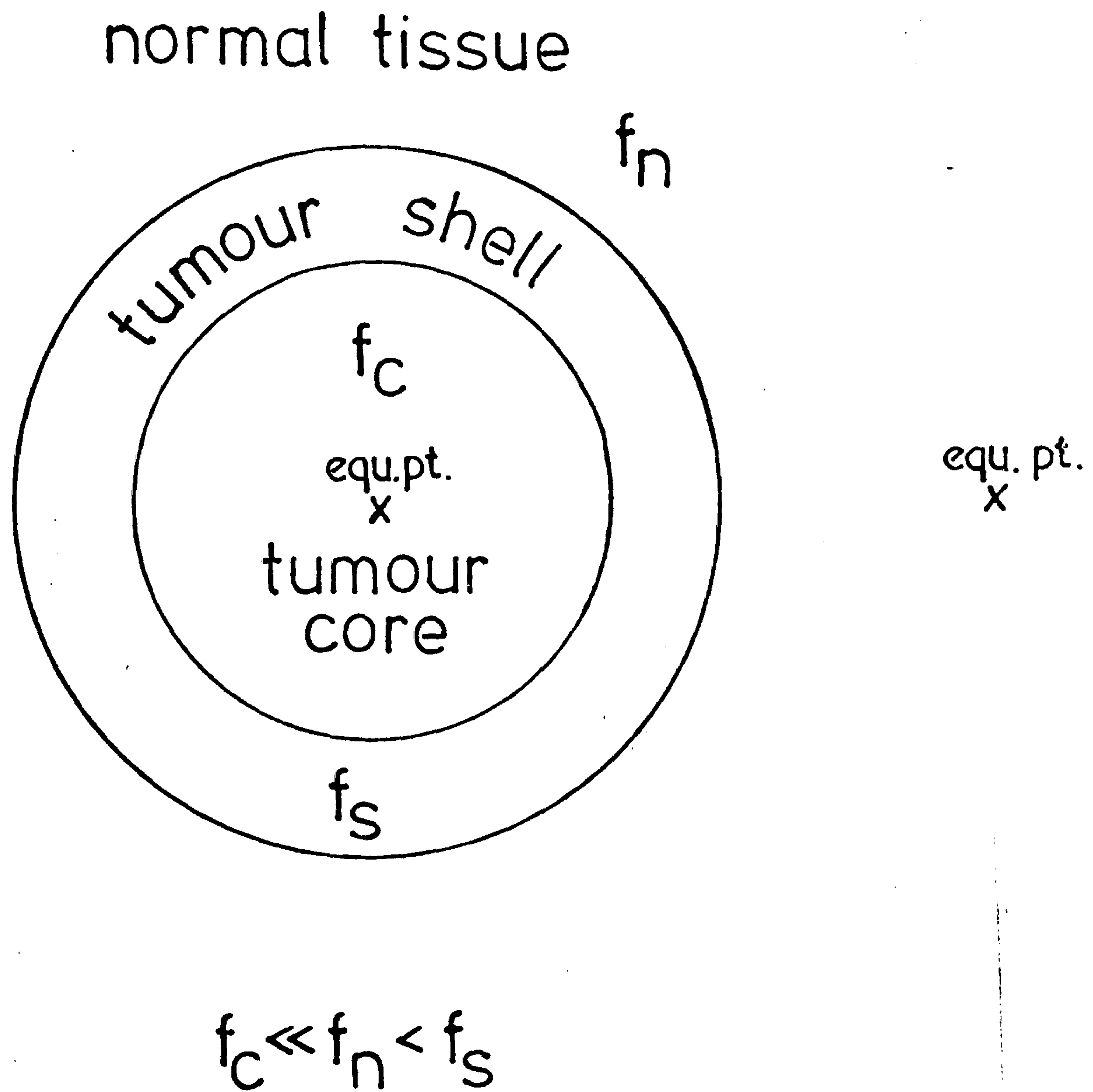


Figure 8.19 Model of non-uniformly perfused tumour.
 f_n , f_c and f_s represent the blood flow
 in the normal tissue, tumour core and tumour
 shell respectively.

TABLE 8.2Tissue sizes and blood flows for tumour models

	<u>Core</u> <u>Blood Flow</u>	<u>Shell</u> <u>Blood Flow</u>	<u>Normal</u> <u>Tissue</u> <u>Blood Flow</u>	<u>Core</u> <u>Radius</u>	<u>Shell</u> <u>Radius</u>
Small Tumour	1	20	10	0.5 cm	1 cm
Large Tumour	1	20	10	2 cm	2.5 cm

All blood flows are given in ml/100g/min

the absence of blood flow (Figure 8.13), which show a continual rise in temperature within the tissue with time, in the presence of blood flow a steady state is reached relatively quickly. Figures 8.20 and 8.21 show the temperature profiles for spherical regions of 2 cm and 5 cm diameter respectively, for the blood flows as shown. The achievement of a steady state means that a stage is reached when the blood flow in the tissue is carrying away heat as fast as it can be delivered by the conduction process. The centre of the tissue is then effectively protected by the blood flow in the outer layers and the rise in temperature of this point is therefore limited as shown. For blood flows of 10 ml/100g/min or greater only the outer 2 mm or so of the tissue is above 42°C . To increase the temperature of a significant portion of the tissue above 42°C would require a surface temperature well in excess of 42.5°C which may, of course, be unacceptable. For a tissue of 2 cm diameter and a flow less than 5 ml/100g/min most of the tissue will attain a temperature of greater than 42°C .

The effect of an increase in the thermal conductivity, which may be a second consequence of blood flow, is shown by a dotted line on both graphs, for a flow of 10 ml/100g/min. As expected this increases the amount of tissue above 42°C , substantially in the case of the 2 cm tissue but only marginally in the other example.

It can be seen from these results that in this

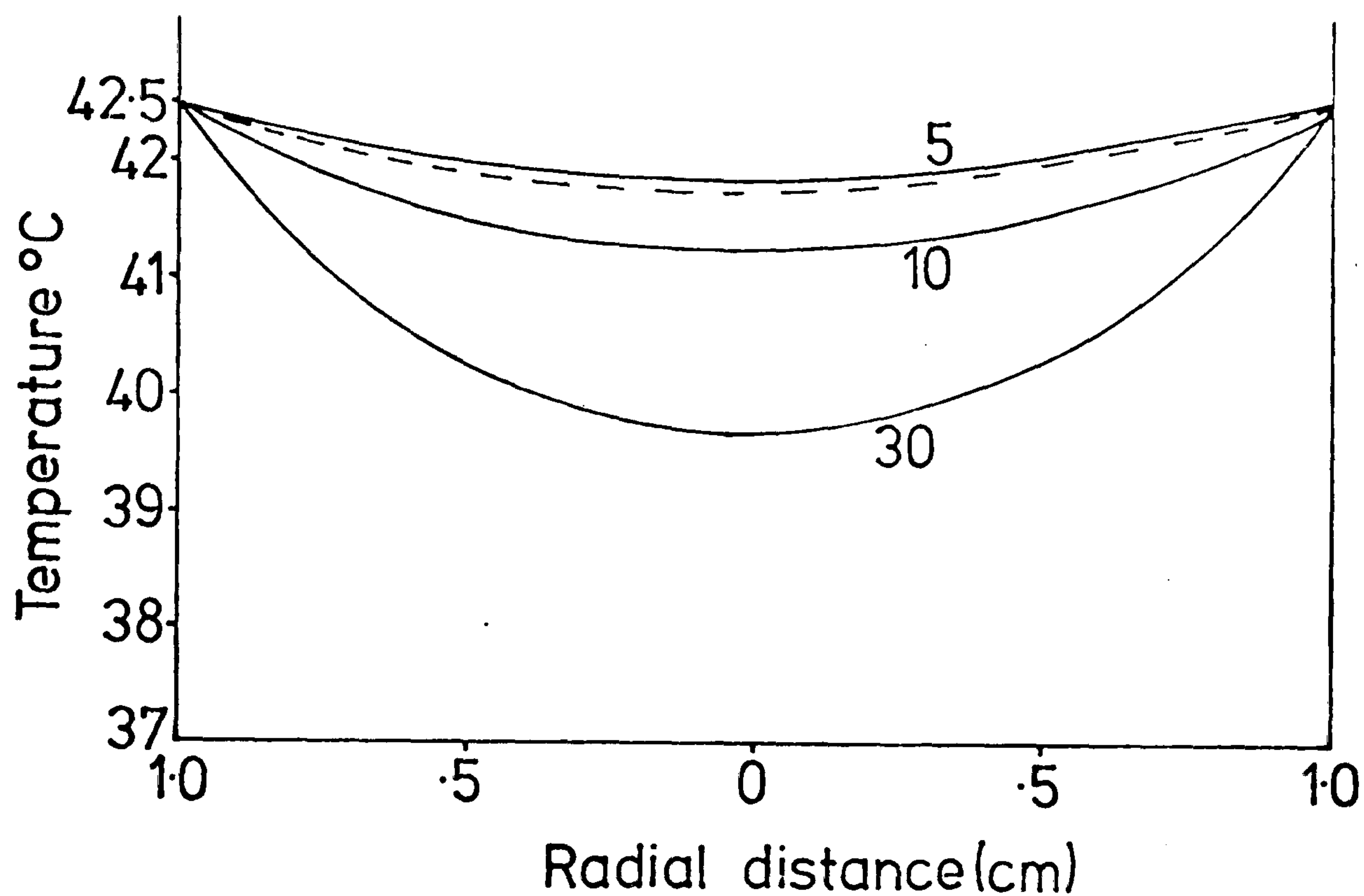


Figure 8.20 Heating by thermal conduction - steady state temperature profiles across spherical volumes of muscle tissue, of diameter 2 cm, with blood flows of 5, 10 and 30 ml/100g/min. The surface of the tissue is maintained at 42.5°C. Dotted line - the temperature profile obtained for a thermal conductivity value of 2x that of muscle and a blood flow of 10 ml/100g/min.

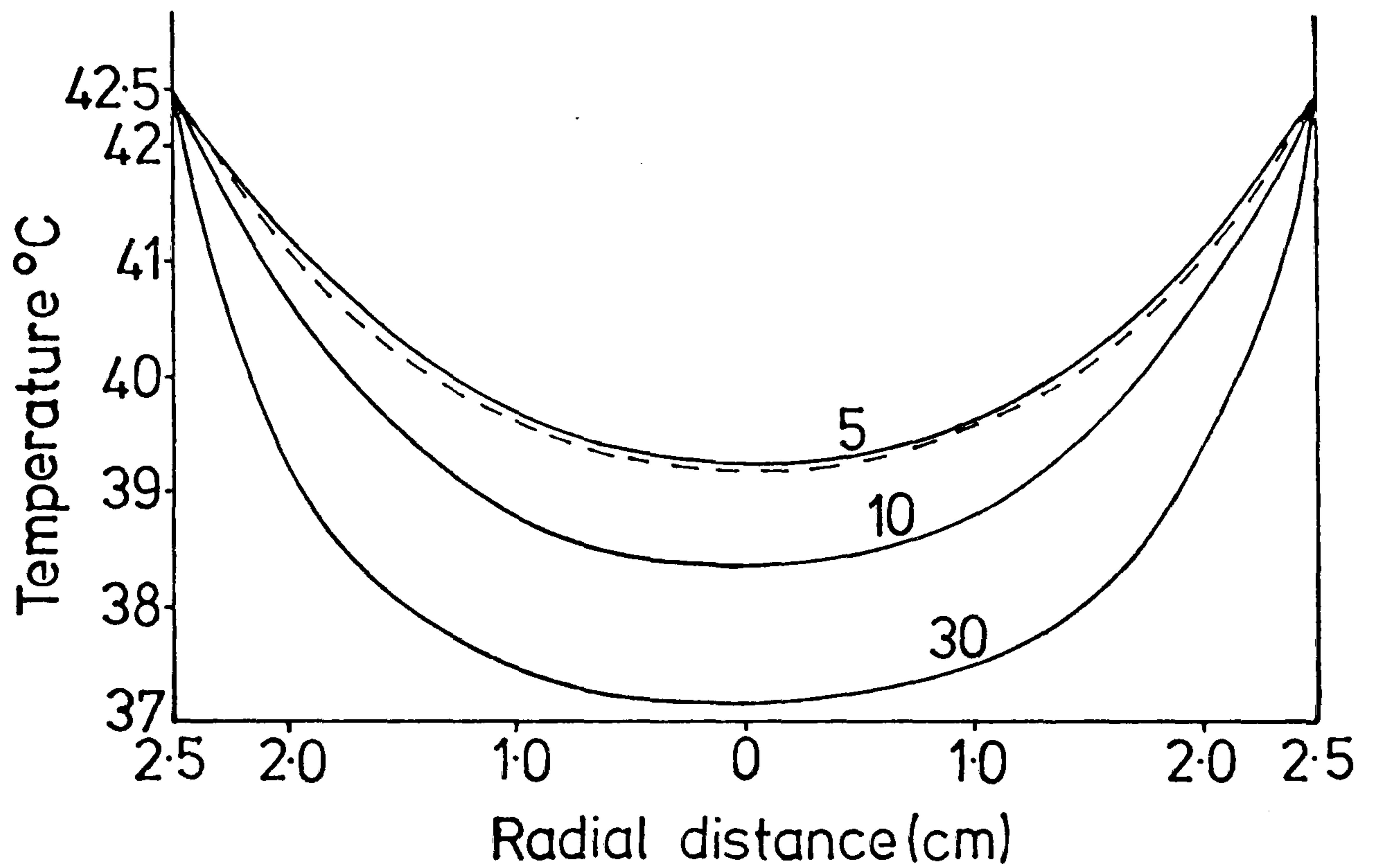


Figure 8.21 Heating by thermal conduction - steady state temperature profiles across spherical volumes of muscle tissue, of diameter 5 cm, with blood flows of 5, 10 and 30 ml/100g/min. The surface of the tissue is maintained at 42.5°C. Dotted line - the temperature profile obtained for a thermal conductivity value of 2x that of muscle and a blood flow of 10 ml/100g/min.

situation blood flow dominates the transfer of heat in tissues greater than 2 cm in size, but below this conduction may assume greater importance.

Model 2 - A non-uniformly perfused tumour

Figures 8.22 and 8.23 show the temperature profiles, taken 20 minutes after the start of heating, for the small and large tumours respectively. The profiles change only marginally with time, the variation being about 0.1°C from 10 minutes after the start to 40 minutes after. First of all, Figure 8.22 shows that, with the equilibration point at the centre of the tumour the temperature does not fall below 42°C at any part of the volume. Instead the normal tissue temperature rises to 43°C . With the equilibration point in the normal tissue a large part of the tumour is then at a temperature less than 42°C . Both of these represent potentially serious situations, one in which the normal tissue may be overdosed and the other where the tumour may be underdosed. Considering the equilibration point at the centre of the tumour the shape of the profile results from the fact that heat is being removed at a fast rate by the relatively high blood flow in the shell of the tumour. Because of the small size of the tumour core the equilibration point is then influenced by conduction from the core to the outer shell. This results in an increased heat input by the external source in an attempt to maintain the equilibration temperature. The conduction from the core and the increased heat input mean

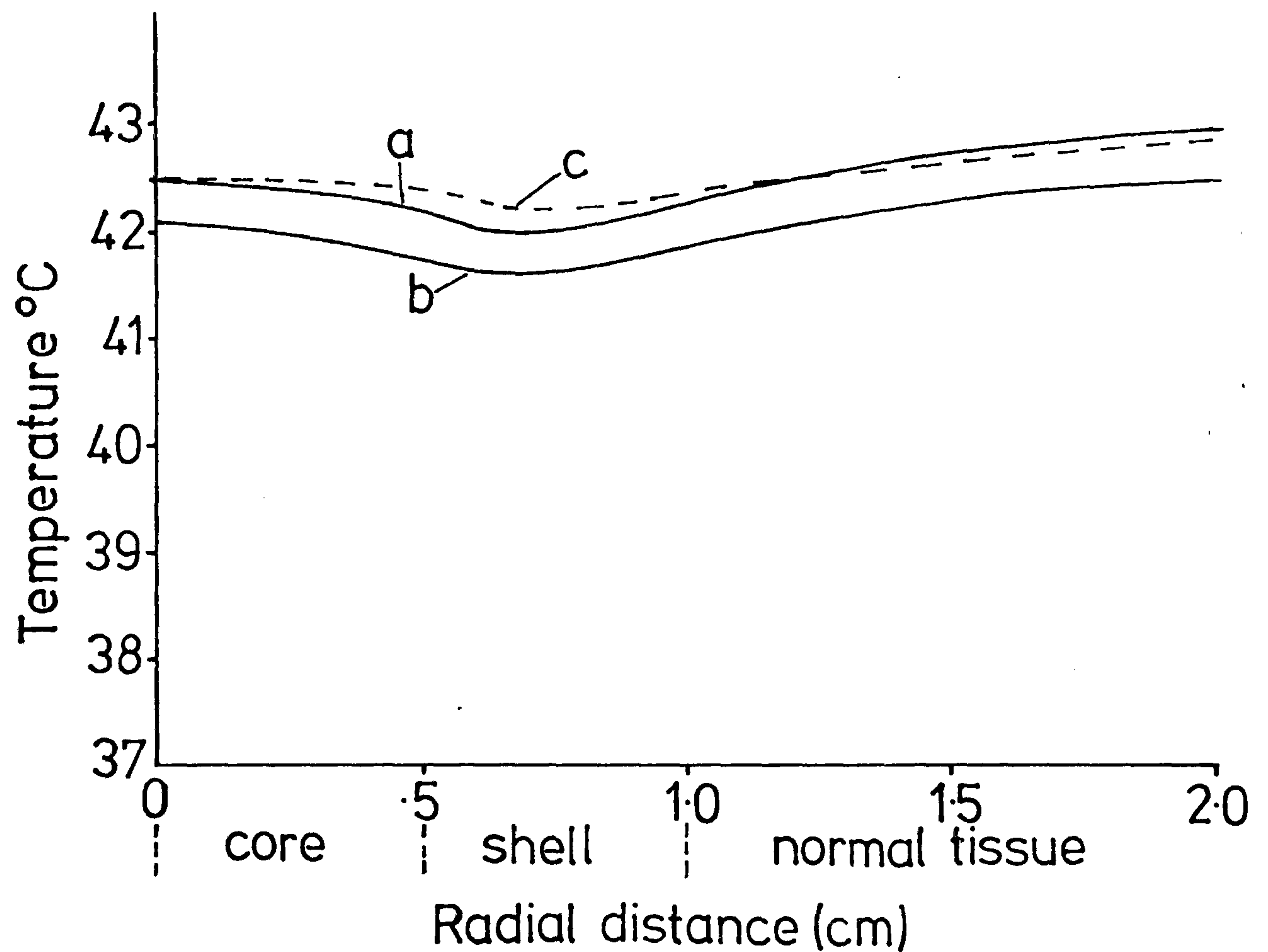


Figure 8.22 Heating of a non-uniformly perfused tumour - steady state temperature profiles across a spherical tumour with a core blood flow of 1 ml/100g/min, a shell blood flow 20 ml/100g/min and normal tissue blood flow 10 ml/100g/min. The core is 1 cm in diameter and the shell is 0.5 cm wide. The heat input maintains the equilibration point at 42.5°C . The equilibration point is a) at the centre of the tumour, b) in the normal tissue. Dotted line - the temperature profile obtained for a thermal conductivity value of 2x that of muscle.

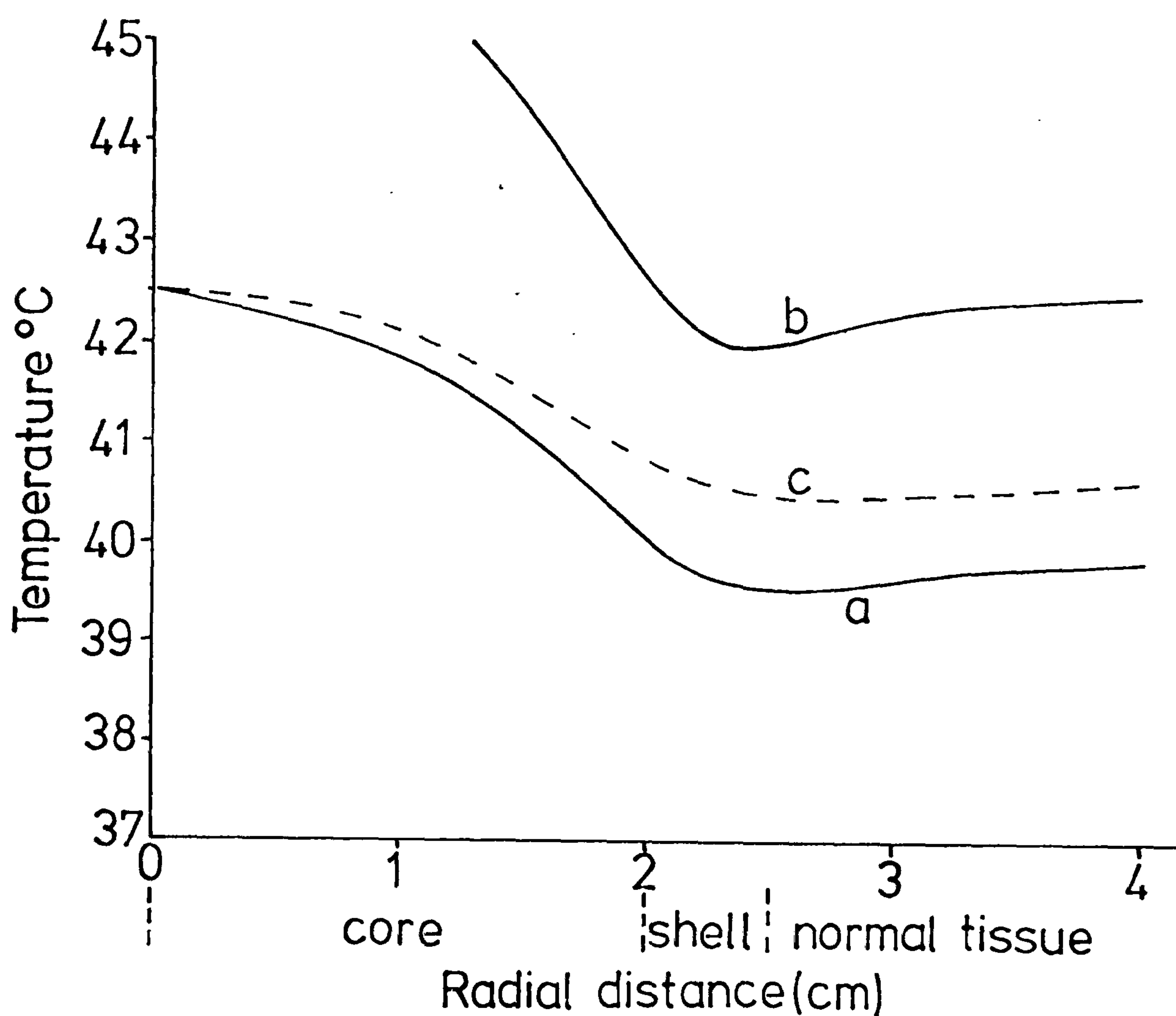


Figure 8.23 Heating of a non-uniformly perfused tumour - steady state temperature profiles across a spherical tumour with a core blood flow of 1 ml/100g/min, a shell blood flow 20 ml/100g/min and normal tissue blood flow 10 ml/100g/min. The core is 4 cm in diameter and the shell is 0.5 cm wide. The heat input maintains the equilibration point at 42.5°C. The equilibration point is a) at the centre of the tumour, b) in the normal tissue. Dotted line - the temperature profile obtained for a thermal conductivity value of 2x that of muscle.

that the temperature in the shell does not fall as much as might have been expected on the basis of its blood flow. However the heat input also results in the temperature of the normal tissue reaching a possibly dangerous level. A similar explanation applies when the equilibration point is in the normal tissue. The important factor then is that although the tumour core does not have a high blood flow, and may be expected to maintain a high temperature, it is small enough to allow a considerable loss of heat by conduction to the outer shell.

A much worse situation is obtained in the case of the large tumour (Fig. 8.23). Here, with the equilibration point at the centre, the temperature falls steadily within the core and shell of the tumour until it is below 40°C at the junction with the normal tissue. However with the equilibration point in the normal tissue the temperature at the centre of the tumour reaches 46°C and is above 42.5°C throughout the tumour. In this case, then, conduction is less able to smooth out the temperature gradients and to influence the equilibration point and the temperature profile is more dependent on blood flow non-uniformity.

The effect of increasing the thermal conductivity is shown on Figures 8.22 and 8.23 by the dotted lines, in both cases assuming that the equilibration point is at the centre of the tumour. As expected this produces a more uniform temperature profile, particularly

with the small tumour. It should be noted that if the blood flow in the core of the tumour was zero instead of 1 ml/100g/min then this correction to the thermal conductivity would not be applicable.

8.5.3 Discussion

Although conduction heating of tumours has been adopted in many studies, detailed temperature profiles have only rarely been measured and in many cases the assumption is made that the tumour attains the water bath temperature (Robinson et al, 1974; Hall et al, 1974; Hume et al, 1979). The above results show that the temperature obtained at any depth within tissue is mainly dependent on the blood flow and that, in general, only a very thin layer close to the surface of the tissue will be within 0.5°C of the water bath temperature. This is consistent with Dickson and Calderwood's (1980) suggestion that the temperature of a water bath must be up to 4°C higher than the desired temperature within the tissue. Robinson et al (1978) have measured temperature profiles across a tumour implanted in a mouse leg. Their results, with water bath heating, are of the same form as Figure 8.20 and show a temperature $1^{\circ} - 2^{\circ}\text{C}$ lower at the tumour centre. They suggest that this is due to large blood vessels at the centre but from above this is equally likely to be due to the diffuse blood flow throughout the tissue. Indeed, on heating with microwaves, an essentially uniform profile is obtained which is compatible with a technique of

local deposition compared to one which depends on the transfer of heat from the outer layers. Hall et al (1974) treated superficial tumours of the urinary bladder by irrigation with heated saline but measured only the temperature of the saline. Since the above results show that the thermal dose at depth is limited and highly dependent on blood flow it is not surprising that a wide response to this treatment was observed.

The number of examples of practical hyperthermia models presented here has been necessarily limited. The two models, based on a description of a solid tumour have, however, been sufficient to demonstrate the importance of blood flow and thermal conduction and the difficulty in predicting the interaction which occurs between the two. In particular they have shown that the normal practice of monitoring the temperature at only one point in tissue gives a limited, and possibly mistaken, impression of the thermal effect. Most clinical studies monitor the temperature at the centre of a tumour (Storm et al, 1980; Raymond et al, 1980; Areangeli et al, 1980) but Figure 8.23 shows that for a fairly large tumour this will lead to an ineffective thermal dose to the outer parts. The region between the core and shell of a tumour may be especially important since it contains the hypoxic cells, which are resistant to treatment by ionising radiation (Cater et al, 1964). In this case, then, it may be advantageous to position the equilibration point in the normal

tissue. Unfortunately, for a small tumour the opposite is true, where an effective tumour dose is only obtained by monitoring the tumour temperature. It is clear from these results that the particular geometry of a tumour is crucial and that the monitoring of temperature at a single point does not necessarily provide information on the true thermal dose. Furthermore it is seen that the existence of a low blood flow within the core of a tumour does not guarantee an effective thermal dose throughout, as has been inferred in the literature (Dickson and Calderwood, 1980).

Variation of the thermal conductivity value in Figures 8.22 and 8.23, which may occur in the presence of blood flow, also emphasises that the thermal characteristics play a vital role in determining the temperature profiles.

8.6 CONCLUSIONS

For localised hyperthermia to be a useful modality in treating cancer the factors influencing the temperature distributions within a tissue must be known and understood. This study has been concerned with defining the roles played by the blood flow and thermal conduction in modifying these temperature distributions. The effects of these processes have been assessed only with regard to the temperature non-uniformity produced and no account has been taken of other factors, which may be equally important, such as the chemical

environment within the tumour, the release of toxic substances as the tissue is damaged, the inherent thermal sensitivity and the immunological response (Dickson and Calderwood, 1980). On this basis it is the lowest temperature within a tumour which will determine whether it will be capable of re-growth. Two criteria, based on published results, have been used to assess the thermal effectiveness in any situation. Several particular conclusions have been obtained.

a) Significant exchange of heat between the blood and tissues occurs not only in the capillaries but also in the arterioles and venules and to a lesser extent in the small arteries and veins. The consequences of this are that, for small tissues, the accurate description of heat transfer might require a complex model which will take into account the "convection" of heat by the blood flow. In addition a blood flow dependent value of the thermal conductivity may be necessary.

b) Where blood vessels do not come to complete equilibrium with tissue, a considerable volume surrounding the blood vessel may be protected from the thermal dose by the "cold" blood. This occurs in large arteries and veins and also to a lesser extent in small arteries and veins although the latter may be more important because of their large number.

c) A diffuse model of blood flow, which is applicable to large tissues, shows that flow limits the temperature obtained within a tissue for a particular heat input and

produces non-uniformities in the tissue temperature or effective heating time, in tissues with different flows.

d) Thermal conduction has important effects in smoothing temperature gradients, although this is only significant over small distances, and can considerably reduce the effective heated volume of a tissue.

e) The interaction of blood flow and conduction results in complex effects which depend on a very large number of variables, including the particular tissue dimensions. In the treatment of tumours the placement of a temperature monitor may be of vital importance. The existence of a low flow within the core of a tumour does not necessarily lead to a thermally effective dose throughout it.

Thus the mathematical models presented in this study have allowed the general, and some specific, effects of blood flow and thermal conduction to be defined. In the light of these findings it is perhaps not surprising that, in clinical use, hyperthermia has shown variable results. In many situations localised hyperthermia will be severely limited by the effects of blood flow and procedures such as occlusion of the blood supply or perfusion of the region with heated fluid may be required to produce more uniform temperatures. While mathematical models are useful to assess the effect of particular variables they would appear to have little future in terms of predicting

the temperature distribution for a specific treatment. Such treatment planning would require accurate knowledge of the tissue and tumour dimensions, and the blood flows and thermal properties within each region. Although several recent studies have attempted to measure blood flow in tumours (Mantyla, 1979; Taylor et al, 1979; Song et al, 1980) it is unlikely that this could be achieved with sufficient accuracy, and with the necessary regional information, to allow a precise definition of the temperature distribution during heating. The clinical use of hyperthermia will demand a full knowledge of the temperature distribution and it would appear more fruitful to investigate methods of measuring this directly.

CHAPTER 9HEAT AND MATTER TRANSFER - CONCLUSIONS

The purpose of this study has been to examine the ways in which both matter, specifically an inert gas, and heat are redistributed within living biological tissues by the processes of blood flow, diffusion and thermal conduction. Two specific clinical problems, one concerning the measurement of skin blood flow using ^{133}Xe and the other the use of localised hyperthermia in cancer therapy, have been investigated using analagous analytical and numerical models. While simplifying assumptions have clearly been required, solutions to the models have been obtained which are compatible with empirical data. The results of the study have emphasised the important interaction which takes place between, in one case, blood flow and diffusion and in the other, blood flow and thermal conduction.

A truly quantitative method of measuring skin blood flow would be of immense value in plastic surgery. The clearance of a radioactive inert gas, ^{133}Xe , from the skin has been proposed and, indeed, used for such a purpose. Motivated by the present finding of clearance of ^{133}Xe in the absence of blood flow this study set out to re-examine the processes involved in this technique.

^{133}Xe can be transported in a tissue both by bulk diffusion and by the blood flow. Before the latter process can occur, however, the ^{133}Xe must obviously be

able to diffuse through the tissue and into the blood vessels. Traditionally it has been assumed that significant transfer of an inert gas from the tissue to the blood can only take place in the capillaries. The present study, however, has shown that such exchange is dependent on the particular combination of the length, velocity of flow and radius of the blood vessel and, for typical values of these, exchange may occur not only in the capillaries but also in larger blood vessels. While the traditional description of the clearance of ^{133}Xe from a tissue, by the blood flow, is still applicable in uniformly labelled regions whose dimensions are much greater than the length of the exchange vessels, such a description is thus insufficient in smaller labelled regions. A rigorous model of this would require complete knowledge of the properties and architecture of the vascular system in a tissue, and has therefore not been attempted in the present study. However, the implications of large vessel exchange have been outlined. After epicutaneous application of ^{133}Xe to the skin surface, ^{133}Xe will be present within the dermis in a very thin layer. Instead of simply being cleared from the skin by the blood flow it may be re-deposited, by the flow, at deeper levels within the dermis and subcutaneous fat. The rate of clearance in the initial stages will be dependent not only on blood flow but also on the particular characteristics of the blood vessels in the lower layer of the dermis and in the subcutaneous fat.

A full model of the transport of ^{133}Xe in skin, incorporating bulk diffusion and clearance by blood flow, with a correction for the above transfer process, has shown that, after epicutaneous application, the clearance rate is dependent not only on blood flow but also very much on diffusion back out of the avascular epidermal barrier. The result of this is that an apparent clearance is present even in the absence of blood flow, and thus the clearance rate is just as likely to reflect the diffusion characteristics of the epidermal barrier. For this reason the method is unable to provide an accurate measurement of skin blood flow and is unsuitable for use in the clinical situation of plastic surgery. The measurement of skin blood flow, however, remains a problem. It may be that, in some situations and especially in the absence of any other suitable technique, the intra-cutaneous ^{133}Xe method may provide sufficient accuracy, if a proper analysis of the clearance curve is made. This, of course, applies only where the inherent disadvantages of the method, namely the necessity of injection and the effect of injection on blood flow, are acceptable.

The investigation of the ways in which blood flow and thermal conduction can modify temperature distributions produced during localised hyperthermia has also firstly involved an assessment of the exchange blood vessels. Again it has been shown that the exchange occurs in vessels larger than capillaries, although in the case of

heat larger vessels are capable of such exchange than for ^{133}Xe . The implications of this are that where temperature gradients are present over small distances (of about 1 cm) within a perfused tissue, the transfer of heat in and out of blood vessels may result in a higher effective thermal conductivity in that region than is measured in excised tissue. A further consequence of the exchange of heat between a blood vessel and tissue has been shown to be the thermal protection afforded to the tissue surrounding a large blood vessel, in a heated region. In this case, while the total exchange is minimal the local reduction in temperature is highly significant in terms of biological effect.

The models of localised hyperthermia, using a capillary description of blood flow, have shown that the temperature distributions produced in a living tissue are highly dependent on that blood flow and on thermal conduction. The blood flow produces an efficient heat sink within the tissue, resulting in non-uniform temperatures in the presence of non-uniform flows. Thermal conduction is able, in a limited way, to smooth out temperature gradients within a tissue and also to provide a form of heating when the tissue is surrounded by a heated fluid. The effects of blood flow and conduction are interdependent and the interaction between them may be difficult to predict. Two specific tumour models have highlighted the problem of producing an effective thermal dose throughout a tumour. The monitor-

ing of temperature at one point within a treatment volume has, in addition, been shown to provide limited information on the likely therapeutic effects.

The above results suggest that considerable limitations are introduced by blood flow and thermal conduction to the use of localised hyperthermia in clinical practice. It should, however, be emphasised again that the possible biological effects have been assessed solely on the basis of the tissue temperature, although it is realised that other factors may also be of importance. Despite this it is clear that not enough attention has been paid to the possible non-uniformities in temperature distributions which may be produced even with ideal heating techniques.

It has been shown that both heat and matter transfer can be described by analagous mathematical models. The essential difference between the two models is in the diffusivity term and a clear example of this is reflected in the size of blood vessels which are capable of significant exchange with the surrounding tissue. Because of its much higher diffusivity heat can be exchanged with blood vessels of a larger radius and flow rate than can ^{133}Xe . An important consequence of this difference is that the effective blood flow, in relation to heat exchange, may have to take account of flow in these larger vessels. This means that the blood flow assessed by an inert gas clearance or microsphere technique might not reflect the thermally effective blood flow, since different sizes of blood vessels are involved. Therefore

if a model of hyperthermia is to be constructed and requires a value for the blood flow, it may be necessary to assess this flow using a technique based on the clearance of heat itself.

Further work required

The results of the models have shown very good agreement with the experimental work carried out on ^{133}Xe clearance from skin and are also compatible with published, but limited, empirical data on hyperthermia. In the present study no experimental work was carried out on the mapping of tissue temperatures in localised hyperthermia but it is clear that much more work is required in this area. Development of the models to include a rigorous description in small tissue regions would appear to be limited because of the lack of information available on blood vessel characteristics and arrangements. Such a description may itself have to be based on empirical results. Whether modelling will play a significant part in the clinical use of hyperthermia remains to be seen but certainly the above results suggest that a large number of, often varying, factors can affect the temperature distributions. With this in mind there is no doubt that accurate and thorough temperature measurement will be of prime importance in clinical practice.

REFERENCES

- ABRAMS, M.E., CRAWLEY, J.C.W., GREEN, J.R. and VEALL, N. (1969) A comparative study of digital and analogue computer techniques for deconvolution procedures in clinical tracer studies. *Phys. Med. Biol.* 14, 225-232.
- AMERY, A., BOSSAERT, H., DERUYTTERE, M. and VANDERLINDEN, L. (1973) Influence of body posture on leg blood flow. *Scand. J. Clin. Lab. Invest.* 31, Suppl. 128, 29-37.
- ANDERSEN, A.M. and LADEFOGED, J. (1967) Partition coefficient of ^{133}Xe between various tissues and blood in vivo. *Scand. J. Clin. Lab. Invest.* 19, 72-78.
- ARCANGELI, G., BAROCAS, A., MAURO, F., NERVI, C., SPANO, M. and TABOCCHINI, A. (1980) Multiple daily fractionation (MDF) radiotherapy in association with hyperthermia and/or Misonidazole: Experimental and clinical results. *Cancer*, 45, 2707-2711.
- BAIN, W.H. and HARPER, A.M. (Eds.) (1967) Blood flow through organs and tissues. Livingstone, Edinburgh.
- BARRON, J.N., VEALL, N. and ARNOTT, D.G. (1951) The measurement of the local clearance of radioactive sodium in tubed skin pedicles. *Brit. J. Plast. Surg.* 4, 16-27.
- BASSINGTHWAIGHTE, J.B., KNOPP, T.J. and HAZELRIG, J.B. (1970) A concurrent flow model for capillary tissue exchanges. In: *Capillary Permeability*. Eds. Crone, C. and Lassen, N.A. Copenhagen, Munksgaard, pp. 60-80.

BAZETT, H.C. (1948) The regulation of body temperatures. In: Physiology of heat regulation and the science of clothing. Ed. Newburgh, L.H. Philadelphia, W. B. Saunders Co. pp. 109-192.

BAZETT, H.C., LOVE, L., NEWTON, M., EISENBURG, L., DAY, R. and FORSTER, R. (1948) Temperature changes in blood flowing in arteries and veins in man. J. App. Physiol. 1, 3-19.

BELCHER, E.H. and VETTER, H. (Eds.) (1971) Radioisotopes in Medical Diagnosis. Butterworths, London.

BERENSON, G.S. and BURCH, G.H. (1951) Studies of diffusion through dead human skin. Am. J. Trop. Med. Hyg. 31, 842-853.

BERGER, M.J. (1971) Distribution of absorbed dose around point sources of electrons and β -particles in water and other media. J. Nucl. Med. 12, Suppl. 5.

BETZ, E., INGVAR, D.H., LASSEN, N.A. and SCHMAHL, F.W. (1966) Local blood flow in the cortex of the brain studied simultaneously by heat and inert gas clearance techniques. Acta Physiol. Scand. 67, 1-9.

BICHER, H.I., HETZEL, F.W., SANDHU, T.S., FRINAK, S., VAUPEL, P., O'HARA, M.D., and O'BRIEN, T. (1980) Effects of hyperthermia on normal and tumor micro-environment. Radiology 137, 523-530.

BLANK, I.H. (1953) Further observations on factors which influence the water content of stratum corneum.

J. Invest. Dermat. 21, 259-269.

BLANK, I.H., SCHEUPLEIN, R.J. and McFARLANE, D.J. (1967) Mechanism of percutaneous absorption. J. Invest. Dermat. 49, 582-589.

BOWMAN, H.F., CRAVALHO, E.G. and WOODS, M. (1975) Theory, measurement and application of thermal properties of biomaterials. Ann. Rev. Biophys. Bioeng. 4, 43-80.

BRAITHWAITE, F., FARMER, F.T. and HERBERT, F.I. (1951) Observations on the vascular channels of tubed pedicles using radioactive sodium III. Brit. J. Plast. Surg. 4, 38-47.

BRODERSEN, P., SEJRSEN, P. and LASSEN, N.A. (1973) Diffusion bypass of Xenon in brain circulation. Circ. Res. 32, 363-369.

BURTON, A.C. (1972) Physiology and Biophysics of the Circulation. Year Book Medical Publishers, Chicago.

BUSCH, W. (1866) "Über den Einfluss welchen heftigere Erysipeln zuweilen auf organisierte Neubildungen ausüben. Verhand naturhist Ver Preuss. Rheinl. 23, 28-30.

CARSLAW, H.S. and JAEGER, J.C. (1959) Conduction of heat in solids. Clarendon Press, Oxford.

- CATER, D.B., SILVER, I.A. and WATKINSON, D.A. (1964) Combined therapy with 220 KV roentgen and 10 cm micro-wave heating in rat hepatoma. *Acta Radiol.* 2, 321-336.
- CAVALIERE, R., CIOCATTO, E.C., GIOVANELLA, B.C., HEIDELBERGER, C., JOHNSON, R.O., MARGOTTINI, M., MONDOVI, B., MORICCA, G. and ROSSI, F.A. (1967) Selective heat sensitivity of cancer cells. *Cancer* 20, 1351-1381.
- CHALLONER, A.V.J. (1972) Measurement of cutaneous blood flow by isotope clearance and thermal conductance methods. In: *Methods in Microcirculatory Studies*. Ed. Ryan, T.J. London, H. K. Lewis. pp. 43-50.
- CHALLONER, A.V.J. (1973) Ph.D. Thesis. CNAAL, London.
- CHAN, A.K., SIGELMANN, R.A., GUY, A.W. and LEHMANN, J.F. (1973) Calculation by the method of finite differences of the temperature distribution in layered tissues. *IEEE Trans. Biomed. Eng.* 20, 86-90.
- CHEN, M.M. and HOLMES, K.R. (1980) Microvascular contributions in tissue heat transfer. *Ann. N.Y. Acad. Sci.* 335, 137-150.
- CHIMOSKEY, J.E. (1972) Skin blood flow by ^{133}Xe disappearance validated by venous occlusion plethysmography. *J. Appl. Physiol.* 32, 432-435.

- COLEY, W.B. (1893) The treatment of malignant tumours by repeated inoculations of erysipelas with a report of ten original cases. *Amer. J. Med. Sci.* 105, 487-511.
- CONN, H.L. (1961) Equilibrium distribution of radioxenon in tissue: xenon-hemoglobin dissociation curve. *J. Appl. Physiol.* 16, 1065-1070.
- CONNOR, W.G., GERNER, E.W., MILLER, R.C. and BOONE, M.L.M. (1977) Prospects for hyperthermia in human cancer therapy. *Radiology* 123, 497-503.
- CONWAY, H., STARK, R.B. and JOSLIN, D. (1951) Cutaneous histamine reaction as a test of circulatory efficiency in tubed pedicles and flaps. *Surg. Gynec. Obstet.* 93, 185-190.
- COOK, H.F. (1952) A physical investigation of heat production in human tissues when exposed to microwaves. *Brit. J. Appl. Physics* 3, 1-6.
- CRC HANDBOOK OF CHEMISTRY AND PHYSICS Ed. WEAST, R.C. (1978) Chemical Rubber Publ. Co., Florida.
- CRANK, J. (1975) The mathematics of diffusion. Clarendon Press, Oxford.
- CRAVALHO, E.G., FOX, L.R., KAN, J.C. (1980) The application of the bioheat equation to the design of thermal protocols for local hyperthermia. *Ann. N.Y. Acad. Sci.* 335, 86-97.

- CRILE, G. (1963) The effects of heat and radiation on cancers implanted on the feet of mice. *Cancer Res.* 23, 372-380.
- CROFT, D.R. and LILLEY, D.G. (1977) Heat transfer calculations using finite difference equations. Applied Science Publ., London.
- DALY, M.J. and HENRY, R.E. (1980) Quantitative measurement of skin perfusion with Xenon-133. *J. Nucl. Med.* 21, 156-160.
- DAVIDSON, D., EGGLETON, P. and FOGGIE, P. (1952) The diffusion of atmospheric gases through fats and oils. *Quant. J. Exptl. Physiol.* 37, 91-105.
- DICKSON, J.A. (1975) Hazards and potentiators of hyperthermia. In: *Proc. Int. Symp. on Cancer Therapy by Hyperthermia and Radiation*. Baltimore, Amer. Coll. Radiol. Press. pp. 134-150.
- DICKSON, J.A. (1977) The effect of hyperthermia in animal tumor systems. *Recent Results Cancer Res.* 59, 43-111.
- DICKSON, J.A. (1979) Hyperthermia in the treatment of cancer. *The Lancet*, I, 202-205.
- DICKSON, J.A. and CALDERWOOD, S.K. (1980) Temperature range and selective sensitivity of tumours to hyperthermia: a critical review. *Ann. N.Y. Acad. Sci.* 335, 180-205.

- DILLMAN, L.T. (1970) Radionuclide decay schemes and nuclear parameters for use in radiation dose estimation. *J. Nucl. Med.* 11, Suppl. 4.
- DOSS, J.D. and McCABE, C.W. (1976) A technique for localised heating in tissue - An adjunct to tumor therapy. *Medical Instrum.* 10, 16-21.
- DOUGLAS, B. and BUCHHOLZ, R.R. (1943) The blood circulation in pedicle flaps. *Annals Surgery* 117, 692-709.
- DRAPER, J.W. and BOAG, J.W. (1971) Skin temperature distributions over veins and tumours. *Phys. Med. Biol.* 16, 645-654.
- DREW, T.B. (1931) Mathematical attacks on forced convection problems. *Trans. Am. Inst. Chem. Engrs.* 26, 26-35.
- ENDRICH, B., REINHOLD, H.S., GROSS, J.E. and INTAGLIETTA, M. (1979) Tissue perfusion inhomogeneity during early tumor growth in rats. *J. Natl. Cancer Inst.* 62, 387-395.
- EVANS, A.L., BUSUTTIL, A., GILLESPIE, F.C. and UNSWORTH, J. (1974) The rate of clearance of Xenon from rat liver sections in vitro and its significance in relation to intracellular diffusion rates. *Phys. Med. Biol.* 19, 303-316.

ESPAGNO, J. and LAZORTHEs, Y. (1965) Measurement of regional CBF in man by local injections of Xenon-133. In: Proc. Int. Symp. on Regional Cerebral Blood Flow. Eds. Ingvar, D.H. and Lassen, N.A. Copenhagen, Munksgaard, pp. 58-62.

FICK, A. (1855) Ueber Diffusion. Pogg. Ann. 94, 59.

FICK, A. (1870) Uber die Messung des Blutquartums in den Herzventrikeln. Verhandl d. phys. - med. Ges zu Wurzburg. 2, xvi. Quoted in full by Hoff, H.E. and Scott, H.J. (1948) New Eng. J. Med. 239, 122.

FIELD, S.B. and BLEEHEN, N.M. (1979) Hyperthermia in the treatment of cancer. Cancer Treatment Reviews 6, 63-94.

FOLKOW, B. and NEIL, E. (1971) Circulation. Oxford Univ. Press, London.

FOURIER, J.B. (1822) The Analytical Theory of Heat. Republished by A. Freeman, New York (1955).

FOX, M.J., KEYE, G.D. and MILLIKEN, J.C. (1972) A new non-intrusive technique for assessing digital blood flow. J. Irish Med. Assoc. 65, 410-411.

FRC - Federal Radiation Council (1960) Radiation protection guidance for federal agencies. Report No. 1. FRC, Washington DC.

- FREEMAN, L. and BLAUFOX, M.D. (1976) Blood flow. Seminars in Nucl. Med. 6, 141-216.
- GEDDES, L.A. and BAKER, L.E. (1967) The specific resistance of biological material. A compendium of data for the biomedical engineer and physiologist. Med. Biol. Eng. 5, 271-280.
- GILLESPIE, F.C. (1967) Some factors influencing the interpretation of regional blood flow measurements using inert gas clearance techniques. In: Blood Flow through Organs and Tissues. Eds. Bain, W.H. and Harper, A.M. Edinburgh, Livingstone. pp. 185-206.
- GLASS, H.I. and DE GARRETA, A.C. (1967) Quantitative analysis of exponential curve fitting for biological applications. Phys. Med. Biol. 12, 379-388.
- GLASS, H.I. and DE GARRETA, A.C. (1971) The quantitative limitations of exponential curve fitting. Phys. Med. Biol. 16, 119-130.
- GRABB, W.C. and SMITH, J.W. (Eds.) (1973) Plastic Surgery. Little, Brown & Co., Boston.
- GRAETZ, L. (1883) "Über die Wärmeleitfähigkeit von Flüssigkeiten. Ann. Phys. (N.F.) 18, 79-94.

GREESON, T.P., LEVAN, N.E., FREEDMAN, R.I. and WONG, W.H. (1973) Cortico-steroid induced vasoconstriction studied by Xenon-133 clearance. *J. Invest. Dermat.* 61, 242-244.

GUTHRIE, R.H., GOULIAN, D. and CUCIN, R.L. (1972) Predicting the extent of viability in flaps by measurement of gas tensions, using a mass spectrometer. *Plast. Reconst. Surg.* 50, 385-389.

GUY, A.W., LEHMANN, J. and STONEBRIDGE, J.B. (1974) Therapeutic applications of electromagnetic power. *Proc. IEEE* 62, 55-75.

HACKETT, M.E.J. (1974) The use of thermography in the assessment of depth of burn and blood supply of flaps. *Brit. J. Plast. Surg.* 27, 311-317.

HAGGENDAL, E., NILSSON, N.J. and NORBACK, B. (1965) On the components of Kr^{85} clearance curves from the brain of the dog. *Acta Physiol. Scand. Suppl.* 258, 5-26.

HAHN, E.W. and KIM, J.H. (1980) Clinical observations on the selective heating of cutaneous tumors with the radio-frequency inductive method. *Ann. N.Y. Acad. Sci.* 335, 347-351.

HALL, R.R., SCHADE, R.O.K. and SWINNEY, J. (1974) Effects of hyperthermia on bladder cancer. *Brit. Med. J.* 2, 593-594.

HAND, J.W., HUME, S.P., ROBINSON, J.E., MARIGOLD, J.C. and FIELD, S.B. (1979) A microwave heating system for improving temperature uniformity in heated tissue. *J. Microwave Power* 14, 145-149.

HANDEL, N., ZAREM, H.A. and GRAHAM, S.L. (1976) Computerised determination of blood flow in pedicle flaps by the clearance of epicutaneously applied ¹³³Xenon. *J. Surg. Res.* 20, 579-587.

HARDY, J.D., GAGGE, A.P. and STOLWIJK, J.A.J. (Eds.) (1970) *Physiological and Behavioural Temperature Regulation*. C. C. Thomas, Illinois.

HATFIELD, H.S. and PUGH, L.G.C. (1951) Thermal conductivity of human fat and muscle. *Nature*, 168, 918-919.

HENNESSY, T.R. (1971) Inert gas diffusion in heterogeneous tissue. *Bull. Math. Biophys.* 33, 235-257.

HENNESSY, T.R. (1974) The interaction of diffusion and perfusion in homogeneous tissue. *Bull. Math. Biophys.* 36, 505-526.

HENSON, P.W. (1972) A note on some aspects of skin contamination by certain radionuclides in common use. *Brit. J. Radiol.* 45, 938-942.

HENSON, P.W. (1973) Skin contamination: dose rates at a reduced depth of basal layer. *Brit. J. Radiol.* 46, 645-647.

HERTZMAN, A.B., RANDALL, W.C. and JOCHIM, K.E. (1946)
Estimation of cutaneous blood flow with the photoelectric
plethysmograph. Amer. J. Physiol. 145, 716-725.

HERTZMAN, A.B. (1961) Effects of heat on the cutaneous
blood flow. In: Advances in Biology of Skin. Eds.
Montagna, W. and Ellis, R.A. London, Pergamon Press.
pp. 117-122.

HILLS, B.A. (1967) Diffusion versus blood perfusion in
limiting the rate of uptake of inert non-polar gases by
skeletal rabbit muscle. Clin. Sci. 33, 67-87.

HMSO (1972) Code of Practice for the Protection of
Persons against Ionising Radiations arising from Medical
and Dental Use. HMSO, London.

HOEDT-RASMUSSEN, K., SVEINSDOTTIR, E. and LASSEN, N.A.
(1966) Regional cerebral blood flow in man determined
by intra-arterial injection of radioactive inert gas.
Circ. Res. 18, 237-247.

HOLBROOK, K.A. and ODLAND, G.F. (1974) Regional
differences in the thickness (cell layers) of the
human stratum corneum: an ultrastructural analysis.
J. Invest. Dermat. 62, 415-420.

HOLLENBERG, N.K. (1973) Renal disease. In: The
Microcirculation in Clinical Disease. Ed. Wells, R.
London, Academic Press. pp. 61-80.

HOLTI, G. (1955) Measurement of the vascular responses in skin at various time intervals after damage with histamine and U.V. radiation. *Clin. Sci.* 14, 143-153.

HUME, S.P., ROBINSON, J.E. and HAND, J.W. (1979) The influence of blood flow on temperature distribution in the exteriorised mouse intestine during treatment by hyperthermia. *Brit. J. Radiol.* 52, 219-222.

HYNES, W. (1948) A simple method of estimating blood flow with special reference to the circulation in pedicled skin flaps and tubes. *Brit. J. Plast. Surg.* 1, 159-171.

ICRP - International Commission on Radiological Protection (1966) Recommendations of the ICRP. Publication 9. Pergamon Press, Oxford.

ICRP - International Commission on Radiological Protection (1969) Radiosensitivity and Spatial Distribution of Dose. Publication 14. Pergamon Press, Oxford.

ICRP - International Commission on Radiological Protection (1971) Protection of the Patient in Radionuclide Investigations. Publication 17. Pergamon Press, Oxford.

JAIN, R.K. and WEI, J. (1977) Dynamics of drug transport in solid tumors distributed parameter model. *J. Bioeng.* 1, 313-330.

JAKOB, M. (1959) Heat Transfer. Chapman and Hall, London.

JANIAK, M. and SZMIGIELSKI, S. (1978) Membrane injury in cells exposed in vitro to microwave and water-bath hyperthermia. In: Cancer Therapy by Hyperthermia and Radiation. Ed. Streffer, C. Baltimore USA, Urban and Schwarzenberg.

JONES, H.B. (1950) Nitrogen elimination in the respiratory system. In: Medical Physics. Ed. Glasser, O. Chicago, Year Book Publishers. 2, 855-871.

JOST, W. (1960) Diffusion in Solids, Liquids and Gases. Academic Press, New York.

KETY, S.S. (1948) Measurement of regional circulation by the local clearance of radioactive sodium. Am. J. Med. Sci. 215, 352-362.

KETY, S.S. (1951) The theory and applications of the exchange of inert gas at the lungs and tissues. Pharm. Rev. 3, 1-41.

KIM, J.H. and HAHN, E.W. (1979) Clinical and biological studies of localised hyperthermia. Cancer Res. 39, 2258-2261.

KLIGMAN, A.M. (1965) In: Skin Bacteria and Their Role in Infection. Ed. Maibach, H.I. and Hildick-Smith, H. New York, McGraw-Hill. p. 296.

KLINGER, H.G. (1974) Heat transfer in perfused biological tissue. 1. General theory. Bull. Math. Biol. 36, 403-415.

KOSTUIK, J.P., WOOD, D., HORNBY, R., FEINGOLD, S. and MATHEWS, V. (1976) The measurement of skin blood flow in peripheral vascular disease by epicutaneous application of ^{133}Xe . J. Bone Joint Surg. 58, 833-837.

KRISTENSEN, J.K. and WADSKOV, S. (1977) Studies of ^{133}Xe washout from human skin: quantitative measurements of blood flow in normal and corticosteroid treated skin. J. Invest. Dermat. 68, 196-200.

KROGH, A. (1919) The supply of oxygen to the tissues and the regulation of the capillary circulation. J. Physiol. 52, 457-474.

LADEFOGED, J. (1964) The significance of recirculation for the determination of intrarenal blood flow distribution with Kr-85 and Xe-133. Scand. J. Clin. Lab. Invest. 16, 479-480.

LADEFOGED, J. and ANDERSON, A.M. (1967) Solubility of Xenon-133 at 37°C in water, saline, olive oil, liquid paraffin, solutions of albumin, and blood. Phys. Med. Biol. 12, 353-358.

LARSEN, O.A. and LASSEN, N.A. (1967) Fatty tissue blood flow measured by Xenon-133 clearance. Scand. J. Clin. Lab. Invest. Suppl. 99, 46-49.

LASSEN, N.A. (1964) Muscle blood flow in normal man and in patients with intermittent claudication evaluated by simultaneous Xe-133 and Na-24 clearances. J. Clin. Invest. 43, 1805-1812.

LASSEN, N.A., LINBJERG, F. and DAHN, I. (1965) Validity of the ^{133}Xe method for measurement of muscle blood flow by simultaneous venous occlusion plethysmography. Circ. Res. 16, 287-293.

LEROY, E.C., DOWNEY, J.A. and CANNON, P.J. (1971) Skin capillary blood flow in scleroderma. J. Clin. Invest. 50, 930-939.

LEHMANN, J.F., DeLATEUR, B.J., and STONEBRIDGE, J.B. (1969) Selective muscle heating by shortwave diathermy with a helical coil. Arch. Phys. Med. 50, 117-132.

LeVEEN, H.H., WAPNICK, S., PICCONE, V. et al (1976) Tumour eradication by radiofrequency therapy. J.A.M.A. 235, 2198-2200.

LIN, S.H. (1972) Analytical solutions for transient thermal behaviour of biological systems. Bull. Math. Biophys. 34, 413-418.

LINDBJERG, I.F. (1965) Measurement of muscle blood flow with Xe-133 after histamine injection as a diagnostic method in peripheral arterial disease. Scand. J. Clin. Lab. Invest. 17, 371-380.

- LOEVINGER, R., JAPHA, E.H. and BROWNELL, G.L. (1956) Discrete radioisotope sources. In: Radiation dosimetry. Eds. Hine, G.J. and Brownell, G.L. New York, Academic Press. p. 693.
- LUIKOV, A.V. (1968) Analytical heat diffusion theory. Academic Press, New York.
- MANTYLA, M., KUIKKAM J. and REKONEN, A. (1976) Regional blood flow in human tumors with special reference to the effect of radiotherapy. Br. J. Radio. 49, 335-338.
- MANTYLA, M.J. (1979) Regional blood flow in human tumours. Cancer Res. 39, 2304-2306.
- MAPLESON, W.W. (1963) An electric analogue for uptake and exchange of inert gases and other agents. J. Appl. Physiol. 18, 197-206.
- MARMOR, J.B., HAHN, N. and HAHN, G.M. (1977) Tumor core and cell survival after localised radiofrequency heating. Cancer Res. 37, 879-883.
- MARTINSSON, A. (1967) On the composition of human adipose tissue. Acta Med. Scand. 182, 795-803.
- MAYERSON, H.S. (1963) The physiologic importance of lymph. In: Handbook of Physiology, Section 2: Circulation Vol. II. Section Editor Hamilton, W.F. Washington, Americal Physiological Society. p. 1042.

MELLANDER, S. and JOHANSSON, B. (1968) Control of resistance, exchange and capacitive functions in the peripheral circulation. *Pharmacol. Rev.* 20, 117-196.

MENDECKI, J., FRIEDENTHAL and BOTSTEIN, C. (1978) Microwave induced hyperthermia in cancer treatment: apparatus and preliminary results. *Int. J. Radiat. Oncol. Biol. Phys.* 4, 1095-1103.

MINARD, D. (1970) Body heat content. In: *Physiological and Behavioral Temperature Regulation*. Eds. Hardy, J.D., Gagge, M.P. and Stolwijk, J.A.J. Illinois, C. C. Thomas. pp. 345-357.

MITCHELL, J.W., GALVEZ, T.L., HENGLE, J., MYERS, G.E. and SIEBECKER, K.L. (1970) Thermal response of human legs during cooling. *J. Appl. Physiol.* 29, 859-865.

MONDOVI, B., STROM, R. and ROTILIO, G. (1969a) The biochemical mechanism of selective heat sensitivity of cancer cells. I. Studies on cellular respiration. *Eur. J. Cancer* 5, 129-136.

MONDOVI, B., FINAZZI, A.A., ROTILIO, G. et al (1969b) The biochemical mechanism of selective heat sensitivity of cancer cells. II. Studies on nucleic acids and protein synthesis. *Eur. J. Cancer* 5, 137-146.

MOORE, W.S. (1973) Determination of amputation level. *Arch. Surg.* 107, 798-802.

MORALES, M.F. and SMITH, R.E. (1948) On the theory of blood-tissue exchange of inert gases. VI - Validity of approximate uptake expressions. *Bull. Math. Biophys.* 10, 191-200.

MORIMOTO, T. (1978) Variations of sweating activity due to sex, age and race. In: *The Physiology and Pathophysiology of the Skin*. Ed. Jarrett, A. London, Acad. Press. pp. 1655-1666.

McGREGOR, I.A. (1970) *Fundamental Techniques of Plastic Surgery*. Churchill Livingstone, Edinburgh.

McGREGOR, I.A. and MORGAN, G. (1973) Axial and random pattern flaps. *Brit. J. Plast. Surg.* 26, 202-213.

McLURE, W.B. and ALDRICH, C.A. (1923) Time required for disappearance of intradermally injected salt solution. *J.A.M.A.* 81, 293-298.

NCRP - National Committee on Radiation Protection and Measurements (1960) *Radiology* 75, 122-126.

NEVINS, R.G. and DARWISH, M.A. (1970) Heat transfer through subcutaneous tissue as heat generating porous material. In: *Physiological and Behavioral Temperature Regulation*. Eds. Hardy, J.D., Gagge, M.P. and Stolwijk, J.A.J. Illinois, C. C. Thomas. pp. 281-301.

NEWBURGH, L.H. (1968) *Physiology of heat regulation and the science of clothing*. Hafner Publishing Co., New York. p. 120.

- NIELSEN, S.L. (1972) Measurement of blood flow in adipose tissue from the washout of ^{133}Xe after atraumatic labelling. *Acta Physiol. Scand.* 84 187-193.
- NIELSEN, S.L. (1973) Relationship of subcutaneous adipose tissue blood flow to thickness of subcutaneous tissue and total body fat mass. *Scand. J. Clin. Lab. Invest.* 31, 383-388.
- NILSSON, N.J. (1965) Observations on the clearance rate of β radiation from Kr-85 dissolved in saline and injected in microliter amounts into the grey and white matter of the brain. In: *Proc. Int. Symp. on RCBF*. Eds. Ingvar, D.H. and Lassen, N.A. Copenhagen, Munksgaard. p . 53-57.
- NUSSELT, W. (1910) Die Abhängigkeit der Wärmeübergangszahl von der Rohrlänge. *Zeitschrift VDI* 54, 1154-1158.
- NYFORS, A. and ROTHENBORG, H.W. (1970) Cutaneous blood flow in psoriasis measured by $^{133}\text{Xenon}$ clearance. *J. Invest. Dermat.* 54, 381-385.
- OLESEN, J., PAULSON, O.B. and LASSEN, N.A. (1971) Regional cerebral blood flow in man determined by the initial slope of the clearance of intra-arterially injected ^{133}Xe . *Stroke* 2, 519-540.
- OSBURN, J.O., STITZELL, J.A. and PETERSON, R.E. (1969) Diffusion of argon, krypton and xenon in olive oil. *J. Appl. Physiol.* 27, 624-629.

OVERGAARD, K. and OVERGAARD, J. (1972) Investigations on the possibility of a thermic tumor therapy.

Europ. J. Cancer 8, 65-78.

OVERGAARD, K. and OVERGAARD, J. (1977) Hyperthermia tumor-cell devitalisation in vivo. Acta Radiologica Therapy Physics Biol. 16, 1-16.

PAULSON, O.B., CRONQVIST, S. and RISBERG, J. (1969) Regional cerebral blood flow: comparison of 8 detector and 16 detector instrumentation. J. Nucl. Med. 10, 164-173.

PENNES, H.H. (1948) Analysis of tissue and arterial blood temperatures in the resting human forearm. J. Appl. Physiol. 1, 93-122.

PERL, W. (1960) A method for curve-fitting by exponential functions. Int. J. Appl. Rad. Isotop. 8, 211-222.

PERL, W. (1962) Heat and matter distribution in body tissues and the determination of tissue blood flow by local clearance methods. J. Theoret. Biol. 2, 201-235.

PERL, W., RACKOW, H., SALANITRE, E., WOLF, G.L. and EPSTEIN, R.M. (1965) Intertissue diffusion effect for inert fat soluble gases. J. Appl. Physiol. 20, 621-627.

PETTIGREW, R.T., GALT, J.M., LUDGATE, C.M. and SMITH, A.N. (1974) Clinical effects of whole body hyperthermia in advanced malignancy. Br. Med. J. 4, 679-682.

PRATHER, A., BLACKBURN, J.P., WILLIAMS, T.R. and LYNN, J.A. (1979) Evaluation of tests for predicting the viability of axial pattern skin flaps in the pig. *Plast. Reconst. Surg.* 63, 250-262.

PRIEBE, L. (1970) Heat transfer and specific blood flow in homogeneously and isotropically perfused tissue. In: *Physiological and Behavioural Temperature Regulation*. Eds. Hardy, J.D., Gagge, M.P. and Stolwijk, J.A.J. Illinois, C. C. Thomas. pp. 272-280.

RAYMOND, U., NOELL, K.T., WOODWARD, K.T. and WORDE, B.T. (1980) Microwave induced local hyperthermia in combination with radiotherapy of human malignant tumours. *Cancer* 45, 638-646.

REINERSTON, R.P. and WHEATLEY, V.R. (1959) Studies on the chemical composition of human epidermal lipids. *J. Invest. Dermat.* 32, 49-60.

REINISCH, J.F. (1974) The pathophysiology of skin flap circulation. *Plast. Reconst. Surg.* 54, 585-598.

RENKIN, E.M. (1952) Capillary permeability to lipid soluble molecules. *Am. J. Physiol.* 168, 538-545.

RENKIN, E.M. (1964) Transport of large molecules across capillary walls. *Physiologist*, 7, 13-28.

RIGGS, D.S. (1963) *The mathematical approach to physiological problems*. Williams and Wilkins, Baltimore.

ROBINSON, J.E., WIZENBERG, M.J. and McCREADY, W.A. (1974)
Radiation and hyperthermal response of normal tissue in
situ. *Radiology* 113, 195-198.

ROBINSON, J.E., HARRISON, G.H., McCREADY, W.A. and
SAMARAS, G.M. (1978) Good thermal dosimetry is essential
to good hyperthermia research. *Brit. J. Radiol.* 51,
532-534.

ROOK, A., WILKINSON, D.S. and EBLING, F.J. (1972)
Textbook of Dermatology Vol. I. Blackwell Scientific
Publications, Oxford.

RYAN, T.J. (1973) Structure, pattern and shape of the
blood vessels of the skin. In: *The Physiology and
Pathophysiology of the Skin*. Ed. Jarrett, A. London,
Academic Press. pp. 577-601.

RYAN, T.J. (1976) The blood vessels of the skin.
J. Invest. Dermat. 67, 110-118.

SCHEUPLEIN, R.J. and BLANK, I.H. (1971) Permeability
of the skin. *Physiol. Rev.* 51, 702-747.

SCHEUPLEIN, R. (1978) The skin as a barrier.
In: *The Physiology and Pathophysiology of the Skin*.
Ed. Jarrett, A. London, Academic Press. pp. 1669-1752.

SCHMIDT-NIELSEN, K. and TAYLOR, E. (1952) Use of a
quartz fiber microbalance for histochemical investigations
of the skin. *J. Invest. Dermat.* 19, 157-163.

SCHWAN, H.P. (1967) Absorption and energy transfer of microwaves and ultrasound in tissues. *Med. Phys.* 3, 1-7.

SEJRSEN, P. (1966) Cutaneous blood flow in man studied by freely diffusible radioactive indicators. *Scand. J. Clin. Lab. Invest. Suppl.* 99, 52-59.

SEJRSEN, P. (1967) Diffusion processes invalidating the intra-arterial ^{85}Kr beta-particle clearance method for measurement of skin blood flow in man. *Circ. Res.* 21, 281-295.

SEJRSEN, P. (1968) Epidermal diffusion barrier to ^{133}Xe in man and studies of clearance of ^{133}Xe by sweat. *J. Appl. Physiol.* 24, 211-216.

SEJRSEN, P. (1969) Blood flow in cutaneous tissue in man studied by washout of radioactive Xenon. *Circ. Res.* 25, 215-229.

SEJRSEN, P. (1970) Convection and diffusion of inert gases in cutaneous, subcutaneous and skeletal muscle tissue. In: *Capillary Permeability*. Eds. Crone, C. and Lassen, N.A. Copenhagen, Munksgaard. pp. 586-604.

SEJRSEN, P. (1971) Measurement of cutaneous blood flow by freely diffusible radioactive isotopes. *Dan. Med. Bull.* 18 (Suppl.)3, 9-38.

SEJRSEN, P. and TONNESSEN, K.H. (1968) Concentration profiles for gas diffusion in skeletal muscle in vitro and in vivo. *Acta Physiol. Scand.* 22A, 74.

- SEJRSEN, P. and TONNESSEN, K.H. (1972) Shunting by diffusion of inert gas in skeletal muscle. *Acta Physiol. Scand.* 86, 82-91.
- SHEPHERD, J.T. and WEBB-PEPLOE, M.M. (1970) Cardiac output and blood flow distribution during work in heat. In: *Physiological and behavioral temperature regulation*. Eds. Hardy, J.D., Gagge, A.P. and Stolwijk, J.A.J. Illinois, C. C. Thomas. Ch. 18.
- SHITZER, A. and KLEINER, M.K. (1976) Thermal behaviour of biological tissues - A general analysis. *Bull. Math. Biol.* 38, 369-386.
- SONG, C.W., KANG, M.S., RHEE, J.G. and LEVITT, S.H. (1980) The effect of hyperthermia on vascular function, pH and cell survival. *Radiology* 137, 795-803.
- SOUTHWOOD, W.F.W. (1955) The thickness of the skin. *Plast. Reconst. Surg.* 15, 423-430.
- SPECTOR, W.S. (Ed.) (1956) Vertebrate tissues and organs: chemical composition. In: *Handbook of Biological Data*. Philadelphia, Saunders. p. 70.
- STEHLIN, J.S., GIOVANELLA, B.C., De IPOLYI, P.D., MUENZ, L.R., ANDERSON, R.F. and GUTIERREL, A.A. (1975) Results of hyperthermia perfusion for melanoma of the extremities. *Surg. Gynecol. Obstet.* 140, 338-348.

STEWART, A., ALLOTT, P.R., COWLES, A.L. and MAPLESON, W.W. (1973) Solubility coefficients for inhaled anaesthetics for water, oil and biological media. *Brit. J. Anaesth.* 45, 282-293. /

STORM, F.K., HARRISON, W.H., ELLIOTT, R.S. and MORTON, D.L. (1980) Hyperthermia therapy for human neoplasms. *Cancer* 46, 1849-1854.

STOSSEK, K. (1970) Hydrogen exchange through the pial vessel wall and its meaning for the determination of the local cerebral blood flow. *Pfleugers. Arch.* 320, 111-119.

STRANC, W.E., FOX, R.H. and MUIR, I.F.K. (1971) The blood flow in tubed pedicles. *Brit. J. Plast. Surg.* 26, 10-14.

STRANG, R. (1977) The determination of the diffusion coefficient of Krypton in rabbit ocular tissue. *Invest. Ophthalmol.* 16, 183-186.

STRANG, R., HORTON, P.W. and GILLESPIE, F.C. (1979) Theoretical basis of the measurement of choroidal blood flow using a radioactive inert gas clearance method. *Phys. Med. Biol.* 24, 964-970.

STRAW, J.A., HART, M.M., KLUBES, P., ZAHARKO, D.S. and DEDRICK, R.L. (1974) Distribution of anticancer agents in spontaneous animal tumors. I. Regional blood flow and methotrexate distribution in canine lymphosarcoma. *J. Natl. Cancer Inst.* 52, 1327-1331.

STREFFER, C., VAN BEUNINGEN, D., DIETZEL, F. et al (1978)
Cancer therapy by Hyperthermia and Radiation. Proc. of
2nd Int. Symp. 1977, Essen, Germany. Urban and
Schwarzenberg, Baltimore.

TAUBENFLIGEL, W., WAJDA, Z. and LEWINSKY, A. (1965)
Determination of the condition of vascularisation of
pedicle skin grafts by the thermoelement. Acta Chir.
Plast. 7, 236-240.

TAUXE, W.N., SIMONS, J.N., LIPSCOMB, P.R. and HAMAMOTO,
K. (1970) Determination of vascular status of pedicle
skin flaps by use of radioactive pertechnetate (^{99m}Tc).
Surg. Gynec. Obstet. 130, 87-93.

TAYLOR, L., BENNETT, R., SHERRIFF, S. (1979) The blood
supply of colorectal liver metastasis. Br. J. Cancer
39, 749-756.

TEICH-ALASIA, S. (1971) A study of vascularisation of
pedicle flaps using disulphine blue. Brit. J. Plast.
Surg. 24, 282-288.

TEORELL, T. (1937) Kinetics of distribution of
substances administered to the body. Arch. internat. de
Pharmacodyn et de therap. 57, 205-240.

TEORELL, L.M. and NILSSON, S.K. (1978) Temperature
gradients in low flow vessels. Phys. Med. Biol. 23,
106-117.

TER HAAR, G. (1979) Temperature distributions obtainable in tissue as a result of ultrasonic irradiation.

Presented at: European Group of Hyperthermia in Radiation Oncology, Cambridge.

TREGGAR, R.T. (1966) Physical Functions of Skin.

London, Academic Press. pp. 1-52.

TRAP-JENSEN, J., ALPERT, J.S., GARCIA DEL-RIO, H. and

LASSEN, N.A. (1967) Capillary diffusion capacity for sodium in skeletal muscle in long term juvenile diabetes mellitus. Acta Med. Scand. Suppl. 476, 135-146.

TSUCHIDA, Y. and TSUYA, A. (1978) Skin blood flow - ^{133}Xe injection. Plast. Reconst. Surg. 62, 763-770.

UNSWORTH, J. and GILLESPIE, F.C. (1971) Diffusion coefficients of Xenon and Krypton in water from 0°C to 80°C and in biological tissues at 37°C . In: Diffusion Processes. London, Gordon and Breach. p.75.

VAN MASTRIGT, R. (1977) Constant step approximation of multi-exponential signals using a least squares criterion. Comput. Biol. Med. 7, 231-247.

VEALL, N. and MALLETT, B.L. (1965) The partition of trace amounts of xenon between human blood and brain tissues at 37°C . Phys. Med. Biol. 10, 375-380.

VEALL, N. (1968) In: Blood Flow through Organs and Tissues. Eds. Bain, W. and Harper, A.M. Edinburgh, Livingstone. p. 369..

WESTERMARK, N. (1927) Effect of heat upon rat tumours. Skandin. Arch. f. Physiol. 52, 257-263.

WESTRA, A. and DEWEY, W.C. (1971) Variation in sensitivity to heat shock during the cell cycle of chinese hamster cells in vitro. Int. J. Radiot. Biol. 19, 467-477.

WHITMORE, R.L. (1968) Rheology of the circulation. Pergamon Press, London.

WHITTON, J.T. and EVERALL, J.D. (1972) Epidermal and dermal thickness. Brit. J. Radiol. 45, 611-612.

WOODCOCK, J. (Ed.) (1976) Clinical Blood Flow Measurement. Sector Publ. Ltd., London.

YANG, W.J. and WANG, J.H. (1979) Shortwave and microwave diathermy for deep tissue heating. Med. Biol. Eng. and Comput. 17, 518-523.

YERUSHALMI, A. (1975) Cure of a solid tumour by simultaneous administration of microwaves and X-ray irradiation. Radiation Res. 64, 602-610.

YEH, S.Y. and PETERSON, R.E. (1963) Solubility of carbon dioxide, krypton and xenon in lipids. J. Pharm. Sci. 52, 452-458.

YEH, S.H. and PETERSON, R.E. (1965) Solubility of krypton and xenon in blood, protein solutions, and tissue homogenates. J. Appl. Physiol. 20, 1041-1047.

ZIERLER, K.L. (1965) Equations for measuring blood flow by external monitoring of radioisotopes. *Circ. Res.* 16, 309-321.

APPENDIX ACALCULATION OF THE RADIATION DOSE IN THE USE OF ^{133}Xe A.1 Epicutaneous diffusion technique

With this technique the dose arises mainly from the ^{133}Xe sitting on the surface of the skin during the initial diffusion period. Figure A1 is a model of the system with the ^{133}Xe uniformly distributed in a depot of unit density material (saline) sitting on the surface of the skin, represented in a similar way. The depot is a disc of diameter b cm and thickness h cm.

The dose is calculated from the equations given by Loevinger et al (1956), which are basically empirical, but also show good agreement with the results of Henson (1972) who used the theoretical data of Berger (1971).

Firstly the dose in Gy/hour at a distance y from an infinite plane slab of infinite thickness is given by

$$D(y, \infty) = 0.005 D_{\beta} \alpha \left[c^2 \left\{ 3 - \exp(1 - \nu y/c) - \nu y/c (2 + \ln c/2y) \right\} + \exp(1 - \nu y) \right] \quad \text{A.1}$$

where the term $\left\{ \right\} = 0$ for $y \geq \frac{c}{\nu} = 0.021 \text{ g cm}^{-2}$ for ^{133}Xe

D_{β} is the β^{-} particle dose in Gy/hour in the interior of a large source with the same concentration of radioactivity as the slab and is given by

$$D_{\beta} = 0.57 \bar{E}_{\beta} \tau$$

where \bar{E}_{β} is the average energy of the β^{-} particles and

τ is the concentration of the source in MBq g^{-1} .

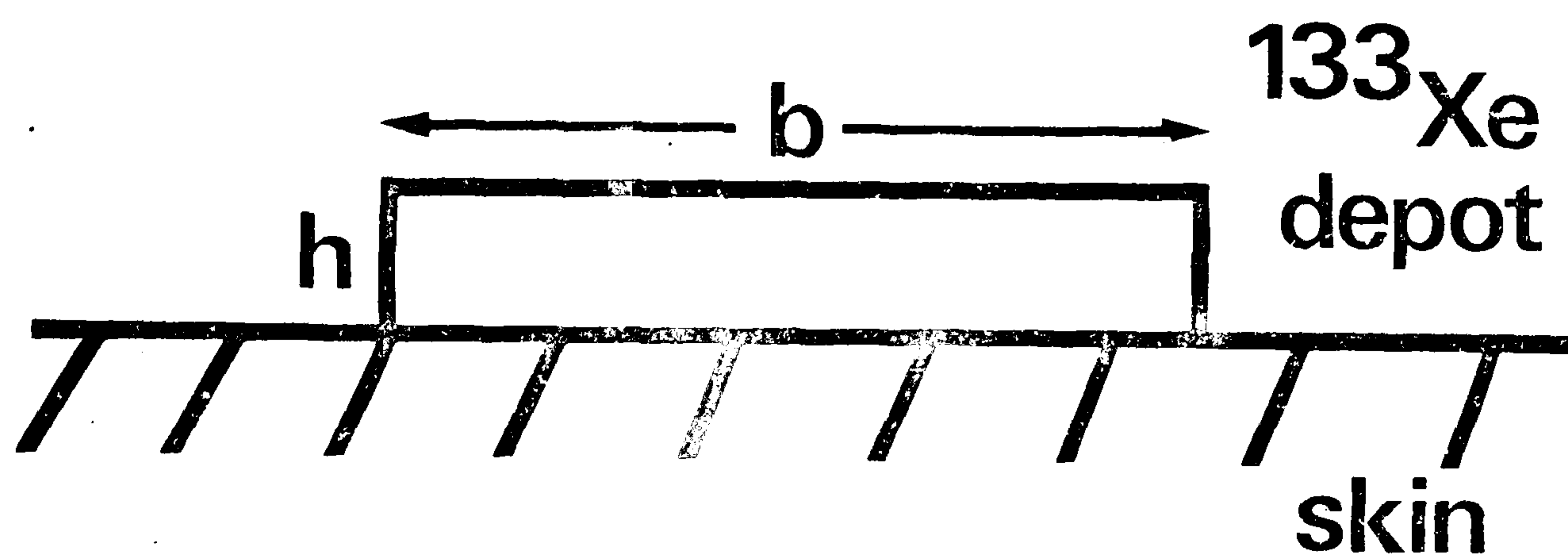


Figure A.1 Model of the chamber on the surface of the skin producing a disc-shaped depot of ¹³³Xe of diameter b and thickness h.

c is an empirically determined constant which depends on the energy of the β^- particles. For ^{133}Xe $c = 2$.

$$\alpha = \left(3c^2 - (c^2 - 1) e \right)^{-1} = 0.260 \text{ for } ^{133}\text{Xe}$$

ν is again energy dependent and is known as the apparent mass absorption coefficient.

$$= \frac{18.6}{(E_0 - 0.036)1.37} \text{ for tissue} \quad \nu = 95.5 \text{ cm}^2/\text{g for } ^{133}\text{Xe}$$

E_0 is the maximum energy of the β^- particles.

y is the distance from the slab in g/cm^2 .

νy is thus a dimensionless quantity.

Now to find the dose from an infinite slab of thickness h , the following is used

$$D(y, h) = D(y, \infty) - D(y + h, \infty) \quad \text{A2}$$

In the situation being considered here the source is a circular disc of finite diameter and thickness. However, Loevinger et al (1956) have shown that if the diameter of the disc is greater than $\frac{5}{\nu}$ ($= 0.052 \text{ cm}$ for ^{133}Xe) then the disc can be approximated by an infinite plane.

Thus equation A2 is used to calculate the dose at a distance y from a depot of thickness h .

The average energy of β^- particles emitted by ^{133}Xe is 0.1006 MeV (Dillman, 1970). However, conversion electrons are also emitted, the most common one being of 0.045 MeV. As an approximation to their effect Loevinger et al (1956) suggest adding

$$\frac{E_{\gamma} \alpha_K}{1 + \alpha_K} \text{ to the } \beta^- \text{ particle energy}$$

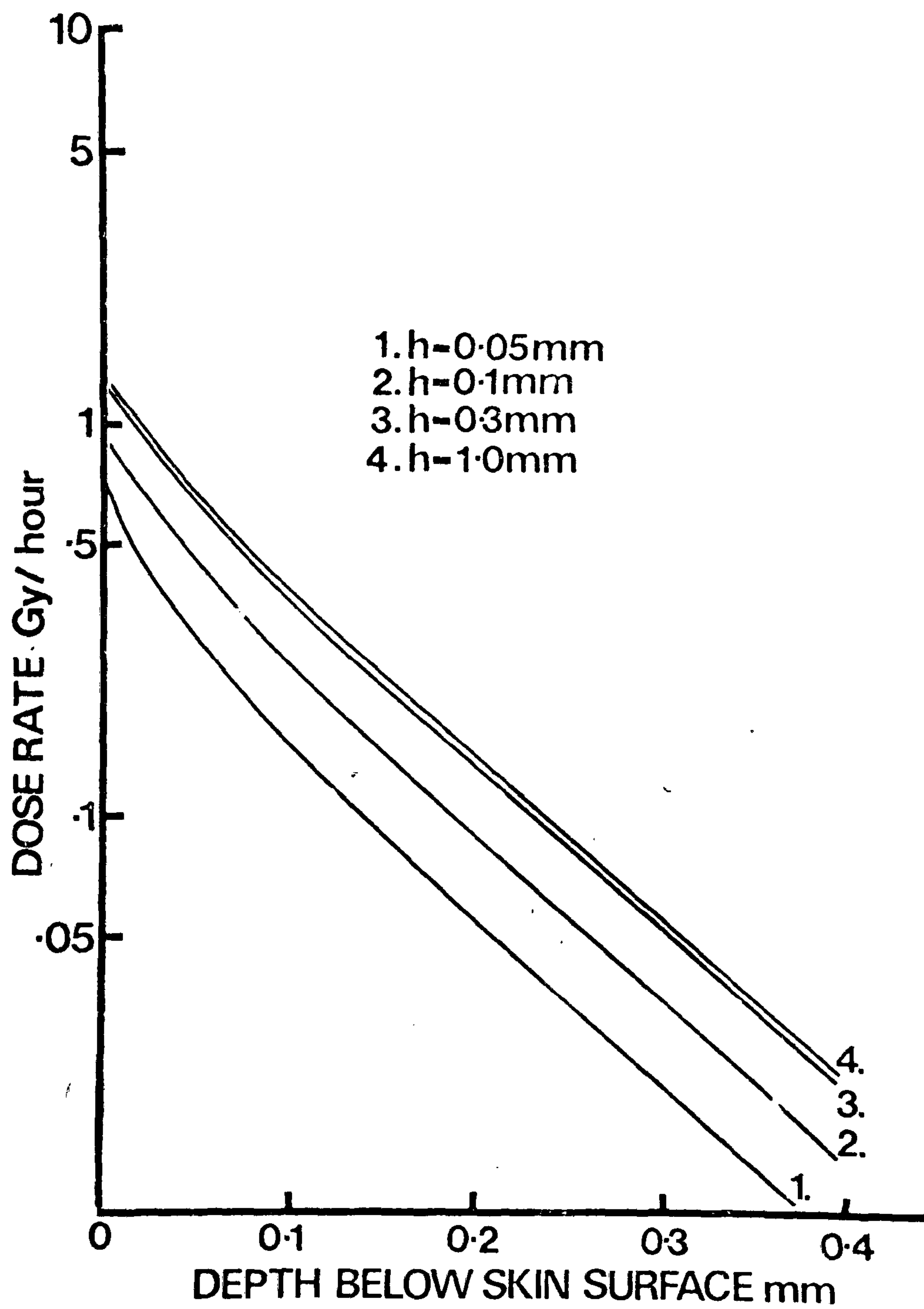


Figure A.2 Variation of dose rate with depth below skin surface for a ^{133}Xe depot of activity 40 MBq g^{-1} and various thicknesses h mm.

where E_γ is the energy of the γ rays giving rise to the conversion electrons, and α_K is the γ ray conversion coefficient.

Thus, in the equations, for ^{133}Xe

$$\begin{aligned}\bar{E}_\beta &= 0.1006 + \frac{0.081 \times 0.64}{1.64} \\ &= \underline{0.131 \text{ MeV}}\end{aligned}$$

The dose rate at a depth y mm from the base of the depot for a ^{133}Xe concentration of 40 MBq g^{-1} has been calculated and is given for several values of h in Figure A2.

A.2 Calculation of the radiation dose - injection technique

The dose in this case is calculated from an equation given by Loevinger et al (1956b)

$$R = 0.0135 C_0 E_\beta T_{\text{eff}} \text{ (Gy)}$$

where R = total absorbed dose to the tissue ^{in Gy} for complete removal of the radionuclide

C_0 = activity concentration in the tissue in MBq g^{-1}

E_β = mean β^- particle energy in MeV

T_{eff} = effective half-life of the ^{133}Xe in the tissue in minutes.

The above equation is for an infinite medium containing a uniform distribution of ^{133}Xe and for an injected depot the dose will be

$$R = \frac{0.0135}{2} C E_\beta T_{\text{eff}} \text{ Gy} \quad (\text{Barron et al, 1951})$$

where C is now the concentration of the injected solution.

T_{eff} is, of course, dependent on the blood flow within the tissue and will be infinite, (ignoring diffusion processes) for zero blood flow. Figure A3 shows the dose plotted against T_{eff} for different concentrations of injected solution.

Although the ^{133}Xe is removed from the tissue mainly by the blood flow it is also dispersed at a very slow rate by diffusion down into the subcutaneous tissue. The effect of this is to reduce the dose, particularly at high values of T_{eff} . This is shown in Figure A3 by the broken line, which was calculated using the finite difference diffusion model of skin described in Chapter 5.

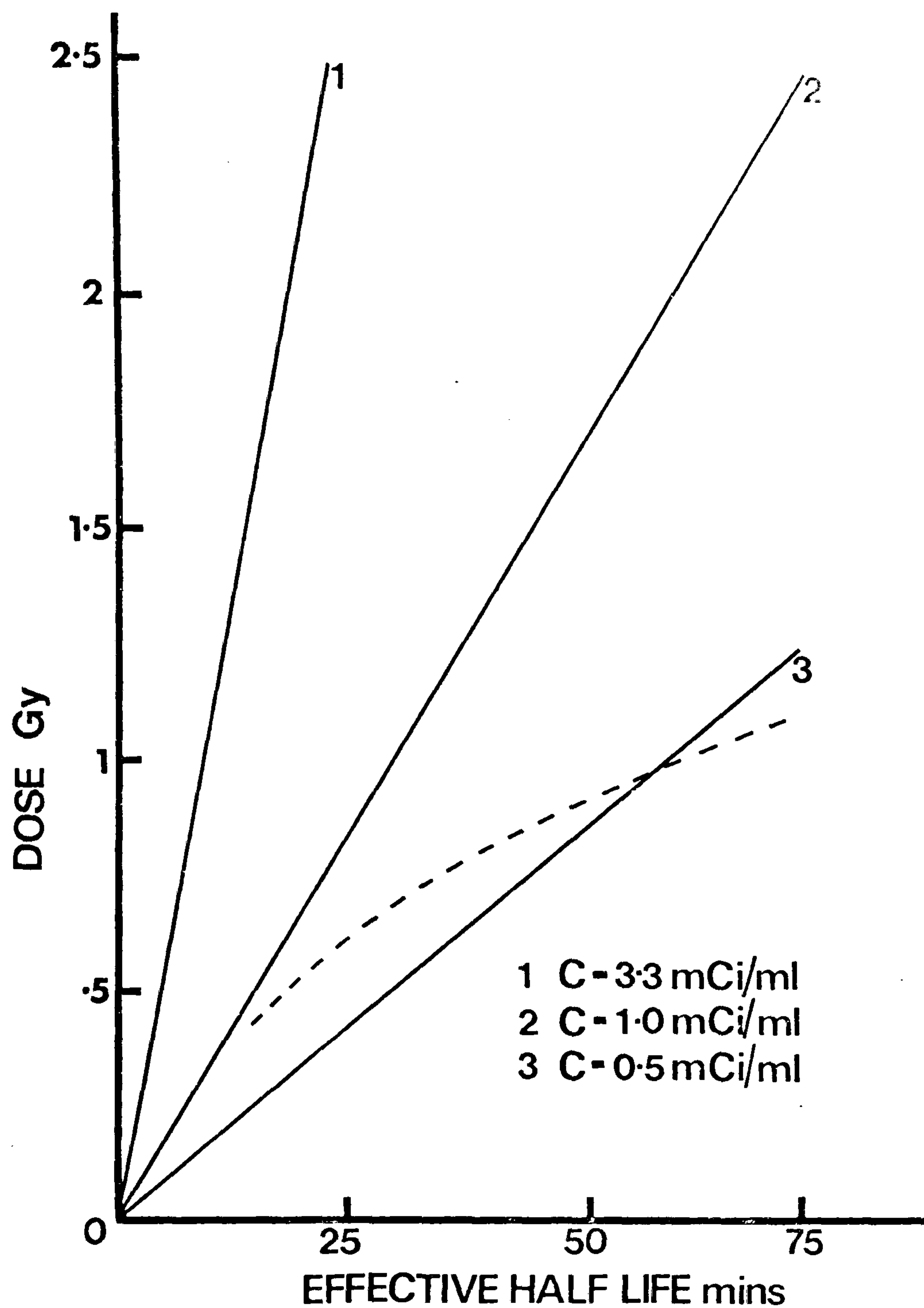


Figure A.3 Variation of dose with effective half-life of injected depot of ^{133}Xe of various concentrations $C \text{ MBq g}^{-1}$. Broken line shows the effect of diffusion of the ^{133}Xe on the dose for a concentration of 40 MBq g^{-1} .
 Concentrations 1 - 120 MBq g^{-1}
 2 - 40 MBq g^{-1}
 3 - 20 MBq g^{-1}

APPENDIX BPROGRAM TO FIT CLEARANCE CURVE WITH DOUBLE
EXPONENTIAL FUNCTION

```

0001      COMMON U(30,6),C(6),K,N,PHI,B(4),G,D(3),IRMAX
          1,K1,V(4)
C      ***** INPUT DATA *****
          *** V(1)V(2) - INITIAL ESTIMATES OF EXPONENTS ***
          *** D(1)D(2) - MIN EXPONENT STEP IN ITERATION ***
          *** IRMAX - MAX NO OF ITERATIONS ***
          *** G - DEFINES MAX STEP SIZE ***
0002      TYPE *, 'V(1),V(2)?'
0003      ACCEPT *,V(1),V(2)
0004      TYPE *, 'D(1),D(2)?'
0005      ACCEPT *,D(1),D(2)
0006      G=8
0007      IRMAX=100
0008      N=2
0009      ACCEPT *,N
0010      DO 6 J=1,6
0011      DO 6 I=1,N
0012      6 U(I,J)=0.
0013      TYPE *, 'INPUT T VALUES'
0014      DO 1 I=1,N
0015      1 ACCEPT *,U(I,6)
0016      TYPE *, 'INPUT Y VALUES'
0017      DO 2 I=1,N
0018      2 ACCEPT *,U(I,5)
0019      K=2
0020      K1=K+1
0021      CALL STEP
0022      TYPE *, 'CONSTANTS CC(1),C(2)='
0023      TYPE *,C(1),C(2)
0024      WRITE (7,3) B(1),B(2)
0025      3 FORMAT (5H B1= ,F8.4,/,5H B2= ,F8.4,/,)
0026      WRITE (7,4) PHI
0027      4 FORMAT (6H PHI= ,E14.6,/,)
0028      WRITE (7,5) (U(I,4),I=1,N)
0029      5 FORMAT (30(E14.6,/,))
0030      STOP
0031      END

          *** SUBROUTINE STEP - DETERMINES THE DIRECTION
          AND SIZE OF THE NEXT STEP IN THE ITERATION ***
0032      SUBROUTINE STEP
0034      COMMON U(30,6),C(6),K,N,PHI,B(4),G,D(3),IRMAX,K1,
          1V(4)
0035      DIMENSION BB(3,7)
0036      8 FORMAT (/,I3,3F10.5,F15.2,I10)
0037      9 FORMAT(/,'NR',11X,'EXPONENTS',20X,'PHI',12X,'JTE')
0038      K2=2*K+1
0039      DO 14 I=1,K
0040      D TYPE *, 'STEP LINE 8'
0041      14 B(I)=V(I)

```

```

0042      DD=G
0043      CALL LIN
0044      AKLE=PHI
0045      JTE=1
0046 D    TYPE *, 'STEP LINE 14'
0047      IR=0.
0048      WRITE (7,9)
0049 D    TYPE *, 'STEP LINE 17'
0050      DO 17 I=K1,4
0051      17 B(I)=0.
0052      WRITE (7,8) IR,(B(I),I=1,3),PHI, JTE
0053      DO 7 IR=1,IRMAX
0054      JTEV=JTE
0055      JTE=1
0056      DO 18 J=1,K2
0057      DO 18 I=1,K
0058      18 BB(I,J)=B(I)
0059      DO 19 J=2,K2
0060      I=J/2
0061      INT=1
0062      IF (2*I.EQ.J)INT=-1
0063      19 BB(I,J)=BB(I,J)+INT*DD*D(I)
0064      PHIT=AKLE
0065      DO 13 J=2,K2
0066      IF ((JTEV/2*4-JTEV+1).EQ.J) GOTO 13
0067 D    TYPE *, 'STEP LINE 36'
0068      DO 4 I=1,K
0069      4 B(I)=BB(I,J)
0070      CALL LIN
0071      IF (PHI.GE.PHIT) GOTO 13
0072      IF (PHI.GE.AKLE) GOTO 16
0073      JTE=J
0074      AKLE=PHI
0075      16 IF (J/2*2.EQ.J) J=J+1
0076 D    TYPE *, 'STEP LINE 48'
0077      13 CONTINUE
0078      DO 6 I=1,K
0079      6 B(I)=BB(I,JTE)
0080      WRITE (7,8) IR,(B(I),I=1,3),AKLE,JTE
0081      IF (JTE.NE.1) GOTO 7
0082      11 IF (DD.EQ.1) GOTO 12
0083      DD=DD/2
0084      7 CONTINUE
0085      12 CALL LIN
0086      RETURN
0087      END

```

***SUBROUTINE LIN - CALCULATES THE COEFFICIENTS
AND SUM OF LEAST SQUARES FOR EACH ITERATION ***

```

0088      SUBROUTINE LIN
0089      COMMON U(30,6),C(6),K,N,PHI,B(4),G,D(3),IRMAX,K1,
1V(4)
0090      DIMENSION A(6,6)
0091      K2=K+2

```

```

0092      K3=K+3
0093      DO 21 J=1,K
0094      I=1
0095  23   ARG=B(J)*U(I,6)
0096      IF (ARG.LT.-20) GOTO 22
0097      U(I,J)=EXP(+ARG)
0098      IF (I.GT.N) GOTO 21
0099      I=I+1
0100      GOTO 23
0101  22   U(I,J)=0.
0102      IF (I.GT.N) GOTO 21
0103      I=I+1
0104      GOTO 22
0105  21   CONTINUE
0106      DO 33 I=1,N
0107      U(I,K2)=U(I,5)
0108  D    TYPE *, 'LIN LINE 24'
0109  33   U(I,K1)=0.
0110      DO 24 L=1,K2
0111      SOM=0.
0112      DO 25 I=1,N
0113  25   SOM=SOM+U(I,L)
0114      A(1,L)=SOM
0115      DO 24 M=1,K
0116      M1=M+1
0117      SOM=0.
0118      DO 27 I=1,N
0119  27   SOM=SOM+U(I,M)*U(I,L)
0120  24   A(M1,L)=SOM
0121      DO 28 I=2,K1
0122      DO 28 M=I,K1
0123      DO 28 L=I,K2
0124  28   A(M,L)=A(M,I-1)*A(I-1,L)-A(I-1,I-1)*A(M,L)
0125      DO 29 I1=2,K1
0126      I=K2-I1
0127      C(I)=A(I,K2)
0128  D    TYPE *, 'LIN LINE 44'
0129      DO 30 J1=2,I1
0130      J=K3-J1
0131  30   C(I)=C(I)-A(I,J)*C(J)
0132  29   C(I)=C(I)/A(I,I)
0133      SOM=0.
0134      DO 31 I=1,N
0135      U(I,4)=0.
0136      DO 32 J=1,K
0137  32   U(I,4)=U(I,4)+C(J)*U(I,J)
0138  31   SOM=SOM+(U(I,4)-U(I,5))*(U(I,4)-U(I,5))
0139      PHI=SOM
0140      RETURN
0141      END

```

APPENDIX C

PROGRAM TO CALCULATE THE PARTIAL PRESSURE OF
XENON-133 THROUGHOUT THE SKIN

```

0001 DIMENSION PP1(400),PP2(400)
0002 INTEGER C1,C2,C3,A1,A2,A3,A4,D1,D2,D3,E1,E2,E3,M,N
0003 REAL K1,K2,K3,K4
      ***** INPUT DATA *****
      *** M - TOTAL NO OF NODAL POINTS ***
      *** N = 1 FOR EPICUTANEOUS DIFFUSION TECHNIQUE ***
      *** DSTEP1 TO 4 - DISTANCE STEPS FOR EACH LAYER ***
      *** SOL1 TO 4 - SOLUBILITIES FOR EACH LAYER ***
      *** K1 TO K4 - BLOOD FLOW TERMS FOR EACH LAYER
      *** EE - FRACTION OF XENON TRANSFERRED BY BLOOD TO
      SUB-CUT ***
      *** DF1 TO DF4 - DIFFUSION COEFFICIENTS FOR EACH
      LAYER ***
      *** TSTEP - TIME STEP ***
      *** C1 TO C3 - END POINTS FOR EACH LAYER ***
0004 TYPE *, 'INPUT M,N'
0005 ACCEPT *,M,N
0006 TYPE *, 'INPUT DSTEP1 TO 4'
0007 ACCEPT *,DSTEP1,DSTEP2,DSTEP3,DSTEP4
0008 TYPE *, 'INPUT SOLUBILITIES'
0009 ACCEPT *,SOL1,SOL2,SOL3,SOL4
0010 TYPE *, 'INPUT K1,K2,K3,K4,EE'
0011 ACCEPT *,K1,K2,K3,K4,EE
0012 TYPE *, 'INPUT DIFF. COEFFS 1 TO 4'
0013 ACCEPT *,DF1,DF2,DF3,DF4
0014 TYPE *, 'INPUT TSTEP,BOUNDARIES'
0015 ACCEPT *,TSTEP,C1,C2,C3
      C ***** CALCULATION OF STABILITY CRITERIA *****
0016 R1=TSTEP*DF1/DSTEP1**2
0017 R2=TSTEP*DF2/DSTEP2**2
0018 R3=TSTEP*DF3/DSTEP3**2
0019 R4=TSTEP*DF4/DSTEP4**2
0020 TYPE *, 'FOR STABILITY R SHOULD BE LESS THAN 0.125'
0021 TYPE *,R1,R2,R3,R4
      C ***** DEFINITION OF POINTS NEAR BOUNDARY *****
0022 A1=C1-1
0023 A2=C2-1
0024 A3=C3-1
0025 A4=M-1
0026 D1=C1+1
0027 D2=C2+1
0028 D3=C3+1
0029 E1=C1+2
0030 E2=C2+2
0031 E3=C3+2
      C ***** INPUT INITIAL VALUES OF PARTIAL PRESSURE *****
0032 TYPE *, 'INPUT PARTIAL PRESSURES B,C,D,E'
0033 ACCEPT *,B,C,D,E
0034 DO 12 I=1,C1

```

```

0035     PP1(I)=B
0036  12  CONTINUE
0037     DO 13 I=D1,C2
0038  13  PP1(I)=C
0039     DO 14 I=D2,C3
0040  14  PP1(I)=D
0041     DO 15 I=D3,M
0042  15  PP1(I)=E
0043     TTIME=0
0044  28  Z=0
0045  27  Y=0
0046  25  TOT1=0
0047     TOT2=0
0048     TOT3=0
0049     TOT4=0
0050     V=0
0051     TOT5=0
0052     TOT=0
0053     TTIME=TTIME+TSTEP
0054     IF (N-1) 7,4,7
0055  4   IF (TTIME-180.0) 7,5,5
0056  5   DO 6 I=1,C1
0057  6   PP1(I)=0.0
0058     DSTEP1=2.0
0059     SOL1=1.3
0060     DF1=0.07
0061     R1=TSTEP*DF1/DSTEP1**2
0062  7   CONTINUE
      C   *****BLOOD FLOW CALCULATIONS *****
0063     DO 39 I=1,C1
0064  39  PP1(I)=PP1(I)-K1*TSTEP*PP1(I)
0065     DO 40 I=D1,C2
0066     W=K2*TSTEP*PP1(I)
0067  40  PP1(I)=PP1(I)-W
0068     DO 42 I=D2,C3
0069     V=V+K3*TSTEP*PP1(I)*SOL3*DSTEP3
0070  42  PP1(I)=(1.0-K3*TSTEP)*PP1(I)
0071     DO 43 I=D3,M
0072     PP1(I)=PP1(I)+(EE*V)/(SOL4*DSTEP4)
0073  43  PP1(I)=PP1(I)-K4*TSTEP*PP1(I)
      C   ***** MEDIUM 1 CALCULATIONS *****
0074     DO 17 I=2,A1
0075     PP2(I)=(1.0-(2.0*R1) )*PP1(I)+R1*(PP1(I+1)+PP1(I-1) )
0076     TOT1=TOT1+PP2(I)*DSTEP1*SOL1
0077  17  CONTINUE
      C   ***** MEDIUM 2,3,4 CALCULATIONS *****
0078     DO 18 I=E1,A2
0079     PP2(I)=(1.0-(2.0*R2) )*PP1(I)+R2*(PP1(I+1)+PP1(I-1) )
0080     TOT2=TOT2+PP2(I)*DSTEP2*SOL2
0081  18  CONTINUE
0082     DO 19 I=E2,A3
0083     PP2(I)=(1.0-(2.0*R3) )*PP1(I)+R3*(PP1(I+1)+PP1(I-1) )
0084     TOT3=TOT3+PP2(I)*DSTEP3*SOL3
0085  19  CONTINUE
0086     DO 20 I=E3,A4
0087     PP2(I)=(1.0-(2.0*R4) )*PP1(I)+R4*(PP1(I+1)+PP1(I-1) )

```

```

0088     TOT4=TOT4+PP2(I)*DSTEP4*SOL4
0089  20  CONTINUE
C      ***** CALCULATION OF BOUNDARY VALUES *****
0090     B12=(DF1*DSTEP2*PP1(C1)/2.0+(DF2*DSTEP1*PP1(D1)*
1SOL2)/(2.0+SOL1) )/(DF1*DSTEP2/2.0+(DF2*DSTEP1*SOL2)
2/(2.0*SOL1) )
0091     B23=(DF2*DSTEP3*PP1(C2)/2.0+(DF3*DSTEP2*PP1(D2)*
1SOL3)/(2.0*SOL2) )/(DF2*DSTEP3/2.0+(DF3*DSTEP2*SOL3)
2/(2.0*SOL2) )
0092     B34=(DF3*DSTEP4*PP1(C3)/2.0+(DF4*DSTEP3*PP1(D3)*
1SOL4)/(2.0*SOL3) )/(DF3*DSTEP4/2.0+(DF4*DSTEP3*SOL4)
2/(2.0*SOL3) )
C
C      ***** CALC OF POINTS NEAR BOUNDARY *****
0093     PP2(C1)=PP1(C1)*(1.0-(4.0*R1) )+R1*( (8.0*B12)/3.0+
1(4.0*PP1(A1) )/3.0)
0094     PP2(C2)=PP1(C2)*(1.0-(4.0*R2) )+R2*( (8.0*B23)/3.0+
1(4.0*PP1(A2) )/3.0)
0095     PP2(C3)=PP1(C3)*(1.0-(4.0*R3) )+R3*( (8.0*B34)/3.0+
1(4.0*PP1(A3) )/3.0)
0096     PP2(D1)=PP1(D1)*(1.0-(4.0*R2) )+R2*( (8.0*B12)/3.0+
1(4.0*PP1(E1) )/3.0)
0097     PP2(D2)=PP1(D2)*(1.0-(4.0*R3) )+R3*( (8.0*B23)/3.0+
1(4.0*PP1(E2) )/3.0)
0098     PP2(D3)=PP1(D3)*(1.0-(4.0*R4) )+R4*( (8.0*B34)/3.0+
1(4.0*PP1(E3) )/3.0)
C      ***** CALC OF FIRST AND LAST POINTS *****
0099     PP2(1)=PP2(2)+(PP2(2)-PP2(3) )
0100     IF (PP2(1)-0.0) 21,22,22
0101  21  PP2(1)=0.0
0102  22  PP2(M)=PP2(A4)+(PP2(A4)-PP2(M-2) )
0103     IF (PP2(M)-0.0) 23,24,24
0104  23  PP2(M)=0.0
C      ***** CALC OF AMOUNTS IN EACH LAYER *****
0105  24  TOT1=TOT1+(PP2(1)+PP2(C1) )*SOL1*DSTEP1
0106     TOT2=TOT2+(PP2(D1)+PP2(C2) )*SOL2*DSTEP2
0107     TOT3=TOT3+(PP2(D2)+PP2(C3) )*SOL3*DSTEP3
0108     TOT4=TOT4+(PP2(D3)+PP2(M) )*SOL4*DSTEP4
0109     TOT5=TOT2+TOT3+TOT4
0110     TOT=TOT1+TOT2+TOT3+TOT4
0111     DO 26 I+1,M
0112  26  PP1(I)=PP2(I)
0113     Y=Y+TSTEP
0114     Z=Z+TSTEP
0115     IF (Y-60.0) 25,32,32
0116  32  WRITE (7,30) TTIME,TOT1,TOT2,TOT3,TOT4,TOT5,TOT
0117  30  FORMAT (8H TIME = ,F8.3,6H(SECS),/,8H TOT1 = ,E14.6,
1/,8H TOT2 = ,E14.6,/,8H TOT3 = ,E14.6,/,8H TOT4 = ,
2E14.6,/,8H TOT5 = ,E14.6,/,7H TOT = ,E14.6,/,)
0118     IF (Z-60.0) 27,33,33
0119  33  WRITE (7,31) (PP1(I),I=1,M)
0120  31  FORMAT (50(3X,5E14.6,/) )
0121     IF (TTIME-7200.0) 28,41,41
0122  41  STOP
0123     END

```

APPENDIX D

PROGRAM TO CALCULATE THE TEMPERATURE DISTRIBUTION
IN TISSUE DURING HYPERTHERMIA

```

C ***** PROGRAM CALCULATES TEMPERATURE FOR
      SPHERICAL DIFFUSION EQUATION AND LCF
      HEATING *****
0001  DIMENSION TEMP1(100),TEMP2(100),TOUT(20),DIST
      1(100)
0002  INTEGER A(100),COT,COTT,MAXX,S,SS,X1,X2,F,FX1,
      1FX2
0003  INTEGER G,DOT1,DOT2,BLANK,SYMBOL(100)
0004  BLANK=1H
0005  DOT1=1H*
0006  DOT2=1HX
C ***** INPUT DATA *****
C ***** PARAMETER LIST *****
C TSTEP = TIME INTERVAL
C DSTEP = DISTANCE INTERVAL
C THDIFF = THERMAL DIFFUSIVITY
C MAXX = MAX. NO. OF NODAL POINTS
C NOP = NUMBER OF OUTPUT TIMES
C TOUT = OUTPUT TIMES
C FLOW = BLOOD FLOW REMOVAL TERM
C HEAT = LCF HEATING TERM
C EQTEMP = EQUILIBRATION TEMPERATURE AT POINT XT
C *****
0007  ACCEPT "TSTEP,DSTEP ",TSTEP,DSTEP
0008  ACCEPT "THDIFF ",THDIFF
0009  ACCEPT "TIMAX ",TIMAX
0010  ACCEPT "NO. OF OUTPUT POINTS ",NOP
0011  ACCEPT "MAX. NO. OF NODAL POINTS ",MAXX
0012  DO 13 I=1,NOP
0013  13 ACCEPT "TOUT (I) ",TOUT(I)
0014  ACCEPT "INITIAL TEMPS. ",T1,T2
0015  ACCEPT "CO-ORD OF T1/T2 ",COT
0016  COTT=COT+1
0017  ACCEPT "INITIAL AND FINAL NODAL PTS OF HEATED
      1REGION? ",HX1,HX2
0018  ACCEPT "EQUILIBRATION TEMP? ",EQTEMP
0019  ACCEPT "FEEDBACK NODAL POINT? " XT
0020  ACCEPT "LCF HEATING TERM? ",HEAT
0021  ACCEPT "ARE SOME PTS. MAINTAINED AT CONST. TEMP.
      11=YES,0=NO",SS
0022  IF (SS.EQ.0) GO TO 12
0023  ACCEPT "INITIAL & FINAL NODAL PTS. OF CONST.
      1TEMP",X1,X2
0024  ACCEPT "WHAT IS THE CONSTANT TEMPERATURE?",C
      1TEMP
0025  12 ACCEPT "BLOOD FLOW PRESENT - 1=YES,0=NO",F
0026  IF (F.EQ.0) GO TO 14
0027  ACCEPT "INITIAL & FINAL NODAL POINTS OF FLOW"
      1,FX1,FX2

```

```

0028 ACCEPT "FLOW VALUE",FLOW
0029 14 WRITE (12,20)
0030 WRITE (12,21) TSTEP,DSTEP
0031 WRITE (12,22) THDIFF
0032 WRITE (12,23) T1,COT,T2,COTT,MAXX
0033 ACCEPT "GRAPH (LP) O/P 1=YES,0+NO",G
0034 IF (SS.EQ.0) GO TO 17
0035 WRITE (12,24) CTEMP,X1,X2
0036 17 CONTINUE
0037 IF (F.EQ.0) GO TO 18
0038 WRITE (12,25) FLOW,FX1,FX2
0039 18 CONTINUE
0040 20 FORMAT (1H1,/,13H PROGRAM RS08,/,20H PROGRAM
1CALCULATES, 47HTEMPERATURES FOR SPHERICAL
2DIFFUSION EQUATION,/)
0041 21 FORMAT (9H TSTEP = ,F6.3,6H(SECS),5X,8HDSTEP =
1,F6.3,5H(CMS),/)
0042 22 FORMAT (10H THDIFF = ,E9.3,11H(CM**2/SEC)/)
0043 23 FORMAT (21H INITIAL TEMPERATURES,/,2X,F6.3,19H
1'C FROM I=1 TO I =,1X,I3,/,2X,F6.3,13H 'C FROM
2I = ,I3,8H TO I = ,I3)
0044 24 FORMAT (22H CONSTANT TEMPERATURE,,F5.1,22H
1BETWEEN NODAL POINTS ,I3,5H AND ,I3,/)
0045 25 FORMAT (15H BLOOD FLOW (K=,F6.3,22H BETWEEN
1NODAL POINTS ,I3,5H AND ,I3,/)
C ***** INITIAL TEMPERATURE DISTRIBUTION *****
0046 DO 30 I=1,COT
0047 30 TEMP1(I)=T1
0048 DO 31 I=COTT,MAXX
0049 31 TEMP1(I)=T2
0050 TE=0
0051 DUM=1.0
0052 TT=0.0
0053 S=1
0054 MMAX = MAXX-1
0055 400 TT=TT+TSTEP
C *** LCF HEATING ***
0056 DO 300 I=HX1,HX2
0057 300 TEMP1(I)=TEMP1(I)+DUM*HEAT
C *****THERMAL DIFFUSIVITY CALCULATIONS *****
0058 DO 50 I=2,MMAX
0059 R=(THDIFF*TSTEP)/(DSTEP**2*(I-1))
0060 TEMP2(I)=(I-1)*R*TEMP1(I-1)+(R*(I+1)*TEMP1
1(I+1))-(((2*I)*R)-1)*TEMP1(I)
0061 50 CONTINUE
C ***** END POINTS OF ARRAY *****
0062 TEMP2(1)=2*TEMP2(2)-TEMP2(3)
0063 TEMP2(MAXX)=TEMP2(MMAX)*2-TEMP2(MAXX-2)
0064 IF (F.EQ.0) GO TO 32
C ***** BLOOD FLOW REMOVAL *****
0065 DO 52 I=FX1,FX2
0066 52 TEMP2(I)=TEMP2(I)-(FLOW*(TEMP2(I)-37.0))
0067 32 CONTINUE
0068 IF (SS.EQ.0) GO TO 16
C ***** MAINTAIN CONSTANT TEMPERATURES *****

```



```

0069     DO 15 I=X1,X2
0070  15 TEMP2(I)=CTEMP
0071  16 CONTINUE
      C ***** HEAT FEEDBACK *****
0072     IF (TEMP2(XT).LT.EQTEMP.AND.TE.EQ.0) GO TO 309
0073     IF (TEMP2(XT).GE.EQTEMP) GO TO 306
0074     DUM=EQTEMP-TEMP2(XT)
0075     DUM=DUM/HEAT
0076     GO TO 309
0077  306 IF (TE.EQ.0) WRITE (12,307)TT
0078  307 FORMAT (////22H EQUILIBRATION TIME = ,F6.1,6H
      1(SECS))
0079     TE=1
0080     DUM=0
0081  309 CONTINUE
      C ***** RESET TEMP1 *****
0082     DO 51 I=1,MAXX
0083  51 TEMP1(I)=TEMP2(I)
      C ***** OUTPUT *****
0084     IF (TT.GT.TOUT(S)-0.05.AND.TT.LT.TOUT(S)+0.05)
      1GO TO 210
0085     IF (TT.GE.TIMAX) GO TO 220
0086     GO TO 400
0087  210 WRITE (12,215) TT
0088  215 FORMAT (//1H1,5X,7HTIME = ,F6.1,8H (SECS) )
0089     RMAX = MAXX/15.0 + 1.0
0090     NN=INT(RMAX)
0091     DO 60 J=1,NN
0092     II=(J*15-14)
0093     III=II+14
0094     IF (J.EQ.NN) GO TO 66
0095     DO 61 I=II,III
0096  61 A(I)=I
0097     WRITE (12,62) (A(I),I=II,III)
0098  62 FORMAT (12H NODAL POINT,3X,I2,14(5X,I2))
0099     DO 63 I=II,III
0100  63 DIST(I)=DSTEP*(I-1)
0101     WRITE(12,64) (DIST(I),I=II,III)
0102  64 FORMAT (12H DIST. (CMS),15(1X,F6.3))
0103     WRITE (12,65) (TEMP1(I),I=II,III)
0104  65 FORMAT (9H TEMP. 'C,6X,F4.1,14(3X,F4.1)/)
0105     GO TO 2
0106  66 NNN=MAXX-(NN-1)*15
0107     DO 67 I=II,MAXX
0108  67 A(I)=I
0109     WRITE (12,62) (A(I),I=II,MAXX)
0110     DO 69 I=II,MAXX
0111  69 DIST(I)=DSTEP*(I-1)
0112     WRITE (12,64) (DIST(I),I=II,MAXX)
0113     WRITE (12,65) (TEMP1(I),I=II,MAXX)
0114     2 CONTINUE
0115  60 CONTINUE
0116     IF (G.EQ.0) GO TO 1
      C ***** GRAPH (LP) OUTPUT *****
0117     WRITE (12,99) TT

```

```
0118     WRITE (12,100)
0119     WRITE (12,101)
0120     WRITE (12,102)
0121     WRITE (12,103)
0122  99  FORMAT (1H1,15X,7HTIME = ,F6.1,8H (SECS) )
0123 100  FORMAT (//,30X,14HTEMPERATURE 'C)
0124 101  FORMAT (1H ,10X,2H37,8X,2H38,8X,2H39,8X,2H40,
          18X,2H41,8X,2H42,8X,2H43,8X,2H44,8X,2H45)
0125 102  FORMAT (1H ,10X,1HI,8(9X,1HI) )
0126 103  FORMAT (1H ,9X,41(2H==))
0127     M=MAXX
0128     MM=0
0129     IF (MAXX.GT.50) M=50
0130     DO 105 I=1,100
0131 105  SYMBOL(I)=BLANK
0132     DO 104 K=1,M
0133     MM=MM+1
0134     KK=INT(TEMP1(K)*10+0.5)
0135     KK=KK-369
0136     IF (KK.LT.1) GO TO 110
0137     SYMBOL(KK)=DOT1
0138     GO TO 111
0139 110  KK=1
0140     SYMBOL(KK)=DOT2
0141 111  CONTINUE
0142     IF (K.EQ.10) GO TO 112
0143     IF (K.EQ.12) GO TO 113
0144     IF (MM.EQ.2) GO TO 114
0145     IF (MM.EQ.1) GO TO 120
0146 112  WRITE (12,115) K,(SYMBOL(I),I=1,85)
0147 115  FORMAT (6H NODAL,2X,I2,1HI,85A1)
0148     GO TO 116
0149 113  WRITE (12,117) K,(SYMBOL(I),I=1,85)
0150 117  FORMAT (6H POINT,2X,I2,1HI,85A1)
0151     GO TO 116
0152 114  WRITE (12,118) K,(SYMBOL(I),I=1,85)
0153 118  FORMAT (1H ,7X,I2,1HI,85A1)
0154     GO TO 116
0155 120  WRITE (12,119) (SYMBOL(I),I=1,85)
0156 119  FORMAT (1H ,9X,1HI,85A1)
0157 116  SYMBOL(KK)=BLANK
0158     IF (MM.EQ.2) MM=0
0159 104  CONTINUE
0160  1   CONTINUE
0161     IF (TT.GT.TIMAX) GO TO 220
0162     S=S+1
0163     GO TO 400
0164 220  STOP
0165     END
```

APPENDIX ECONVERSION FACTORS TO SI UNITS

<u>Term</u>	<u>Units used</u>	<u>Multiply by to convert to</u>	<u>SI units</u>
Diffusion coefficient	$\text{cm}^2 \text{s}^{-1}$	10^{-4}	$\text{m}^2 \text{s}^{-1}$
Blood flow	ml/100g/min	10^{-2}	l/kg/min
Density	g cm^{-3}	10^{-3}	kg m^{-3}
Velocity of fluid	cm s^{-1}	10^{-2}	m s^{-1}
Thermal conductivity	$\text{Wcm}^{-1} \text{ } ^\circ\text{C}^{-1}$	10^{-2}	$\text{Wm}^{-1} \text{ } ^\circ\text{C}^{-1}$
Specific heat	$\text{Jg}^{-1} \text{ } ^\circ\text{C}^{-1}$	10^3	$\text{Jkg}^{-1} \text{ } ^\circ\text{C}^{-1}$
Thermal diffusivity	$\text{cm}^2 \text{s}^{-1}$	10^{-4}	$\text{m}^2 \text{s}^{-1}$